frontiers | Research Topics

Oxidative stress, inflammation and atherosclerosis-related diseases: From basic to clinical research

Edited by
Qiang Liu, Mark Slevin and Wen-Jun Tu

Published in
Frontiers in Cardiovascular Medicine

ISSN 1664-8714
ISBN 978-2-8325-3931-6
DOI 10.3389/978-2-8325-3931-6

About Frontiers

Frontiers is more than just an open access publisher of scholarly articles: it is a pioneering approach to the world of academia, radically improving the way scholarly research is managed. The grand vision of Frontiers is a world where all people have an equal opportunity to seek, share and generate knowledge. Frontiers provides immediate and permanent online open access to all its publications, but this alone is not enough to realize our grand goals.

Frontiers journal series

The Frontiers journal series is a multi-tier and interdisciplinary set of open-access, online journals, promising a paradigm shift from the current review, selection and dissemination processes in academic publishing. All Frontiers journals are driven by researchers for researchers; therefore, they constitute a service to the scholarly community. At the same time, the *Frontiers journal series* operates on a revolutionary invention, the tiered publishing system, initially addressing specific communities of scholars, and gradually climbing up to broader public understanding, thus serving the interests of the lay society, too.

Dedication to quality

Each Frontiers article is a landmark of the highest quality, thanks to genuinely collaborative interactions between authors and review editors, who include some of the world's best academicians. Research must be certified by peers before entering a stream of knowledge that may eventually reach the public - and shape society; therefore, Frontiers only applies the most rigorous and unbiased reviews. Frontiers revolutionizes research publishing by freely delivering the most outstanding research, evaluated with no bias from both the academic and social point of view. By applying the most advanced information technologies, Frontiers is catapulting scholarly publishing into a new generation.

What are Frontiers Research Topics?

Frontiers Research Topics are very popular trademarks of the *Frontiers journals series*: they are collections of at least ten articles, all centered on a particular subject. With their unique mix of varied contributions from Original Research to Review Articles, Frontiers Research Topics unify the most influential researchers, the latest key findings and historical advances in a hot research area.

Find out more on how to host your own Frontiers Research Topic or contribute to one as an author by contacting the Frontiers editorial office: frontiersin.org/about/contact

Oxidative stress, inflammation and atherosclerosis-related diseases: From basic to clinical research

Topic editors

Qiang Liu — Chinese Academy of Medical Sciences and Peking Union Medical College, China

Mark Slevin — Manchester Metropolitan University, United Kingdom

Wen-Jun Tu — Chinese Academy of Medical Sciences and Peking Union Medical College, China

Citation

Liu, Q., Slevin, M., Tu, W.-J., eds. (2023). *Oxidative stress, inflammation and atherosclerosis-related diseases: From basic to clinical research*. Lausanne: Frontiers Media SA. doi: 10.3389/978-2-8325-3931-6

Table of contents

frontiers | Frontiers in Cardiovascular Medicine

REVIEW
published: 16 June 2022
doi: 10.3389/fcvm.2022.918056

Endoplasmic Reticulum Stress and Pathogenesis of Vascular Calcification

Zhenqi Rao[1], Yidan Zheng[2], Li Xu[1], Zihao Wang[1], Ying Zhou[1], Ming Chen[1], Nianguo Dong[1], Zhejun Cai[3] and Fei Li[1]**

[1] Department of Cardiovascular Surgery, Union Hospital, Tongji Medical College, Huazhong University of Science and Technology, Wuhan, China, [2] Basic Medical School, Tongji Medical College, Huazhong University of Science and Technology, Wuhan, China, [3] Department of Cardiology, The Second Affiliated Hospital, Zhejiang University School of Medicine, Hangzhou, China

OPEN ACCESS

Edited by:
Wen-Jun Tu, Chinese Academy of Medical Sciences and Peking Union Medical College, China

Reviewed by:
Florent Allagnat, Centre Hospitalier Universitaire Vaudois (CHUV), Switzerland
Mabruka Alfaidi, Louisiana State University Health Shreveport, United States

***Correspondence:**
Zhejun Cai
caizhejun@zju.edu.cn
Fei Li
lifei_union@hust.edu.cn

Specialty section:
This article was submitted to Atherosclerosis and Vascular Medicine, a section of the journal Frontiers in Cardiovascular Medicine

Received: *12 April 2022*
Accepted: *30 May 2022*
Published: *16 June 2022*

Citation:
Rao Z, Zheng Y, Xu L, Wang Z, Zhou Y, Chen M, Dong N, Cai Z and Li F (2022) Endoplasmic Reticulum Stress and Pathogenesis of Vascular Calcification. Front. Cardiovasc. Med. 9:918056. doi: 10.3389/fcvm.2022.918056

Vascular calcification (VC) is characterized by calcium phosphate deposition in blood vessel walls and is associated with many diseases, as well as increased cardiovascular morbidity and mortality. However, the molecular mechanisms underlying of VC development and pathogenesis are not fully understood, thus impeding the design of molecular-targeted therapy for VC. Recently, several studies have shown that endoplasmic reticulum (ER) stress can exacerbate VC. The ER is an intracellular membranous organelle involved in the synthesis, folding, maturation, and post-translational modification of secretory and transmembrane proteins. ER stress (ERS) occurs when unfolded/misfolded proteins accumulate after a disturbance in the ER environment. Therefore, downregulation of pathological ERS may attenuate VC. This review summarizes the relationship between ERS and VC, focusing on how ERS regulates the development of VC by promoting osteogenic transformation, inflammation, autophagy, and apoptosis, with particular interest in the molecular mechanisms occurring in various vascular cells. We also discuss, the therapeutic effects of ERS inhibition on the progress of diseases associated with VC are detailed.

Keywords: vascular calcification, endoplasmic reticulum stress, unfolded protein response, chronic kidney disease, atherosclerosis, diabetes

INTRODUCTION

Vascular calcification (VC) commonly occurs with aging, atherosclerosis, diabetes, and chronic kidney disease (CKD) owing to accumulation of apatite calcium salts in the media and/or intima of arteries (1). Based on the location of hydroxyapatite, three main types of VC have been reported, namely, intimal calcification, Mönckeberg medial arterial calcification, and valvular calcification (2). Intimal calcification is closely associated with lipid deposits, inflammatory cell infiltration, atherosclerosis, and atherosclerotic plaque rupture (3). Medial calcification occurs when smooth muscle cells transform into osteoblast-like cells. This transformation is associated with various

genes, including bone morphogenetic protein-2 (*BMP2*), MSH homeobox 2 (*MSX2*), and alkaline phosphatase (*ALP*; 4). Valvular calcification occurs in aortic valves as a result of long-term mechanical stress and the effects of proinflammatory cytokines, which can cause aortic stenosis.

The endoplasmic reticulum (ER) is an intracellular organelle with important roles in protein folding and maturation, lipid biosynthesis, and intracellular calcium homeostasis. However, the capacity of the ER protein maturation machinery can become overwhelmed in certain physiological or pathological conditions, leading to the accumulation of defective or superfluous proteins and ER stress (ERS; 5). Over the past two decades, ERS has been widely recognized as an important mechanism implicated in the development of several human diseases. Moreover, numerous studies have shown that ERS contributes to VC through various mechanisms in vascular cells. VC research is currently focused on the intima and tunica media; involvement of the former is observed in atherosclerosis and that of the latter in degenerative vascular diseases, such as CKD and diabetes; however, no effective clinical therapy is available for VC.

In this review, we summarize the roles of ERS in the initiation and progression of VC. Furthermore, we discuss the current understanding of how ERS can promote VC through various mechanisms involving vascular smooth muscle cells (VSMCs), vascular endothelial cells (VECs), and immune cells, leading to an increase in the unfolded protein response (UPR). Finally, we evaluate emerging therapeutic strategies to target VC-associated ERS.

KEY PLAYERS IN THE UNFOLDED PROTEIN RESPONSE

The UPR is a highly conserved mechanism mediated by three ER transmembrane sensor proteins: PKR-like ER kinase (PERK), activating transcription factor 6 (ATF6), and inositol-requiring enzyme 1 (IRE1; **Figure 1**). In the absence of stress, these proteins are maintained in an inactive state by the binding of their luminal domains with the ER intraluminal glucose-regulated protein 78 (GRP78; 6). ERS conditions activate these proteins and increase the binding of GRP78 to misfolded or unfolded proteins. This results in the dissociation of GRP78 from ATF6, IRE1, and PERK and the subsequent activation of UPR signaling (7).

Inositol-Requiring Enzyme 1

Inositol-requiring enzyme 1, the most conserved UPR transducer, is a transmembrane protein responsible for protein kinase and endoribonuclease activity (8, 9). IRE1 homodimerizes and is transphosphorylated upon dissociation from GRP78, facilitating subsequent allosteric activation of its C-terminal endoribonuclease domain (10, 11). This domain specifically recognizes and cleaves a 26-base fragment from the mRNA transcript of the X-box binding protein 1 (XBP1). The 26-base transcript fragment is subsequently translated into spliced XBP1s (XBP1s), which act as a transcription factors by inducing the expression of genes involved in protein folding, autophagy, and ER-associated degradation to help maintain ER homeostasis (12). In addition, IRE1 forms a complex with tumor necrosis factor receptor-associated factor 2 and apoptosis signal-regulating kinase 1, leading to the activation of c-Jun N-terminal kinases and caspase proteases, which promote apoptosis (13).

PKR-Like Endoplasmic Reticulum Kinase

PKR-like ER kinase, a type I ER-resident protein kinase, is activated through autophosphorylation and homodimerization after dissociating from GRP78 (14). Once activated, PERK phosphorylates the alpha subunit of eukaryotic translation initiation factor (eIF) 2α, leading to downregulation of overall protein synthesis. This reduces the accumulation of unfolded proteins. However, phosphorylation of eIF2α also induces the translation of ATF4 (15), which stimulates the expression of C/EBP homologous protein (CHOP). Subsequently, ATF4 and CHOP synergistically induce the expression of genes involved in apoptosis, autophagy, and antioxidant response (16).

Activating Transcription Factor 6

Activating transcription factor 6 is a type II ER transmembrane protein with a basic leucine zipper transcription activation domain at the N-terminus. The ATF6 C-terminus is localized in the ER cavity. ATF6 has multiple GRP78 binding sites and two Golgi positioning signals. GRP78 dissociates from the luminal domain of ATF6 in response to ERS, exposing two Golgi localization signals and causing ATF6 translocation to the Golgi (17). Following translocation, ATF6 is cleaved by site-1 protease and site-2 protease to release its active N-terminal fragment (18). The N-terminus protein then binds to the ATF/cyclic adenosine monophosphate response element and ERS response element and subsequently migrates into the nucleus to activate transcription. Furthermore, to reduce unfolded protein accumulation, ATF6 regulates the transcription of various genes, such as those encoding ER chaperones and protein folding enzymes. This process is mediated by activating specific UPR-related genes (including *XBP1*) and three main branches of the UPR (including *ATF4*, *XBP1*, and *ATF6*; 12).

VASCULAR CALCIFICATION

Vascular calcification occurs when calcium phosphate crystals (hydroxyapatite) accumulate in the media and/or intima of vessel walls and is strongly correlated with cardiovascular mortality in patients with CKD, atherosclerosis, and diabetes (19, 20). Hence, delaying and reversing VC can theoretically reduce the case fatality rate of these high-risk groups. However, the specific mechanisms underlying VC development and pathogenesis are not fully understood.

Predisposition of Vascular Calcification

Multiple factors contribute to the occurrence of VC. Physiological calcification is a normal process occurring in bones and teeth; however, its occurrence is closely associated with aging, advanced atherosclerosis, diabetes mellitus, and CKD (21). Moreover, numerous risk factors, including calcium

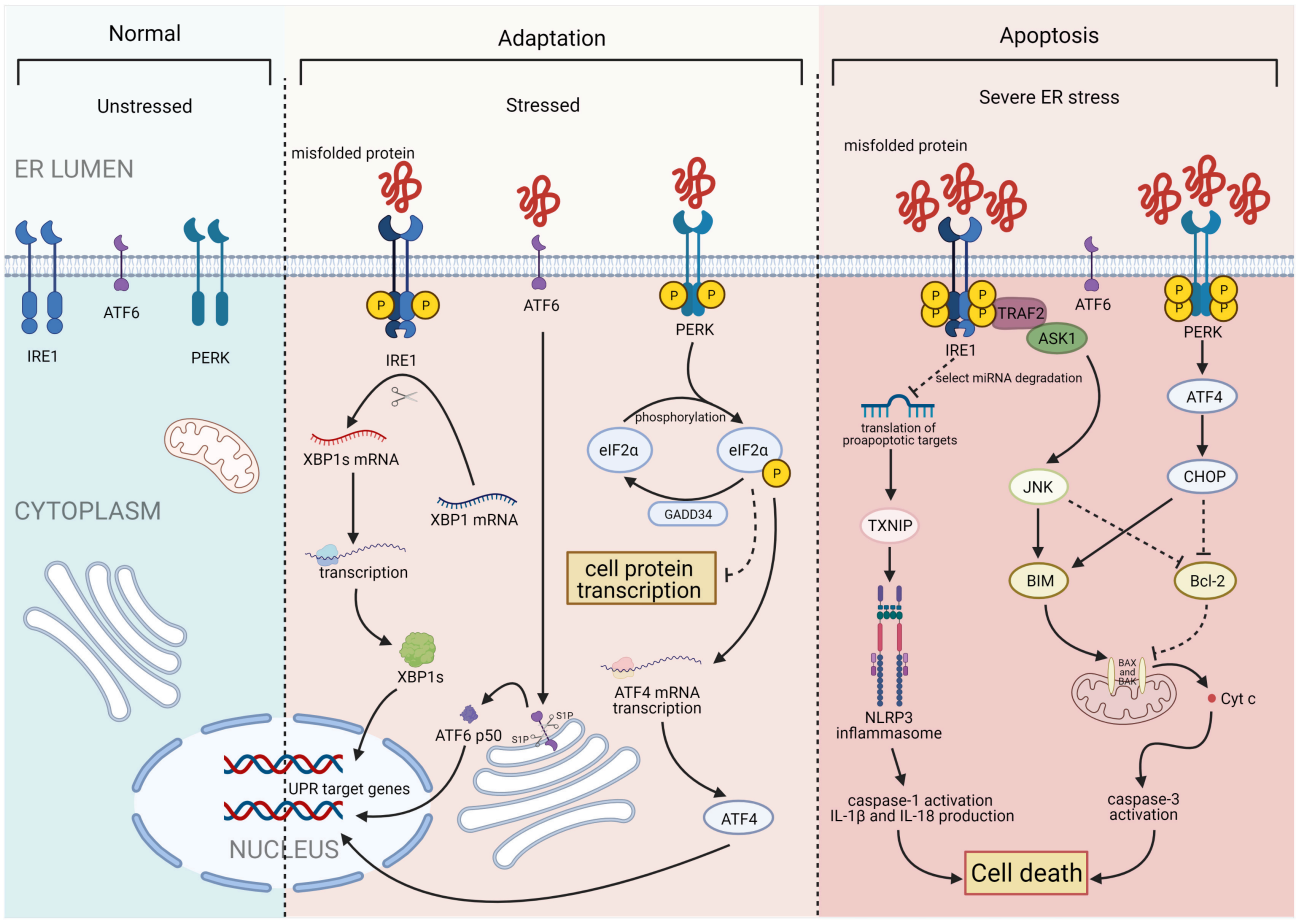

FIGURE 1 | Three major states of endoplasmic reticulum stress (ERS): unstressed, stressed, and severe ERS. In the absence of stress, PKR-like ER kinase (PERK), activating transcription factor 6 (ATF6), and inositol-requiring enzyme 1 (IRE1) are maintained in an inactive state. Upon activation, the IRE1 endoribonuclease domain specifically recognizes and cleaves a 26-base fragment from the X-box binding protein 1 (XBP1) mRNA transcript, resulting in XBP1s. PERK phosphorylates the alpha subunit of eukaryotic translation initiation factor 2 (eIF2α), that leads to a downregulation of overall mRNA translation, which reduces the accumulation of unfolded proteins. Phosphorylation of eIF2α also induces the translation of ATF4. ATF6 will be cleaved by two Golgi resident proteases to release its N-terminal transcriptionally active 50-kDa fragment. Thereafter, the 50-kDa N-terminus protein will translocate into the nucleus to activate transcription. Finally, after activation of ATF6, IRE1, and PERK, the unfolded protein response (UPR) is constitutively activated. Under severe ERS, IRE1 forms a complex with tumor necrosis factor receptor-associated factor 2 (TRAF2) and apoptosis signal-regulating kinase 1 (ASK1) to activate c-Jun N-terminal kinase (JNK) and the caspase family. This process activates the NACHT, LRR, and PYD domain-containing protein 3 (NLRP3) inflammasome. ATF4 and C/EBP homologous protein (CHOP) synergistically induce the expression of multiple genes involved in apoptosis, autophagy, and antioxidant responses, which all lead to cell death. Figures were created using BioRender.com.

and phosphorus metabolism disorder, inflammation, oxidative stress, apoptosis, autophagy, and aging, can also contribute to VC (22).

Mechanisms of Vascular Calcification

In the past decade, VC was defined as a passive, degenerative condition. However, more recent studies have suggested that VC is a highly regulated process resulting from multiple factors acting together over a certain period of time. For example, the transformation of smooth muscle cells from a contractile phenotype to an osteoblast-like phenotype, together with extracellular matrix remodeling, apoptosis, and elevated calcium and phosphorus levels, is involved in the development of VC. Under the action of calcification-stimulating factors, the expression levels of osteoblast cell markers, including Runt-related transcription factor 2 (Runx2), become increased, as does the activity of the transcription factor core binding factor alpha1 and the expression of genes containing the core binding factor alpha1 binding site (i.e., osteopontin, osteocalcin, and ALP; 23). By contrast, the expression levels of smooth muscle cell markers, such as SM22-α and smooth muscle α-actin, are decreased, thereby promoting the transformation of smooth muscle cells from a contractile phenotype to an osteoblast cell phenotype (23). Moreover, disorder of calcium (Ca^{2+}) and phosphorus (Pi) metabolism promotes VC. That is, high Ca^{2+} and Pi concentrations can promote the expression of BMP2, Runx2, MSX2, and osteocalcin in VSMCs, thus promoting osteogenic-like differentiation of VSMCs. In addition, imbalanced Ca^{2+} and Pi concentrations can cause accumulation of Ca^{2+} in VSMCs, thereby promoting

the release and mineralization of matrix vesicles as well as the apoptosis of VSMCs (24, 25). However, despite the abundance of research on the various risk factors for VC, including hyperphosphatemia, hypercalcemia, oxidative stress, inflammation, and apoptosis, there is a dearth of information regarding the associated regulatory pathways and molecules. Therefore, as a calcium reservoir, the ER has high value in the field of VC research.

ENDOPLASMIC RETICULUM STRESS AND VASCULAR CALCIFICATION

Numerous recent studies have shown that ERS can regulate VC through various mechanisms in vascular cells (**Table 1**; 26).

Endoplasmic Reticulum Stress in Vascular Smooth Muscle Cells

Vascular smooth muscle cells are the most abundant cell type in the arterial vessel wall, and play a key role in regulating atherosclerotic plaque formation and VC (27). In response to ERS, VSMCs differentiate into calcified vascular cells through multiple mechanisms, including osteogenic differentiation (28), apoptosis (29), autophagy induction (30), cellular senescence (31), and oxidative stress (32). Many of these processes also occur with bone formation. Importantly, ERS and the UPR are crucial for bone development. All three branches of the UPR are activated during bone formation to regulate the expression of osteogenic genes. ERS is strongly associated with VC, particularly in VSMCs (**Figure 2**; 33, 34).

Endoplasmic Reticulum Stress Promotes Osteogenic Differentiation of Vascular Smooth Muscle Cells

The process of VC involves vascular cells, mainly VSMCs, undergoing osteogenic processes that resemble osteoblast formation, such as osteogenic differentiation, matrix maturation, and matrix mineralization stages. The osteogenic differentiation of VSMCs induced by ERS plays an important role in VC development. This is supported by studies demonstrating that ERS can promote osteogenic differentiation of VSMCs through three pathways, namely IRE1-XBP1, PERK-eIF2α-ATF4, and ATF6. Downregulation of the expression of genes involved in the UPR, including *HSPA5*, *XBP1*, *ATF4*, *DDIT3*, and *ATF6*, has been shown to suppress osteogenic gene expression and mineralization of VSMCs (35). Runx2 is a key transcription factor involved in osteoblast differentiation and its expression can be directly regulated by XBP1 (36). ATF4 is a key transcription factor involved in osteoblastogenesis and ERS-induced apoptosis. Notably, ATF4 deficiency has been reported to inhibits osteogenic differentiation and calcification of VSMCs, both *in vitro* and *in vivo* (37, 38).

Endoplasmic Reticulum Stress Promotes Vascular Smooth Muscle Cell Apoptosis

Apoptosis is closely related to calcification. Calcified VSMCs are prone to apoptosis, and apoptosis can in turn promote calcification. VSMC apoptosis provides a suitable microenvironment for the nucleation of hydroxyapatite crystals, which play a key role in the initiation of VC. Moreover, VSMC apoptosis directly affects the morphology and structure of advanced atherosclerosis and plaque stability (39). VSMC apoptosis process can be activated by ERS through three apoptotic pathways: the IRE1α-ASK-JNK, PERK-eIF2α-CHOP signaling, and caspase-12 pathways. CHOP, an ERS-specific transcription factor, is activated by the PERK-eIF2α-ATF4 pathway and induces apoptosis by decreasing the expression of the anti-apoptotic protein, B-cell lymphoma 2. Shiozaki et al. found that transgenic mice with SMC-specific CHOP expression develop severe vascular apoptosis and medial calcification with CKD (40). They further demonstrated that the cyclin-dependent kinase 9 (CDK9)-cyclin T1 complex mediates VC through CHOP induction and phosphorylation-mediated ATF4 activation. Caspase-12, activated exclusively by ERS, activates caspase-9 directly, which subsequently activates caspase-3, resulting in apoptosis (41). Shi et al. found that the metabolic hormone fibroblast growth factor 21 (FGF21) inhibits VC progression by alleviating ERS-mediated apoptosis in rats. The caspase-12 pathway, but not the phospho-JNK-JNK pathway, is involved in FGF21 expression (34). Moreover, expression levels of JNK, which plays a key role in cell differentiation, inflammation, and apoptosis, did not change with ERS-induced apoptosis in a rat model of periodontitis and VC (42). Therefore, the role of the IRE1α-ASK-JNK pathway in VC development needs further investigation.

Crosstalk Between Endoplasmic Reticulum Stress and Autophagy in Vascular Smooth Muscle Cells

Autophagy is a catabolic and tightly regulated subcellular process in which long-lived proteins and damaged organelles are degraded by lysosomes. Autophagy can regulate endothelial cell homeostasis, VSMC phenotype transition, and Ca^{2+} homeostasis in VSMCs (2). Emerging evidence has demonstrated that autophagy directly protects against VC. Morciano et al. found that the autophagy and mitochondrial phagocytosis levels of caveolins increased and that rapamycin can enhance the calcification phenotype by promoting autophagy *in vitro* (43). In addition, crosstalk among endosomes, dysfunctional mitochondria, autophagic vesicles, and Ca^{2+}- and Pi-enriched matrix vesicles (MVs) may underlie the pathogenesis of VC. Autophagy is an adaptive response that protects against phosphate-induced VSMC calcification by regulating apoptosis and releasing mineralizing MVs from VSMCs (44–46). Moreover, autophagosomes are formed by shedding the double-layer membrane of the ribosome free attachment area of the rough ER and wrapping some cytoplasmic and intracellular organelles, proteins, and other components that need to be degraded. Therefore, the ER plays an indispensable role in autophagy regulation. ERS activates autophagy through the UPR and calcium-mediated signaling cascade pathway. However, the associations of ERS, autophagy, and VC remain poorly understood. Furmanik et al. reported that ERS mediates VSMC calcification *via* increased release of extracellular vesicles, induced by increased expression of GRP78 and ATF4 (47).

TABLE 1 | Reference table to the specific cell type, signaling pathway leading to ERS, and the mechanism of VCd LDL.

Specific cell-type	Pathway	Biological effect	References
Vascular smooth muscle cell	IRE1	Osteogenic differentiation	(36)
	ATF4	Osteogenic differentiation	(37, 38)
		VSMC apoptosis	(40)
		VSMC autophagy	(47)
	ATF6	Osteogenic differentiation	(35)
	Caspase-12	VSMC apoptosis	(41)
	Matrix vesicles (MVs)	VSMC autophagy	(48, 49)
VEC	IRE1-EndMT	Osteogenic differentiation	(58)
	IRE1	VEC apoptosis	(65)
	ATF6	VEC apoptosis	(66)
Macrophages	ATF4	Macrophage-derived foam cell formation and apoptosis	(80)
	ATF6, p-IRE1α	Alleviated inflammation of macrophages	(94)
Inflammasomes	ATF4	Subsequent inflammation triggered by NLRP3	(87)

However, another study on VC revealed that autophagy results in the release of MVs, which attract inflammatory cells and induce VC (48, 49). Therefore, further studies of the mechanisms linking ERS and autophagy in VSMCs are warranted.

Endoplasmic Reticulum Stress in Vascular Endothelial Cells

Vascular endothelial cells, which form a biological barrier that controls the passage of immune cells and biomolecules between the vascular walls and mediates physiological functions, are the main components of the vascular intima. During homeostatic conditions, endothelial cells maintain microvascular integrity and exert vasodilatory, anti-inflammatory, and antithrombotic activities (50). However, under various pathological conditions, these biological functions become compromised (51) and may lead to VC through osteogenic differentiation, endothelial microparticles, or cytokines. ERS plays an important role in these changes primarily by inducing osteogenic differentiation and apoptosis of VECs (**Figure 3**).

Endoplasmic Reticulum Stress Promotes Osteogenic Differentiation of Vascular Endothelial Cells

Similar to VSMCs, VECs promote VC by inducing osteogenic differentiation (52). Changes in VEC physiological homeostasis promotes osteoblastic differentiation *via* the extracellular signal-regulated protein kinase 1/2 and nuclear factor kappa B (NF-κB) signaling pathways, leading to VC (53). Moreover, studies have substantiated that endothelial-to-mesenchymal transition (EndMT) plays a critical role in the osteogenic differentiation of VECs (54–56). EndMT is a process through which endothelial lineage cells lose cell polarity, acquire migratory and aggressive characteristics, and differentiate into mesenchymal stem cells. Moreover, the EndMT gives VECs the potential for osteogenesis differentiation in different physiological states. Yao et al. found that reducing the EndMT by knocking out serine protease or Sox2 in *in vitro* experiments improves VC (57). EndMT occurs when endothelial cells acquire mesenchymal and stem-cell-like characteristics and is closely related to ERS (58, 59). ERS can aggravate EndMT *via* the IRE1α-XBP1 axis and thereby contribute to VC (58).

Endoplasmic Reticulum Stress Promotes Vascular Endothelial Cell Apoptosis

Apoptosis of endothelial cells plays a pivotal role in the development of VC. Increased endothelial cell apoptosis has been observed in the atherosclerosis-prone regions of the vasculature (60) and in the endothelium of human atherosclerotic plaques (61). Under homeostatic conditions, clearance of apoptotic cells occurs in the absence of immune activation and is mediated by various phagocytic cells (7, 62). However, dysregulation of apoptotic cell clearance can lead to secondary necrosis and release of proinflammatory intracellular contents (62). Moreover, this can promote the development of chronic inflammatory diseases, such as atherosclerosis (63). ERS-induced VEC apoptosis plays an important role in the pathogenesis and development of several vascular diseases (64, 65). Recent studies have demonstrated that high expression of active ATF6 may exacerbate VEC apoptosis through the mitochondrial apoptotic pathway (66). Similarly, the activation of IRE1α may enhance VEC apoptosis *via* the pro-apoptotic molecule JNK and the p38-mitogen-activated protein kinase pathway (65). Furthermore, VEC apoptosis changes the balance between pro-apoptotic and anti-apoptotic proteins of the Bcl-2 family, leading to VC (67).

Endoplasmic Reticulum Stress and Inflammation

Vascular calcification is associated with the development of chronic inflammation, as inflammatory cell infiltration has been detected in all stages of VC (68–71). Therefore, in addition to VSMCs and VECs, VC therapeutic strategies targeting inflammation warrant further investigation. ERS is associated with various pathological conditions linked to chronic inflammation (72, 73). Studies indicate that ERS can trigger inflammatory pathways and proinflammatory stimuli, such as Toll-like receptor ligands, reactive oxygen species, and cytokines. These proinflammatory signals can then initiate ERS and result in UPR activation, which further amplifies inflammatory

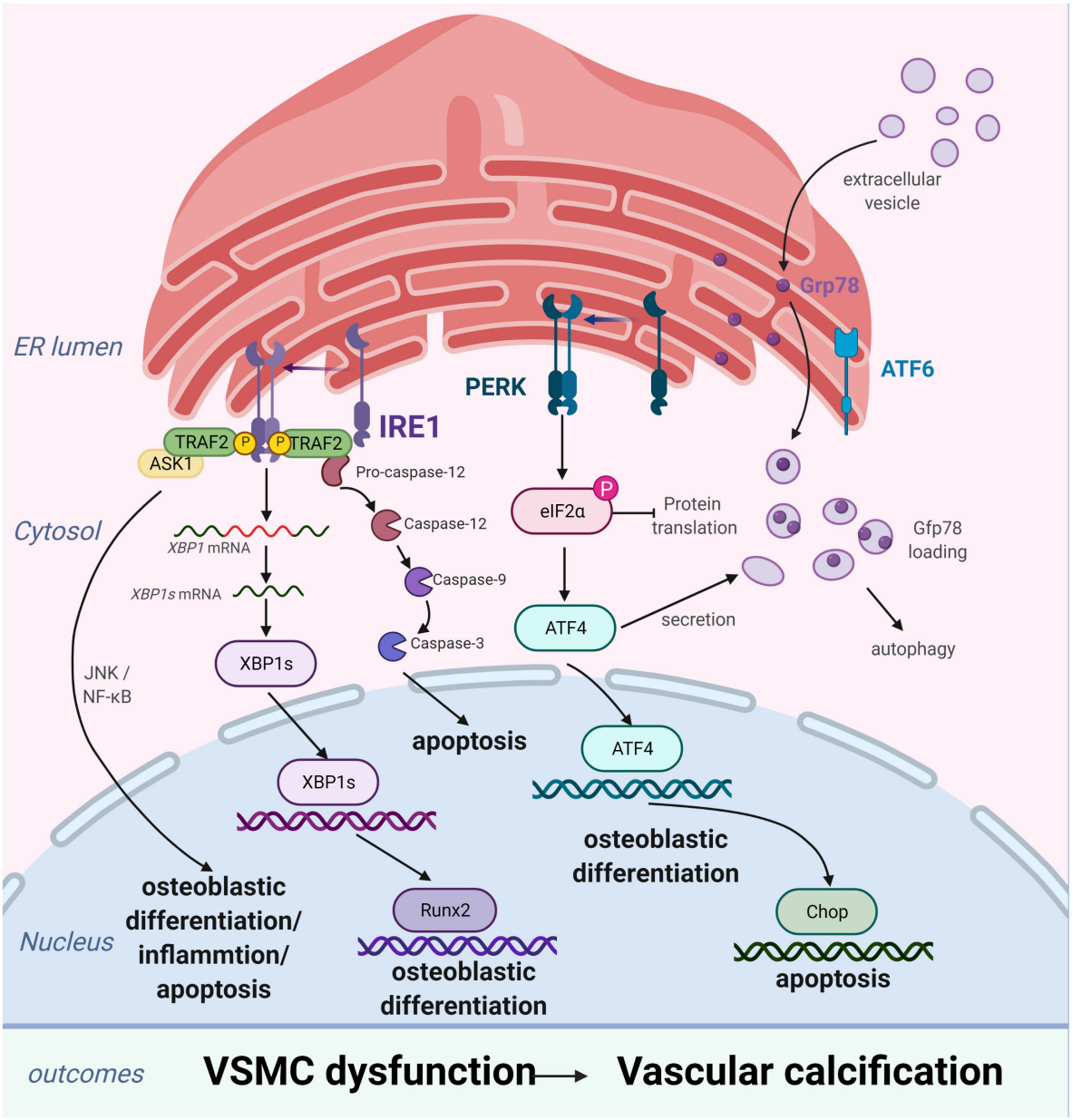

FIGURE 2 | Endoplasmic reticulum stress (ERS) promotes vascular calcification (VC) by inducing the osteogenic differentiation, autophagy, and apoptosis of vascular smooth muscle cells (VSMCs). In response to ERS, VSMCs differentiate into calcifying VSMCs *via* multiple mechanisms, including osteogenic differentiation, apoptosis, and autophagy. Inositol-requiring enzyme 1 (IRE1) can promote osteoblastic differentiation *via* nuclear factor kappa B (NF-κB), the IRE1α-XBP1 axis, and RUNX2 signaling pathways and aggravate apoptosis by the IRE1α-ASK-JNK and caspase-12 pathways. PKR-like ER kinase (PERK) induces apoptosis *via* the PERK-eIF2α-CHOP signaling pathway and osteogenic differentiation *via* ATF4 activation. Extracellular vesicles, induced by increased expression of Grp78 and ATF4, attract inflammatory cells and induce VC. Figures were created using BioRender.com.

responses (74). Collectively, these processes increase the chances of developing VC (75).

Endoplasmic Reticulum Stress in Macrophages

Macrophages are central effectors of innate immunity and play a crucial role in VC development. Studies have shown that activated macrophages contribute to VC by differentiating into osteoclasts (76) and secreting inflammatory factors (77). ERS induces an inflammatory response in macrophages *via* IRE1α-XBP1 (78) and PERK-ATF4 (79). Yao et al. found that D4F, an apoA-I mimetic peptide, can alleviate macrophage-derived foam cell formation and apoptosis by inhibiting CD36-mediated ox-LDL uptake and subsequent activation of the ERS-CHOP pathway (80). Ren et al. found that intermedin1-53, a cardiovascular protective peptide, protects against homocysteine-promoted atherosclerotic calcification in

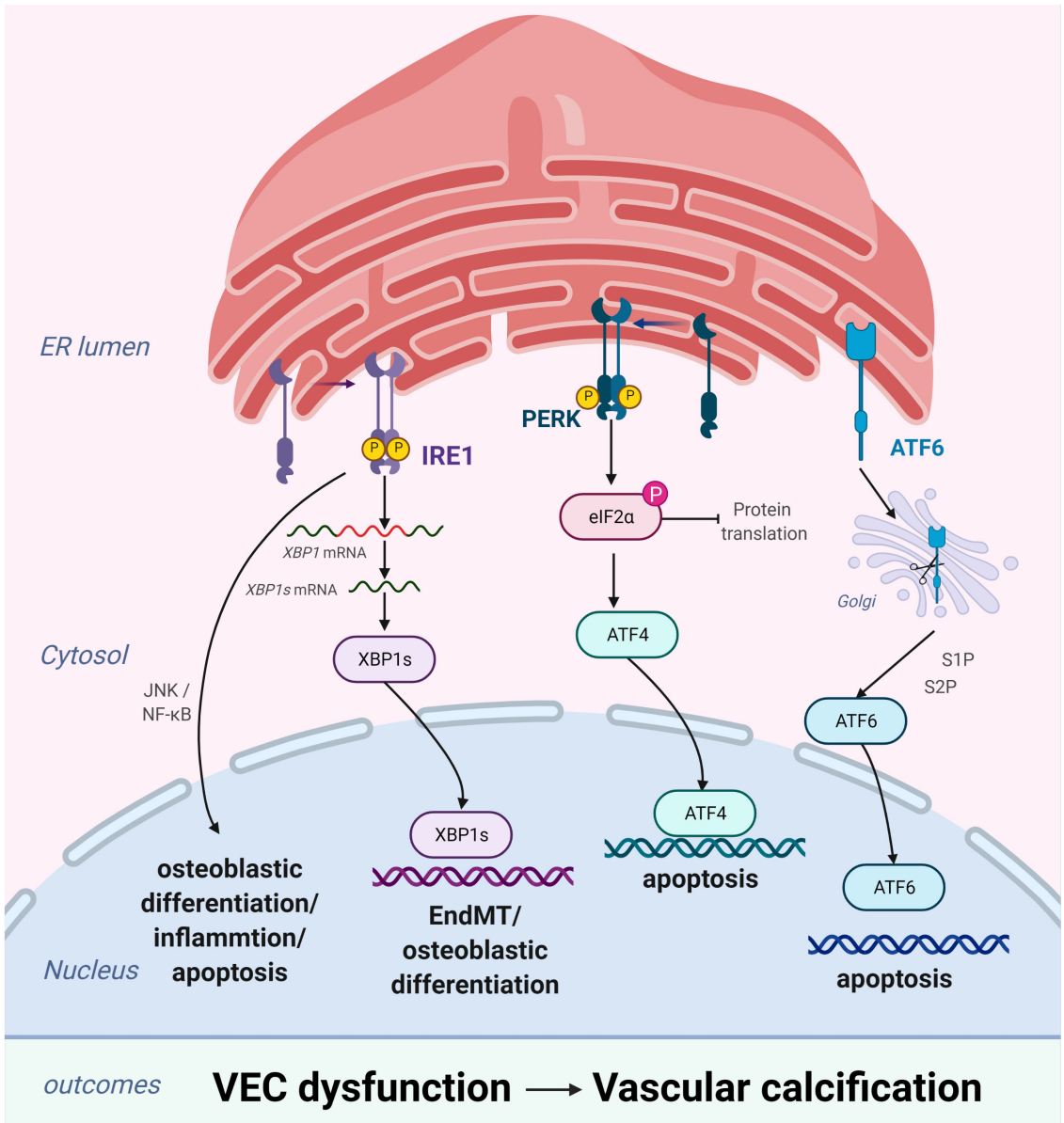

FIGURE 3 | Endoplasmic reticulum stress (ERS) promotes vascular calcification (VC) by inducing the osteogenic differentiation and apoptosis of vascular endothelial cells (VECs). In response to ERS, inositol-requiring enzyme 1 (IRE1) can aggravate EndMT through the IRE1α-XBP1 axis, promote osteoblastic differentiation *via* the nuclear factor kappa B (NF-κB) signaling pathway and the IRE1α-XBP1 axis, and induce apoptosis *via* the IRE1α-ASK-JNK pathway. PKR-like ER kinase (PERK) promotes apoptosis *via* the PERK-eIF2α-ATF4 signaling pathway. High expression of active ATF6 may exacerbate VEC apoptosis through the mitochondrial apoptotic pathway. Figures were created using BioRender.com.

ApoE$^{-/-}$ mice by inhibiting ERS markers in rat VSMCs and mouse peritoneal macrophages (81). Further investigation is needed to better understand the role of ERS in macrophage-induced VC.

Endoplasmic Reticulum Stress and Inflammasomes

The NACHT, LRR, and PYD domains-containing protein 3 (NLRP3) inflammasome is an essential component of the innate immune system and can induce the secretion of the proinflammatory cytokine interleukin 1 beta (IL-1β) in a caspase-1-dependent manner (82, 83). Moreover, IL-1β can activate the secretion of the receptor activator of NF-κB ligand, which promotes the formation of osteoclasts, leading to VC (84, 85). ERS stimulates the NLRP3 inflammasome activation through oxidative stress, NF-κB activation, and calcium homeostasis (86). Ren et al. found that intermedin may attenuate the progression of atherosclerotic lesions and plaque susceptibility by inhibiting ERS-CHOP-mediated macrophage apoptosis and subsequent inflammation triggered by NLRP3 both *in vivo* and *in vitro* (87). Therefore, further studies are needed to elucidate

the mechanisms of ERS-mediated and NLRP3 inflammasome-mediated VC.

ENDOPLASMIC RETICULUM STRESS-MEDIATED REGULATION OF VASCULAR CALCIFICATION IN DISEASES

It is important to identify effective treatments for the globally prevalent metabolic disorders, such as aging, CKD, diabetes, and atherosclerosis-related VC (88). However, no effective clinical therapy is currently available. ERS is a key feature of metabolic disorders. Hence, herein we aim to identify new therapeutic targets for the treatment of VC by discussing the effects of ERS in different diseases.

Chronic Kidney Disease

Although there have been recent improvements in the systemic management of CKD, cardiovascular disease remains a leading cause of death in patients with CKD (89, 90). VC is a common complication in patients with CKD and is associated with increased cardiovascular disease-related mortality. Recent evidence suggests that ERS is the primary cause of VC in CKD *via* several pathways. Tumor necrosis factor α induces the PERK-eIF2α-ATF4-CHOP axis of the ERS response, leading to CKD-associated VC (91). Other positive regulators of the PERK-eIF2α-ATF4-CHOP axis of the ERS response in VSMCs include high phosphate levels, oxidized lipids, *BMP2*, and basic fibroblast growth factor (92, 93). Furthermore, oxysterol accumulation in the ER induces ERS and activates CKD-dependent VC *via* the PERK-eIF2α-ATF4-CHOP pathway. Oxysterol-mediated ERS can be reduced by ezetimibe-simvastatin combination therapy, thereby attenuating CKD-dependent vascular diseases (94). In addition, ATF4 activity, which is activated by the CDK9-cyclin T1 complex during ERS, can lead to VC in CKD. Moreover, inhibition of the cyclin T1-CDK9-CHOP pathway may decrease ERS-induced CHOP expression and CKD-dependent VC (40).

Atherosclerosis

Atherosclerosis is a chronic inflammatory disease characterized by the progressive accumulation of lipids and plaques in arteries (95). Pathological conditions, such as inflammation, oxidized lipids, and metabolic stress, can activate ERS (96, 97). The UPR is chronically activated in atherosclerotic lesion cells, particularly advanced lesional macrophages, and endothelial cells. Tabas found that ERS is a significant cause of apoptosis of endothelial cells and macrophages in advanced lesions (60). In addition, Oh et al. reported that suppression of macrophage ERS can lead to polarization of differentiated M2 macrophages toward an M1 phenotype and can subsequently suppressed foam cell formation (98). Furthermore, intermedin1-53 protects against homocysteine-related atherosclerotic calcification in Apoe$^{-/-}$ mice by inhibiting ERS (81). These studies indicate that ERS plays a significant role in atherosclerosis and that inhibiting ERS can alleviate the pathological damage associated with atherosclerotic calcification.

Diabetes

Despite improvements in CVD treatment over the past few decades, diabetes remains a significantly independent cardiovascular risk factor (61, 99). Therefore, reducing adverse events caused by diabetes-induced CVD is a clinical challenge (100). Diabetes-related VC presents with disturbed vessel wall homeostasis, endothelial dysfunction, and phenotypic switching of VSMCs (101–103). High glucose levels trigger apoptosis and phenotypic transformation of VSMCs (in the presence of ERS). In addition, compared with continued high glucose conditions, increased glycemic variability is more strongly associated with VC (104). Chronic exposure of VSMCs to high glucose conditions can exacerbate inflammation and calcification through the induction of CD36 scavenger receptors (71). Moreover, CD36 signaling may contribute to diabetic atherosclerosis *via* ERS induction. Collectively, these findings suggest that ERS crucially contributes to diabetes; however, further investigation is warranted.

CURRENT CLINICAL TRIALS ASSESSING ENDOPLASMIC RETICULUM STRESS-RELATED VASCULAR CALCIFICATION TREATMENT

Endoplasmic reticulum stress plays a key pathological role in promoting the occurrence and development of CVDs. Over

TABLE 2 | Table summarizing ERS blockade attempt in diseases and their main outcome on VC.

Blockade	Main outcome on VC	References
IMD1-53	Attenuates VSMC calcification in rats by inhibiting ERS through cAMP/PKA signaling	(105)
Sodium selenite	Suppresses apoptosis of calcifying VSMCs by inhibiting oxidative-stress-activated ERS	(106)
Cyclin T2 and cyclin K	Decreases ERS-induced CHOP expression and CKD-dependent VC	(40)
Spermidine	Ameliorates VSMC calcification through sirtuin 1-mediated inhibition of ERS	(109)
Stellate ganglion block (SGB)	Prevents the activation of ERS by inhibiting the sympathetic nervous system to regulate vascular dilation	(110)
Fibroblast growth factor 21 (FGF21)	Inhibits the progress of VC by alleviating ERS mediated apoptosis in rats	(34)
Death-associated protein kinase 3 (DAPK3)	Regulates VSMC calcification *via* AMPK-mediated ERS signaling	(111)
Ezetimibe-simvastatin	Attenuates CKD-dependent vascular diseases	(99)

the past few decades, research has focused on the signaling proteins involved in ERS, resulting in the development of an increasing array of drugs (**Table 2**). This section aims to explain the fundamentals, value, and limitations of existing drugs targeting ERS.

Intermedin1-53, a paracrine/autocrine peptide in the vasculature, attenuates VSMC calcification in rats by inhibiting ERS through cyclic adenosine monophosphate-protein kinase A signaling (105). Sodium selenite may suppress apoptosis of calcifying VSMCs, in part, by inhibiting oxidative-stress-activated ERS (106). The CDK9-cyclin T1 complex, an essential component in ERS, mediates pro-apoptotic CHOP expression and VC by activating ATF4. Cyclin T2 and cyclin K inhibit CHOP induction by competitively binding CDK9. Hence, inhibition of the cyclin T1/CDK9-CHOP pathway may be a potential therapeutic strategy for VC treatment (107). Spermidine, an endogenously synthesized polyamine, has been shown to protect against CVD and extend lifespan (108). VSMC calcification has recently been shown to be ameliorated through sirtuin 1-mediated inhibition of ERS (109). Stellate ganglion block, which regulates vascular dilation through sympathetic blockade, is used to treat several CVDs. Recently, stellate ganglion block has been shown to prevent the activation of ERS by inhibiting sympathetic nervous activity (110). For the first time, FGF21 has been shown to reduce ERS-mediated VC progression in rats. Some studies suggest that FGF21 has the potential to regulate many metabolic diseases and CVDs because of its pleiotropic biological effects. Thus, FGF21 is a promising new therapeutic target for preventing and treating VC (34). Death-associated protein kinase 3 is involved in hypertension-related vascular remodeling and has been shown to regulate VSMC calcification *via* AMPK-mediated ERS signaling (111). Although these studies provide important translational insights into ERS-targeted prevention of VC, they present only basic experiments and therefore, clinical studies are needed. Notably, inappropriate alteration of ERS may also cause harm, as it is a key mechanism in body maintenance. Hence, the safety of ERS inhibitors requires further evaluation prior to their clinical application.

CONCLUSION AND PERSPECTIVE

Despite various clinical prevention strategies, CVD remains a common complication of aging, atherosclerosis, hypertension, diabetes, and CKD. Accumulating evidence indicates that ERS can regulate the development of VC by promoting osteogenic transformation, inflammation, autophagy, and apoptosis, and by increasing the UPR. Although these studies comprehensively demonstrate that ERS inhibitors can ameliorate VC, they all have certain limitations. That is, most of these studies conducted basic experiments that did not fully nor accurately reflect the pathological changes in human diseases. Additionally, considering that the ERS-UPR pathway is ubiquitous in humans and sensitive to external stimuli, the repression of excessive ERS can promote cellular damage and lead to increased disease progression. Therefore, clinical trials are needed to validate the results of these studies; this may aid in the development of new therapies for VC.

AUTHOR CONTRIBUTIONS

ZR, LX, YDZ, ZW, YZ, MC, ND, ZC, and FL: conceptualization. All authors writing-original draft preparation, editing, and revising. FL and ZC: supervision.

FUNDING

This work was supported by funding from the National Natural Science Foundation of China (82170377 and 81974034).

REFERENCES

1. Shanahan CM, Crouthamel MH, Kapustin A, Giachelli CM. Arterial calcification in chronic kidney disease: key roles for calcium and phosphate. *Circ Res.* (2011) 109:697–711. doi: 10.1161/CIRCRESAHA.110.234914
2. Phadwal K, Feng D, Zhu D, MacRae VE. Autophagy as a novel therapeutic target in vascular calcification. *Pharmacol Ther.* (2020) 206:107430. doi: 10.1016/j.pharmthera.2019.107430
3. Amann K. Media calcification and intima calcification are distinct entities in chronic kidney disease. *Clin J Am Soc Nephrol.* (2008) 3:1599–605. doi: 10.2215/CJN.02120508
4. Chen Y, Zhao X, Wu H. Arterial stiffness: a focus on vascular calcification and its link to bone mineralization. *Arterioscler Thromb Vasc Biol.* (2020) 40:1078–93. doi: 10.1161/ATVBAHA.120.313131
5. Wang M, Kaufman RJ. Protein misfolding in the endoplasmic reticulum as a conduit to human disease. *Nature.* (2016) 529:7586. doi: 10.1038/nature17041
6. Braakman I, Hebert DN. Protein folding in the endoplasmic reticulum. *Cold Spring Harb Perspect Biol.* (2013) 5:a013201. doi: 10.1101/cshperspect.a013201
7. Malhotra JD, Kaufman RJ. The endoplasmic reticulum and the unfolded protein response. *Semin Cell Dev Biol.* (2007) 18:716–31. doi: 10.1016/j.semcdb.2007.09.003
8. Hassler J, Cao SS, Kaufman RJ. IRE1, a double-edged sword in pre-miRNA slicing and cell death. *Dev Cell.* (2012) 23:921–3. doi: 10.1016/j.devcel.2012.10.025
9. Shamu CE, Walter P. Oligomerization and phosphorylation of the Ire1p kinase during intracellular signaling from the endoplasmic reticulum to the nucleus. *EMBO J.* (1996) 15:3028–39.
10. Tringali G, Mancuso C, Mirtella A, Pozzoli G, Parente L, Preziosi P, et al. Evidence for the neuronal origin of immunoreactive interleukin-1 beta released by rat hypothalamic explants. *Neurosci Lett.* (1996) 219:143–6. doi: 10.1016/s0304-3940(96)13195-5
11. Korennykh AV, Korostelev AA, Egea PF, Finer-Moore J, Stroud RM, Zhang C, et al. Structural and functional basis for RNA cleavage by Ire1. *BMC Biol.* (2011) 9:47. doi: 10.1186/1741-7007-9-47
12. Walter P, Ron D. The unfolded protein response: from stress pathway to homeostatic regulation. *Science.* (2011) 334:1081–6. doi: 10.1126/science.1209038
13. Sano R, Reed JC. ER stress-induced cell death mechanisms. *Biochim Biophys Acta.* (2013) 1833:3460–70. doi: 10.1016/j.bbamcr.2013.06.028
14. Shen J, Chen X, Hendershot L, Prywes R. ER stress regulation of ATF6 localization by dissociation of BiP/GRP78 binding and unmasking of Golgi localization signals. *Dev Cell.* (2002) 3:99–111. doi: 10.1016/s1534-5807(02)00203-4

15. Hetz C. The unfolded protein response: controlling cell fate decisions under ER stress and beyond. *Nat Rev Mol Cell Biol.* (2012) 13:89–102. doi: 10.1038/nrm3270
16. Brewer JW. Regulatory crosstalk within the mammalian unfolded protein response. *Cell Mol Life Sci.* (2014) 71:1067–79. doi: 10.1007/s00018-013-1490-2
17. Chen X, Shen J, Prywes R. The luminal domain of ATF6 senses endoplasmic reticulum (ER) stress and causes translocation of ATF6 from the ER to the Golgi. *J Biol Chem.* (2002) 277:13045–52. doi: 10.1074/jbc.M110636200
18. Ye J, Rawson RB, Komuro R, Chen X, Davé UP, Prywes R, et al. ER stress induces cleavage of membrane-bound ATF6 by the same proteases that process SREBPs. *Mol Cell.* (2000) 6:1355–64. doi: 10.1016/s1097-2765(00)00133-7
19. Duer MJ, Friscić T, Proudfoot D, Reid DG, Schoppet M, Shanahan CM, et al. Mineral surface in calcified plaque is like that of bone: further evidence for regulated mineralization. *Arterioscler Thromb Vasc Biol.* (2008) 28:2030–4. doi: 10.1161/atvbaha.108.172387
20. Rennenberg RJ, Kessels AG, Schurgers LJ, van Engelshoven JM, de Leeuw PW, Kroon AA. Vascular calcifications as a marker of increased cardiovascular risk: a meta-analysis. *Vasc Health Risk Manage.* (2009) 5:185–97. doi: 10.2147/vhrm.s4822
21. Jing L, Li L, Sun Z, Bao Z, Shao C, Yan J, et al. Role of matrix vesicles in bone-vascular cross-talk. *J Cardiovasc Pharmacol.* (2019) 74:372–8. doi: 10.1097/FJC.0000000000000720
22. Pescatore LA, Gamarra LF, Liberman M. Multifaceted mechanisms of vascular calcification in aging. *Arterioscler Thromb Vasc Biol.* (2019) 39:1307–16. doi: 10.1161/ATVBAHA.118.311576
23. Steitz SA, Speer MY, Curinga G, Yang HY, Haynes P, Aebersold R, et al. Smooth muscle cell phenotypic transition associated with calcification: upregulation of Cbfa1 and downregulation of smooth muscle lineage markers. *Circ Res.* (2001) 89:1147–54. doi: 10.1161/hh2401.101070
24. Abbasian N. Vascular calcification mechanisms: updates and renewed insight into signaling pathways involved in high phosphate-mediated vascular smooth muscle cell calcification. *Biomedicines.* (2021) 9:804. doi: 10.3390/biomedicines9070804
25. Li T, Yu H, Zhang D, Feng T, Miao M, Li J, et al. Matrix vesicles as a therapeutic target for vascular calcification. *Front Cell Dev Biol.* (2022) 10:825622. doi: 10.3389/fcell.2022.825622
26. Lee SJ, Lee IK, Jeon JH. Vascular calcification-new insights into its mechanism. *Int J Mol Sci.* (2020) 21:2685. doi: 10.3390/ijms21082685
27. Ma WQ, Sun XJ, Zhu Y, Liu NF. PDK4 promotes vascular calcification by interfering with autophagic activity and metabolic reprogramming. *Cell Death Dis.* (2020) 11:991. doi: 10.1038/s41419-020-03162-w
28. Durham AL, Speer MY, Scatena M, Giachelli CM, Shanahan CM. Role of smooth muscle cells in vascular calcification: implications in atherosclerosis and arterial stiffness. *Cardiovasc Res.* (2018) 114:590–600. doi: 10.1093/cvr/cvy010
29. Grootaert MOJ, Moulis M, Roth L, Martinet W, Vindis C, Bennett MR, et al. Vascular smooth muscle cell death, autophagy and senescence in atherosclerosis. *Cardiovasc Res.* (2018) 114:622–34. doi: 10.1093/cvr/cvy007
30. Dong Y, Chen H, Gao J, Liu Y, Li J, Wang J. Molecular machinery and interplay of apoptosis and autophagy in coronary heart disease. *J Mol Cell Cardiol.* (2019) 136:27–41. doi: 10.1016/j.yjmcc.2019.09.001
31. Shi J, Yang Y, Cheng A, Xu G, He F. Metabolism of vascular smooth muscle cells in vascular diseases. *Am J Physiol Heart Circ Physiol.* (2020) 319:H613–31. doi: 10.1152/ajpheart.00220.2020
32. Basatemur GL, Jørgensen HF, Clarke MCH, Bennett MR, Mallat Z. Vascular smooth muscle cells in atherosclerosis. *Nat Rev Cardiol.* (2019) 16:727–44. doi: 10.1038/s41569-019-0227-9
33. Dong Q, Chen Y, Liu W, Liu X, Chen A, Yang X, et al. 25-Hydroxycholesterol promotes vascular calcification via activation of endoplasmic reticulum stress. *Eur J Pharmacol.* (2020) 880:173165. doi: 10.1016/j.ejphar.2020.173165
34. Shi Y, Wang S, Peng H, Lv Y, Li W, Cheng S, et al. Fibroblast growth factor 21 attenuates vascular calcification by alleviating endoplasmic reticulum stress mediated apoptosis in rats. *Int J Biol Sci.* (2019) 15:138–47. doi: 10.7150/ijbs.28873
35. Duangchan T, Tawonsawatruk T, Angsanuntsukh C, Trachoo O, Hongeng S, Kitiyanant N, et al. Amelioration of osteogenesis in iPSC-derived mesenchymal stem cells from osteogenesis imperfecta patients by endoplasmic reticulum stress inhibitor. *Life Sci.* (2021) 278:119628. doi: 10.1016/j.lfs.2021.119628
36. Liberman M, Johnson RC, Handy DE, Loscalzo J, Leopold JA. Bone morphogenetic protein-2 activates NADPH oxidase to increase endoplasmic reticulum stress and human coronary artery smooth muscle cell calcification. *Biochem Biophys Res Commun.* (2011) 413:436–41. doi: 10.1016/j.bbrc.2011.08.114
37. Masuda M, Miyazaki-Anzai S, Keenan AL, Shiozaki Y, Okamura K, Chick WS, et al. Activating transcription factor-4 promotes mineralization in vascular smooth muscle cells. *JCI Insight.* (2016) 1:e88646. doi: 10.1172/jci.insight.88646
38. Duan XH, Chang JR, Zhang J, Zhang BH, Li YL, Teng X, et al. Activating transcription factor 4 is involved in endoplasmic reticulum stress-mediated apoptosis contributing to vascular calcification. *Apoptosis.* (2013) 18:1132–44. doi: 10.1007/s10495-013-0861-3
39. Zeini M, Lopez-Fontal R, Traves PG, Benito G, Hortelano S. Differential sensitivity to apoptosis among the cells that contribute to the atherosclerotic disease. *Biochem Biophys Res Commun.* (2007) 363:444–50. doi: 10.1016/j.bbrc.2007.09.004
40. Shiozaki Y, Okamura K, Kohno S, Keenan AL, Williams K, Zhao X, et al. The CDK9-cyclin T1 complex mediates saturated fatty acid-induced vascular calcification by inducing expression of the transcription factor CHOP. *J Biol Chem.* (2018) 293:17008–20. doi: 10.1074/jbc.RA118.004706
41. Garcia de la Cadena S, Massieu L. Caspases and their role in inflammation and ischemic neuronal death. Focus on caspase-12. *Apoptosis.* (2016) 21:763–77. doi: 10.1007/s10495-016-1247-0
42. Song X, Li J, Jiao M, Chen Y, Pan K. Effect of endoplasmic reticulum stress-induced apoptosis in the role of periodontitis on vascular calcification in a rat model. *J Mol Histol.* (2021) 52:1097–104. doi: 10.1007/s10735-021-10015-z
43. Morciano G, Patergnani S, Pedriali G, Cimaglia P, Mikus E, Calvi S, et al. Impairment of mitophagy and autophagy accompanies calcific aortic valve stenosis favoring cell death and the severity of disease. *Cardiovasc Res.* (2021). [Epub ahead of print]. doi: 10.1093/cvr/cvab267
44. Pi S, Mao L, Chen J, Shi H, Liu Y, Guo X, et al. The P2RY12 receptor promotes VSMC-derived foam cell formation by inhibiting autophagy in advanced atherosclerosis. *Autophagy.* (2021) 17:980–1000. doi: 10.1080/15548627.2020.1741202
45. Smith M, Wilkinson S. ER homeostasis and autophagy. *Essays Biochem.* (2017) 61:625–35. doi: 10.1042/EBC20170092
46. Zhao Y, Zhao MM, Cai Y, Zheng MF, Sun WL, Zhang SY, et al. Mammalian target of rapamycin signaling inhibition ameliorates vascular calcification via Klotho upregulation. *Kidney Int.* (2015) 88:711–21. doi: 10.1038/ki.2015.160
47. Furmanik M, van Gorp R, Whitehead M, Ahmad S, Bordoloi J, Kapustin A, et al. Endoplasmic reticulum stress mediates vascular smooth muscle cell calcification via increased release of Grp78 (Glucose-regulated protein, 78 kDa)-loaded extracellular vesicles. *Arterioscler Thromb Vasc Biol.* (2021) 41:898–914. doi: 10.1161/atvbaha.120.315506
48. Zazzeroni L, Faggioli G, Pasquinelli G. Mechanisms of arterial calcification: the role of matrix vesicles. *Eur J Vasc Endovasc Surg.* (2018) 55:425–32. doi: 10.1016/j.ejvs.2017.12.009
49. Mizushima N, Komatsu M. Autophagy: renovation of cells and tissues. *Cell.* (2011) 147:728–41. doi: 10.1016/j.cell.2011.10.026
50. Guglielmetti G, Quaglia M, Sainaghi PP, Castello LM, Vaschetto R, Pirisi M, et al. "War to the knife" against thromboinflammation to protect endothelial function of COVID-19 patients. *Crit Care.* (2020) 24:365. doi: 10.1186/s13054-020-03060-9
51. Werner N, Wassmann S, Ahlers P, Kosiol S, Nickenig G. Circulating CD31+/annexin V+ apoptotic microparticles correlate with coronary endothelial function in patients with coronary artery disease. *Arterioscler Thromb Vasc Biol.* (2006) 26:112–6. doi: 10.1161/01.ATV.0000191634.13057.15
52. Cianciolo G, Capelli I, Cappuccilli M, Scrivo A, Donadei C, Marchetti A, et al. Is chronic kidney disease-mineral and bone disorder associated with the presence of endothelial progenitor cells with a calcifying phenotype? *Clin Kidney J.* (2017) 10:389–96. doi: 10.1093/ckj/sfw145
53. Cheng ZY, Ye T, Ling QY, Wu T, Wu GY, Zong GJ. Parathyroid hormone promotes osteoblastic differentiation of endothelial cells via the extracellular

signal-regulated protein kinase 1/2 and nuclear factor-kappaB signaling pathways. *Exp Ther Med.* (2018) 15:1754–60. doi: 10.3892/etm.2017.5545
54. Cheng SL, Shao JS, Behrmann A, Krchma K, Towler DA. Dkk1 and MSX2-Wnt7b signaling reciprocally regulate the endothelial-mesenchymal transition in aortic endothelial cells. *Arterioscler Thromb Vasc Biol.* (2013) 33:1679–89. doi: 10.1161/ATVBAHA.113.300647
55. Bostrom KI, Yao J, Guihard PJ, Blazquez-Medela AM, Yao Y. Endothelial-mesenchymal transition in atherosclerotic lesion calcification. *Atherosclerosis.* (2016) 253:124–7. doi: 10.1016/j.atherosclerosis.2016.08.046
56. Sanchez-Duffhues G, Garcia de Vinuesa A, van de Pol V, Geerts ME, de Vries MR, Janson SG, et al. Inflammation induces endothelial-to-mesenchymal transition and promotes vascular calcification through downregulation of BMPR2. *J Pathol.* (2019) 247:333–46. doi: 10.1002/path.5193
57. Yao J, Guihard PJ, Blazquez-Medela AM, Guo Y, Moon JH, Jumabay M, et al. Serine protease activation essential for endothelial-mesenchymal transition in vascular calcification. *Circ Res.* (2015) 117:758–69. doi: 10.1161/CIRCRESAHA.115.306751
58. Luo R, Li L, Liu X, Yuan Y, Zhu W, Li L, et al. Mesenchymal stem cells alleviate palmitic acid-induced endothelial-to-mesenchymal transition by suppressing endoplasmic reticulum stress. *Am J Physiol Endocrinol Metab.* (2020) 319:E961–80. doi: 10.1152/ajpendo.00155.2020
59. Ying R, Wang XQ, Yang Y, Gu ZJ, Mai JT, Qiu Q, et al. Hydrogen sulfide suppresses endoplasmic reticulum stress-induced endothelial-to-mesenchymal transition through Src pathway. *Life Sci.* (2016) 144:208–17. doi: 10.1016/j.lfs.2015.11.025
60. Tabas I. The role of endoplasmic reticulum stress in the progression of atherosclerosis. *Circ Res.* (2010) 107:839–50. doi: 10.1161/circresaha.110.224766
61. Malmberg K, Yusuf S, Gerstein HC, Brown J, Zhao F, Hunt D, et al. Impact of diabetes on long-term prognosis in patients with unstable angina and non-Q-wave myocardial infarction: results of the OASIS (organization to assess strategies for ischemic syndromes) registry. *Circulation.* (2000) 102:1014–9. doi: 10.1161/01.cir.102.9.1014
62. Poon IK, Hulett MD, Parish CR. Molecular mechanisms of late apoptotic/necrotic cell clearance. *Cell Death Differ.* (2010) 17:381–97. doi: 10.1038/cdd.2009.195
63. Szondy Z, Garabuczi E, Joos G, Tsay GJ, Sarang Z. Impaired clearance of apoptotic cells in chronic inflammatory diseases: therapeutic implications. *Front Immunol.* (2014) 5:354. doi: 10.3389/fimmu.2014.00354
64. Toya SP, Malik AB. Role of endothelial injury in disease mechanisms and contribution of progenitor cells in mediating endothelial repair. *Immunobiology.* (2012) 217:569–80. doi: 10.1016/j.imbio.2011.03.006
65. Legeay S, Fautrat P, Norman JB, Antonova G, Kennard S, Bruder-Nascimento T, et al. Selective deficiency in endothelial PTP1B protects from diabetes and endoplasmic reticulum stress-associated endothelial dysfunction via preventing endothelial cell apoptosis. *Biomed Pharmacother.* (2020) 127:110200. doi: 10.1016/j.biopha.2020.110200
66. Huang J, Wan L, Lu H, Li X. High expression of active ATF6 aggravates endoplasmic reticulum stress-induced vascular endothelial cell apoptosis through the mitochondrial apoptotic pathway. *Mol Med Rep.* (2018) 17:6483–9. doi: 10.3892/mmr.2018.8658
67. Lu CL, Liao MT, Hou YC, Fang YW, Zheng CM, Liu WC, et al. Sirtuin-1 and its relevance in vascular calcification. *Int J Mol Sci.* (2020) 21:1593. doi: 10.3390/ijms21051593
68. Demer LL, Tintut Y. Inflammatory, metabolic, and genetic mechanisms of vascular calcification. *Arterioscler Thromb Vasc Biol.* (2014) 34:715–23. doi: 10.1161/ATVBAHA.113.302070
69. Goody PR, Hosen MR, Christmann D, Niepmann ST, Zietzer A, Adam M, et al. Aortic valve stenosis: from basic mechanisms to novel therapeutic targets. *Arterioscler Thromb Vasc Biol.* (2020) 40:885–900. doi: 10.1161/ATVBAHA.119.313067
70. Chernomordik F, Cercek B, Lio WM, Mihailovic PM, Yano J, Herscovici R, et al. The role of T cells reactive to the cathelicidin antimicrobial peptide LL-37 in acute coronary syndrome and plaque calcification. *Front Immunol.* (2020) 11:575577. doi: 10.3389/fimmu.2020.575577
71. Navas-Madronal M, Castelblanco E, Camacho M, Consegal M, Ramirez-Morros A, Sarrias MR, et al. Role of the scavenger receptor CD36 in accelerated diabetic atherosclerosis. *Int J Mol Sci.* (2020) 21:7360. doi: 10.3390/ijms21197360
72. Bettigole SE, Glimcher LH. Endoplasmic reticulum stress in immunity. *Annu Rev Immunol.* (2015) 33:107–38. doi: 10.1146/annurev-immunol-032414-112116
73. Di Conza G, Ho PC. ER stress responses: an emerging modulator for innate immunity. *Cells.* (2020) 9:695. doi: 10.3390/cells9030695
74. Grootjans J, Kaser A, Kaufman RJ, Blumberg RS. The unfolded protein response in immunity and inflammation. *Nat Rev Immunol.* (2016) 16:469–84. doi: 10.1038/nri.2016.62
75. Bailey KA, Haj FG, Simon SI, Passerini AG. Atherosusceptible shear stress activates endoplasmic reticulum stress to promote endothelial inflammation. *Sci Rep.* (2017) 7:8196. doi: 10.1038/s41598-017-08417-9
76. Byon CH, Sun Y, Chen J, Yuan K, Mao X, Heath JM, et al. Runx2-upregulated receptor activator of nuclear factor kappaB ligand in calcifying smooth muscle cells promotes migration and osteoclastic differentiation of macrophages. *Arterioscler Thromb Vasc Biol.* (2011) 31:1387–96. doi: 10.1161/ATVBAHA.110.222547
77. Buendia P, Montes de Oca A, Madueno JA, Merino A, Martin-Malo A, Aljama P, et al. Endothelial microparticles mediate inflammation-induced vascular calcification. *FASEB J.* (2015) 29:173–81. doi: 10.1096/fj.14-249706
78. Kim S, Joe Y, Kim HJ, Kim YS, Jeong SO, Pae HO, et al. Endoplasmic reticulum stress-induced IRE1alpha activation mediates cross-talk of GSK-3beta and XBP-1 to regulate inflammatory cytokine production. *J Immunol.* (2015) 194:4498–506. doi: 10.4049/jimmunol.1401399
79. Iwasaki Y, Suganami T, Hachiya R, Shirakawa I, Kim-Saijo M, Tanaka M, et al. Activating transcription factor 4 links metabolic stress to interleukin-6 expression in macrophages. *Diabetes.* (2014) 63:152–61. doi: 10.2337/db13-0757
80. Yao S, Tian H, Miao C, Zhang DW, Zhao L, Li Y, et al. D4F alleviates macrophage-derived foam cell apoptosis by inhibiting CD36 expression and ER stress-CHOP pathway. *J Lipid Res.* (2015) 56:836–47. doi: 10.1194/jlr.M055400
81. Ren JL, Hou YL, Ni XQ, Zhu Q, Chen Y, Zhang LS, et al. Intermedin1-53 ameliorates homocysteine-promoted atherosclerotic calcification by inhibiting endoplasmic reticulum stress. *J Cardiovasc Pharmacol Ther.* (2020) 25:251–64. doi: 10.1177/1074248419885633
82. Chen TC, Yen CK, Lu YC, Shi CS, Hsieh RZ, Chang SF, et al. The antagonism of 6-shogaol in high-glucose-activated NLRP3 inflammasome and consequent calcification of human artery smooth muscle cells. *Cell Biosci.* (2020) 10:5. doi: 10.1186/s13578-019-0372-1
83. Schuchardt M, Herrmann J, Henkel C, Babic M, van der Giet M, Tolle M. Long-term treatment of azathioprine in rats induces vessel mineralization. *Biomedicines.* (2021) 9:327. doi: 10.3390/biomedicines9030327
84. Yu C, Zhang C, Kuang Z, Zheng Q. The role of NLRP3 inflammasome activities in bone diseases and vascular calcification. *Inflammation.* (2021) 44:434–49. doi: 10.1007/s10753-020-01357-z
85. Zhang X, Li Y, Yang P, Liu X, Lu L, Chen Y, et al. Trimethylamine-N-Oxide promotes vascular calcification through activation of NLRP3 (Nucleotide-binding domain, leucine-rich-containing family, pyrin domain-containing-3) inflammasome and NF-kappaB (Nuclear Factor kappaB) signals. *Arterioscler Thromb Vasc Biol.* (2020) 40:751–65. doi: 10.1161/ATVBAHA.119.313414
86. Li W, Cao T, Luo C, Cai J, Zhou X, Xiao X, et al. Crosstalk between ER stress, NLRP3 inflammasome, and inflammation. *Appl Microbiol Biotechnol.* (2020) 104:6129–40. doi: 10.1007/s00253-020-10614-y
87. Ren JL, Chen Y, Zhang LS, Zhang YR, Liu SM, Yu YR, et al. Intermedin1-53 attenuates atherosclerotic plaque vulnerability by inhibiting CHOP-mediated apoptosis and inflammasome in macrophages. *Cell Death Dis.* (2021) 12:436. doi: 10.1038/s41419-021-03712-w
88. Poterucha TJ, Goldhaber SZ. Warfarin and vascular calcification. *Am J Med.* (2016) 129:635.e1–4. doi: 10.1016/j.amjmed.2015.11.032
89. Parikh NI, Hwang SJ, Larson MG, Levy D, Fox CS. Chronic kidney disease as a predictor of cardiovascular disease (from the Framingham heart study). *Am J Cardiol.* (2008) 102:47–53. doi: 10.1016/j.amjcard.2008.02.095
90. Go AS, Chertow GM, Fan D, McCulloch CE, Hsu CY. Chronic kidney disease and the risks of death, cardiovascular events, and hospitalization. *N Engl J Med.* (2004) 351:1296–305. doi: 10.1056/NEJMoa041031

91. Masuda M, Miyazaki-Anzai S, Levi M, Ting TC, Miyazaki M. PERK-eIF2α-ATF4-CHOP signaling contributes to TNFα-induced vascular calcification. *J Am Heart Assoc.* (2013) 2:e000238. doi: 10.1161/jaha.113.000238
92. Masuda M, Ting TC, Levi M, Saunders SJ, Miyazaki-Anzai S, Miyazaki M. Activating transcription factor 4 regulates stearate-induced vascular calcification. *J Lipid Res.* (2012) 53:1543–52. doi: 10.1194/jlr.M025981
93. Ting TC, Miyazaki-Anzai S, Masuda M, Levi M, Demer LL, Tintut Y, et al. Increased lipogenesis and stearate accelerate vascular calcification in calcifying vascular cells. *J Biol Chem.* (2011) 286:23938–49. doi: 10.1074/jbc.M111.237065
94. Miyazaki-Anzai S, Masuda M, Demos-Davies KM, Keenan AL, Saunders SJ, Masuda R, et al. Endoplasmic reticulum stress effector CCAAT/enhancer-binding protein homologous protein (CHOP) regulates chronic kidney disease-induced vascular calcification. *J Am Heart Assoc.* (2014) 3:e000949. doi: 10.1161/jaha.114.000949
95. Weber C, Noels H. Atherosclerosis: current pathogenesis and therapeutic options. *Nat Med.* (2011) 17:1410–22. doi: 10.1038/nm.2538
96. Ivanova EA, Orekhov AN. The role of endoplasmic reticulum stress and unfolded protein response in atherosclerosis. *Int J Mol Sci.* (2016) 17:193. doi: 10.3390/ijms17020193
97. Zhang C, Syed TW, Liu R, Yu J. Role of endoplasmic reticulum stress, autophagy, and inflammation in cardiovascular disease. *Front Cardiovasc Med.* (2017) 4:29. doi: 10.3389/fcvm.2017.00029
98. Oh J, Riek AE, Weng S, Petty M, Kim D, Colonna M, et al. Endoplasmic reticulum stress controls M2 macrophage differentiation and foam cell formation. *J Biol Chem.* (2012) 287:11629–41. doi: 10.1074/jbc.M111.338673
99. Mukamal KJ, Nesto RW, Cohen MC, Muller JE, Maclure M, Sherwood JB, et al. Impact of diabetes on long-term survival after acute myocardial infarction: comparability of risk with prior myocardial infarction. *Diabetes Care.* (2001) 24:1422–7. doi: 10.2337/diacare.24.8.1422
100. Barrett H, O'Keeffe M, Kavanagh E, Walsh M, O'Connor EM. Is matrix Gla protein associated with vascular calcification? a systematic review. *Nutrients.* (2018) 10:415. doi: 10.3390/nu10040415
101. Zhu L, Liu J, Gao C, Zhao W, Que J, Wang X, et al. Comparison of coronary plaque, coronary artery calcification and major adverse cardiac events in Chinese outpatients with and without type 2 diabetes. *Springerplus.* (2016) 5:1678. doi: 10.1186/s40064-016-3373-0
102. Casella S, Bielli A, Mauriello A, Orlandi A. Molecular pathways regulating macrovascular pathology and vascular smooth muscle cells phenotype in type 2 diabetes. *Int J Mol Sci.* (2015) 16:24353–68. doi: 10.3390/ijms161024353
103. Dhananjayan R, Koundinya KS, Malati T, Kutala VK. Endothelial dysfunction in type 2 diabetes mellitus. *Indian J Clin Biochem.* (2016) 31:372–9. doi: 10.1007/s12291-015-0516-y
104. Zhang L, Sun H, Liu S, Gao J, Xia J. Glycemic variability is associated with vascular calcification by the markers of endoplasmic reticulum stress-related apoptosis, Wnt1, galectin-3 and BMP-2. *Diabetol Metab Syndr.* (2019) 11:67. doi: 10.1186/s13098-019-0464-4
105. Chang JR, Duan XH, Zhang BH, Teng X, Zhou YB, Liu Y, et al. Intermedin1-53 attenuates vascular smooth muscle cell calcification by inhibiting endoplasmic reticulum stress via cyclic adenosine monophosphate/protein kinase A pathway. *Exp Biol Med (Maywood).* (2013) 238:1136–46. doi: 10.1177/1535370213502619
106. Liu H, Li X, Qin F, Huang K. Selenium suppresses oxidative-stress-enhanced vascular smooth muscle cell calcification by inhibiting the activation of the PI3K/AKT and ERK signaling pathways and endoplasmic reticulum stress. *J Biol Inorg Chem.* (2014) 19:375–88. doi: 10.1007/s00775-013-1078-1
107. Yao S, Yang N, Song G, Sang H, Tian H, Zhang Y, et al. Induction of mildly oxidized low-density lipoprotein on endoplasmic reticulum stress in macrophages and its signaling pathway. *Chin J Arterioscl.* (2011) 19:242. doi: 10.1016/j.freeradbiomed.2017.02.006
108. Eisenberg T, Abdellatif M, Schroeder S, Primessnig U, Stekovic S, Pendl T, et al. Cardioprotection and lifespan extension by the natural polyamine spermidine. *Nat Med.* (2016) 22:1428–38. doi: 10.1038/nm.4222
109. Liu X, Chen A, Liang Q, Yang X, Dong Q, Fu M, et al. Spermidine inhibits vascular calcification in chronic kidney disease through modulation of SIRT1 signaling pathway. *Aging Cell.* (2021) 20:e13377. doi: 10.1111/acel.13377
110. Hao W, Yang R, Yang Y, Jin S, Li Y, Yuan F, et al. Stellate ganglion block ameliorates vascular calcification by inhibiting endoplasmic reticulum stress. *Life Sci.* (2018) 193:1–8. doi: 10.1016/j.lfs.2017.12.002
111. Li KX, Du Q, Wang HP, Sun HJ. Death-associated protein kinase 3 deficiency alleviates vascular calcification via AMPK-mediated inhibition of endoplasmic reticulum stress. *Eur J Pharmacol.* (2019) 852:90–8. doi: 10.1016/j.ejphar.2019.03.007

Conflict of Interest: The authors declare that the research was conducted in the absence of any commercial or financial relationships that could be construed as a potential conflict of interest.

Publisher's Note: All claims expressed in this article are solely those of the authors and do not necessarily represent those of their affiliated organizations, or those of the publisher, the editors and the reviewers. Any product that may be evaluated in this article, or claim that may be made by its manufacturer, is not guaranteed or endorsed by the publisher.

frontiers | Frontiers in Cardiovascular Medicine

ORIGINAL RESEARCH
published: 30 June 2022
doi: 10.3389/fcvm.2022.904215

Pemafibrate Prevents Rupture of Angiotensin II-Induced Abdominal Aortic Aneurysms

Naofumi Amioka[1], Toru Miyoshi[1], Tomoko Yonezawa[2], Megumi Kondo[1], Satoshi Akagi[1], Masashi Yoshida[1], Yukihiro Saito[1], Kazufumi Nakamura[1] and Hiroshi Ito[1]*

[1] Department of Cardiovascular Medicine, Faculty of Medicine, Dentistry and Pharmaceutical Sciences, Okayama University, Okayama, Japan, [2] Department of Molecular Biology and Biochemistry, Faculty of Medicine, Dentistry and Pharmaceutical Sciences, Okayama University, Okayama, Japan

Background: Abdominal aortic aneurysm (AAA) is a life-threatening disease that lacks effective preventive therapies. This study aimed to evaluate the effect of pemafibrate, a selective peroxisome proliferator-activated receptor alpha (PPARα) agonist, on AAA formation and rupture.

Methods: Experimental AAA was induced by subcutaneous angiotensin II (AngII) infusion in *ApoE*$^{-/-}$ mice for 4 weeks. Pemafibrate (0.1 mg/kg/day) was administered orally. Dihydroethidium staining was used to evaluate the reactive oxygen species (ROS).

Results: The size of the AngII-induced AAA did not differ between pemafibrate- and vehicle-treated groups. However, a decreased mortality rate due to AAA rupture was observed in pemafibrate-treated mice. Pemafibrate ameliorated AngII-induced ROS and reduced the mRNA expression of interleukin-6 and tumor necrosis factor-α in the aortic wall. Gelatin zymography analysis demonstrated significant inhibition of matrix metalloproteinase-2 activity by pemafibrate. AngII-induced ROS production in human vascular smooth muscle cells was inhibited by pre-treatment with pemafibrate and was accompanied by an increase in catalase activity. Small interfering RNA-mediated knockdown of catalase or PPARα significantly attenuated the anti-oxidative effect of pemafibrate.

Conclusion: Pemafibrate prevented AAA rupture in a murine model, concomitant with reduced ROS, inflammation, and extracellular matrix degradation in the aortic wall. The protective effect against AAA rupture was partly mediated by the anti-oxidative effect of catalase induced by pemafibrate in the smooth muscle cells.

Keywords: pemafibrate, angiotensin II, abdominal aortic aneurysm, oxidative stress, catalase

OPEN ACCESS

Edited by:
Mark Slevin,
Manchester Metropolitan University,
United Kingdom

Reviewed by:
Massimiliano Ruscica,
University of Milan, Italy
Wen-Jun Tu,
Chinese Academy of Medical Sciences and Peking Union Medical College, China

****Correspondence:***
Toru Miyoshi
miyoshit@cc.okayama-u.ac.jp

Specialty section:
This article was submitted to Atherosclerosis and Vascular Medicine, a section of the journal Frontiers in Cardiovascular Medicine

Received: *25 March 2022*
Accepted: *14 June 2022*
Published: *30 June 2022*

Citation:
Amioka N, Miyoshi T, Yonezawa T, Kondo M, Akagi S, Yoshida M, Saito Y, Nakamura K and Ito H (2022) Pemafibrate Prevents Rupture of Angiotensin II-Induced Abdominal Aortic Aneurysms. Front. Cardiovasc. Med. 9:904215. doi: 10.3389/fcvm.2022.904215

INTRODUCTION

Abdominal aortic aneurysm (AAA) is characterized by progressive dilation of the abdominal aorta and associated risk of rupture and sudden death. Multiple factors are associated with the development and fatal rupture of AAA, including infiltration of macrophages that release pro-inflammatory cytokines (1), generation of reactive oxygen species (ROS) (2–5), impairment and

apoptosis of vascular smooth muscle cells (VSMCs) (6), and degradation of the extracellular matrix by activated matrix metalloproteinases (MMPs) (7). Unfortunately, effective preventive treatments have not yet been established despite extensive basic and clinical research on AAA. Previous clinical studies have shown the potential of beta-blockers and angiotensin-converting enzyme inhibitors to prevent the development or rupture of AAA; however, their clinical effectiveness for AAA remains controversial (8–11).

Peroxisome proliferator-activated receptors (PPARs) are transcription factors that belong to the nuclear receptor superfamily, which includes the three following subtypes: PPARα, PPARβ/δ, and PPARγ. PPARs bind to PPAR-responsive regulatory elements and regulate energy homeostasis, insulin sensitivity, and lipid metabolism by promoting the expression of various genes (12–15). In addition, the activation of PPARα can regulate the expression of genes involved in inflammation and oxidative stress (16–18). PPARα is expressed in various types of cells in the body, including vascular component cells such as macrophages, vascular smooth muscle cells, and endothelial cells (17, 19–23). Previous studies showed that fibrates, which are PPARα agonists, decrease the production of inflammatory cytokines, infiltration of monocytes, and expression of MMP genes in the aortic wall (24–27). Fibrates have also been reported to attenuate the reduction of anti-oxidative enzymes, including superoxide dismutase and catalase, in the aortic wall impaired by diabetic stress (28). Accumulating evidence showing the counteraction of fibrates on the pathogenesis of AAA suggests the potential of PPARα as a therapeutic target for the development and rupture of AAA (29).

However, the side effects of conventional PPARα agonists, especially off-target effects such as liver damage and elevated serum creatinine levels, are major concerns in clinical practice (30–32). Recently, pemafibrate, a selective PPARα modulator, has been discovered (33, 34). Pemafibrate is more potent in activating PPARα than conventional PPARα agonists, as indicated by its lower effective concentration and higher selectivity toward PPAR subtypes with reduced off-target side effects (35, 36).

In primary studies, angiotensin II (AngII)-infused hypercholesterolemic mice are widely used to develop experimental AAA. AngII infusion has been reported to promote AAA formation in mice by inducing ROS, inflammation, and activating MMPs in the aortic wall (37–40). Thus, AngII infusion in mice is a technically facile animal model that recapitulates multiple facets of AAA in human.

In this study, we investigated the protective effect of pemafibrate on AAA formation and rupture in an experimental murine model, with a focus on AngII-induced ROS production and inflammation.

MATERIALS AND METHODS

Animals and Treatments

All animal experiments were conducted in accordance with experimental protocols approved by the Institutional Animal Care and Use Committee of Okayama University (OKU-2021372). Male $ApoE^{-/-}$ mice were purchased from Jackson Laboratory (Bar Harbor, ME, United States). **Figure 1** shows the experimental animal protocol. For the AAA model, 8-week-old $ApoE^{-/-}$ male mice were stimulated with a continuous infusion of AngII (1,000 ng/min/kg) for 4 weeks. AngII was dissolved in sterile saline and infused using Alzet osmotic pumps (Model 2004, Durect Corp., Cupertino, United States). Osmotic pumps filled with AngII were implanted subcutaneously in the neck under ketamine and xylazine anesthesia. A saline infusion was used as the control. To evaluate the effect of pemafibrate on AAA, treatment with pemafibrate (0.1 mg/kg/day) or vehicle was commenced a week before the administration of AngII or saline. Mice were anesthetized by intraperitoneal injection of ketamine (80 mg/kg) and xylazine (5 mg/kg) before euthanization. To evaluate early changes in the aortic wall after AngII infusion, another set of mice was euthanized at 1 week. Catalase staining, dihydroethidium (DHE) staining, gelatin zymography, and gene expression analysis were performed in mice euthanized at 1 week. In addition, the evaluation of blood pressure, serum lipid profile, the incidence of AAA rupture, the maximum diameter of the abdominal aortas, plaque volume of the thoracic aorta, and histology of the abdominal aorta [elastin van Gieson (EVG) staining] were performed in mice euthanized at 4 weeks. The sample size of each group for the 1-week infusion of saline or AngII was 5. The sample size of each treatment group infused with saline or AngII for 4 weeks was as follows: vehicle-treated saline-infused mice (n = 10), pemafibrate-treated saline-infused mice (n = 10), vehicle-treated AngII-infused mice (n = 25), and pemafibrate-treated AngII-infused mice (n = 25). All mice were euthanized at their respective endpoints under anesthesia.

Measurement of Blood Pressure

Blood pressure was measured using the tail-cuff method (MK-2000; Muromachi, Tokyo, Japan) at the start of the experiment (baseline) and 4 weeks after AngII infusion.

Analysis of Serum Lipid Profile

Mice were fasted overnight at the endpoint of this study (4 weeks after the beginning of AngII or saline infusion). Blood was collected from the right ventricle. Serum samples were separated by centrifugation of blood samples at 3,000 rpm for 20 min. The serum was stored at -80°C. The general serum lipid profile was analyzed using high-performance liquid chromatography (Skylight Biotech Inc., Akita, Japan).

Evaluation of the Incidence of Aortic Rupture, Abdominal Aortic Diameter, and Extent of Atherosclerosis

To assess the incidence of aortic rupture, each mouse was monitored intensively every day to ensure immediate dissection of dead mice. After termination, the abdominal aortic diameter was measured at the suprarenal lesion of the aorta using *ex vivo* imaging. In addition, thoracic aortas were used for Oil Red O staining (Sigma-Aldrich, St. Louis, MO, United States) to compare the percentage of plaque areas among the treatment

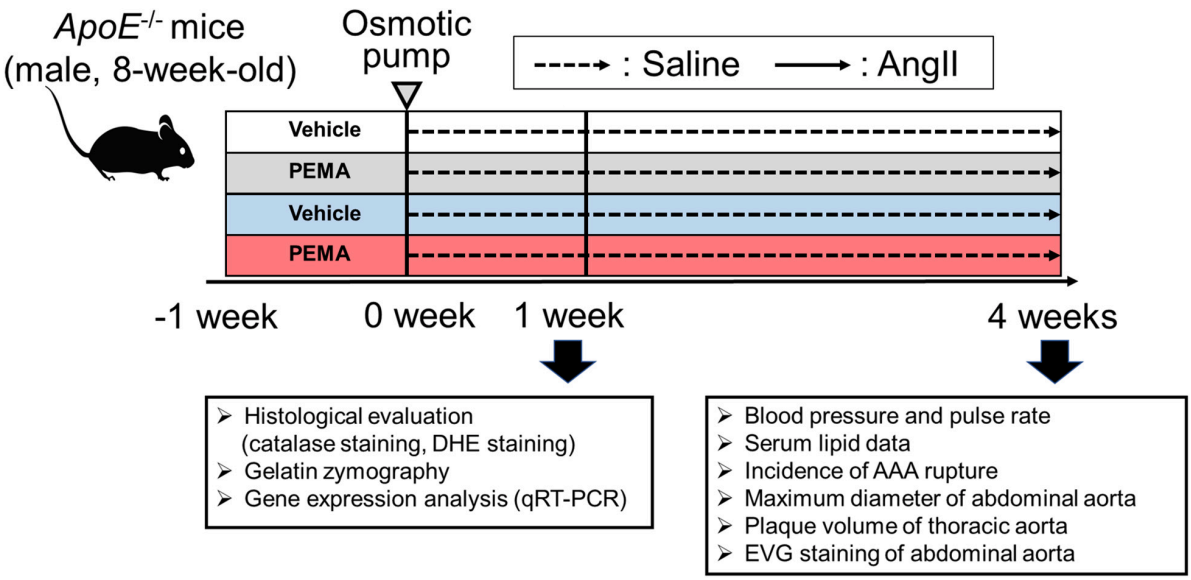

FIGURE 1 | Animal experiment protocol. To develop an experimental abdominal aortic aneurysm (AAA) model, 8-week-old *ApoE-/-* male mice were infused with angiotensin II (AngII) (1,000 ng/min/kg) or saline for 4 weeks. To assess the effect of pemafibrate, treatment with vehicle or pemafibrate (PEMA) (0.1 mg/kg/day) was initiated 1 week before administration of AngII or saline, resulting in four treatment groups: vehicle-treated saline-infused (n = 10), pemafibrate-treated saline-infused (n = 10), vehicle-treated AngII-infused (n = 25), and pemafibrate-treated AngII-infused (n = 25). Five mice in each group were euthanized to evaluate the early changes after AngII infusion. Blood pressure and heart rate were measured using the tail-cuff method before and 4 weeks after AngII infusion. All mice were euthanized at their respective endpoints under anesthesia. DHE, dihydroethidium; EVG, Elastica van Gieson; qRT-PCR, quantitative reverse transcription polymerase chain reaction.

groups. The plaque area was quantified using the ImageJ software (National Institutes of Health, Bethesda, MD, United States).

Histological Assessment

Suprarenal abdominal aortic segments were fixed in 4% paraformaldehyde, embedded in paraffin, and cut into 5-μm-thick sections. Three sets of serial sections obtained at 500 μm intervals were stained with EVG using a standard protocol to evaluate the abdominal aorta longitudinally. To detect catalase in the aortic wall, immunostaining was performed using the following method. First, deparaffinized tissue sections were incubated with 0.3% H_2O_2 in Tris buffer for 15 min at room temperature (RT), 0.025% Triton in Tris buffer for three times, and streptavidin/biotin blocking kit (SP-2002, Vector Labs, Burlingame, CA, United States) for 15 min, respectively, at RT. Subsequently, the slides were incubated with blocking solution (X0909, DAKO, Santa Clara, CA, United States) for 15 min at RT and then incubated with a rabbit anti-mouse catalase primary antibody (1 μg/mL, ab16731, Abcam, Cambridge, United States) overnight at 4°C. Next, the sections were incubated for 30 min at room temperature with a biotinylated swine anti-rabbit IgG secondary antibody (1:500, E0353, DAKO). Finally, a biotinylated protein detection kit (SA-5704, Vector Labs) and diaminobenzidine (DAB) substrate (SK-4105, Vector Labs) were used. EVG- and catalase-stained samples were photographed using an Axioskop 2 Plus light microscope (Zeiss, Oberkochen, Germany). The percentage of catalase-positive areas in the tunica media in five different fields and 7–8 different samples were analyzed using ImageJ software.

Cell Culture

Human aortic VSMCs were obtained from Lonza (Basel, Germany) and cultured in SmGM-2 Bullet Kit medium (Lonza) supplemented with 5% fetal bovine serum (FBS), 0.2% human fibroblast growth factor-B, 0.1% gentamicin/amphotericin B solution, 0.1% human epidermal growth factor, and 0.1% insulin. To analyze the effect of pemafibrate on ROS, cells were first grown in a reduced-serum medium for 24 h and then cultured in the respective basal medium supplemented with 1% FBS. The cells were treated with pemafibrate (0.1–10 μM) or vehicle (dimethyl sulfoxide) for 24 h. To evaluate the anti-oxidative effect of catalase activity induced by pemafibrate, 3-amino-1,2,4-triazole (3AT) (Sigma Aldrich) (50 mM), a catalase inhibitor, was co-administered with pemafibrate.

Small Interfering Ribonucleic Acid Transfection

Gene silencing experiments were performed by transfecting VSMCs with 10 μM small interfering ribonucleic acid (siRNAs) (Ambion, Life Technologies, Darmstadt, Germany) targeting catalase (*CAT*), *PPARα*, or the negative control, using Lipofectamine RNAiMAX (Invitrogen, Carlsbad, CA, United States), and Opti-MEM (Gibco, Waltham, MA, United States) for 24 h, before each treatment.

Catalase Activity

The catalase activity of VSMCs was determined using a simple visual assay as described previously (41). Briefly, catalase powder (Sigma Aldrich) dissolved in 100 μL of distilled water was used

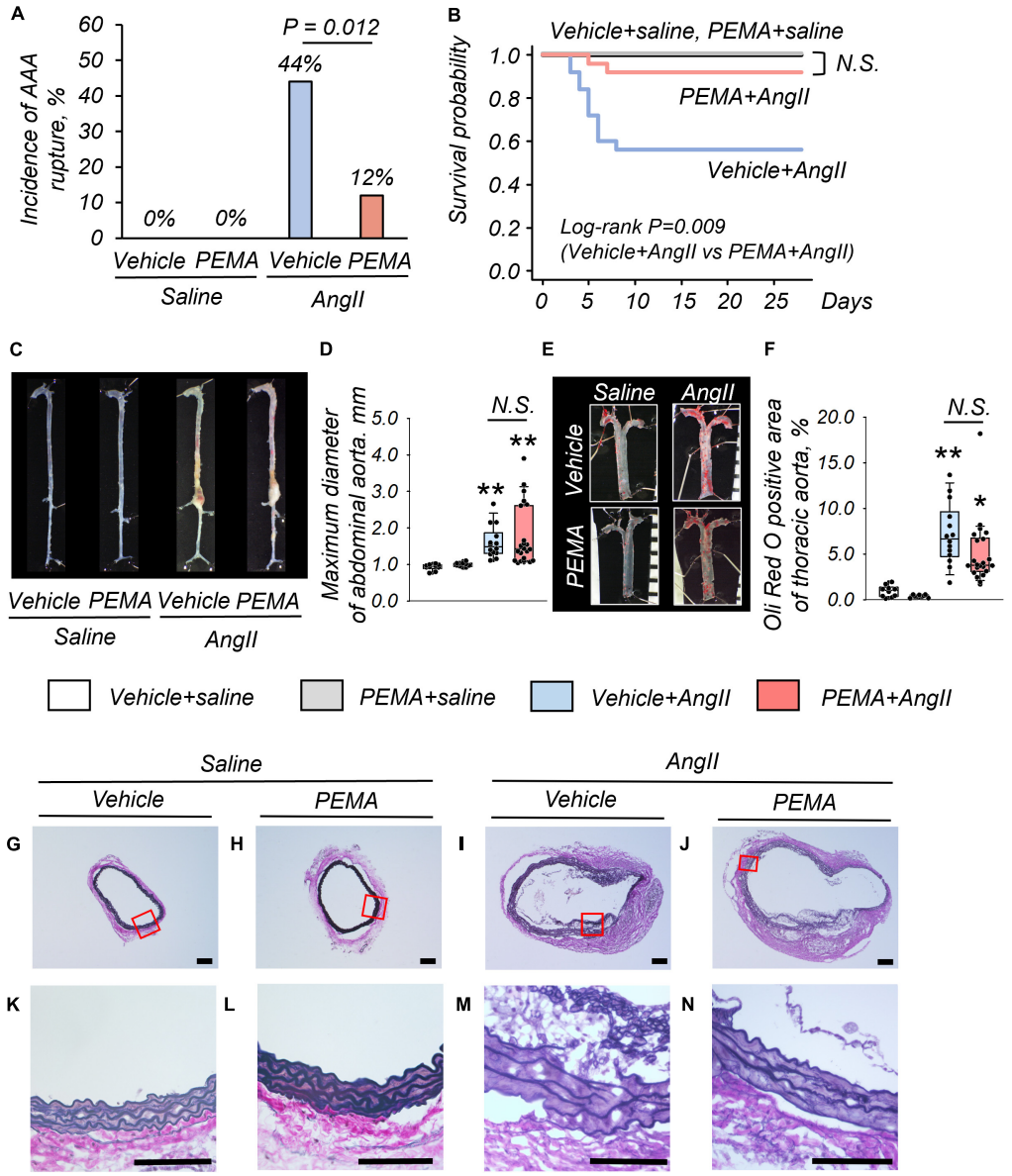

FIGURE 2 | Impact of pemafibrate (PEMA) on abdominal aortic aneurysm (AAA) in a murine model. Incidence of aortic rupture in the vehicle-treated saline-infused (vehicle + saline) (n = 10), PEMA-treated saline-infused (PEMA + saline) (n = 10), vehicle-treated angiotensin II-infused (vehicle + AngII) (n = 25), and PEMA-treated angiotensin II-infused (PEMA + AngII) (n = 25) groups **(A)**. Kaplan–Meier survival curve for AngII- or saline-infused mice in the presence or absence of PEMA **(B)**. Representative findings of aortas **(C)** and maximum diameter of suprarenal abdominal aortas **(D)** extracted from surviving mice. Representative findings of Oil Red O staining **(E)** and Oil Red O-positive area **(F)** of thoracic aortas extracted from surviving mice [n = 10 (vehicle + saline group), n = 10 (PEMA + saline group), n = 14 (vehicle + AngII group), and n = 22 (PEMA + AngII group)]. Representative results of Elastica van Gibson staining **(G–N)**. Data are expressed as frequencies for categorical variables and analyzed by chi-square test **(A)** or as median (interquartile range) and analyzed using the Kruskal–Wallis test followed by Bonferroni corrections **(D,F)**. Survival probabilities were compared using the log-rank test **(B)**. *p < 0.01 vs. vehicle + saline group; **p < 0.001 vs. vehicle + saline. N.S., not significant. Scale bar = 100 μm.

to prepare catalase standards. Next, VSMCs (1.0×10^7 cells) were suspended in 100 μL of phosphate-buffered saline (PBS). Catalase standard or sample solution (100 μL) was transferred to a Pyrex test tube (13 mm diameter × 100 mm height), and 100 μL each of 1% Triton X-100 (MP Biomedicals, Santa Ana, CA, United States) and 30% hydrogen peroxide (Wako, Osaka, Japan) were added, mixed gently, and incubated at 20°C. After the completion of the reaction, the height of the O_2-forming foam, which remained constant for 15 min, was measured in millimeters using a ruler.

Detection of Reactive Oxygen Species

The presence of ROS in the aortic walls of mice and VSMCs was analyzed using DHE staining (Molecular Probes, Eugene, United States). Briefly, VSMCs were plated on glass coverslips

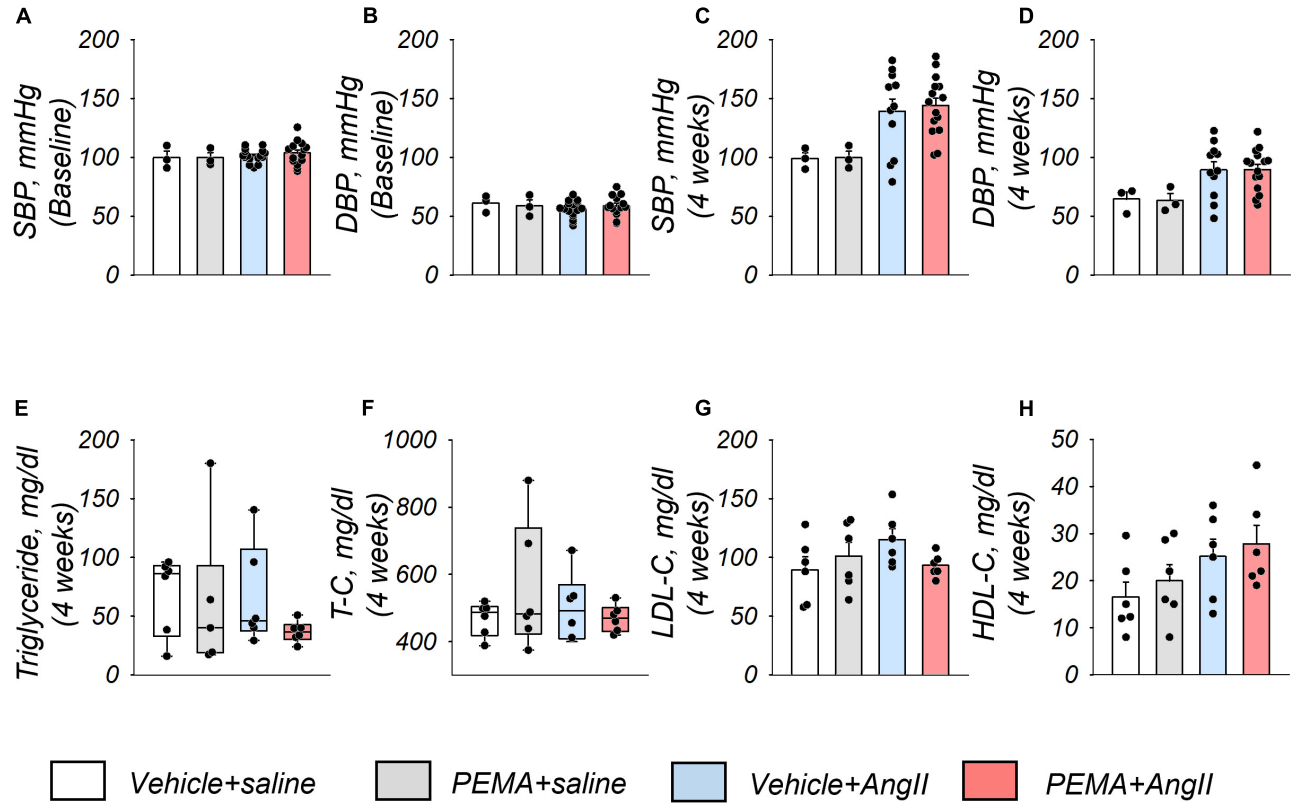

FIGURE 3 | Blood pressure and serum lipid profiles of study mice. Systolic blood pressure (SBP) and diastolic blood pressure (DBP) at the start of the experiment (baseline) **(A,B)** and 4 weeks after the administration of AngII or saline infusion **(C,D)** in each group. Sample size: $n = 3$ (vehicle + saline and PEMA + saline group] and $n = 11$–16 (vehicle + AngII and PEMA + AngII group) in triplicate. Samples that matched the median body weights of each group were selected. Serum levels of triglycerides, total cholesterol (T-C), low-density lipoprotein cholesterol (LDL-C), and high-density lipoprotein cholesterol (HDL-C) 4 weeks after the administration of AngII or saline infusion in each group **(E–H)**, respectively. Sample size: $n = 6$ per group. Samples that matched the median body weights of each group were selected. Data are expressed as mean ± standard error of the mean and analyzed by one-way analysis of variance for normally distributed continuous variables **(A–D,G,H)** or expressed as median (interquartile range) and analyzed using the Kruskal–Wallis test **(E,F)**. $p < 0.05$.

placed in 12-well plates. Subsequently, sub-confluent cells were stimulated with AngII (100 nM) for 30 min, washed with PBS, incubated with DHE (5 μM) for 30 min, and analyzed for fluorescence. Red fluorescence intensity (FI) (585 nm) was measured using an OLYMPUS IX71 fluorescence microscope (Tokyo, Japan). The mean FIs of 10–20 nuclei per image, 5 images per coverslip, and 3 coverslips per sample were measured using the ImageJ software. The aortas of mice treated for 1 week were perfused with PBS (pH 7.4) for 5 min at 4°C. Subsequently, the aortic tissue was harvested from the abdominal aorta, embedded in Tissue-Tek O.C.T. Compound (Sakura Finetek United States, Torrance, CA, United States), and snap-frozen. Freshly cut frozen aortic sections (5 μm) were incubated with DHE for 30 min at 37°C to detect ROS. For *in vivo* experiments, the mean FI of 10–20 nuclei per image and five images per sample were analyzed using the ImageJ software.

Gelatin Zymography

The enzymatic activities of MMP-2 and MMP-9 were analyzed in the aortic walls of mice treated with vehicle or pemafibrate for 1 week. Briefly, 10 μg of total protein isolated from the abdominal aorta was subjected to 10% sodium dodecyl sulfate-polyacrylamide gel electrophoresis containing 1 mg/mL gelatin added before heating. After electrophoresis, the gel was washed with 2.5% Triton X-100 solution for 30 min and then incubated in a solution containing 50 mM Tris-HCl, 5 mM $CaCl_2$, and 1 μM $ZnCl_2$ for 16 h at 37°C. Following incubation, the gel was stained with 0.05% Coomassie Brilliant Blue R-250 for 30 min at room temperature, washed with buffer, and photographed. Pro-MMP-2, active MMP-2, and pro-MMP-9 were visualized as colorless bands against a blue background. The color density of the band formation area was determined using the ImageJ software.

Quantitative Reverse Transcription-Polymerase Chain Reaction

RNA was extracted from the aortic tissue of mice in the acute model or from VSMCs using the RNeasy Mini Kit (Qiagen,

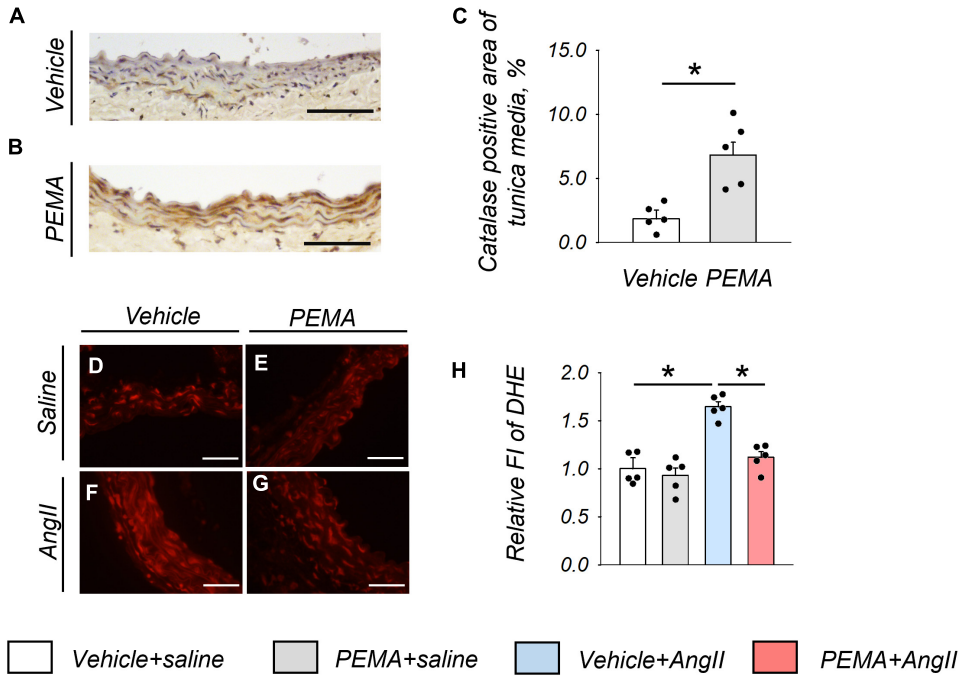

FIGURE 4 | Catalase expression and the reduction in reactive oxygen species (ROS) in the aortic wall at 1 week after angiotensin (AngII) infusion. Representative findings of anti-catalase staining **(A,B)** and quantitative evaluation of catalase expression **(C)** in the suprarenal aorta from vehicle-treated saline-infused mice and in pemafibrate (PEMA)-treated saline-infused mice (n = 5 per group, performed in duplicate). Representative results of dihydroethidium (DHE) staining **(D–G)** and relative fluorescence intensity (FI) of DHE staining (n = 5 per group, performed in duplicate) **(H)** in the suprarenal aorta extracted from vehicle-treated saline-infused, PEMA-treated saline-infused, vehicle-treated AngII-infused, and PEMA-treated AngII-infused mice. Data are expressed as the mean ± standard error of the mean. All analyses were performed using analysis of variance and Bonferroni corrections. *$p < 0.01$. Scale bar = 50 μm.

Valencia, United States). Complementary diribonucleic acid (cDNA) was synthesized from 1.0 μg of extracted total RNA using ReverTra Ace (TOYOBO, Osaka, Japan). The synthesized cDNAs were subjected to polymerase chain reaction (PCR) using the TaqMan Gene Expression Master Mix (Applied Biosystems, Foster City, United States) and predesigned gene-specific primer and probe sets (TaqMan Gene Expression Assays; Applied Biosystems). TaqMan gene expression probe-and-primer sets for *PPARα*, superoxide dismutases (*SOD1* and *SOD2)*, nicotinamide adenine dinucleotide phosphate oxidases (*NOX2* and *NOX4*), *CAT*, heme oxygenase-1 (*HO-1*), interleukin-6 (*IL-6*), tumor necrosis factor-α (*TNFα*), and transforming growth factor-β1 (*TGF-β1*) were purchased from Applied Biosystems. Real-time PCR was performed in triplicate for each sample using the QuantStudio 1 real-time PCR System (Applied Biosystems) described previously (42). The results were quantified using the relative Ct method and normalized to the internal control, glyceraldehyde 3-phosphate dehydrogenase. See **Supplementary Table 1** for PCR primer details.

Statistical Analyses

All analyses were performed using EZR version 1.41 (Saitama Medical Center, Jichi Medical University, Saitama, Japan) (43), a graphical user interface of R (The R Foundation for Statistical Computing, Vienna, Austria), or SigmaPlot version 14.5 (Systat Software Inc., San Jose, CA, United States). For normally distributed continuous variables, results are expressed as the mean ± standard error of the mean. One-way analysis of variance with Bonferroni *post-hoc* test was used to examine the differences among groups. Non-normally distributed continuous variables were expressed as median (interquartile range) and analyzed using the Kruskal–Wallis tests. Categorical variables are presented as absolute values and frequencies, and categorical variables were compared using the chi-square test. Kaplan–Meier survival curves were used to evaluate survival rates, and significance was assessed using the log-rank test. In some experiments, technical replicates were performed as described in each figure legend. Differences with $p < 0.05$ were considered statistically significant.

RESULTS

Pemafibrate Reduced Angiotensin II-Induced Abdominal Aortic Rupture

At 4 weeks, no fatal aortic rupture was observed in vehicle- or pemafibrate-treated mice without AngII infusion (**Figure 2A**). The incidence of fatal aortic rupture in the pemafibrate-treated AngII-infused group was significantly lower than that in the vehicle-treated AngII-infused group [3/25 (12%) vs. 11/25 (44%),

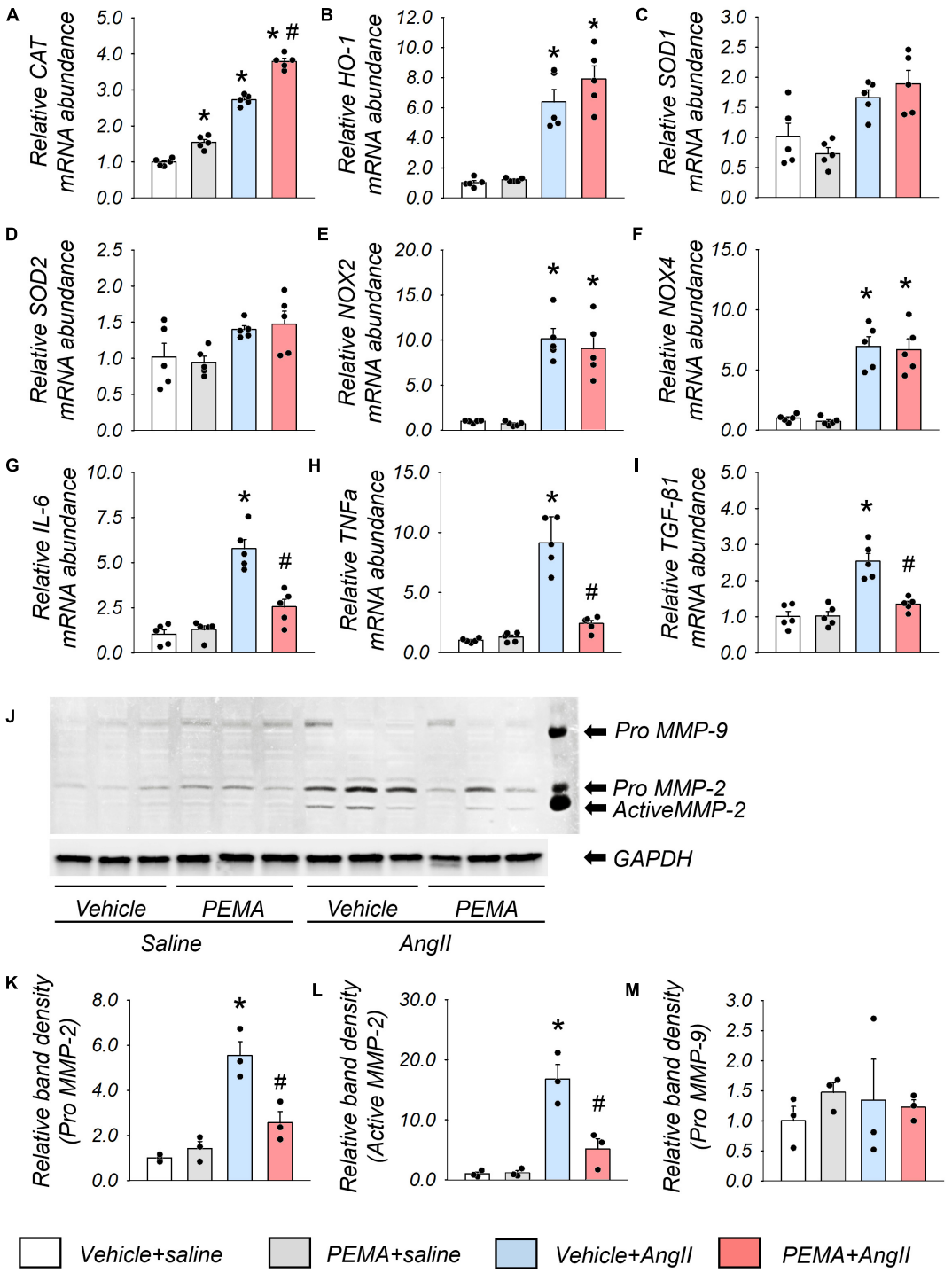

FIGURE 5 | Gene expression and matrix metalloproteinase (MMP) activity in the aortic tissues extracted from the acute model of ApoE$^{-/-}$ mice. **(A–I)** mRNA expression levels of catalase (*CAT*), heme oxygenase-1 (*HO-1*), superoxide dismutase 1 (*SOD-1*), *SOD-2*, nicotinamide adenine dinucleotide phosphate oxidases (*NOX2* and *NOX4*), Interleukin-6 (*IL-6*), tumor necrosis factor-α (*TNFα*), and transforming growth factor-β1 (*TGF-β1*) in the suprarenal aortic tissues extracted from vehicle-treated saline-infused (vehicle + saline), pemafibrate-treated saline-infused (PEMA + saline), vehicle-treated angiotensin II-infused (vehicle + AngII), and PEMA-treated angiotensin II-infused (PEMA + AngII) mice (n = 5 per group, performed in duplicates). All gene expression analyses were conducted using quantitative reverse transcription-polymerase chain reaction, and each gene expression level was normalized using glyceraldehyde 3-phosphate dehydrogenase (*GAPDH*). **(J)** MMP-2, and MMP-9 activities in the abdominal aorta of mice infused with saline or AngII for 4 weeks were analyzed using gelatin zymography. Quantitative analysis of pro-MMP-2 **(K)**, active MMP-2 **(L)**, and pro-MMP-9 **(M)** in the abdominal aorta (*n* = 3 per group, performed in duplicates). For gelatin zymography, the samples matched to the median body weight of each group were selected. Data are expressed as mean ± standard error of the mean. All analyses were performed using analysis of variance and Bonferroni corrections. $^{*}p < 0.05$ vs. the vehicle-treated saline-infused group; $^{\#}p < 0.05$ vs. the vehicle-treated AngII-infused group.

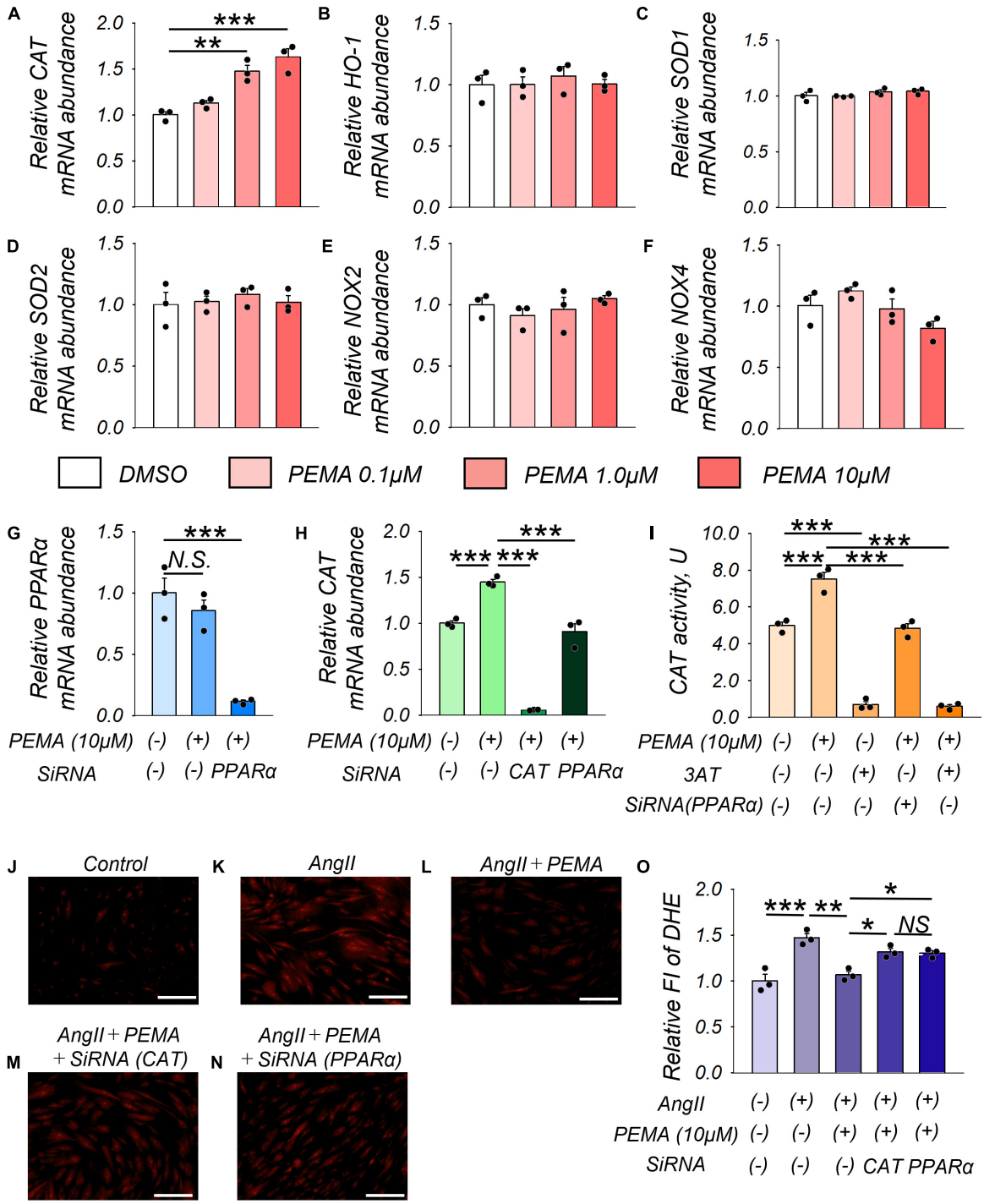

FIGURE 6 | Pemafibrate (PEMA)-mediated gene expression changes and the reduction in ROS in vascular smooth muscle cells (VSMCs). **(A–F)** mRNA expression levels of catalase (*CAT*), heme oxygenase-1 (*HO-1*), superoxide dismutase 1 (*SOD-1*), *SOD-2*, nicotinamide adenine dinucleotide phosphate oxidases (*NOX2* and *NOX4*) in VSMCs treated with dimethyl sulfoxide (DMSO) and PEMA (0.1, 1.0, and 10 μM) for 24 h. **(G)** mRNA expression levels of peroxisome proliferator-activated receptor alpha (*PPARα*) in VSMCs treated with 10 μM PEMA with or without transfection using SiRNA of *PPARα* for 24 h before the PEMA administration. **(H)** mRNA expression levels of *PPARα* in VSMCs treated with 10 μM PEMA with or without transfection using SiRNA of *CAT* or *PPARα*. All gene expression analyses were conducted using quantitative reverse transcription-polymerase chain reaction, and each gene expression level was normalized using glyceraldehyde 3-phosphate dehydrogenase (*GAPDH*). **(I)** CAT activity in VSMCs (1.0×10^7 cells) treated with 10 μM PEMA in the presence or absence of 3-amino-1,2,4-triazole (3AT) treatment and/or transfection using SiRNA of PPARα. Representative results of DHE staining **(J–N)** and relative DHE fluoro-intensity (FI) **(O)** of VSMCs stimulated with AngII (100 nM) with or without PEMA, and/or transfection using SiRNA of CAT or PPARα. All analyses were performed using analysis of variance and Bonferroni corrections; $n = 3$ per group, performed in duplicates. Data are expressed as mean ± standard error of the mean. $^*p < 0.05$; $^{**}p < 0.01$; $^{***}p < 0.001$. N.S., not significant.

p = 0.012]. Immediate dissection of dead mice confirmed that all ruptures had occurred in the suprarenal abdominal aorta. Kaplan–Meier analysis indicated significantly increased survival in the pemafibrate-treated AngII-infused group compared with that in the vehicle-treated AngII-infused group (log-rank p = 0.009) (**Figure 2B**). The maximum abdominal aortic diameter of surviving mice was significantly increased by AngII infusion; however, this increase was not significantly changed by pemafibrate at 4 weeks (**Figures 2C,D**). **Figure 2E** shows representative findings of the thoracic aorta stained with Oil Red O. There was no significant difference in the percentage of plaque area between the vehicle- and pemafibrate-treated AngII-infused mice (**Figure 2F**). Representative findings of EVG staining of the abdominal aorta at 4 weeks are shown in **Figures 2G–N**. Degradation of the elastic lamina was observed in the aortic walls of vehicle- and pemafibrate-treated AngII-infused mice.

Pemafibrate Did Not Influence Serum Lipid Profiles and Blood Pressure

Compared with the baseline of the experiment (**Figures 3A,B**), an increase in systolic and diastolic blood pressure by AngII infusion was observed at 4 weeks (**Figures 3C,D**). Pemafibrate did not ameliorate this increase in blood pressure. Analyses of serum triglyceride, total cholesterol, low-density lipoprotein cholesterol, and high-density lipoprotein cholesterol levels indicated no significant difference among all groups of mice at 4 weeks (**Figures 3E–H**).

Pemafibrate Increased the Expression of Catalase and Reduced Angiotensin II-Induced Reactive Oxygen Species in the Aortic Wall

Representative findings of anti-catalase staining of abdominal aortic tissue extracted from mice at 1 week after AngII infusion are shown in **Figures 4A,B**. Pemafibrate significantly increased the expression of catalase in the tunica media of the aortic wall compared with that in control mice (**Figure 4C**). **Figures 4D–G** represents DHE staining findings in the tunica media of abdominal aorta extracted from mice 1 week after AngII infusion. In addition, pemafibrate pre-treatment significantly attenuated the increase in ROS induced by AngII, as indicated by FI (**Figure 4H**).

Pemafibrate Enhanced the Expression of Catalase and Suppressed the Expression of Genes Associated With Inflammation in the Aortic Tissue

The administration of pemafibrate increased *CAT* mRNA abundance in the aortic wall of mice infused with saline for 1 week. This increase was further enhanced in mice infused with AngII (**Figure 5A**). The mRNA expression levels of *HO-1*, *NOX-2*, and *NOX-4* in the vehicle-treated AngII-infused group were also significantly increased compared with those in the vehicle-treated group; however, these increases were not affected by pemafibrate treatment (**Figures 5B,E,F**). There were no statistically significant differences in the mRNA expression level of *SOD-1* and *SOD-2* between any of the groups (**Figures 5C,D**). Pemafibrate significantly suppressed the enhanced mRNA expression of *IL-6*, *TNF*-α, and *TGF*-β*1* induced by AngII infusion (**Figures 5G–I**). MMP-2 activity was significantly increased by AngII infusion, and this increase was attenuated by pemafibrate treatment (**Figures 5J–L**). The activity of pro-MMP-9 was not affected by AngII infusion or pemafibrate treatment (**Figures 5J,M**).

Pemafibrate Decreased Reactive Oxygen Species by Increasing the Expression and Activity of Catalase in Vascular Smooth Muscle Cells

Treatment of VSMCs with pemafibrate (10 μM) significantly enhanced *CAT* mRNA expression by 1.6-fold compared with that of the untreated control. Furthermore, this increase in expression was dose-dependent (**Figure 6A**). However, pemafibrate treatment did not affect the mRNA expression of any of the other genes analyzed in this study (**Figures 6B–F**). Pemafibrate treatment did not directly influence *PPAR*α mRNA expression, but transfection with siRNA-*PPAR*α significantly suppressed *PPAR*α mRNA expression (**Figure 6G**). Accordingly, the pemafibrate treatment-mediated increase in catalase expression was significantly attenuated by transfection with siRNA-*CAT* and siRNA-*PPAR*α in VSMCs (**Figure 6H**). Catalase activity was enhanced in pemafibrate-treated VSMCs compared with that in the untreated control. This increase in catalase activity was suppressed by adding 3AT, a catalase inhibitor, and was attenuated by siRNA-*PPAR*α (**Figure 6I**). DHE staining of VSMCs treated with a combination of AngII, pemafibrate, and siRNA of *CAT* or *PPAR*α is shown in **Figures 1J–N**. Stimulation with AngII significantly increased ROS by 1.5-fold, which was attenuated by pemafibrate treatment. This effect of pemafibrate treatment was reversed to a moderate extent by transfection with siRNA-*CAT* or siRNA-*PPAR*α in VSMCs (**Figure 6O**).

DISCUSSION

To the best of our knowledge, this is the first study to demonstrate the protective effect of pemafibrate on the prevention of fatal aortic rupture in an experimental AAA model. The primary finding of this study was that pemafibrate did not ameliorate the size of AngII-induced AAAs but significantly prevented fatal aortic rupture, which may be mediated by its anti-oxidative and anti-inflammatory effects. This protective effect against aortic rupture is partly attributable to the enhanced expression and activity of catalase in VSMCs.

Catalase, a strong antioxidant enzyme, mitigates oxidative stress by converting cellular hydrogen peroxide to water and oxygen. Overexpression of the catalase gene is associated with decreased inflammatory markers, VSMC apoptosis, and MMP

activity in the aorta, leading to the prevention of experimental AAA formation in mice (44). PPARα agonists increase the expression and activity of catalase in diverse tissues, including the heart, liver, and kidneys (16, 45–47). In the present study, we demonstrated that pemafibrate treatment significantly decreased ROS levels in AngII-stimulated aortic tissue of mice and VSMCs, both of which were associated with increased catalase gene expression. The ability of pemafibrate to increase catalase activity and gene expression, leading to decreased ROS, was attenuated by knocking down *PPAR*α in VSMCs. PPARα-associated enhanced expression of the catalase gene by pemafibrate is further supported by the presence of PPAR-α-specific binding sites in the promoter region of catalase (48). Pemafibrate-induced reduction in ROS could have contributed to the reduced incidence of aortic rupture in experimental AAA. However, ROS include several components such as superoxide anions and hydrogen peroxide. As DHE staining is mainly used to detect superoxide, further studies are needed to elucidate the impact of other ROS on aortic rupture in experimental AAA.

Inflammation plays a pivotal role in developing cardiovascular diseases, including AAA (49, 50). A previous study showed that pro-inflammatory cytokines, including IL-6, IL-β1, TNF-α, monocyte chemoattractant protein (MCP)-1, and MCP-2, may contribute to pathological changes within the established, pre-ruptured AAA (51). During AAA development, monocytes are recruited into the aortic wall by chemotactic cytokines, including IL-6 and MCP-1 (52). Macrophages produce MMPs, cytokines, and chemokines in mouse and human AAA lesions (1). MMPs secreted by inflammatory cells induce ECM degradation, resulting in a decrease in aortic wall integrity. Our study demonstrated that pemafibrate significantly suppressed the enhanced gene expression of the pro-inflammatory cytokines IL-6, TNF-α, and TGF-β1 in the aortic wall 1 week after AngII infusion. Several studies have reported the preventive effects of PPARα on inflammation and atherosclerosis (53–56). One study showed that PPARα activation could decrease the production of IL-6 (54) and the cytokine-induced expression of adhesion molecules, such as vascular cell adhesion molecule-1, both *in vivo* and *ex vivo* (55). However, few studies have demonstrated the anti-inflammatory effects of pemafibrate on the aortic wall. Administration of pemafibrate decreased the gene expression of vascular cell adhesion molecule-1 and IL-6 in atherosclerotic lesions of *ApoE2*-knock-in mice (53). Previous studies have suggested that pemafibrate may affect the polarization or migration of macrophages through PPARα activation-mediated regulation of gene expression.

Furthermore, pemafibrate attenuated AngII-induced enhancement of MMP-2 activity in the aortic wall of mice. Maintenance of the structural integrity of the aortic wall, together with inhibition of extracellular matrix degradation, is primarily responsible for preventing fatal aortic rupture in AAA (57). ROS are key modulators of MMP activity (37). Accordingly, suppression of ROS in VSMCs protects against AAA formation in mice (58). In this study, MMP-2 activity after 1 week of treatment was significantly reduced in pemafibrate-treated mice compared with that in vehicle-treated mice. Therefore, it is speculated that pemafibrate might prevent extracellular matrix degradation at the early stages in the murine AAA model, thereby ameliorating fatal abdominal aortic rupture.

Pemafibrate is widely used to treat hypertriglyceridemia owing to its high clinical efficacy and minor disadvantages compared with those of conventional PPARα agonists (59). Furthermore, PROMINENT, a large ongoing randomized controlled trial, is investigating the preventive effect of pemafibrate on cardiovascular events in patients with type 2 diabetes mellitus (60). Considering that pemafibrate improved survival in AngII-infused mice by preventing fatal rupture of AAA, it may provide a promising novel treatment strategy for AAA in clinical practice.

This study had several limitations. First, the effects of pemafibrate on different experimental AAA models were not evaluated. It is well known that the AngII-induced AAA model is associated with a higher rate of aortic rupture than other experimental models of AAA induced by $CaCl_2$, $CaPO_4$, or elastase (61). Although it is possible that pemafibrate can attenuate the dilatation and rupture of the abdominal aorta in other AAA models, further studies are required to confirm the reduction in the rupture rate in animal models. Second, this study examined the protection, not regression, of AAA caused by pemafibrate. In clinical practice, treatment is initiated after the establishment of AAA. Prospective clinical studies are required to determine the beneficial effects of pemafibrate on AAA. Third, we did not directly compare the effects of conventional PPARα agonists and pemafibrate on the development and aortic rupture of AAA. It has been reported that fenofibrate, a major conventional PPARα agonist, reduces aortic dilatation in murine models of aortic aneurysms (62, 63). The difference in the effects of pemafibrate and other PPARα agonists on aortic rupture needs to be assessed in the same AAA model. Fourth, we did not examine changes in the lipid profile during treatment. According to previous reports, AngII can affect the plasma levels of triglycerides in rodent models (64, 65). Furthermore, another study showed that serum triglyceride levels were a risk factor for AAA rupture (66). However, in this study, as there were no significant differences in serum lipid profile among the study groups at 4 weeks, serum triglyceride levels may not significantly affect aortic rupture.

CONCLUSION

Pemafibrate significantly prevented aortic rupture in a murine AAA model, concomitant with decreased ROS levels and gene expression of pro-inflammatory cytokines. In addition, pemafibrate-mediated increase in catalase gene expression and activity might be a novel contributing factor associated with its beneficial effects in AAA. Our results suggest that pemafibrate-mediated PPARα modulation is a promising drug for the prevention of AAA rupture.

DATA AVAILABILITY STATEMENT

The raw data supporting the conclusions of this article will be made available by the authors, without undue reservation.

ETHICS STATEMENT

The animal study was reviewed and approved by the Institutional Animal Care and Use Committee, Okayama University.

AUTHOR CONTRIBUTIONS

TM conceptualized the study and acquired funding. NA, TM, TY, MY, MK, YS, and KN designed the methodology. NA, TY, and MK conducted experiments under the supervision of HI. NA wrote the first draft of this manuscript. TM, TY, MY, YS, KN, and HI reviewed and edited the manuscript. All authors contributed to the article and approved the submitted version.

FUNDING

This study was supported by a Grant-in-Aid for Scientific Research (grant no. 18K08758).

SUPPLEMENTARY MATERIAL

The Supplementary Material for this article can be found online at: https://www.frontiersin.org/articles/10.3389/fcvm.2022.904215/full#supplementary-material

REFERENCES

1. Raffort J, Lareyre F, Clément M, Hassen-Khodja R, Chinetti G, Mallat Z. Monocytes and macrophages in abdominal aortic aneurysm. *Nat Rev Cardiol.* (2017) 14:457–71. doi: 10.1038/nrcardio.2017.52
2. Miller FJ, Sharp WJ, Fang X, Oberley LW, Oberley TD, Weintraub NL. Oxidative stress in human abdominal aortic aneurysms: a potential mediator of aneurysmal remodeling. *Arterioscler Thromb Vasc Biol.* (2002) 22:560–5. doi: 10.1161/01.ATV.0000013778.72404.30
3. Zhang J, Schmidt J, Ryschich E, Mueller-Schilling M, Schumacher H, Allenberg JR. Inducible nitric oxide synthase is present in human abdominal aortic aneurysm and promotes oxidative vascular injury. *J Vasc Surg.* (2003) 38:360–7. doi: 10.1016/S0741-5214(03)00148-4
4. Guzik B, Sagan A, Ludew D, Mrowiecki W, Chwała M, Bujak-Gizycka B, et al. Mechanisms of oxidative stress in human aortic aneurysms–association with clinical risk factors for atherosclerosis and disease severity. *Int J Cardiol.* (2013) 168:2389–96. doi: 10.1016/J.IJCARD.2013.01.278
5. McCormick ML, Gavrila D, Weintraub NL. Role of oxidative stress in the pathogenesis of abdominal aortic aneurysms. *Arterioscler Thromb Vasc Biol.* (2007) 27:461–9. doi: 10.1161/01.ATV.0000257552.94483.14
6. Henderson EL, Geng YJ, Sukhova GK, Whittemore AD, Knox J, Libby P. Death of smooth muscle cells and expression of mediators of apoptosis by T lymphocytes in human abdominal aortic aneurysms. *Circulation.* (1999) 99:96–104. doi: 10.1161/01.CIR.99.1.96
7. Longo GM, Xiong W, Greiner TC, Zhao Y, Fiotti N, Baxter BT. Matrix metalloproteinases 2 and 9 work in concert to produce aortic aneurysms. *J Clin Invest.* (2002) 110:625–32. doi: 10.1172/JCI15334
8. Gadowski GR, Pilcher DB, Ricci MA. Abdominal aortic aneurysm expansion rate: effect of size and beta-adrenergic blockade. *J Vasc Surg.* (1994) 19:727–31. doi: 10.1016/S0741-5214(94)70048-6
9. Propanolol Aneurysm Trial Investigators. Propranolol for small abdominal aortic aneurysms: results of a randomized trial. *J Vasc Surg.* (2002) 35:72–9. doi: 10.1067/MVA.2002.121308
10. Hackam DG, Thiruchelvam D, Redelmeier DA. Angiotensin-converting enzyme inhibitors and aortic rupture: a population-based case-control study. *Lancet.* (2006) 368:659–65. doi: 10.1016/S0140-6736(06)69250-7
11. Sweeting MJ, Thompson SG, Brown LC, Greenhalgh RM, Powell JT. Use of angiotensin converting enzyme inhibitors is associated with increased growth rate of abdominal aortic aneurysms. *J Vasc Surg.* (2010) 52:1–4. doi: 10.1016/J.JVS.2010.02.264
12. Evans RM, Barish GD, Wang YX. PPARs and the complex journey to obesity. *Nat Med.* (2004) 10:355–61. doi: 10.1038/nm1025
13. Dunning KR, Anastasi MR, Zhang VJ, Russell DL, Robker RL. Regulation of fatty acid oxidation in mouse cumulus-oocyte complexes during maturation and modulation by PPAR agonists. *PLoS One.* (2014) 9:e87327. doi: 10.1371/journal.pone.0087327
14. Hong F, Pan S, Guo Y, Xu P, Zhai Y. PPARs as nuclear receptors for nutrient and energy metabolism. *Molecules.* (2019) 24:2545. doi: 10.3390/molecules24142545
15. Michalik L, Auwerx J, Berger JP, Chatterjee VK, Glass CK, Gonzalez FJ, et al. International union of pharmacology. LXI. Peroxisome proliferator-activated receptors. *Pharmacol Rev.* (2006) 58:726–41. doi: 10.1124/pr.58.4.5
16. Inoue I, Noji S, Awata T, Takahashi K, Nakajima T, Sonoda M, et al. Bezafibrate has an antioxidant effect: peroxisome proliferator-activated receptor α is associated with Cu2+, Zn2+-superoxide dismutase in the liver. *Life Sci.* (1998) 63:135–44. doi: 10.1016/S0024-3205(98)00249-5
17. Inoue I, Goto SI, Matsunaga T, Nakajima T, Awata T, Hokari S, et al. The ligands/activators for peroxisome proliferator-activated receptor alpha (PPARalpha) and PPARgamma increase Cu^{2+}, Zn^{2+}-superoxide dismutase and decrease p22phox message expressions in primary endothelial cells. *Metabolism.* (2001) 50:3–11. doi: 10.1053/META.2001.19415
18. Rakhshandehroo M, Knoch B, Müller M, Kersten S. Peroxisome proliferator-activated receptor alpha target genes. *PPAR Res.* (2010) 2010:612089. doi: 10.1155/2010/612089
19. Braissant O, Foufelle F, Scotto C, Dauça M, Wahli W. Differential expression of peroxisome proliferator-activated receptors (PPARs): tissue distribution of PPAR-alpha, -beta, and -gamma in the adult rat. *Endocrinology.* (1996) 137:354–66. doi: 10.1210/ENDO.137.1.8536636
20. Auboeuf D, Rieusset J, Fajas L, Vallier P, Frering V, Riou JP, et al. Tissue distribution and quantification of the expression of mRNAs of peroxisome proliferator-activated receptors and liver X receptor-alpha in humans: no alteration in adipose tissue of obese and NIDDM patients. *Diabetes.* (1997) 46:1319–27. doi: 10.2337/DIAB.46.8.1319
21. Chinetti G, Griglio S, Antonucci M, Torra IP, Delerive P, Majd Z, et al. Activation of proliferator-activated receptors alpha and gamma induces apoptosis of human monocyte-derived macrophages. *J Biol Chem.* (1998) 273:25573–80. doi: 10.1074/JBC.273.40.25573
22. Inoue I, Shino K, Noji S, Awata T, Katayama S. Expression of peroxisome proliferator-activated receptor alpha (PPAR alpha) in primary cultures of human vascular endothelial cells. *Biochem Biophys Res Commun.* (1998) 246:370–4. doi: 10.1006/BBRC.1998.8622
23. Zhou Y, Wang X, Guo L, Chen L, Zhang M, Chen X, et al. TRPV1 activation inhibits phenotypic switching and oxidative stress in vascular smooth muscle cells by upregulating PPAR alpha. *Biochem Biophys Res Commun.* (2021) 545:157–63. doi: 10.1016/j.bbrc.2021.01.072
24. Delerive P, De Bosscher K, Besnard S, Vanden Berghe W, Peters JM, Gonzalez FJ, et al. Peroxisome proliferator-activated receptor alpha negatively regulates the vascular inflammatory gene response by negative cross-talk with transcription factors NF-kappaB and AP-1. *J Biol Chem.* (1999) 274:32048–54. doi: 10.1074/JBC.274.45.32048
25. Kooistra T, Verschuren L, de Vries-van der Weij J, Koenig W, Toet K, Princen HMG, et al. Fenofibrate reduces atherogenesis in ApoE*3Leiden

mice: evidence for multiple antiatherogenic effects besides lowering plasma cholesterol. *Arterioscler Thromb Vasc Biol.* (2006) 26:2322–30. doi: 10.1161/01.ATV.0000238348.05028.14
26. Calkin AC, Cooper ME, Jandeleit-Dahm KA, Allen TJ. Gemfibrozil decreases atherosclerosis in experimental diabetes in association with a reduction in oxidative stress and inflammation. *Diabetologia.* (2006) 49:766–74. doi: 10.1007/S00125-005-0102-6
27. Ji YY, Liu JT, Liu N, Wang ZD, Liu CH. PPARalpha activator fenofibrate modulates angiotensin II-induced inflammatory responses in vascular smooth muscle cells via the TLR4-dependent signaling pathway. *Biochem Pharmacol.* (2009) 78:1186–97. doi: 10.1016/J.BCP.2009.06.095
28. Xu N, Wang Q, Jiang S, Wang Q, Hu W, Zhou S, et al. Fenofibrate improves vascular endothelial function and contractility in diabetic mice. *Redox Biol.* (2019) 20:87–97. doi: 10.1016/J.REDOX.2018.09.024
29. Amioka N, Miyoshi T. Fibrates: a possible treatment option for patients with abdominal aortic aneurysm? *Biomolecules.* (2022) 12:74. doi: 10.3390/BIOM12010074
30. Ahmad J, Odin JA, Hayashi PH, Chalasani N, Fontana RJ, Barnhart H, et al. Identification and characterization of fenofibrate-induced liver injury. *Dig Dis Sci.* (2017) 62:3596–604. doi: 10.1007/s10620-017-4812-7
31. Mychaleckyj JC, Craven T, Nayak U, Buse J, Crouse JR, Elam M, et al. Reversibility of fenofibrate therapy-induced renal function impairment in Accord type 2 diabetic participants. *Diabetes Care.* (2012) 35:1008–14. doi: 10.2337/dc11-1811
32. Ncube V, Starkey B, Wang T. Effect of fenofibrate treatment for hyperlipidaemia on serum creatinine and cystatin C. *Ann Clin Biochem.* (2012) 49:491–3. doi: 10.1258/acb.2012.011163
33. Yamamoto Y, Takei K, Arulmozhiraja S, Sladek V, Matsuo N, Han S-I, et al. Molecular association model of PPARα and its new specific and efficient ligand, pemafibrate: structural basis for SPPARMα. *Biochem Biophys Res Commun.* (2018) 499:239–45. doi: 10.1016/j.bbrc.2018.03.135
34. Raza-Iqbal S, Tanaka T, Anai M, Inagaki T, Matsumura Y, Ikeda K, et al. Transcriptome analysis of K-877 (A novel selective PPARα modulator (SPPARMα))-regulated genes in primary human hepatocytes and the mouse liver. *J Atheroscler Thromb.* (2015) 22:754–72. doi: 10.5551/jat.28720
35. Fruchart JC. Selective peroxisome proliferator-activated receptor α modulators (SPPARMα): the next generation of peroxisome proliferator-activated receptor α-agonists. *Cardiovasc Diabetol.* (2013) 12:82. doi: 10.1186/1475-2840-12-82
36. Ferri N, Corsini A, Sirtori C, Ruscica M. PPAR-α agonists are still on the rise: an update on clinical and experimental findings. *Expert Opin Investig Drugs.* (2017) 26:593–602. doi: 10.1080/13543784.2017.1312339
37. Rajagopalan S, Meng XP, Ramasamy S, Harrison DG, Galis ZS. Reactive oxygen species produced by macrophage-derived foam cells regulate the activity of vascular matrix metalloproteinases in vitro. Implications for atherosclerotic plaque stability. *J Clin Invest.* (1996) 98:2572–9. doi: 10.1172/JCI119076
38. Browatzki M, Larsen D, Pfeiffer CAM, Gehrke SG, Schmidt J, Kranzhöfer A, et al. Angiotensin II stimulates matrix metalloproteinase secretion in human vascular smooth muscle cells via nuclear factor-kappaB and activator protein 1 in a redox-sensitive manner. *J Vasc Res.* (2005) 42:415–23. doi: 10.1159/000087451
39. Cao RY, Amand T, Ford MD, Piomelli U, Funk CD. The murine angiotensin II-induced abdominal aortic aneurysm model: rupture risk and inflammatory progression patterns. *Front Pharmacol.* (2010) 1:9. doi: 10.3389/FPHAR.2010.00009
40. Sawada H, Lu HS, Cassis LA, Daugherty A. Twenty years of studying AngII (angiotensin II)-induced abdominal aortic pathologies in mice: continuing questions and challenges to provide insight into the human disease. *Arterioscler Thromb Vasc Biol.* (2022) 42:277–88. doi: 10.1161/ATVBAHA.121.317058
41. Iwase T, Tajima A, Sugimoto S, Okuda KI, Hironaka I, Kamata Y, et al. A simple assay for measuring catalase activity: a visual approach. *Sci Rep.* (2013) 3:3081. doi: 10.1038/srep03081
42. Nakamura K, Miura D, Saito Y, Yunoki K, Koyama Y, Satoh M, et al. Eicosapentaenoic acid prevents arterial calcification in klotho mutant mice. *PLoS One.* (2017) 12:e0181009. doi: 10.1371/journal.pone.0181009
43. Kanda Y. Investigation of the freely available easy-to-use software "EZR" for medical statistics. *Bone Marrow Transplant.* (2013) 48:452–8. doi: 10.1038/bmt.2012.244
44. Parastatidis I, Weiss D, Joseph G, Taylor WR. Overexpression of catalase in vascular smooth muscle cells prevents the formation of abdominal aortic aneurysms. *Arterioscler Thromb Vasc Biol.* (2013) 33:2389–96. doi: 10.1161/ATVBAHA.113.302175
45. Toyama T, Nakamura H, Harano Y, Yamauchi N, Morita A, Kirishima T, et al. PPARalpha ligands activate antioxidant enzymes and suppress hepatic fibrosis in rats. *Biochem Biophys Res Commun.* (2004) 324:697–704. doi: 10.1016/j.bbrc.2004.09.110
46. Brigadeau F, Gelé P, Wibaux M, Marquié C, Martin-Nizard F, Torpier G, et al. The PPARα activator fenofibrate slows down the progression of the left ventricular dysfunction in porcine tachycardia-induced cardiomyopathy. *J Cardiovasc Pharmacol.* (2007) 49:408–15. doi: 10.1097/FJC.0b013e3180544540
47. Tanaka Y, Kume S, Araki SI, Isshiki K, Chin-Kanasaki M, Sakaguchi M, et al. Fenofibrate, a PPARα agonist, has renoprotective effects in mice by enhancing renal lipolysis. *Kidney Int.* (2011) 79:871–82. doi: 10.1038/ki.2010.530
48. Park C, Ji HM, Kim SJ, Kil SH, Lee JN, Kwak S, et al. Fenofibrate exerts protective effects against gentamicin-induced toxicity in cochlear hair cells by activating antioxidant enzymes. *Int J Mol Med.* (2017) 39:960–8. doi: 10.3892/ijmm.2017.2916
49. Ruscica M, Corsini A, Ferri N, Banach M, Sirtori CR. Clinical approach to the inflammatory etiology of cardiovascular diseases. *Pharmacol Res.* (2020) 159:104916. doi: 10.1016/J.PHRS.2020.104916
50. Yuan Z, Lu Y, Wei J, Wu J, Yang J, Cai Z. Abdominal aortic aneurysm: roles of inflammatory cells. *Front Immunol.* (2020) 11:609161. doi: 10.3389/FIMMU.2020.609161
51. Middleton RK, Lloyd GM, Bown MJ, Cooper NJ, London NJ, Sayers RD. The pro-inflammatory and chemotactic cytokine microenvironment of the abdominal aortic aneurysm wall: a protein array study. *J Vasc Surg.* (2007) 45:574–80. doi: 10.1016/J.JVS.2006.11.020
52. Tieu BC, Ju X, Lee C, Sun H, Lejeune W, Recinos A, et al. Aortic adventitial fibroblasts participate in angiotensin-induced vascular wall inflammation and remodeling. *J Vasc Res.* (2011) 48:261–72. doi: 10.1159/000320358
53. Hennuyer N, Duplan I, Paquet C, Vanhoutte J, Woitrain E, Touche V, et al. The novel selective PPARα modulator (SPPARMα) pemafibrate improves dyslipidemia, enhances reverse cholesterol transport and decreases inflammation and atherosclerosis. *Atherosclerosis.* (2016) 249:200–8. doi: 10.1016/j.atherosclerosis.2016.03.003
54. Staels B, Koenig W, Habib A, Merval R, Lebret M, Torra IP, et al. Activation of human aortic smooth-muscle cells is inhibited by PPARα but not by PPARγ activators. *Nature.* (1998) 393:790–3. doi: 10.1038/31701
55. Marx N, Sukhova GK, Collins T, Libby P, Plutzky J. PPARalpha activators inhibit cytokine-induced vascular cell adhesion molecule-1 expression in human endothelial cells. *Circulation.* (1999) 99:3125–31. doi: 10.1161/01.CIR.99.24.3125
56. Babaev VR, Ishiguro H, Ding L, Yancey PG, Dove DE, Kovacs WJ, et al. Macrophage expression of peroxisome proliferator-activated receptor-α reduces atherosclerosis in low-density lipoprotein receptor-deficient mice. *Circulation.* (2007) 116:1404–12. doi: 10.1161/CIRCULATIONAHA.106.684704
57. Rabkin SW. The role matrix metalloproteinases in the production of aortic aneurysm. *Prog Mol Biol Transl Sci.* (2017) 147:239–65. doi: 10.1016/bs.pmbts.2017.02.002
58. Satoh K, Nigro P, Matoba T, O'Dell MR, Cui Z, Shi X, et al. Cyclophilin A enhances vascular oxidative stress and the development of angiotensin II-induced aortic aneurysms. *Nat Med.* (2009) 15:649–56. doi: 10.1038/nm.1958
59. Fruchart JC, Santos RD, Aguilar-Salinas C, Aikawa M, Al Rasadi K, Amarenco P, et al. The selective peroxisome proliferator-activated receptor alpha modulator (SPPARMα) paradigm: conceptual framework and therapeutic potential: a consensus statement from the International atherosclerosis society (IAS) and the Residual risk reduction initiative (R3i) foundation. *Cardiovasc Diabetol.* (2019) 18:71. doi: 10.1186/s12933-019-0864-7
60. Pradhan AD, Paynter NP, Everett BM, Glynn RJ, Amarenco P, Elam M, et al. Rationale and design of the pemafibrate to reduce cardiovascular outcomes

by reducing triglycerides in patients with diabetes (PROMINENT) study. *Am Heart J.* (2018) 206:80–93. doi: 10.1016/j.ahj.2018.09.011
61. Krishna SM, Morton SK, Li J, Golledge J. Risk factors and mouse models of abdominal aortic aneurysm rupture. *Int J Mol Sci.* (2020) 21:7250. doi: 10.3390/IJMS21197250
62. Krishna SM, Seto SW, Moxon JV, Rush C, Walker PJ, Norman PE, et al. Fenofibrate increases high-density lipoprotein and sphingosine 1 phosphate concentrations limiting abdominal aortic aneurysm progression in a mouse model. *Am J Pathol.* (2012) 181:706–18. doi: 10.1016/j.ajpath.2012.04.015
63. Golledge J, Cullen B, Rush C, Moran CS, Secomb E, Wood F, et al. Peroxisome proliferator-activated receptor ligands reduce aortic dilatation in a mouse model of aortic aneurysm. *Atherosclerosis.* (2010) 210:51–6. doi: 10.1016/J.ATHEROSCLEROSIS.2009.10.027
64. Ran J, Hirano T, Adachi M. Chronic ANG II infusion increases plasma triglyceride level by stimulating hepatic triglyceride production in rats. *Am J Physiol Endocrinol Metab.* (2004) 287:E955–61. doi: 10.1152/AJPENDO.00199.2004
65. Rossignoli A, Vorkapic E, Wanhainen A, Länne T, Skogberg J, Folestad E, et al. Plasma cholesterol lowering in an AngII-infused atherosclerotic mouse model with moderate hypercholesterolemia. *Int J Mol Med.* (2018) 42:471–8. doi: 10.3892/IJMM.2018.3619
66. Watt HC, Law MR, Wald NJ, Craig WY, Ledue TB, Haddow JE. Serum triglyceride: a possible risk factor for ruptured abdominal aortic aneurysm. *Int J Epidemiol.* (1998) 27:949–52. doi: 10.1093/IJE/27.6.949

Conflict of Interest: The authors declare that the research was conducted in the absence of any commercial or financial relationships that could be construed as a potential conflict of interest.

Publisher's Note: All claims expressed in this article are solely those of the authors and do not necessarily represent those of their affiliated organizations, or those of the publisher, the editors and the reviewers. Any product that may be evaluated in this article, or claim that may be made by its manufacturer, is not guaranteed or endorsed by the publisher.

frontiers | Frontiers in Cardiovascular Medicine

TYPE Review
PUBLISHED 22 July 2022
DOI 10.3389/fcvm.2022.925254

OPEN ACCESS

EDITED BY
Wen-Jun Tu,
Chinese Academy of Medical Sciences and Peking Union Medical College, China

REVIEWED BY
Sang Joon Ahn,
University of Illinois at Chicago, United States
Monica Y. Lee,
University of Illinois at Chicago, United States

*CORRESPONDENCE
Min Cheng
mincheng@wfmc.edu.cn
Yan-Xia Wang
wangyanxia6666@wfmc.edu.cn

SPECIALTY SECTION
This article was submitted to Atherosclerosis and Vascular Medicine, a section of the journal Frontiers in Cardiovascular Medicine

RECEIVED 21 April 2022
ACCEPTED 04 July 2022
PUBLISHED 22 July 2022

CITATION
Zhang W, Li Q-q, Gao H-y, Wang Y-c, Cheng M and Wang Y-X (2022) The regulation of yes-associated protein/transcriptional coactivator with PDZ-binding motif and their roles in vascular endothelium. *Front. Cardiovasc. Med.* 9:925254. doi: 10.3389/fcvm.2022.925254

The regulation of yes-associated protein/transcriptional coactivator with PDZ-binding motif and their roles in vascular endothelium

Wen Zhang[1], Qian-qian Li[1], Han-yi Gao[2], Yong-chun Wang[3], Min Cheng[4]* and Yan-Xia Wang[1]*

[1]School of Rehabilitation Medicine, Weifang Medical University, Weifang, China, [2]Department of Rehabilitation Medicine, Affiliated Hospital, Weifang Medical University, Weifang, China, [3]The Second Affiliated Hospital of Shandong University of Traditional Chinese Medicine, Jinan, China, [4]School of Basic Medicine, Weifang Medical University, Weifang, China

Normal endothelial function plays a pivotal role in maintaining cardiovascular homeostasis, while endothelial dysfunction causes the occurrence and development of cardiovascular diseases. Yes-associated protein (YAP) and its homolog transcriptional co-activator with PDZ-binding motif (TAZ) serve as crucial nuclear effectors in the Hippo signaling pathway, which are regulated by mechanical stress, extracellular matrix stiffness, drugs, and other factors. Increasing evidence supports that YAP/TAZ play an important role in the regulation of endothelial-related functions, including oxidative stress, inflammation, and angiogenesis. Herein, we systematically review the factors affecting YAP/TAZ, downstream target genes regulated by YAP/TAZ and the roles of YAP/TAZ in regulating endothelial functions, in order to provide novel potential targets and effective approaches to prevent and treat cardiovascular diseases.

KEYWORDS

YAP/TAZ, endothelial cells, oxidative stress, inflammation, angiogenesis

Introduction

The vascular endothelium is a cell layer lining the internal surface of the vascular lumen (1). Endothelial cells can sense factors acting on the vascular inner wall, such as fluid shear stress, stretch stress, and extracellular matrix (ECM) hardness, and then release nitric oxide, prostacyclin, reactive oxygen species (ROS), and other vasoactive substances to maintain the normal function of blood vessels (2, 3). Yes-associated protein (YAP) and transcriptional co-activator with PDZ-binding motif (TAZ), two closely related transcriptional regulators in the classical Hippo signaling pathway, play a crucial role in organ growth, tissue regeneration, and tumor development through the regulation of diverse transcriptional factors (4–6). Recently, researchers have found that YAP/TAZ also play an indispensable role in regulating endothelial biological functions, including inflammation, oxidative stress, and angiogenesis (7–12). In the present review, we aim to describe the YAP/TAZ structural characteristics, summarize the factors regulating YAP/TAZ, and elucidate the

downstream target genes regulated by YAP/TAZ and the effects of YAP/TAZ on vascular endothelial functions.

Structural characteristics of yes-associated protein/transcriptional co-activator with PDZ-binding motif

In 1994, Sudol identified and cloned the cDNA of a new protein that binds to the SRC homology 3 (SH3) domain of Yes proto-oncogene product through an anti-idiotypic antibody (13), and since then YAP has been discovered. Transcriptional regulators YAP and TAZ have quickly attracted the attention of researchers due to their important roles in cell growth and differentiation, tissue regeneration and repair, cancer, and cardiovascular diseases. YAP is mapped at chromosome 11q22 with a molecular weight of 65 kDa (14, 15). The N-terminal of YAP is connected to the proline-rich ligand. Because YAP lacks a DNA binding domain, it can only act as a transcriptional regulator *via* interacting with the TEAD binding domain or other transcription factors (16, 17). TEAD is a pivotal DNA binding platform of YAP and includes the 14-3-3 binding domain. The phosphorylation site of YAP at serine 127 (S127) was found to interact with 14-3-3 protein, resulting in the accumulation of YAP in the cytoplasm (18). YAP, also known as YAP1, contains eight splice isomers, and YAP1-1 and YAP1-2 are the two main isomers (15, 19, 20). The difference is that YAP1-1 has only one WW domain, while YAP1-2 contains two WW domains. The WW domain can identify the PPxY motif (proline/proline/any amino acid/tyrosine), which is present in a series of proteins known to be YAP/TAZ interactors (19). In addition, YAP harbors an SH3 binding domain that is located between the WW domain and coiled-coil domain (17). TAD is the transcriptional activation domain, and the PDZ binding domain is the C-terminal domain (**Figure 1A**).

TAZ, the paralog of YAP, was isolated as 14-3-3 binding protein, and it is located on chromosome 3q23-3q24 (14, 21). YAP and TAZ share several similar structures, but also possess distinctive structural features (**Figure 1**). The important shared structural features are the TEAD binding domain, WW domain, SH3 binding domain, Coiled-coil domain, and C-terminal transactivation domain. The main structurally distinctive feature is a proline-rich motif at the N-terminal end of YAP that is not conserved in TAZ (19) (**Figure 1B**).

YAP and TAZ are located both in the cytoplasm and nucleus. Phosphorylation of YAP/TAZ on multiple serine residues by LATS and other kinases, such as AKT and JNK contributes to YAP/TAZ inactivation and cytoplasmic accumulation (22, 23). Nevertheless, phosphorylation by c-Abl on YAP^{Y357} results in YAP/TAZ activation and the sequestration of YAP/TAZ into the nucleus (24, 25). The nuclear localization of YAP/TAZ plays a vital role in determining cell behaviors, including proliferation, differentiation, and migration.

Regulatory factors of yes-associated protein/transcriptional co-activator with PDZ-binding motif

Effect of mechanical stress on yes-associated protein/transcriptional co-activator with PDZ-binding motif

Studies have shown that YAP and TAZ are not only nuclear sensors in the Hippo pathway, but also signal carriers and amplifiers of mechanical stress in the extracellular microenvironment (26). YAP/TAZ can sense and distinguish diverse mechanical stress and trigger different biomechanical responses. Zhong et al. used a microfluidic perfusion device to demonstrate for the first time that YAP could respond to different magnitudes of shear stress (27). Subsequent studies found that the activity of YAP/TAZ could be regulated by different forms of shear stress, including laminar shear stress (LSS) and oscillatory shear stress (OSS) (28–30). On the one hand, by promoting the LATS1/2-dependent phosphorylation of YAP^{S127} in the Hippo pathway, LSS inhibited the activation of YAP to resist inflammation and maintain the stability in normal endothelial cells (28, 31). On the other hand, LSS could also down-regulate YAP activation through autophagy-dependent pathway to decrease the expression of pro-inflammatory genes and interrupt the formation of atherosclerosis plaque (32). For damaged vascular endothelium, LSS ameliorated endothelial functions by activating YAP/TAZ. For example, in the injury model of cardiac microvascular endothelial cells (CMECs), LSS increased the expression of platelet-endothelial cell adhesion molecule-1 (PECAM1) and phosphorylated endothelial nitric oxide synthase (p-eNOS). The increased PECAM1 and p-eNOS subsequently activated YAP to protect CMECs from ischemia reperfusion injury (33). However, when human umbilical vein endothelial cells (HUVECs) were exposed to OSS, it was observed that YAP/TAZ was activated and translocated from vascular actin to the nucleus. Meantime, the expression of pro-inflammatory factors, including intercellular adhesion molecule-1 (ICAM-1), vascular cell adhesion molecule-1 (VCAM-1), and interleukin-6 (IL-6) were increased (29, 34, 35), which led to vascular endothelial injury and atherosclerosis. A recent study also revealed that HUVECs in the microfluidic chip showed obvious nuclear translocation after being stimulated by OSS for 6 h.

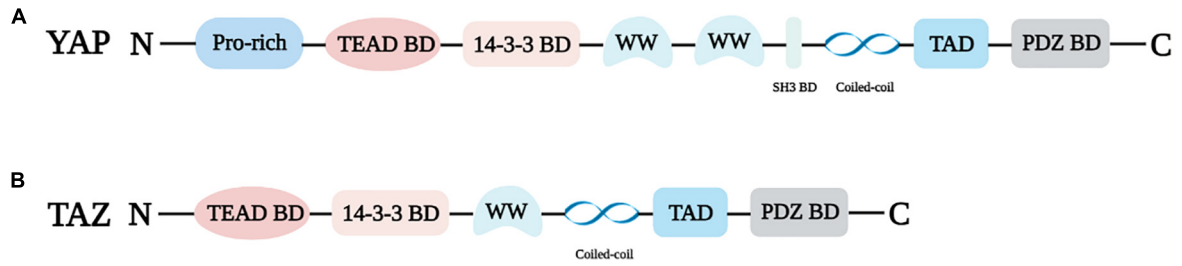

FIGURE 1
Structural properties of YAP **(A)** and TAZ **(B)**. Pro-rich: Proline-rich; TEAD BD: TEAD binding domain; 14-3-3 BD: 14-3-3 binding domain, WW: WW domain; SH3 BD: SH3 binding domain; PDZ BD: PDZ binding domain.

Moreover, the activation of YAP/TAZ in HUVECs induced a significant increase in the expression of molecules related to the occurrence and development of atherosclerosis, such as ICAM-1 and von Willebrand factor (36). In addition, when human adipose-derived microvascular endothelial cells were stimulated with 20% stretch stress based on a normal physiological condition, the nuclear to cytoplasmic ratio of YAP in the experimental group cells was significantly higher than that in the control group (37), which indicated that physiological stretch stress could also promote the activation of YAP. The above evidence shows that mechanical stress, including LSS, WSS and physiological stretch stress, could modulate the activity of YAP/TAZ. Specifically, LSS can promote YAP^{S127} phosphorylation and inactivate YAP, while OSS and physiological stretch stress are able to activate YAP. Exercise is an effective method to improve endothelial functions and maintain vascular homeostasis. Our previous study showed that pulsatile flow shear stress induced by moderate intensity exercise was a key factor in mediating vascular endothelial functions improvement (38). However, the underlying mechanism is not entirely understood. Therefore, whether exercise-induced blood flow shear stress can regulate arterial endothelial functions *via* modulating YAP/TAZ deserves further study.

Effect of extracellular matrix hardness on yes-associated protein/transcriptional co-activator with PDZ-binding motif

Extracellular matrix (ECM) hardness is one of the important factors that determine cell adhesion and diffusion processes, which also has significant impacts on cell growth, migration, and differentiation. The activation of YAP/TAZ could be modulated by the hardness of ECM (39–41). In the early report, YAP activation was observed in breast epithelial cells under the hard matrix. Dupont et al. found that the hard substrate promoted the translocation of YAP/TAZ into the nucleus, whereas the soft substrate remained YAP/TAZ in the cytoplasm (26). Afterward, Shin and Mooney compared the content of YAP in human K-562 cells under different ECM hardness and observed that the expression level of YAP in cells under the hard matrix was higher than that under the soft matrix (42), which again confirmed the previous research results. Relevant studies also pointed out that the process of ECM hardness regulating YAP not only depended on Rho GTPase activity and actin cytoskeleton tension, but also relied on Src family kinases (39, 43, 44). Recently, Deng's team found that the stiff substrate promoted the expression of focal adhesion kinase (FAK) and p-Paxillin, and then elevated the level of Rac1 in cells, contributing to the increase in cytoskeleton tissue stiffness. Subsequently, YAP was transferred to the nucleus, and the expression of target genes was up-regulated to promote the formation of endothelial tip cells (45). Similarly, Matsuo et al. confirmed that YAP activation was decreased in endothelial cells on soft substrate compared to cells on stiff substrate, and the YAP-Dll4-Notch signaling pathway was involved in modulating the effect of substrate stiffness on endothelial cell functions (46). Other studies have pointed out that the change in YAP activity induced by ECM hardness also plays a crucial role in cardiomyocyte regeneration. In addition, in the mouse myocardial infarction model, ECM protein Agrin activated YAP by up-regulating FAK and LRP4-MuSK and then promoted cardiomyocyte proliferation (47–49).

Effect of drugs on yes-associated protein/transcriptional co-activator with PDZ-binding motif

A series of drugs, including anti-atherosclerotic and anti-neoplastic drugs, have previously been found to downregulate YAP/TAZ activity in endothelial cells (25, 29, 31, 50). Anti-atherosclerotic drugs, such as rosuvastatin, simvastatin, and lovastatin, can inhibit YAP/TAZ activation to ameliorate the occurrence and development of cardiovascular diseases (29, 31, 50, 51). For example, rosuvastatin markedly attenuated YAP expression on TNF-α treatment and then decreased ICAM1 and VCAM1 expression in HUVECs, playing anti-inflammatory

and atheroprotective roles (50). Simvastatin treatment significantly suppressed YAP/TAZ activation to attenuate the disturbed flow-induced proliferation and inflammation (29, 31). Lovastatin decreased YAP/TAZ activation and diminished angiotensin II-induced cardiovascular fibrosis (52). Additionally, methotrexate, an anti-neoplastic drug, also markedly inhibited disturbed flow shear stress induced YAP/TAZ activation in an AMPK-dependent manner, and further reduced pro-inflammatory factor secretion and monocyte adhesion in HUVECs (35). Thus, inhibition of YAP/TAZ activation *via* drugs is a promising endothelial protection and athero-protective therapeutic strategy.

Bosutinib, a tyrosine kinase inhibitor, significantly decreased the level of the phosphorylation of YAP at tyrosine 357 (Y357) and YAP activation to alleviate endothelium injury and the development of atherosclerosis (25). Likewise, salvianolic acid B, harmine and tetramethylpyrazine, the extracts from the traditional medicinal plants, inhibited YAP nuclear translocation and activation, and thus played a potent atheroprotective role (8, 9, 53). These inhibitor and extracts from the traditional medicinal plants might serve as potential therapeutical candidates for improving endothelial function and cardiovascular diseases *via* regulating the YAP/TAZ pathway.

Other factors regulating yes-associated protein/transcriptional co-activator with PDZ-binding motif

In addition to the above factors, YAP and TAZ are also regulated by glucose metabolism, hypoxia, and osmotic stress (41, 54–62). Under normal physiological conditions, YAP promoted glucose metabolism by up-regulating glucose transporter 3. Phosphorylation of YAP^{S127} increased when glucose metabolism was insufficient. On the contrary, in response to high glucose stimulation, YAP was activated and unregulated, and YAP activation led to vascular endothelial inflammation and increased monocyte adhesion (41, 54–58). In myocardial fibroblasts, high glucose promoted the increase of YAP expression in the nucleus by down-regulating p-MST1 and p-LATS1, resulting in inflammation, cell proliferation, and invasion (59). High expression of YAP/TAZ and VCAM-1 and vascular intima thickening were also observed in diabetic mice (54, 60). Besides, when the cells were under hypoxia, the production of 3-hydroxymethylglutaryl CoA reductase (HMGCR) increased. The up-regulated HMGCR suppressed the activation of LATS1/2 in the Hippo signaling pathway, and further promoted YAP nuclear accumulation and induced the increase in cysteine-rich angiogenic inducer 61 (CYR61) and connective tissue growth factor (CTGF) (61, 62). In addition, osmotic stress-induced the increase in phosphorylation of YAP^{S128} through NLK kinase localized YAP/TAZ in the nucleus (63).

Taken together, LSS, soft matrix, and abovementioned drugs and potential drugs promote YAP/TAZ inactivation and cytoplasm accumulation to resist inflammation and maintain vascular homeostasis (8, 25, 27, 28, 31, 46). Whereas, OSS, physiological stretch stress, hard matrix, glucose metabolism, hypoxia, and osmotic stress lead to YAP/TAZ activation and nuclear translocation, and further stimulate the expression of their downstream target genes to cause vascular endothelial injury and atherosclerosis (26, 29, 34, 35, 54–60).

Regulation of yes-associated protein/transcriptional co-activator with PDZ-binding motif on downstream target genes

Accumulating evidence has shown that YAP/TAZ induce the expression of downstream target genes after binding with the transcription factors of the TEAD binding domain and then plays an vital role in angiogenesis, ECM remodeling and atherosclerosis by regulating cell proliferation and migration (7, 29, 39, 47, 64–68) (**Table 1**). In a study of $ApoE^{-/-}$ mice fed with high-fat diets, an abnormal increase in YAP/TAZ expression was found in endothelial cells, as well as the augmentation of CYR61, CTGF and ankyrin repeat domain 1 (ANKRD1) contents. Moreover, YAP/TAZ activation induced the up-regulation of abovementioned genes and promoted the proliferation and migration of ECs, contributing to the thickening of common carotid artery wall and narrowing of vascular cavity in mice clearly observed by HE staining. In addition, in *in vitro* cell studies, overexpression of YAP/TAZ also increased the expression levels of the abovementioned genes. Therefore, these results confirmed that CYR61, CTGF, and ANKRD1 were upregulated by YAP/TAZ activation (25, 28, 29, 31, 35). It was also observed that the expression of angiopoietin-2 (Ang-2), a regulator of angiogenesis, decreased accordingly after the targeted knockdown of YAP, revealing that Ang-2 was also unregulated by YAP activation (7, 69, 70). Likewise, target genes such as hear shock protein A12B (HSPA12B), deleted-in-liver-cancer 1 (DLC1), microfibrillar-associated protein 5 (MFAP5), cell division cycle 42 (CDC42), and delta-like ligand 4 (DLL4) were modulated by YAP to further promote vascular germination or the formation of vascular reticular structure (64, 65, 71). In addition, YAP inactivation led to the decrease in expression levels of downstream genes, such as insulin-like growth factor binding protein 3 (IGFBP3) and diaphanous homology 3 (DIAPH3), and the down-regulated IGFBP3 and DIAPH3 destroyed ECM remodeling by inhibiting the increase in ECM hardness (39, 47). In addition, YAP activation reduced the expression of tumor necrosis factor superfamily member 10 (TNFSF10) to cause cells

TABLE 1 Related downstream target genes of YAP/TAZ.

Name (abbreviation)	Expression level	Functions	References
Cysteine-rich angiogenic inducer 61 (CYR61)	↑	CYR61 promotes ECs proliferation and migration, which leads to atherosclerosis	(28, 29, 31, 84)
Connective tissue growth factor (CTGF)	↑	CTGF arouses ECs proliferation and is involved in atherogenesis	(29, 31, 84)
Ankyrin Repeat Domain 1 (ANKRD1)	↑	ANKRD1 triggers the development of atherosclerosis by promoting ECs proliferation and migration	(29, 67)
Angiopoietin-2 (Ang-2)	↑	Ang-2 regulates the germination of new blood vessels and triggers angiogenesis	(7, 70)
Heat shock protein A12B (HSPA12B)	↑	HSPA12B plays an important role in promoting ECs proliferation and regulating endothelial angiogenesis after myocardial infarction	(86)
Deleted-in-Liver-Cancer 1 (DLC1)	↑	DLC1 is crucial for sprouting angiogenesis and vascular homeostasis	(65)
Microfibrillar-associated protein 5 (MFAP5)	↑	MFAP5 promotes the tube formation of ECs	(71)
Cell division cycle 42 (CDC42)	↑	CDC42 regulates endothelial tip cell migration and promotes vascular tubular structure and morphogenesis	(95)
Diaphanous homology 3 (DIAPH3)	↑	DIAPH3 is a positive regulator in inducing ECM remodeling in cancer-associated fibroblasts	(39)
Insulin-like growth factor binding protein 3 (IGFBP3)	↑	IGFBP3 accelerates the process of ECM remodeling *via* promoting an increase in extracellular matrix stiffness	(47)
Delta-like ligand 4 (DLL4)	↑	DLL4 ameliorates damaged vascular endothelium and boosts the production of germinating blood vessels	(64)
Tumor necrosis factor superfamily member 10 (TNFSF10)	↓	TNFSF10 is considered as a regulator involved in cell apoptosis	(71, 72)

Symbols: the expression levels of each target gene in this table was in the context of YAP/TAZ upregulation; ↑, increase; ↓, decrease.

apoptosis (71, 72). In brief, YAP/TAZ activation up-regulate the abovementioned downstream target genes, including CYR61, CTGF, ANKRD1, to affect cells biological functions *via* regulating cells proliferation, migration and apoptosis.

Effect of yes-associated protein/transcriptional co-activator with PDZ-binding motif on the biological functions of the vascular endothelium

Yes-associated protein/transcriptional co-activator with PDZ-binding motif and inflammation

Atherosclerosis is the main inducer of cardiovascular diseases. Studies have confirmed that the activation of YAP/TAZ in endothelial cells plays an important role in the occurrence and development of atherosclerosis by promoting an inflammatory response (12, 67, 73, 74). Overexpression of YAP in an ApoE$^{-/-}$ mouse model upregulated the inflammatory related factors in arterial endothelial cells, such as IL-6, VCAM-1 and IL-8, and thus increased the atherosclerotic plaque and lesion range in aortic arch (8, 33). Moreover, it was found that after activating tumor necrosis factor-α (TNF-α) in HUVECs, YAP/TAZ expression was increased and transferred into the nucleus. The up-regulation of YAP/TAZ further promoted the increase in VCAM-1 and ICAM-1 in HUVECs, leading to inflammation (75). In addition, YAP/TAZ also increased monocyte adhesion by stimulating the JNK signaling pathway, triggering an inflammatory response in HUVECs (31). Yang et al. down-regulated YAP/TAZ in endothelial cells through the application of salvianolic acid B and found that inflammatory related factors, such as IL-6, IL-1β, and TNF-α, were decreased significantly, which confirmed that inhibiting YAP/TAZ reduced the expression of inflammatory factors (9). YAP/TAZ also acted as important regulators of macrophage intervention in the pro-inflammatory response and participated in the development of atherosclerosis through macrophages (73). Many researchers believe that the decrease of YAP/TAZ in cells inhibits the expression of inflammatory factors. However, Lv et al. found that the expression of E-selectin and ICAM-1 in mouse lung endothelial cells and the number of adherent neutrophils in postcapillary venules increased in mice with endothelial-specific deletion of YAP (76). This study suggested that YAP knockout did not suppress the expression of inflammatory factors, but promoted the endothelial cells activation and inflammatory response in pulmonary endothelial cells, which was inconsistent with the aforementioned studies (76). The reason of difference

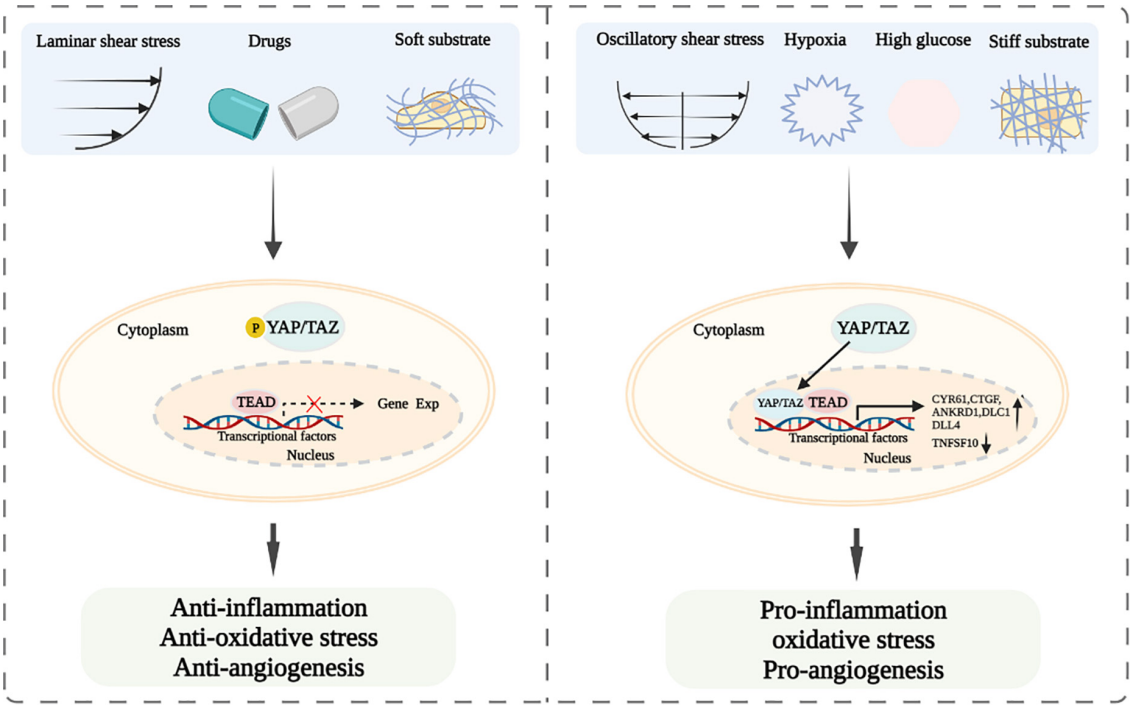

FIGURE 2
Schematic diagram of YAP/TAZ signaling and their modulation of endothelial functions after exposing to laminar and oscillatory shear stress, different drugs, soft and hard substrate, hypoxia or high glucose.

results might due to the cells observed in Lv's research was pulmonary endothelial cells, which was different from HUVECs or other types of endothelial cells used in other investigations.

Yes-associated protein/transcriptional co-activator with PDZ-binding motif and oxidative stress

The dynamic balance between the oxidation and antioxidant system plays an important role in maintaining the homeostasis of the body. Under normal circumstances, the human body has a natural antioxidant system to fight against the oxidation system. When the production of superoxide anion, hydrogen peroxide, hydroxyl radical and other oxides in the body exceeds that of superoxide dismutase (SOD), glutathione, and other antioxidants, oxidative stress occurs (77). Oxidative stress is involved in the pathogenesis of atherosclerosis. Studies have shown that YAP participated in the regulation of oxidative stress, leading to the occurrence of atherosclerosis (78–80). In human aortic endothelial cells induced by ox-LDL, after down-regulating YAP, the expression of ROS was generally reduced. The decrease in ROS alleviated the endothelial injury caused by oxidative stress (11). Other findings showed that knockdown of YAP increased the expression of Rac1 in cells, and the up-regulation of Rac1 further caused excessive production of ROS, which eventually led to cell death related to autophagy (79, 81). Consistent with these, in *in vivo* animal experiments, under the conditions of YAP inhibitors or RNAi silencing, SOD expression content in rats was significantly decreased compared to the control group (58). Additionally, a study found that the activity of YAP was affected by ROS in breast cancer cells. When ROS production was reduced, intracellular YAP and JNK activation was attenuated accordingly, leading to mitochondrial dysfunction and apoptosis (10). The results of abovementioned investigations might suggest that YAP and ROS could promote each other's activation or expression (10, 11, 76–78).

Yes-associated protein/transcriptional co-activator with PDZ-binding motif and angiogenesis

Angiogenesis is a process of forming new capillaries from pre-existing blood vessels, which involves a series of events, including endothelial cells germination, branching, lumen formation, and remodeling into a functional perfusion vascular network (82, 83). The significant role of YAP in angiogenesis has been repeatedly reported. It was found that the expression of YAP was increased in the process of differentiation from endothelial progenitor cells to endothelial cells. YAP nuclear localization further activated the vascular endothelium and

promoted neovascularization, indicating that YAP is closely related to angiogenesis (7, 40). Conversely, YAP deletion seriously hindered the formation of the vascular network structure in endothelial cells (84, 85). In the mouse model of myocardial infarction, YAP overexpression reduced myocardial injury by promoting angiogenesis, improving cardiac function, and elevating the survival rate (86, 87). However, in mice, endothelial-specific deletion of YAP/TAZ induced the reduction and deformity of filopodia at the vascular front and the decrease and disarranged distribution of tight and adherent junction proteins, leading to destruction of vascular barrier network (88). Thus, YAP was shown to be an essential factor in promoting angiogenesis and treating ischemic cardiovascular diseases. YAP binded to signal transducer and activator of transcription 3 (STAT3), resulting in the phosphorylation of STAT3 and the increase of STAT3 expression in the nucleus, which further activated downstream Ang-2 and accelerated angiogenesis (70, 85, 89). Similarly, the miR-205/YAP pathway depended on STAT3 to promote vascular germination and angiogenesis in HUVECs (90, 91). Other studies have found that the DLL4-Notch1 signaling pathway was closely related to angiogenesis. Inhibiting the DLL4-Notch1 signaling pathway promoted the expression of vascular endothelial growth factor receptor 2 (VEGFR2), and VEGFR2 regulated downstream Ang-2 by activating YAP to repair damaged vascular endothelium (46, 64, 92). The abovementioned evidence shows that YAP/TAZ play an important role in angiogenesis and are expected to become potential targets for the clinical treatment of pathological angiogenesis-related diseases.

Conclusion and perspectives

Endothelial dysfunction is one of triggers for the development of cardiovascular diseases (93, 94). YAP and TAZ are important downstream regulators of the Hippo pathway, which are involved in the regulation of vascular endothelial functions and play a prominent role in the development of cardiovascular diseases. Current studies have suggested that LSS, some drugs, and soft matrix induce YAP/TAZ inactivation and cytoplasm accumulation, resulting in the attenuating of inflammation and oxidative stress and the improvement of endothelial functions (25–29, 31). However, OSS, physiological stretch stress, and hard matrix cause YAP/TAZ activation and nuclear translocation, leading to vascular endothelial injury (34, 35, 41, 45) (**Figure 2**). Thus, modulating mechanical stress and matrix stiffness and using drugs might be served as treatment strategies for ameliorating endothelial functions. Our previous study showed that exercise-induced shear stress is a key factor to regulate endothelial function (38). However, the underlying mechanism is not entirely understood. Therefore, whether exercise-induced shear stress can improve arterial endothelial functions *via* modulating YAP/TAZ deserves further clarification. Furthermore, if YAP and TAZ mediate endothelial functions improvement under exercise-induced shear stress, whether the combined effects of exercise-induced shear stress and drugs would be achieve better synergistic effect in improving endothelial functions *via* YAP/TAZ regulation also need further study. In addition, glucose metabolism, hypoxia and osmotic stress can regulate YAP/TAZ and affect endothelial-related biological functions. However, how the abovementioned factors regulate YAP/TAZ and whether there are other downstream target genes modulated by YAP/TAZ are not well clarified. Accumulating evidence has indicated that YAP/TAZ play a central role in modulating biological functions of the vascular endothelium, including inflammation, oxidative stress, and angiogenesis (12, 67, 73–87). Whether there are other biological functions of the vascular endothelium affected by YAP/TAZ are also worthy to be further studied. Further studies of YAP/TAZ related biological functions of vascular endothelium and signal pathways will provide novel targets for the prevention and treatment of endothelial cells functions related cardiovascular diseases.

Author contributions

Y-XW and MC designed the work. WZ, Y-XW, and Q-QL drafted the manuscript. H-YG, Y-CW, and MC revised the manuscript. All authors contributed to the article and approved the submitted version.

Funding

This work was supported by the National Natural Science Foundation of China (Grant Nos. 32000927 and 81870237) and Shandong Province Natural Science Foundation (Grant No. ZR2020QC092).

Conflict of interest

The authors declare that the research was conducted in the absence of any commercial or financial relationships that could be construed as a potential conflict of interest.

Publisher's note

References

1. Rajendran P, Rengarajan T, Thangavel J, Nishigaki Y, Sakthisekaran D, Sethi G, et al. The vascular endothelium and human diseases. *Int J Biol Sci.* (2013) 9:1057–69. doi: 10.7150/ijbs.7502

2. Hsieh HJ, Liu CA, Huang B, Tseng AH, Wang DL. Shear-Induced endothelial mechanotransduction: the interplay between reactive oxygen species (Ros) and nitric oxide (No) and the pathophysiological implications. *J Biomed Sci.* (2014) 21:3. doi: 10.1186/1423-0127-21-3

3. Russell-Puleri S, Ebong EE, Tarbell JM. "Mechanisms of flow-dependent endothelial Cox-2 and Pgi2 expression,"in *Proceedings of the 2014 40th Annual Northeast Bioengineering Conference (NEBEC)*, (Piscataway, NJ: IEEE) (2014).

4. Moya IM, Halder G. Hippo–Yap/taz signalling in organ regeneration and regenerative medicine. *Nat Rev Mol Cell Biol.* (2018) 20:211–26. doi: 10.1038/s41580-018-0086-y

5. Pan D. The hippo signaling pathway in development and cancer. *Dev Cell.* (2010) 19:491–505. doi: 10.1016/j.devcel.2010.09.011

6. Klaihmon P, Lorthongpanich C, Kheolamai P, Luanpitpong S, Issaragrisil S. Distinctive roles of yap and taz in human endothelial progenitor cells growth and functions. *Biomedicines.* (2022) 10:147. doi: 10.3390/biomedicines10010147

7. Choi HJ, Zhang H, Park H, Choi KS, Lee HW, Agrawal V, et al. Yes-Associated protein regulates endothelial cell contact-mediated expression of angiopoietin-2. *Nat Commun.* (2015) 6:6943. doi: 10.1038/ncomms7943

8. Yang Y, Ma Q, Li Z, Wang H, Zhang C, Liu Y, et al. Harmine alleviates atherogenesis by inhibiting disturbed flow-mediated endothelial activation *via* protein tyrosine phosphatase ptpn14 and yap. *Br J Pharmacol.* (2021) 178:1524–40. doi: 10.1111/bph.15378

9. Yang Y, Pei K, Zhang Q, Wang D, Feng H, Du Z, et al. Salvianolic acid B ameliorates atherosclerosis *via* inhibiting Yap/Taz/Jnk signaling pathway in endothelial cells and pericytes. *Biochim Biophys Acta Mol Cell Biol Lipids.* (2020) 1865:158779. doi: 10.1016/j.bbalip.2020.158779

10. Wang L, Wang C, Tao Z, Zhao L, Zhu Z, Wu W, et al. Curcumin derivative Wz35 inhibits tumor cell growth *via* ros-yap-jnk signaling pathway in breast cancer. *J Exp Clin Cancer Res.* (2019) 38:460. doi: 10.1186/s13046-019-1424-4

11. Xie T, Wang C, Jin Y, Meng Q, Liu Q, Wu J, et al. Coenzymeq10-Induced activation of ampk-yap-opa1 pathway alleviates atherosclerosis by improving mitochondrial function. Inhibiting oxidative stress and promoting energy metabolism. *Front Pharmacol.* (2020) 11:1034. doi: 10.3389/fphar.2020.01034

12. Xu K, Zhao H, Qiu X, Liu X, Zhao F, Zhao Y. Vgll4 protects against oxidized-ldl-induced endothelial cell dysfunction and inflammation by activating hippo-Yap/Tead1 signaling pathway. *Mediators Inflamm.* (2020) 2020:8292173. doi: 10.1155/2020/8292173

13. Sudol M. Yes-Associated protein (Yap65) is a proline-rich phosphoprotein that binds to the sh3 domain of the yes proto-oncogene product. *Oncogene.* (1994) 9:2145–52.

14. Chen YA, Lu CY, Cheng TY, Pan SH, Chen HF, Chang NS. WW domain-containing proteins yap and taz in the hippo pathway as key regulators in stemness maintenance, tissue homeostasis, and tumorigenesis. *Front Oncol.* (2019) 9:60. doi: 10.3389/fonc.2019.00060

15. Sudol M, Bork P, Einbond A, Kastury K, Druck T, Negrini M, et al. Characterization of the mammalian yap (yes-associated protein) gene and its role in defining a novel protein module, the Ww domain. *J Biol Chem.* (1995) 270:14733–41. doi: 10.1074/jbc.270.24.14733

16. Zhao B, Lei QY, Guan KL. The hippo-yap pathway: new connections between regulation of organ size and cancer. *Curr Opin Cell Biol.* (2008) 20:638–46. doi: 10.1016/j.ceb.2008.10.001

17. Reggiani F, Gobbi G, Ciarrocchi A, Sancisi V. Yap and Taz are not identical twins. *Trends Biochem Sci.* (2020) 46:154–68. doi: 10.1016/j.tibs.2020.08.012

18. Yu Y, Su X, Qin Q, Hou Y, Zhang X, Zhang H, et al. Yes-Associated protein and transcriptional coactivator with pdz-binding motif as new targets in cardiovascular diseases. *Pharmacol Res.* (2020) 159:105009. doi: 10.1016/j.phrs.2020.105009

19. Sudol M. Yap1 oncogene and its eight isoforms. *Oncogene.* (2013) 32:3922. doi: 10.1038/onc.2012.520

20. Komuro A, Nagai M, Navin NE, Sudol M. Ww domain-containing protein yap associates with Erbb-4 and acts as a co-transcriptional activator for the carboxyl-terminal fragment of Erbb-4 that translocates to the nucleus. *J Biol Chem.* (2003) 278:33334–41. doi: 10.1074/jbc.M305597200

21. Kanai F, Marignani PA, Sarbassova D, Yagi R, Hall RA, Donowitz M, et al. Taz: a novel transcriptional co-activator regulated by interactions with 14-3-3 and pdz domain proteins. *Embo J.* (2000) 19:6778–91. doi: 10.1093/emboj/19.24.6778

22. Piccolo S, Dupont S, Cordenonsi M. The biology of Yap/Taz: hippo signaling and beyond. *Physiol Rev.* (2014) 94:1287–312. doi: 10.1152/physrev.00005.2014

23. Zhao B, Li L, Tumaneng K, Wang CY, Guan KLA. Coordinated phosphorylation by lats and ck1 regulates yap stability through scf(Beta-Trcp). *Genes Dev.* (2010) 24:72–85. doi: 10.1101/gad.1843810

24. Levy D, Adamovich Y, Reuven N, Shaul Y. Yap1 Phosphorylation by C-Abl Is a Critical Step in Selective Activation of Proapoptotic Genes in Response to DNA Damage. *Mol Cell.* (2008) 29:350–61. doi: 10.1016/j.molcel.2007.12.022

25. Li B, He J, Lv H, Liu Y, Lv X, Zhang C, et al. C-Abl regulates yapy357 phosphorylation to activate endothelial atherogenic responses to disturbed flow. *J Clin Invest.* (2019) 129:1167–79. doi: 10.1172/JCI122440

26. Dupont S, Morsut L, Aragona M, Enzo E, Giulitti S, Cordenonsi M, et al. Role of Yap/Taz in Mechanotransduction. *Nature.* (2011) 474:179–83. doi: 10.1038/nature10137

27. Zhong W, Tian K, Zheng X, Li L, Zhang W, Wang S, et al. Mesenchymal stem cell and chondrocyte fates in a multishear microdevice are regulated by yes-associated protein. *Stem Cells Dev.* (2013) 22:2083–93. doi: 10.1089/scd.2012.0685

28. Xu S, Koroleva M, Yin M, Jin ZG. Atheroprotective laminar flow inhibits hippo pathway effector yap in endothelial cells. *Transl Res.* (2016) 176:18–28.e2. doi: 10.1016/j.trsl.2016.05.003

29. Wang KC, Yeh YT, Nguyen P, Limqueco E, Lopez J, Thorossian S, et al. Flow-dependent Yap/Taz activities regulate endothelial phenotypes and atherosclerosis. *Proc Natl Acad Sci U.S.A.* (2016) 113:11525–30. doi: 10.1073/pnas.1613121113

30. Chitragari G, Shalaby SY, Sumpio BJ, Kurita J, Sumpio BE. Regulation of yes-associated protein by laminar flow. *Ann Vasc Surg.* (2018) 52:183–91. doi: 10.1016/j.avsg.2018.03.002

31. Wang L, Luo JY, Li B, Tian XY, Chen LJ, Huang Y, et al. Integrin-YAP/TAZ-JNK cascade mediates atheroprotective effect of unidirectional shear flow. *Nature.* (2016) 540:579–82. doi: 10.1038/nature20602

32. Yuan P, Hu Q, He X, Long Y, Song X, Wu F, et al. Laminar flow inhibits the hippo/yap pathway *via* autophagy and sirt1-mediated deacetylation against atherosclerosis. *Cell Death Dis.* (2020) 11:141. doi: 10.1038/s41419-020-2343-1

33. Zhang Q, Cao Y, Liu Y, Huang W, Ren J, Wang P, et al. Shear stress inhibits cardiac microvascular endothelial cells apoptosis to protect against myocardial ischemia reperfusion injury *via* Yap/Mir-206/Pdcd4 signaling pathway. *Biochem Pharmacol.* (2021) 186:114466. doi: 10.1016/j.bcp.2021.114466

34. Nakajima H, Yamamoto K, Agarwala S, Terai K, Fukui H, Fukuhara S, et al. Flow-dependent endothelial yap regulation contributes to vessel maintenance. *Dev Cell.* (2017) 40:523–36.e6. doi: 10.1016/j.devcel.2017.02.019

35. Liu D, Lv H, Liu Q, Sun Y, Hou S, Zhang L, et al. Atheroprotective effects of methotrexate *via* the inhibition of Yap/Taz under disturbed flow. *J Transl Med.* (2019) 17:378. doi: 10.1186/s12967-019-02135-8

36. Walther BK, Rajeeva Pandian NK, Gold KA, Kiliç ES, Sama V, Gu J, et al. Mechanotransduction-on-Chip: vessel-chip model of endothelial yap mechanobiology reveals matrix stiffness impedes shear response. *Lab Chip.* (2021) 21:1738–51. doi: 10.1039/d0lc01283a

37. Landau S, Ben-Shaul S, Levenberg S. Oscillatory strain promotes vessel stabilization and alignment through fibroblast yap-mediated mechanosensitivity. *Adv Sci.* (2018) 5:1800506. doi: 10.1002/advs.201800506

38. Wang YX, Liu HB, Li PS, Yuan WX, Liu B, Liu ST, et al. Ros and no dynamics in endothelial cells exposed to exercise-induced wall shear stress. *Cell Mol Bioeng.* (2019) 12:107–20. doi: 10.1007/s12195-018-00557-w

39. Calvo F, Ege N, Grande-Garcia A, Hooper S, Jenkins RP, Chaudhry SI, et al. Mechanotransduction and Yap-dependent matrix remodelling is required for the generation and maintenance of cancer-associated fibroblasts. *Nat Cell Biol.* (2013) 15:637–46. doi: 10.1038/ncb2756

40. Jiang X, Hu J, Wu Z, Cafarello ST, Di Matteo M, Shen Y, et al. Protein phosphatase 2a mediates Yap activation in endothelial cells upon vegf stimulation and matrix stiffness. *Front Cell Dev Biol.* (2021) 9:675562. doi: 10.3389/fcell.2021.675562

41. Liu Y, Li M, Lv X, Bao K, Yu Tian X, He L, et al. Yes-associated protein targets the transforming growth factor β pathway to mediate high-fat/high-sucrose diet-induced arterial stiffness. *Circ Res.* (2022) 130:851–67. doi: 10.1161/circresaha.121.320464

42. Shin JW, Mooney DJ. Extracellular matrix stiffness causes systematic variations in proliferation and chemosensitivity in myeloid leukemias. *Proc Natl Acad Sci U.S.A.* (2016) 113:12126–31. doi: 10.1073/pnas.1611338113

43. Yamashiro Y, Thang BQ, Ramirez K, Shin SJ, Kohata T, Ohata S, et al. Matrix mechanotransduction mediated by Thrombospondin-1/Integrin/Yap in the vascular remodeling. *Proc Natl Acad Sci U.S.A.* (2020) 117:9896–905. doi: 10.1073/pnas.1919702117

44. Ma H, Wang J, Zhao X, Wu T, Huang Z, Chen D, et al. Periostin promotes colorectal tumorigenesis through integrin-fak-src pathway-mediated Yap/Taz activation. *Cell Rep.* (2020) 30:793–806. doi: 10.1016/j.celrep.2019.12.075

45. Guo Y, Mei F, Huang Y, Ma S, Wei Y, Zhang X, et al. Matrix stiffness modulates tip cell formation through the P-Pxn-Rac1-Yap signaling axis. *Bioact Mater.* (2021) 7:364–76. doi: 10.1016/j.bioactmat.2021.05.033

46. Matsuo E, Okamoto T, Ito A, Kawamoto E, Asanuma K, Wada K, et al. Substrate stiffness modulates endothelial cell function *via* the Yap-Dll4-Notch1 pathway. *Exp Cell Res.* (2021) 408:112835. doi: 10.1016/j.yexcr.2021.112835

47. Chakraborty S, Njah K, Pobbati AV, Lim YB, Raju A, Lakshmanan M, et al. Agrin as a mechanotransduction signal regulating Yap through the hippo pathway. *Cell Rep.* (2017) 18:2464–79. doi: 10.1016/j.celrep.2017.02.041

48. Wang X, Senapati S, Akinbote A, Gnanasambandam B, Park PS, Senyo SE. Microenvironment stiffness requires decellularized cardiac extracellular matrix to promote heart regeneration in the neonatal mouse heart. *Acta Biomater.* (2020) 113:380–92. doi: 10.1016/j.actbio.2020.06.032

49. Bassat E, Mutlak YE, Genzelinakh A, Shadrin IY, Baruch Umansky K, Yifa O, et al. The extracellular matrix protein agrin promotes heart regeneration in mice. *Nature.* (2017) 547:179–84. doi: 10.1038/nature22978

50. Jia M, Li Q, Guo J, Shi W, Zhu L, Huang Y, et al. Deletion of bach1 attenuates atherosclerosis by reducing endothelial inflammation. *Circ Res.* (2022) 130:1038–55. doi: 10.1161/circresaha.121.319540

51. Sorrentino G, Ruggeri N, Specchia V, Cordenonsi M, Mano M, Dupont S, et al. Metabolic control of Yap and Taz by the mevalonate pathway. *Nat Cell Biol.* (2014) 16:357–66. doi: 10.1038/ncb2936

52. Wu P, Liu Z, Zhao T, Xia F, Gong L, Zheng Z, et al. Lovastatin attenuates angiotensin ii induced cardiovascular fibrosis through the suppression of Yap/Taz signaling. *Biochem Biophys Res Commun.* (2019) 512:736–41. doi: 10.1016/j.bbrc.2019.03.158

53. Zhu X, Shan Y, Yu M, Shi J, Tang L, Cao H, et al. Tetramethylpyrazine ameliorates peritoneal angiogenesis by regulating Vegf/Hippo/Yap signaling. *Front Pharmacol.* (2021) 12:649581. doi: 10.3389/fphar.2021.649581

54. Ortillon J, Le Bail JC, Villard E, Léger B, Poirier B, Girardot C, et al. High glucose activates Yap signaling to promote vascular inflammation. *Front Physiol.* (2021) 12:665994. doi: 10.3389/fphys.2021.665994

55. Wang W, Xiao ZD, Li X, Aziz KE, Gan B, Johnson RL, et al. Ampk modulates hippo pathway activity to regulate energy homeostasis. *Nat Cell Biol.* (2015) 17:490–9. doi: 10.1038/ncb3113

56. Mo JS, Meng Z, Kim YC, Park HW, Hansen CG, Kim S, et al. Cellular energy stress induces ampk-mediated regulation of Yap and the hippo pathway. *Nat Cell Biol.* (2015) 17:500–10. doi: 10.1038/ncb3111

57. Wei F, Wang A, Wang Q, Han W, Rong R, Wang L, et al. Plasma endothelial cells-derived extracellular vesicles promote wound healing in diabetes through Yap and the Pi3k/Akt/Mtor pathway. *Aging.* (2020) 12:12002–18. doi: 10.18632/aging.103366

58. Yu S, Dong X, Yang M, Yu Q, Xiong J, Chen J, et al. (Pro)Renin receptor involves in myocardial fibrosis and oxidative stress in diabetic cardiomyopathy *via* the Prr-Yap pathway. *Sci Rep.* (2021) 11:3259. doi: 10.1038/s41598-021-82776-2

59. Liu J, Xu L, Zhan X. Lncrna malat1 regulates diabetic cardiac fibroblasts through the hippo-Yap signaling pathway. *Biochem Cell Biol.* (2020) 98:537–47. doi: 10.1139/bcb-2019-0434

60. Chao ML, Luo S, Zhang C, Zhou X, Zhou M, Wang J, et al. S-Nitrosylation-mediated coupling of G-protein alpha-2 with Cxcr5 induces hippo/Yap-dependent diabetes-accelerated atherosclerosis. *Nat Commun.* (2021) 12:4452. doi: 10.1038/s41467-021-24736-y

61. Zhao C, Zeng C, Ye S, Dai X, He Q, Yang B, et al. Yes-Associated protein (Yap) and transcriptional coactivator with a Pdz-binding motif (Taz): a nexus between hypoxia and cancer. *Acta Pharm Sin B.* (2020) 10:947–60. doi: 10.1016/j.apsb.2019.12.010

62. Zhang X, Li Y, Ma Y, Yang L, Wang T, Meng X, et al. Yes-Associated protein (Yap) binds to hif-1α and sustains hif-1α protein stability to promote hepatocellular carcinoma cell glycolysis under hypoxic stress. *J Exp Clin Cancer Res.* (2018) 37:216. doi: 10.1186/s13046-018-0892-2

63. Hong AW, Meng Z, Yuan HX, Plouffe SW, Moon S, Kim W, et al. Osmotic stress-induced phosphorylation by Nlk at ser128 activates Yap. *EMBO Rep.* (2017) 18:72–86. doi: 10.15252/embr.201642681

64. Yasuda D, Kobayashi D, Akahoshi N, Ohto-Nakanishi T, Yoshioka K, Takuwa Y, et al. Lysophosphatidic acid-induced Yap/Taz activation promotes developmental angiogenesis by repressing notch ligand Dll4. *J Clin Invest.* (2019) 129:4332–49. doi: 10.1172/jci121955

65. van der Stoel M, Schimmel L, Nawaz K, van Stalborch AM, de Haan A, Klaus-Bergmann A, et al. Dlc1 is a direct target of activated Yap/Taz that drives collective migration and sprouting angiogenesis. *J Cell Sci.* (2020) 133:jcs239947. doi: 10.1242/jcs.239947

66. Shen Z, Stanger BZ. Yap regulates S-phase entry in endothelial cells. *PLoS One.* (2015) 10:e0117522. doi: 10.1371/journal.pone.0117522

67. Coleman PR, Lay AJ, Ting KK, Zhao Y, Li J, Jarrah S, et al. Yap and the rhoc regulator arhgap18, are required to mediate flow-dependent endothelial cell alignment. *Cell Commun Signal.* (2020) 18:18. doi: 10.1186/s12964-020-0511-7

68. Rausch V, Bostrom JR, Park J, Bravo IR, Feng Y, Hay DC, et al. The hippo pathway regulates caveolae expression and mediates flow response *via* caveolae. *Curr Biol.* (2019) 29:242–55. doi: 10.1016/j.cub.2018.11.066

69. Huang Y, Pan M, Shu H, He B, Zhang F, Sun L. Vascular endothelial growth factor enhances tendon-bone healing by activating yes-associated protein for angiogenesis induction and rotator cuff reconstruction in rats. *J Cell Biochem.* (2020) 121:2343–53. doi: 10.1002/jcb.29457

70. He J, Bao Q, Zhang Y, Liu M, Lv H, Liu Y, et al. Yes-associated protein promotes angiogenesis *via* signal transducer and activator of transcription 3 in endothelial cells. *Circ Res.* (2018) 122:591–605. doi: 10.1161/circresaha.117.311950

71. Marti P, Stein C, Blumer T, Abraham Y, Dill MT, Pikiolek M, et al. Yap promotes proliferation, chemoresistance, and angiogenesis in human cholangiocarcinoma through tead transcription factors. *Hepatology.* (2015) 62:1497–510. doi: 10.1002/hep.27992

72. Wang S, El-Deiry WS. Trail and apoptosis induction by tnf-family death receptors. *Oncogene.* (2003) 22:8628–33. doi: 10.1038/sj.onc.1207232

73. Mia MM, Cibi DM, Abdul Ghani SAB, Song W, Tee N, Ghosh S, et al. Yap/Taz deficiency reprograms macrophage phenotype and improves infarct healing and cardiac function after myocardial infarction. *PLoS Biol.* (2020) 18:e3000941. doi: 10.1371/journal.pbio.3000941

74. Xu Q, Zhuo K, Cai R, Su X, Zhang L, Liu Y, et al. Activation of yes-associated protein/Pdz-binding motif pathway contributes to endothelial dysfunction and vascular inflammation in angiotensinii hypertension. *Front Physiol.* (2021) 12:732084. doi: 10.3389/fphys.2021.732084

75. Choi HJ, Kim NE, Kim BM, Seo M, Heo JH. TNF-α-induced Yap/Taz activity mediates leukocyte-endothelial adhesion by regulating vcam1 expression in endothelial cells. *Int J Mol Sci.* (2018) 19:3428. doi: 10.3390/ijms19113428

76. Lv Y, Kim K, Sheng Y, Cho J, Qian Z, Zhao YY, et al. Yap controls endothelial activation and vascular inflammation through Traf6. *Circ Res.* (2018) 123:43–56. doi: 10.1161/circresaha.118.313143

77. Kattoor AJ, Pothineni NVK, Palagiri D, Mehta JL. Oxidative stress in atherosclerosis. *Curr Atheroscler Rep.* (2017) 19:42. doi: 10.1007/s11883-017-0678-6

78. Shao D, Zhai P, Del Re DP, Sciarretta S, Yabuta N, Nojima H, et al. A functional interaction between hippo-Yap signalling and foxo1 mediates the oxidative stress response. *Nat Commun.* (2014) 5:3315. doi: 10.1038/ncomms4315

79. Zhou Y, Wang Y, Zhou W, Chen T, Wu Q, Chutturghoon VK, et al. Yap promotes multi-drug resistance and inhibits autophagy-related cell death in hepatocellular carcinoma *via* the Rac1-Ros-Mtor pathway. *Cancer Cell Int.* (2019) 19:179. doi: 10.1186/s12935-019-0898-7

80. Marchio P, Guerra-Ojeda S, Vila JM, Aldasoro M, Victor VM, Mauricio MD. Targeting Early atherosclerosis: a focus on oxidative stress and inflammation. *Oxid Med Cell Longev.* (2019) 2019:8563845. doi: 10.1155/2019/8563845

81. Patel S, Tang J, Overstreet JM, Anorga S, Lian F, Arnouk A, et al. Rac-Gtpase promotes fibrotic Tgf-B1 signaling and chronic kidney disease *via* egfr. P53, and Hippo/Yap/Taz pathways. *Faseb J.* (2019) 33:9797–810. doi: 10.1096/fj.201802489RR

82. Potente M, Gerhardt H, Carmeliet P. Basic and therapeutic aspects of angiogenesis. *Cell.* (2011) 146:873–87. doi: 10.1016/j.cell.2011.08.039

83. Chung AS, Ferrara N. Developmental and pathological angiogenesis. *Annu Rev Cell Dev Biol.* (2011) 27:563–84. doi: 10.1146/annurev-cellbio-092910-154002

84. Yan Z, Shi H, Zhu R, Li L, Qin B, Kang L, et al. Inhibition of Yap ameliorates choroidal neovascularization via inhibiting endothelial cell proliferation. *Mol Vis.* (2018) 24:83–93.

85. Zhu M, Liu X, Wang Y, Chen L, Wang L, Qin X, et al. Yap via interacting with stat3 regulates vegf-induced angiogenesis in human retinal microvascular endothelial cells. *Exp Cell Res.* (2018) 373:155–63. doi: 10.1016/j.yexcr.2018.10.007

86. Fan M, Yang K, Wang X, Wang Y, Tu F, Ha T, et al. Endothelial cell Hspa12b and yes-associated protein cooperatively regulate angiogenesis following myocardial infarction. *JCI Insight.* (2020) 5:e139640. doi: 10.1172/jci.insight.139640

87. Lin Z, von Gise A, Zhou P, Gu F, Ma Q, Jiang J, et al. Cardiac-specific yap activation improves cardiac function and survival in an experimental murine mi model. *Circ Res.* (2014) 115:354–63. doi: 10.1161/circresaha.115.303632

88. Kim J, Kim YH, Kim J, Park DY, Bae H, Lee DH, et al. Yap/Taz regulates sprouting angiogenesis and vascular barrier maturation. *J Clin Invest.* (2017) 127:3441–61. doi: 10.1172/jci93825

89. Fan X, Shan X, Jiang S, Wang S, Zhang F, Tian Q, et al. Yap promotes endothelial barrier repair by repressing Stat3/Vegf signaling. *Life Sci.* (2020) 256:117884. doi: 10.1016/j.lfs.2020.117884

90. Du YE, Tu G, Yang G, Li G, Yang D, Lang L, et al. Mir-205/Yap1 in activated fibroblasts of breast tumor promotes vegf-independent angiogenesis through stat3 signaling. *Theranostics.* (2017) 7:3972–88. doi: 10.7150/thno.18990

91. Shen Y, Wang X, Liu Y, Singhal M, Gürkaşlar C, Valls AF, et al. Stat3-Yap/Taz signaling in endothelial cells promotes tumor angiogenesis. *Sci Signal.* (2021) 14:eabj8393. doi: 10.1126/scisignal.abj8393

92. Hultgren NW, Fang JS, Ziegler ME, Ramirez RN, Phan DTT, Hatch MMS, et al. Slug regulates the Dll4-Notch-Vegfr2 axis to control endothelial cell activation and angiogenesis. *Nat Commun.* (2020) 11:5400. doi: 10.1038/s41467-020-18633-z

93. Gimbrone MA Jr, García-Cardeña G. Endothelial cell dysfunction and the pathobiology of atherosclerosis. *Circ Res.* (2016) 118:620–36. doi: 10.1161/circresaha.115.306301

94. Bai T, Li M, Liu Y, Qiao Z, Wang Z. Inhibition of ferroptosis alleviates atherosclerosis through attenuating lipid peroxidation and endothelial dysfunction in mouse aortic endothelial cell. *Free Radic Biol Med.* (2020) 160:92–102. doi: 10.1016/j.freeradbiomed.2020.07.026

95. Sakabe M, Fan J, Odaka Y, Liu N, Hassan A, Duan X, et al. Yap/Taz-Cdc42 signaling regulates vascular tip cell migration. *Proc Natl Acad Sci U.S.A.* (2017) 114:10918–23. doi: 10.1073/pnas.1704030114

frontiers | Frontiers in Cardiovascular Medicine

TYPE Systematic Review
PUBLISHED 27 July 2022
DOI 10.3389/fcvm.2022.936817

OPEN ACCESS

EDITED BY
Mark Slevin,
Manchester Metropolitan University, United Kingdom

REVIEWED BY
Natalia G. Vallianou,
Evaggelismos General Hospital, Greece
Xiaolong Wang,
Shanghai University of Traditional Chinese Medicine, China
Wei Mao,
Zhejiang Chinese Medical University, China

*CORRESPONDENCE
Jianqing Ju
jujianqing@163.com
Hao Xu
xuhaotcm@hotmail.com

†These authors have contributed equally to this work and share first authorship

SPECIALTY SECTION
This article was submitted to Atherosclerosis and Vascular Medicine, a section of the journal Frontiers in Cardiovascular Medicine

RECEIVED 05 May 2022
ACCEPTED 04 July 2022
PUBLISHED 27 July 2022

CITATION
Zhang J, Wang X, Tian W, Wang T, Jia J, Lai R, Wang T, Zhang Z, Song L, Ju J and Xu H (2022) The effect of various types and doses of statins on C-reactive protein levels in patients with dyslipidemia or coronary heart disease: A systematic review and network meta-analysis. *Front. Cardiovasc. Med.* 9:936817. doi: 10.3389/fcvm.2022.936817

The effect of various types and doses of statins on C-reactive protein levels in patients with dyslipidemia or coronary heart disease: A systematic review and network meta-analysis

Jie Zhang[1,2†], Xinyi Wang[1,3†], Wende Tian[1,3], Tongxin Wang[1,2], Jundi Jia[1,2], Runmin Lai[1,3], Tong Wang[1,2], Zihao Zhang[1,2], Luxia Song[1,2], Jianqing Ju[1*] and Hao Xu[1*]

[1]National Clinical Research Center for Chinese Medicine Cardiology, Xiyuan Hospital, China Academy of Chinese Medical Sciences, Beijing, China, [2]Graduate School, Beijing University of Chinese Medicine, Beijing, China, [3]Graduate School, China Academy of Chinese Medical Sciences, Beijing, China

Objective: The objective of this study was to measure the efficacy of various types and dosages of statins on C-reactive protein (CRP) levels in patients with dyslipidemia or coronary heart disease.

Methods: Randomized controlled trials were searched from PubMed, Embase, Cochrane Library, OpenGray, and ClinicalTrials.gov. We followed the Preferred Reporting Items for Systematic Reviews and Meta-Analyses guidelines for data extraction and synthesis. The pairwise meta-analysis compared statins and controls using a random-effects model, and a network meta-analysis compared the types and dosages of statins using the Bayesian random-effects model. The PROSPERO registration number is CRD42021242067.

Results: The study included 37 randomized controlled trials with 17,410 participants and 20 interventions. According to the pairwise meta-analysis, statins significantly decreased CRP levels compared to controls (weighted mean difference [WMD] = −0.97, 95% confidence interval [CI] [−1.31, −0.64], $P < 0.0001$). In the network meta-analysis, simvastatin 40 mg/day appeared to be the best strategy for lowering CRP (Rank $P = 0.18$, WMD = −4.07, 95% CI = [−6.52, −1.77]). The same was true for the high-sensitivity CRP, non-acute coronary syndrome (ACS), <12 months duration, and clear measurement subgroups. In the CRP subgroup (rank $P = 0.79$, WMD = −1.23, 95% CI = [−2.48, −0.08]) and ≥12-month duration subgroup (Rank $P = 0.40$, WMD = −2.13, 95% CI = [−4.24, −0.13]), atorvastatin 80 mg/day was most likely to be the best. There were no significant differences in the dyslipidemia and ACS subgroups ($P > 0.05$). Node-splitting analysis showed no significant inconsistency ($P > 0.05$), except for the coronary heart disease subgroup.

Conclusion: Statins reduced serum CRP levels in patients with dyslipidemia or coronary heart disease. Simvastatin 40 mg/day might be the most effective therapy, and atorvastatin 80 mg/day showed the best long-term effect. This study provides a reference for choosing statin therapy based on LDL-C and CRP levels.

KEYWORDS

statin, C-reactive protein, coronary heart disease, dyslipidemia, network meta-analysis

The chemical compounds studied in this article

Atorvastatin (PubChem CID: 60823); Pravastatin (PubChem CID: 54687); Pitavastatin (PubChem CID: 5282452); Rosuvastatin (PubChem CID: 446157); Simvastatin (PubChem CID: 54454).

Introduction

Dyslipidemia is the primary risk factor and a prerequisite for atherosclerotic cardiovascular disease (ASCVD) (1). Long-term prospective epidemiological studies have consistently demonstrated the critical role of managing dyslipidemia in reducing ASCVD morbidity and mortality (2). Nevertheless, cardiovascular events continue to occur even with a substantial reduction in low-density lipoprotein cholesterol (LDL-C) (3). Coronary heart disease (CHD) is a chronic inflammatory disease in which inflammation involves the entire process from plaque formation to rupture (4, 5). Recently, clinical trials using anti-inflammatory drugs [e.g., canakinumab (6) and colchicine (7, 8)] confirmed the direct vasculo-protective effects of primarily targeting inflammation, which may partly explain the residual risk after the normalization of LDL-C. These findings suggest that anti-inflammatory therapy provides insights into treating CHD in addition to lipid-lowering.

Statins (i.e., 3-hydroxy-methylglutaryl coenzyme A [HMG-CoA] reductase inhibitors) are used to lower cholesterol in the primary and secondary prevention of ASCVD (9). Their primary effect is to lower serum cholesterol levels by competitively inhibiting HMG-CoA reductase, thereby inhibiting hepatic cholesterol biosynthesis (9, 10). Furthermore, statins exert cardiovascular protective effects independent of lowering LDL-C (called "pleiotropic" effects) with anti-inflammatory effects that are attracting attention (11).

C-reactive protein (CRP) is a pentameric protein consisting of five identical non-covalently bound subunits of 206 amino acid residues (12). It is a major acute-phase protein in humans, a multifunctional component of the human innate host defense mechanism (12), and an indicator and predictor of ASCVD risk associated with inflammation (13, 14). CRP and high-sensitivity CRP (hs-CRP) were used for measuring the same substance, while hs-CRP is more sensitive than CRP at low CRP levels (15). The measurements include immunoturbidimetry, nephelometry, enzyme-linked immunosorbent assay, chemiluminescent enzyme immunometric assay, and radial immunodiffusion assay; a meta-analysis showed that these multiple methods could not influence the CRP results (16).

The initial statin prescription is generally based on the lipid-lowering intensity (9). It might be more beneficial if clinicians considered statins' anti-inflammatory and lipid-lowering effects (11). Previous clinical and experimental studies have shown that statins effectively reduced CRP levels (14, 17); however, comparisons of various types and doses of statins for CRP-lowering effects are inconsistent. A docking experiment *in silico* showed that rosuvastatin, fluvastatin, pitavastatin, and atorvastatin had the most substantial interactions with CRP (18). Some clinical trials demonstrated that various types and dosages of statins showed differing effects on lowering CRP levels (19, 20). In contrast, other trials found no significant differences among several statin therapies (21–23). Therefore, this study aimed to assess the effect of different types and dosages of statins on lowering CRP levels using a pairwise and network meta-analysis (NMA).

Methods

We followed the Preferred Reporting Items for Systematic Reviews and Meta-Analyses (PRISMA) guidelines (24) for this study, and the PRISMA checklist is listed in Supplementary Table 1. This study was registered on PROSPERO (CRD42021242067).

Eligibility criteria

We included studies that met the following criteria: (1) randomized controlled trials (RCTs); (2) participants with dyslipidemia and/or CHD (including stable angina pectoris and acute coronary syndromes); (3) studies comparing patients

treated with statin vs. placebo, blank, or other types or doses of statins; (4) studies providing sufficient information on the baseline and follow-up CRP or hs-CRP level; (5) participants who were taking statins with a fixed-dose once a day; and (6) studies published in English.

The exclusion criteria were as follows: (1) Participants suffering from autoimmune diseases, malignant tumors, liver failure, kidney failure, acute inflammation, or during a perioperative period; (2) participants who were taking statins before enrollment and did not experience a washout period; (3) intervention duration of <8 weeks; and (4) fewer than 30 people per arm in the study.

Search strategy

We searched PubMed, Embase, Cochrane Library databases, OpenGray, and ClinicalTrials.gov for eligible studies from the inception to April 1, 2021. We used a combination strategy of keywords and MeSH keywords, including "dyslipidemia," "hypertriglyceridemia," "hypercholesterolemia," "coronary heart disease," "atherosclerosis," "atherosclerotic," "hydroxymethylglutaryl-CoA reductase inhibitors," "atorvastatin," "fluvastatin," "lovastatin," "pravastatin," "rosuvastatin," "simvastatin," "pitavastatin," "C reactive protein," "CRP," and "hs-CRP." We also scanned the references of included studies and published systematic reviews to avoid omissions. Supplementary Text 1 displays the detailed search strategy.

Literature screening and data extraction

Two authors (WT and TXW) independently screened studies and extracted data. Disagreements were resolved through discussions with a third investigator (HX). We recorded the publication information (first author's name and year), characteristics of trials (design, location, and registration), participants (age, sex, sample size, and disease), interventions (types, dosage, and duration), other treatments, and outcomes (CRP/hs-CRP and its measurement). If possible, we extracted the results from the intention-to-treat analysis.

Risk of bias assessment and quality assessment

Two authors (WT and TXW) independently evaluated the risk of bias according to the Cochrane Collaboration Recommendations assessment tools (25). Because CRP is an objective indicator uninfluenced by allocation concealment and blinding, it is rated as low risk regardless of allocation concealment and blinding (25). Thus, we assessed the risk of bias from the following categories: sequence generation, incomplete outcome data, selective outcome reporting, and other biases (e.g., whether or not to specify the method for measuring CRP/hs-CRP). Discrepancies were resolved by discussions with a third investigator (HX). The quality of evidence for each outcome in the pairwise meta-analysis and significant results in the network meta-analyses were evaluated based on the GRADE (Grading of Recommendations Assessment, Development, and Evaluation) process.

Statistical analysis

The outcome was plasma CRP/hs-CRP level at the final measured point. Data were standardized to mean and standard deviation (*SD*) (26), and units of CRP were converted to mg/L. Placebo and no-interventions were combined as the control groups to provide more evidence for comparisons among statins. We presented the pooled results as weighted mean differences (WMD) and 95% confidence intervals (CI) (16, 27). *P*-values of <0.05 were considered significant.

We performed a pairwise meta-analysis to compare the efficacy of statins and control on serum CRP levels using the Review Manager 5.4 software (The Cochrane Collaboration, Software Update, Oxford, UK). Multi-arm studies were split into comparisons between statins and controls, and the number of participants in the control group was proportionally divided into a new control group to ensure that the total number of participants was exact (25, 28). Due to the high heterogeneity of included studies, we chose a random-effects model to estimate the overall effect, which might provide more conservative results (29). For sensitivity analyses, the robustness of the pooled results was tested by leave-one-out influence analysis.

For NMA, we produced an evidence network plot using the Stata 16 software (STATA Corporation, College Station, TX, USA). The aggregate data drug information system ADDIS 1.16.5 software (Drug Information System, Groningen, The Netherlands) was used to generate the Bayesian random-effects model. We generated a Markov Chain Monte Carlo (MCMC) model to incorporate the efficacy of direct and indirect comparisons and rank the interventions with ranking probabilities (30, 31). The convergence of the MCMC model was assessed using the Brooks-Gelman-Rubin method, which compares within-chain and between-chain variance to calculate the potential scale reduction factor (PSRF) (32). The closer PSRF approaches 1, the better the convergence. Typically, an acceptable PSRF is <1.05 (33). To evaluate the inconsistency of NMA, we used a node-split model to assess the consistency of direct and indirect comparisons. The consistency model was adopted if the *P*-value of >0.05; otherwise, the inconsistent model was used (34).

CRP and hs-CRP have different measurement accuracies, and some studies did not mention the actual measurement

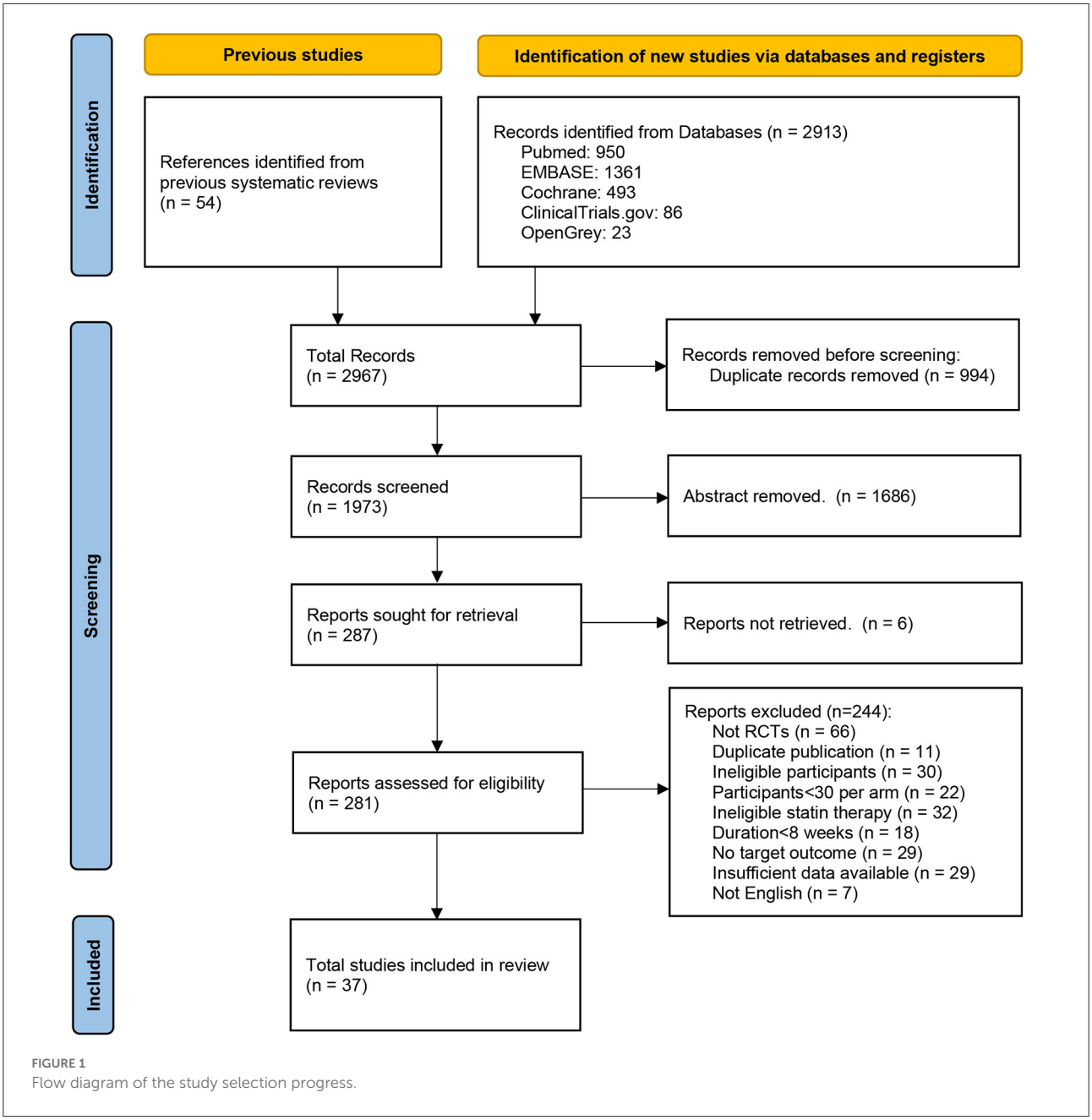

FIGURE 1
Flow diagram of the study selection progress.

clearly; moreover, participants with different diseases, especially those with acute coronary syndromes (ACS), might have higher inflammation levels (35). Therefore, we performed subgroup analyses for CRP measurement (including CRP, hs-CRP, and CRP/hs-CRP with a clear measurement method), population (including CHD, dyslipidemia, ACS, and non-ACS), and treatment duration (less than or more than 12 months). If a study included a population with ACS and dyslipidemia, it would belong to the CHD and ACS subgroups. If there were inconsistencies in the evidence, conclusions were treated cautiously.

Results

Eligible studies, risks of bias assessment, and quality of evidence

According to the search strategy, we retrieved 2,804 potential eligible papers from the three databases. After screening, 37 studies (19–23, 36–69) with 17,410 participants and 20 interventions were included (Figure 1). Among them, nine studies directly compared a statin with control, 22 compared two different types or doses of statins, and six were multi-arm

TABLE 1 Baseline characteristics of the included studies.

Study ID	Location	Disease	Sample size (*n*)	Mean age (year)	Male sex (%)	Intervention (per day)	Course	Other intervention
Allen, 2002 (36) (ARBITER)	USA	hypercholesterolemia	161	59.53	71.46	Atorvastatin 80 mg vs. Pravastatin 40 mg	12 m	Unclear
Andrew, 2015 (37) (LIPID)	Australia and New Zealand	CHD (history of ACS)	7,863	60.9	82.5	Pravastatin 40 mg vs. Placebo	12 m	Routine therapy
Cheuk-Man, 2007 (38)	unclear	CHD and hypercholesterolemia	112	66	81.81	Atorvastatin 10 mg vs. Atorvastatin 80 mg	26 w	Unclear
Dan, 2017 (39)	China	NSTE-ACS	83	60.55	73.5	Rosuvastatin 10 mg vs. Rosuvastatin 20 mg	12 w	NSTE-ACS standard therapy (including aspirin, clopidogrel, β-blockers, and angiotensin-converting enzyme inhibitors/ angiotensin II receptor antagonists)
Guo, 2017 (40)	China	ACS	137	60.59	50.58	Rosuvastatin 10 mg vs. Rosuvastatin 20 mg vs. Blank	12 w	PCI; routine therapy
Haiyan, 2009 (41)	China	hypercholesterolemia	69	58.46	52.18	Atorvastatin 10 mg vs. Rosuvastatin 10 mg	12 w	Unclear
Haralampos, 2004 (23)	Greece	Dyslipidemia	180	58.3	61.1	Atorvastatin 40 mg vs. Simvastatin 40 mg	3 m	National Cholesterol Education Program diet
Hiro, 2009 (42) (JAPAN-ACS)	Japan	ACS and hypercholesterolemia (The patients were enrolled within 72 h after PCI.)	307	62.45	81.74	Atorvastatin 20 mg vs. Pitavastatin 4 mg	8–12 m	ACS standard treatment
Jung Wook, 2019 (43)	Republic of Korea	NSTE-ACS and T2DM	72	64.1	69.16	Pitavastatin 1 mg vs. Pitavastatin 4 mg	12 m	Not mentioned
Komukai, 2014 (44) (EASY-FIT)	Japan	ACS (UA) and untreated dyslipidemia	60	65.45	79.97	Atorvastatin 5mg vs. Atorvastatin 20 mg	12 m	Unclear
Kuei Chuan, 2008 (45)	China	CHD	60	64.95	71.48	Atorvastatin 10 mg vs. Blank	6 m	PCI; diet control; sulfonylurea if necessary
Kwang Kon, 2004 (46)	Korea	CHD	63	31.49	40.6	Simvastatin 20 mg vs. Placebo	14 w	American Heart Association Step I Diet; aspirin; β-blocker therapy
Kwang Kon, 2008 (47)	Korea	hypercholesterolemia	160	58.61	46.82	Simvastatin 10 mg vs. Simvastatin 20 mg vs. Simvastatin 40 mg vs. Simvastatin 80 mg vs. Placebo	2 m	Low-fat diet

(Continued)

10.3389/fcvm.2022.936817

TABLE 1 Continued

Study ID	Location	Disease	Sample size (*n*)	Mean age (year)	Male sex (%)	Intervention (per day)	Course	Other intervention
Kwang Kon, 2010 (48)	Korea	Hyperlipidemia	138	58.68	44.74	Simvastatin 20 mg vs. Simvastatin 40 mg vs. Placebo	2 m	Unclear
Kwang Kon, 2015 (49)	Korea	hypercholesterolemia	102	57	52.9	Simvastatin 20 mg vs. Placebo	2 m	Unclear
Kwang Kon, 2016 (50)	Korea	hypercholesterolemia	190	57.01	50	Rosuvastatin 5 mg vs. Rosuvastatin 10 mg vs. Rosuvastatin 20 mg vs. Placebo	2 m	Low-fat diet
Mehmet, 2006 (51)	Turkey	ACS	122	57.58	88.13	Atorvastatin 40 mg vs. Blank	6 m	AMI standard treatment (STE-MI: thrombolytic drug; NSTE-MI: clopidogrel, aspirin, heparin, nitrate, β-blocker, and angiotensin- converting enzyme inhibitor)
Moutzouri, 2011 (21)	Greece	Hypercholesterolemia and insulin resistance	100	55.3	34.83	Rosuvastatin 10 mg vs. Simvastatin 40 mg	12 w	Unclear
Nakagomi, 2015 (52)	Japan	Dyslipidemia	153	66	50	Atorvastatin 5 mg vs. Pitavastatin 1 mg	12 m	Unclear
Naohisa, 2015–Kazuo, 2017 (53) (J-STARS)	Japan	Hyperlipidemia and ischemic stroke	1095	66.35	68.95	Pravastatin 10 mg vs. Blank	2 m	Diet and exercise therapies
Qianqian, 2017 (54)	China	CHD (including ACS and SAP)	203	61.38	69.15	Atorvastatin 20 mg vs. Atorvastatin 40 mg	12 w	Unclear
Rehab, 2021 (55)	Egypt	Dyslipidemia and T2DM	197	54.92	46.25	Atorvastatin 40 mg vs. Rosuvastatin 10 mg	6 m	Oral hypoglycemic agents
Robert, 2011 (56)	Poland	Mixed Dyslipidemia and T2DM	96	53	57.46	Simvastatin 40 mg vs. Placebo	90 d	Unclear
Robert, 2011(2) (57)	Poland	Hypercholesterolemia	65	52.87	60.52	Simvastatin 40 mg vs. Placebo	90 d	Diet and exercise counseling
Schwartz, 2001-Kinlay et al. (58) (MIRACL)	122 centers in Europe, North America, South Africa, and Australasia.	ACS	2,402	64	66.01	Atorvastatin 80 mg vs. Placebo	16 w	Unclear

(Continued)

10.3389/fcvm.2022.936817

TABLE 1 Continued

Study ID	Location	Disease	Sample size (*n*)	Mean age (year)	Male sex (%)	Intervention (per day)	Course	Other intervention
Seung-Jung, 2016 (59) (STABLE)	Korea	CHD	225	62.34	72.94	Rosuvastatin 10 mg vs. Rosuvastatin 40 mg	12 m	Unclear
Shigemasa, 2015 (60)	Japan	Hypercholesterolemia	108	59.85	62.52	Atorvastatin 10 mg vs. Pitavastatin 2 mg	6 m	Unclear
Smilde, 2001 - Sanne, 2002 (ASAP) (20)	Netherlands	Heterozygous familial hypercholesterolemia	268	47.99	39.51	Atorvastatin 80 mg vs. Simvastatin 40 mg	24 m	Unclear
Stephen, 2011 (61)	USA	Dyslipidemia	159	57.98	40.91	Atorvastatin 20 mg vs. Rosuvastatin 10 mg vs. Simvastatin 40 mg vs. Placebo	12 w	Unclear
Stephen, 2011 (62) (SATURN)	USA, Australia, France, German,	CHD	1039	57.65	73.65	Atorvastatin 80 mg vs. Rosuvastatin 40 mg	24 m	Unclear
Steven, 2004 (63) (REVERSAL)	USA	CHD	502	56.2	71.99	Atorvastatin 80 mg vs. Pravastatin 40 mg	18 m	Unclear
Suxia, 2012 (11)	China	CHD	244	60.49	86.84	Atorvastatin 10 mg vs. Atorvastatin 20 mg vs. Atorvastatin 40 mg vs. Atorvastatin 80 mg vs. Placebo	3–6 m	Aspirin (100 mg/day)
Tsuyoshi, 2012–Tsuyoshi, 2013 (64) (TRUTH)	Japan	CHD	101	66.5	83.06	Pitavastatin 4 mg vs. Pravastatin 20 mg	8 m	Unclear
Xin, 2013 (65)	China	ACS (UA)	100	65	60	Atorvastatin 20 mg vs. Atorvastatin 80 mg	9 m	Aspirin (100 mg/day)
Young Joon, 2011 (22)	Korea	CHD	128	58.51	74.02	Atorvastatin 40 mg vs. Rosuvastatin 20 mg	11 m	Unclear
Zamani, 2014 (66)	Iran	ACS	180	59.09	64.49	Atorvastatin 20 mg vs. Atorvastatin 40 mg	3 m	Unclear
Zhuo, 2009 (67)	China	ACS (UA)	166	71	65.1	Atorvastatin 20 mg vs. Atorvastatin 80 mg	8 w	UA routine therapy

ACS, acute coronary syndrome; CHD, coronary heart disease; NSTE-ACS, non-ST segment elevation acute coronary syndrome; UA, unstable angina pectoris; NSTE-MI, non-ST segment elevation myocardial infarction; STE-MI, ST-segment elevation myocardial infarction; SAP, stable angina pectoris; T2DM, type 2 diabetes mellitus; m, month; w, week; d, days.

10.3389/fcvm.2022.936817

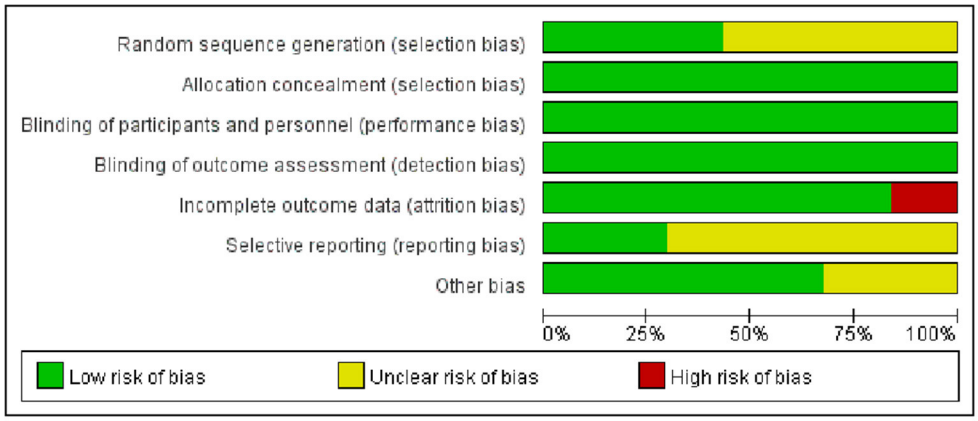

FIGURE 2
Risk of bias graph of the included studies.

trials that performed a comparison between at least two different types or dosages of statins and control. The RCTs included five statins (atorvastatin, rosuvastatin, pitavastatin, simvastatin, and pravastatin) at varying dosages. Table 1 shows the baseline characteristics of each included study.

The assessments for bias risk are summarized in Figure 2. All 37 trials reported random assignment, while only 16 studies (20, 21, 36, 38, 39, 42, 49, 52–54, 60–64, 67) explicitly mentioned appropriate random sequence generation methods. Because CRP is an objective measure, the risk of allocation concealment and blinding was low for all studies (25). Concerning incomplete outcome data, five trials (40, 43, 45, 51, 66) did not report the number or reason of loss to follow-up; one trial (65) had a loss to follow-up rate higher than 35%. Regarding selective outcome reporting, 11 studies (19, 39, 42–44, 53, 55, 58, 59, 61, 64) published the protocols and reported the complete results, whereas others were unclear. In addition, 25 studies (20–23, 36–38, 40, 41, 43, 45–52, 54–58, 60, 61) described the detailed methods of measuring CRP/hs-CRP, while the remaining 12 (19, 39, 42, 44, 53, 59, 62–67) were unclear. In the pairwise meta-analysis, the quality of evidence for comparison between statins and non-statin controls was rated as high. In network meta-analyses, the quality of evidence for significant results was rated as high or moderate (Supplementary Table 2).

Pairwise meta-analysis

The pairwise meta-analysis compared the effects of statins and control on serum CRP levels. As shown in Figure 3, compared with control, statins significantly reduced CRP levels (WMD = −0.97, 95% CI [−1.31, −0.64], $P < 0.0001$, $I^2 = 95\%$). The leave-one-out influence analyses showed that the associations between statins and CRP levels were not determined by any individual study (Supplementary Table 3).

Network meta-analysis

Network evidence

Figure 4 shows the network evidence of 19 statin therapies and control (placebo and no intervention). As shown in Figure 4, control was the most used intermediary comparator. The most common comparisons occurred between pravastatin 40 mg/day and control, followed by atorvastatin 80 mg/day vs. control.

NMA of statins on CRP

All 37 studies were included in the NMA (Supplementary Table 4). Overall, only simvastatin 40 mg/day (WMD = −4.07, 95% CI= [−6.52, −1.77]) and atorvastatin 80 mg/day (WMD = −3.32, 95% CI= [−6.02, −0.83]) were significantly better than control among 19 statin therapies. We performed the rank-possibility of statins on lowering CRP. Rank 1 was the worst, and rank 20 was the best (70). Supplementary Figure 1A shows that simvastatin 40 mg/day has the highest P-value of rank 20; therefore, it also indicates that simvastatin 40 mg/day might be the best method for lowering CRP (rank $P = 0.18$).

We performed a subgroup analysis based on the measurement method of CRP, including CRP, hs-CRP, and CRP/hs-CRP with a clear measurement method (Supplementary Table 4). The CRP subgroup contained three studies with three interventions and 1,679 participants. We performed both consistency model and inconsistency model because there were no closed loops to conduct node-splitting analysis for assessing inconsistency. Atorvastatin 80 mg/day might be the best at lowering CRP levels (rank $P = 0.79$) among atorvastatin 80 mg/day, pravastatin 40 mg/day, and rosuvastatin 40 mg/day (Supplementary Figure 1B). Moreover, atorvastatin 80 mg/day was significantly better than pravastatin 40 mg/day in both the consistency model (WMD = −1.23, 95% CI = [−2.48,

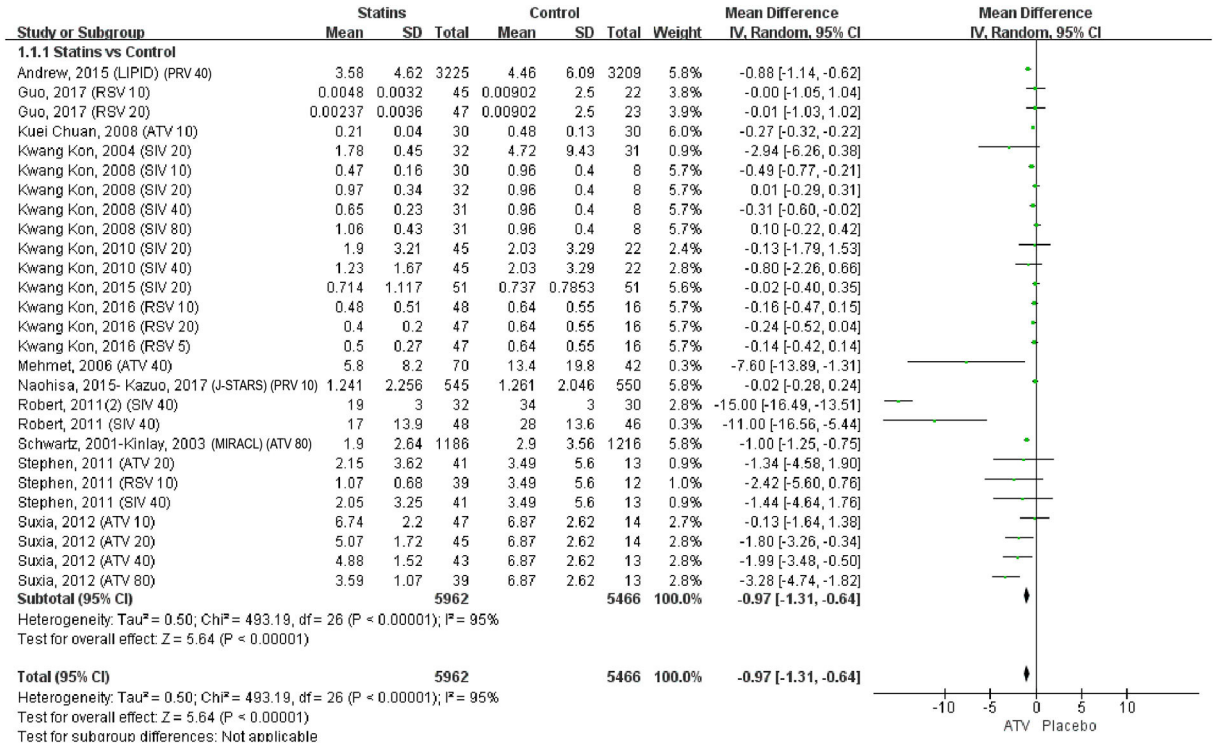

FIGURE 3
Forest plot of pairwise meta-analysis between statins and control. Note: PRV 40: Pravastatin 40 mg/d; RSV 10: Rosuvastatin 10 mg/d; Rosuvastatin 20 mg/d; ATV 10: Atorvastatin 10 mg/d; SIV 20: Simvastatin 20 mg/d; SIV 10: Simvastatin 10 mg/d; SIV 40: Simvastatin 40 mg/d; SIV 80: Simvastatin 80 mg/d; RSV 5: Rosuvastatin 5 mg/d; ATV 40: Atorvastatin 40 mg/d; PRV 10: Pravastatin 10 mg/d; ATV 80: Atorvastatin 80 mg/d; ATV 20: Atorvastatin 20 mg/d.

−0.08]) and the inconsistency model (WMD = −1.25, 95% CI= [−2.53, −0.08]). However, owing to the limited studies, the results should be interpreted with caution. The hs-CRP subgroup included 33 studies with 20 interventions. According to the ranking possibility, the best statins for reducing CRP might be pravastatin 40 mg/day (rank $P = 0.15$), simvastatin 40 mg/day (rank $P = 0.12$), or rosuvastatin 40 mg/day (rank $P = 0.10$) (Supplementary Figure 1C). Nevertheless, only simvastatin 40 mg/day (WMD = −4.10, 95% CI= [−6.83, −1.60]) and atorvastatin 80 mg/day (WMD = −3.66, 95% CI = [−7.01, −0.58]) were significantly better than control. Comprehensive considering the ranking and *P*-value, simvastatin 40 mg/day might be the best therapy for lowering CRP levels. The subgroup of CRP/hs-CRP with a clear measurement method contained 23 studies with 14 interventions. Among them, simvastatin 40 mg/day appeared to be the best (rank $P = 0.20$) (Supplementary Figure 1D). Furthermore, only simvastatin 40 mg/day showed a statistically significant difference compared to control (WMD = −4.28, 95% CI = [−7.21, −1.43]).

We conducted another subgroup analysis in terms of population, including CHD, dyslipidemia, ACS, and non-ACS subgroups. The CHD subgroup included 21 studies with 14 interventions. However, there are two inconsistent comparisons; thus, we used the inconsistency model (Supplementary Table 4), which should be interpreted cautiously. In total, 14 studies were included in the dyslipidemia subgroup. The results showed that pitavastatin 2 mg/day tends to be the best (rank $P = 0.18$) (Supplementary Figure 1E); however, there were no significant differences among the 15 interventions ($P > 0.05$). The ACS subgroup included 11 studies. Compared with other interventions, atorvastatin 80 mg/day might be the most effective strategy to reduce the CRP levels (rank $P = 0.30$). However, the comparisons among the nine interventions also showed no significant difference ($P > 0.05$) (Supplementary Figure 1F). Although 29 studies met the criteria of the non-ACS subgroup, only 27 studies were available for indirect comparisons. Simvastatin 40 mg/day has the highest probability of being the best for reducing CRP levels (rank $P = 0.21$) (Supplementary Figure 1G). Furthermore, simvastatin 40 mg/day (WMD = −4.34, 95% CI= [−7.10, −1.76]) was also significantly better than control among 16 interventions ($P < 0.05$).

We conducted the third subgroup analysis according to the treatment duration. For the <12-month duration subgroup, simvastatin 40 mg/day (rank $P = 0.21$) appeared to be the best strategy (Supplementary Figure 1H). Moreover, simvastatin 40 mg/day (WMD = −4.29, 95% CI = [−7.18,

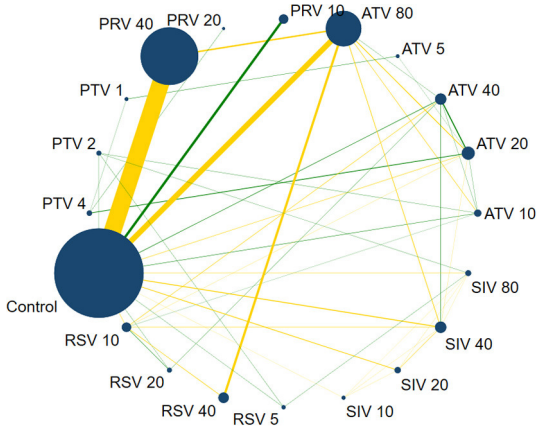

FIGURE 4
Network evidence plot on CRP. The size of nodes is directly proportional to the number of studies. The lines link two direct-comparison interventions, their thickness is proportional to the number of comparisons, and the green links represent at least one double-blind comparison. PTV 4: Pitavastatin 4 mg/d; PTV 2: Pitavastatin 2 mg/d; PTV 1: Pitavastatin 1 mg/d; PRV 40: Pravastatin 40 mg/d; PRV 20: Pravastatin 20 mg/d; PRV 10: Pravastatin 10 mg/d; ATV 80: Atorvastatin 80 mg/d; ATV 5: Atorvastatin 5 mg/d; ATV 40: Atorvastatin 40 mg/d; ATV 20: Atorvastatin 20 mg/d; ATV 10: Atorvastatin 10 mg/d; SIV 80: Simvastatin 80 mg/d; SIV 40: Simvastatin 40 mg/d; SIV 20: Simvastatin 20 mg/d; SIV 10: Simvastatin 10 mg/d; RSV 5: Rosuvastatin 5 mg/d; RSV 40: Rosuvastatin 40 mg/d; RSV 20: Rosuvastatin 20 mg/d; RSV 10: Rosuvastatin 10 mg/d.

−1.55]) and atorvastatin 80 mg/day (WMD = −3.66, 95% CI = [−7.37, −0.19]) were significantly better than control for reducing CRP levels. Although 9 studies were eligible for the ≥12-month duration subgroup, only six studies were available for NMA analysis. Given that there were no closed loops to assess inconsistency, we conducted consistency and inconsistency models. In the consistency model, atorvastatin 80 mg/day (rank $P = 0.40$) and simvastatin 40 mg/day (rank $P = 0.36$) were most likely to be the best for reducing CRP levels (Supplementary Figure 1I). Atorvastatin 80 mg/day was significantly better than pravastatin 40 mg/day (WMD = −1.27, 95% CI = [−2.56, −0.11]) and control (WMD = −2.13, 95% CI = [−4.24, −0.13]) in the consistency and inconsistency models (Supplementary Table 4).

Consistency and convergence analysis

We performed node-splitting analysis to evaluate inconsistency by comparing direct and indirect effects (Supplementary Table 5). In ten comparisons, seven showed no significant inconsistency, suggesting that the consistency model is reliable. The CRP and ≥12-month duration subgroups could not form closed loops to conduct node-splitting analysis; therefore, we conducted both consistency and inconsistency models; the results of the two models were consistent, suggesting that the results are reliable. The CHD subgroup had two inconsistent comparisons between direct effect and indirect effect ($P < 0.05$); therefore, we generated an inconsistency model; however, the results of these two subgroups should be interpreted with caution (34, 71). In addition, the PSRF was between 1.00 and 1.05, indicating that the analysis had good convergence (70).

Discussion

To the best of our knowledge, this is the first study to compare the effects of different types and doses of statins on plasma CRP levels in patients with dyslipidemia or CHD.

The pairwise meta-analysis showed that, compared with control, statins decreased CRP levels, which was consistent with previous studies. The JUPITER (Justification for the Use of Statins in Prevention: an Intervention Trial Evaluating Rosuvastatin) was an RCT investigating the anti-inflammatory effects of rosuvastatin in apparently healthy people with elevated hs-CRP levels (72). It showed that rosuvastatin reduced LDL-C levels by 50% and hs-CRP levels by 37%; rosuvastatin significantly reduced the occurrence of major adverse cardiovascular events. Similarly, the HOPE-3 (Heart Outcomes Prevention Evaluation-3) study on intermediate-risk participants without cardiovascular disease supported the hs-CRP-lowering effect of rosuvastatin regardless of CRP and lipid levels at baseline (73). Other systematic reviews supported the role of statins in reducing hs-CRP in patients with cardiovascular diseases (74), stroke (75), and apparently healthy people or patients with chronic diseases (76). Inconsistently, a meta-analysis (77) showed no significant difference between statins and control in lowering the hs-CRP level in atherosclerosis (WMD = −1.61, $P = 0.09$); however, this subgroup only included three trials with 236 participants, which was too few to obtain reliable results.

Dyslipidemia and inflammation are closely interconnected drivers of atherosclerotic heart disease (78). Correspondingly, statins are pleiotropic drugs that lower serum cholesterol by inhibiting hepatic cholesterol biosynthesis and exert cardiovascular protective effects such as anti-inflammation (10). It remains inconclusive whether the anti-inflammatory effects of statins are independent of their lipid-lowering efficacy. Labos et al. used Egger regression to reanalyze the available previous RCT data of statins (79). The study showed that each 1 mmol/L change in LDL-C with statin therapy was associated with a hazard ratio of 0.77 in cardiovascular endpoints with an intercept indistinguishable from zero, suggesting that statins' cardiovascular benefits were entirely derived from LDL-C lowering. Fernando et al. suggested that this analysis should use multivariable (and not "standard") Egger regression (80). In contrast, in the Cholesterol and Recurrent Events

(CARE) trial that investigated inflammation and coronary events after myocardial infarction, statins reduced CRP levels independently of LDL-C (81). Subsequently, a *post-hoc* analysis of the Air Force/Texas Coronary Atherosclerosis Prevention Study (AFCAPS/TexCAPS) reported that compared to individuals with low levels of LDL-C and CRP, those with low LDL-C but elevated CRP levels benefited markedly from lovastatin, suggesting anti-inflammatory activity independent of lipid-lowering (82). The Pravastatin Inflammation/CRP Evaluation (PRINCE) trial demonstrated that pravastatin 40 mg/day significantly reduced plasma CRP levels independent of any changes in LDL levels (83). Unlike clinical studies with inconsistent conclusions, experimental studies assessed the anti-inflammatory effects of statins independent of their lipid-lowering action (17).

C-reactive protein is considered a nonspecific marker of inflammation, produced in response to the action of IL-6, IL-1, or TNF-α (17). It remains unclear whether patients would benefit if CRP were a therapeutic target, although CRP has attracted attention for its applications in screening and risk stratification (84–86). Nevertheless, anti-inflammatory therapies have shown compelling effects in preventing cardiovascular events recently. The Canakinumab Anti-inflammatory Thrombosis Outcome Study (CANTOS) demonstrated that canakinumab, an IL-1β blocker (150 mg for every 3 months), reduced the incidence of nonfatal myocardial infarction, nonfatal stroke, and cardiovascular death (6). Colchicine is an anti-inflammatory drug for treating gout, familial Mediterranean fever, and pericarditis. It has shown promising efficacy in atherosclerotic heart disease. The Colchicine Cardiovascular Outcomes Trial (COLCOT) found that 0.5 mg of colchicine daily significantly lowered the risk of ischemic cardiovascular events in patients who suffered a myocardial infarction within 30 days (7). Subsequently, the Low-Dose Colchicine 2 trial (LoDoCo2), an RCT that involved 5,522 patients with chronic coronary disease, revealed that 0.5 mg/day of colchicine significantly lowered the risk of cardiovascular events (8). The evidence of these anti-inflammatory therapies suggests an approach to treating atherosclerotic disease besides lipid-lowering. Recently, a position paper of the European Society of Cardiology stated that, given the strong association among inflammation, lipids, and atherosclerosis, it would be helpful to assess the inflammatory response to lipid-lowering interventions, thereby establishing the optimal dose and type of lipid-lowering therapy for cardiovascular prevention (11).

The results of NMA showed that simvastatin 40 mg/day appeared to be the best for lowering CRP among the included statin therapies. Simvastatin is a lipophilic statin and an inactive prodrug hydrolyzed in the liver to its major active β-hydroxy acid metabolite (87). Compared with other lipid-lowering agents, simvastatin might be superior in reducing the risk of major adverse cardiovascular events in hypertriglyceridemic patients (88). Consistent with our findings, Mitra et al. supported the notion that lipophilic statins (such as simvastatin) at high-intensity dosage could significantly decrease inflammatory factor TNF-α (89). In contrast, Neda et al. tested the orientation of ligands (statins) and phosphorylcholine (the standard ligand of CRP) at the CRP active site using Molecular Operating Environment software (18). The docking experiments showed that rosuvastatin had the most robust interaction with CRP, followed by fluvastatin, pitavastatin, atorvastatin, pravastatin, simvastatin, and lovastatin. However, in addition to directly acting on CRP, statins reduce inflammation *via* ICAM-1 and VCAM-1 (17), and the evidence from *in silico* studies requires experimental studies for support. In terms of dosage, according to the 2013 ACC/AHA Guideline (90), 40 mg/day is the maximum recommended dose of simvastatin because of the risk of rhabdomyolysis at higher doses, although it is classified as moderate-intensity statin therapy. Similar to our results, a higher intensity dosage is more likely to have better anti-inflammatory effects (89). In addition, high-dose statins (e.g., simvastatin 40 mg/day and atorvastatin 80 mg/day) are associated with the most significant benefits of secondary prevention in patients with ischemic stroke or transient ischemic attack (91).

We performed subgroup analyses to determine the heterogeneity. In the hs-CRP, non-ACS, <12-month duration, and clear measurement method subgroups, simvastatin 40 mg/day appeared to be the best strategy for CRP-lowering, consistent with the NMA. In the ≥12-month duration subgroup, atorvastatin 80 mg/day was most likely to be the best. The evidence from the ≥12-month duration subgroup is more clinically meaningful because statins are long-term drugs. In the CRP subgroup, atorvastatin 80 mg/day was most likely to be the best for reducing CRP levels, while there were only three studies, which made the results unpersuasive. Conversely, there were no significant differences in dyslipidemia and ACS subgroups. Previous research showed a significant difference between statins and placebo in ACS (76). This discrepancy might be caused by the limited number and heterogeneity of included trials.

Our study has some advantages. First, we performed an NMA of RCTs, which could compare multiple treatments and enable us to synthesize data with direct and indirect evidence (30). Compared to previous meta-analyses (76, 77), this study could incorporate all available data to assess interventions more accurately (70). Second, the results were highly consistent between the direct meta-analysis and NMA and the NMA and NMA subgroups, suggesting a stable result. Finally, our study provides the ranking possibilities of different statins, which can help clinicians make choices when faced with elevated CRP levels in patients with CHD.

Although we strictly followed the PRISMA extension statement for NMA, there are some limitations. First, it would be

more clinically meaningful if we included a subgroup of baseline CRP levels; however, this is challenging because these studies chose participants according to disease rather than CRP level. Second, there was significant heterogeneity among included studies. To resolve the heterogeneity, we used a random-effects model, which may have influenced differences in study design and trial populations, as well as statistical heterogeneity in some of our results (70). In addition, we conducted subgroup analyses in terms of the measurement method of CRP, the population, or the treatment duration. A leave-one-out influence analysis was performed to test the robustness of the pooled results. The results of this study can still be considered credible. Third, owing to the limited number of trials, we could not include all statin therapies recommended by the guidelines (90) and did not differentiate among statins from various brands, which might lead to errors; nevertheless, this study covered statin prescriptions commonly used in clinical, and all statins are approved, commercially available drugs. Fourth, serum CRP levels are influenced by treatment duration, while the traditional meta-analysis and NMA cannot elucidate the changing effects over time (92). We thereby excluded the studies with treatment <8 weeks and performed a subgroup analysis of treatment duration to partly solve the problem. Finally, our study only included patients with dyslipidemia or CHD, whereas statins are used more widely; however, this also reduced the clinical heterogeneity.

Conclusion

Statins reduce serum CRP levels in patients with dyslipidemia or CHD. Simvastatin 40 mg/day might be the most effective therapy, and atorvastatin 80 mg/day showed the best long-term effect. This study provides a reference for choosing statin therapy based on LDL-C and CRP levels.

Data availability statement

The original contributions presented in the study are included in the article/Supplementary material, further inquiries can be directed to the corresponding authors.

Author contributions

HX, JQJ, and JZ designed this study. JZ and XW searched the databases and wrote the original draft. WT and TXW screened the publications and extracted data. RL and JDJ specified the data. JZ and LS performed the analysis. XW and HX provided methodological guidance. TW and ZZ normalized the figures and tables. All authors reviewed the manuscript.

Funding

The study was supported by the Chinese Academy of Chinese Medical Sciences Innovation Fund (CACMS Innovation Fund, CI2021A00917), Chinese Academy of Traditional Chinese Medicine Science and Technology Major Achievement Guidance Project (ZZ13-ZD-03), and Central Public Welfare Research Institutes of China Academy of Chinese Medical Sciences (ZZ13-YQ-017-C1).

Acknowledgments

The authors would like to thank the National Clinical Research Center for Chinese Medicine Cardiology for supporting the study.

Conflict of interest

All authors declare that the research was conducted in the absence of any commercial or financial relationships that could be construed as a potential conflict of interest.

Publisher's note

Supplementary material

The Supplementary Material for this article can be found online at: https://www.frontiersin.org/articles/10.3389/fcvm.2022.936817/full#supplementary-material

References

1. Jellinger PS, Handelsman Y, Rosenblit PD, Bloomgarden ZT, Fonseca VA, Garber AJ, et al. American Association of Clinical Endocrinologists and American College of Endocrinology Guidelines for management of dyslipidemia and prevention of cardiovascular disease. *Endocr Pract.* (2017) 23:479–97. doi: 10.4158/EP171764.GL

2. Kopin L, Lowenstein C. Dyslipidemia. *Ann Intern Med.* (2017) 167:ITC81–ITC96. doi: 10.7326/AITC201712050

3. Hoogeveen RC, Ballantyne CM. Residual cardiovascular risk at low LDL: Remnants, Lipoprotein(a), and Inflammation. *Clin Chem.* (2021) 67:143–53. doi: 10.1093/clinchem/hvaa252

4. Zhu Y, Xian X, Wang Z, Bi Y, Chen Q, Han X, et al. Research progress on the relationship between atherosclerosis and inflammation. *Biomolecules.* (2018) 8:80. doi: 10.3390/biom8030080

5. Ross R. Atherosclerosis–an inflammatory disease. *N Engl J Med.* (1999) 340:115–26. doi: 10.1056/NEJM199901143400207

6. Ridker PM, Everett BM, Thuren T, MacFadyen JG, Chang WH, Ballantyne C, et al. Antiinflammatory therapy with canakinumab for atherosclerotic disease. *N Engl J Med.* (2017) 377:1119–31. doi: 10.1056/NEJMoa1707914

7. Tardif JC, Kouz S, Waters DD, Bertrand OF, Diaz R, Maggioni AP, et al. Efficacy and safety of low-dose colchicine after myocardial infarction. *N Engl J Med.* (2019) 381:2497–505. doi: 10.1056/NEJMoa1912388

8. Nidorf SM, Fiolet ATL, Mosterd A, Eikelboom JW, Schut A, Opstal TSJ, et al. Colchicine in patients with chronic coronary disease. *N Engl J Med.* (2020) 383:1838–47. doi: 10.1056/NEJMoa2021372

9. Mach F, Baigent C, Catapano AL, Koskinas KC, Casula M, Badimon L, et al. 2019 ESC/EAS Guidelines for the management of dyslipidaemias: lipid modification to reduce cardiovascular risk. *Eur Heart J.* (2020) 41:111–88. doi: 10.1093/eurheartj/ehz455

10. Oesterle A, Laufs U, Liao JK. Pleiotropic effects of statins on the cardiovascular system. *Circ Res.* (2017) 120:229–43. doi: 10.1161/CIRCRESAHA.116.308537

11. Tuñón J, Badimón L, Bochaton-Piallat ML, Cariou B, Daemen MJ, Egido J, et al. Identifying the anti-inflammatory response to lipid lowering therapy: a position paper from the working group on atherosclerosis and vascular biology of the European Society of Cardiology. *Cardiovasc Res.* (2019) 115:10–9. doi: 10.1093/cvr/cvy293

12. Pathak A, Agrawal A. Evolution of C-reactive protein. *Front Immunol.* (2019) 10:943. doi: 10.3389/fimmu.2019.00943

13. Grundy SM, Stone NJ, Bailey AL, Beam C, Birtcher KK, Blumenthal RS, et al. 2018 AHA/ACC/AACVPR/AAPA/ABC/ACPM/ADA/AGS/APHA/ASPC/NLA/PCNA Guideline on the management of blood cholesterol: executive summary: a report of the American College of Cardiology/American Heart Association Task force on clinical Practice Guidelines. *J Am Coll Cardiol.* (2019) 73:3168–209. doi: 10.1016/j.jacc.2018.11.002

14. Golia E, Limongelli G, Natale F, Fimiani F, Maddaloni V, Pariggiano I, et al. Inflammation and cardiovascular disease: from pathogenesis to therapeutic target. *Curr Atheroscler Rep.* (2014) 16:435. doi: 10.1007/s11883-014-0435-z

15. Pearson TA, Mensah GA, Alexander RW, Anderson JL, Cannon RO III, Criqui M, et al. Markers of inflammation and cardiovascular disease: application to clinical and public health practice: a statement for healthcare professionals from the Centers for Disease Control and Prevention and the American Heart Association. *Circulation.* (2003) 107:499–511. doi: 10.1161/01.CIR.0000052939.59093.45

16. Machado V, Botelho J, Escalda C, Hussain SB, Luthra S, Mascarenhas P, et al. Serum C-reactive protein and periodontitis: a systematic review and meta-analysis. *Front Immunol.* (2021) 12:706432. doi: 10.3389/fimmu.2021.706432

17. Satny M, Hubacek JA, Vrablik M. Statins and inflammation. *Curr Atheroscler Rep.* (2021) 23:80. doi: 10.1007/s11883-021-00977-6

18. Shakour N, Ruscica M, Hadizadeh F, Cirtori C, Banach M, Jamialahmadi T, et al. Statins and C-reactive protein: *in silico* evidence on direct interaction. *Arch Med Sci.* (2020) 16:1432–9. doi: 10.5114/aoms.2020.100304

19. Guo S, Wang R, Yang Z, Li K, Wang Q. Effects of atorvastatin on serum lipids, serum inflammation and plaque morphology in patients with stable atherosclerotic plaques. *Exp Ther Med.* (2012) 4:1069–74. doi: 10.3892/etm.2012.722

20. van Wissen S, Trip MD, Smilde TJ, de Graaf J, Stalenhoef AF, Kastelein JJ. Differential hs-CRP reduction in patients with familial hypercholesterolemia treated with aggressive or conventional statin therapy. *Atherosclerosis.* (2002) 165:361–6. doi: 10.1016/S0021-9150(02)00280-0

21. Moutzouri E, Liberopoulos E, Mikhailidis DP, Kostapanos MS, Kei AA, Milionis H, et al. Comparison of the effects of simvastatin vs. rosuvastatin vs. simvastatin/ezetimibe on parameters of insulin resistance. *Int J Clin Pract.* (2011) 65:1141–8. doi: 10.1111/j.1742-1241.2011.02779.x

22. Hong YJ, Jeong MH, Hachinohe D, Ahmed K, Choi YH, Cho SH, et al. Comparison of effects of rosuvastatin and atorvastatin on plaque regression in Korean patients with untreated intermediate coronary stenosis. *Circ J.* (2011) 75:398–406. doi: 10.1253/circj.CJ-10-0658

23. Milionis HJ, Kakafika AI, Tsouli SG, Athyros VG, Bairaktari ET, Seferiadis KI, et al. Effects of statin treatment on uric acid homeostasis in patients with primary hyperlipidemia. *Am Heart J.* (2004) 148:635–40. doi: 10.1016/j.ahj.2004.04.005

24. Page MJ, McKenzie JE, Bossuyt PM, Boutron I, Hoffmann TC, Mulrow CD, et al. The prisma 2020 statement: an updated guideline for reporting systematic reviews. *BMJ.* (2021) 372:n71. doi: 10.1136/bmj.n71

25. P.T. HJ, James T, Jacqueline C, Miranda C, Tianjing L, J. PM, et al. *Cochrane Handbook for Systematic Reviews of Interventions*. Chichester: John Wiley & Sons, Ltd. (2019).

26. McGrath S, Zhao X, Steele R, Thombs BD, Benedetti A, Collaboration DESD. Estimating the sample mean and standard deviation from commonly reported quantiles in meta-analysis. *Statistical Methods Med Res.* (2020) 29:2520–37. doi: 10.1177/0962280219889080

27. Wang X, Yang Q, Liao Q, Li M, Zhang P, Santos HO, et al. Effects of intermittent fasting diets on plasma concentrations of inflammatory biomarkers: a systematic review and meta-analysis of randomized controlled trials. *Nutrition.* (2020) 79–80:110974. doi: 10.1016/j.nut.2020.110974

28. Chiavaroli L, Lee D, Ahmed A, Cheung A, Khan TA, Blanco S, et al. Effect of low glycaemic index or load dietary patterns on glycaemic control and cardiometabolic risk factors in diabetes: systematic review and meta-analysis of randomised controlled trials. *Bmj.* (2021) 374:n1651. doi: 10.1136/bmj.n1651

29. Laird NM, Mosteller F. Some statistical methods for combining experimental results. *Int J Technol Assess Health Care.* (1990) 6:5–30. doi: 10.1017/S0266462300008916

30. Salanti G, Higgins JP, Ades AE, Ioannidis JP. Evaluation of networks of randomized trials. *Stat Methods Med Res.* (2008) 17:279–301. doi: 10.1177/0962280207080643

31. Jansen JP, Crawford B, Bergman G, Stam W. Bayesian meta-analysis of multiple treatment comparisons: an introduction to mixed treatment comparisons. *Value Health.* (2008) 11:956–64. doi: 10.1111/j.1524-4733.2008.00347.x

32. Brooks SP, Gelman A. General methods for monitoring convergence of iterative simulations. *J Comput Gr Stat.* (1998) 7:434–55. doi: 10.1080/10618600.1998.10474787

33. van Valkenhoef G, Lu G, de Brock B, Hillege H, Ades AE, Welton NJ. Automating network meta-analysis. *Res Synth Methods.* (2012) 3:285–99. doi: 10.1002/jrsm.1054

34. Dias S, Welton NJ, Caldwell DM, Ades AE. Checking consistency in mixed treatment comparison meta-analysis. *Stat Med.* (2010) 29:932–44. doi: 10.1002/sim.3767

35. Libby P, Theroux P. Pathophysiology of coronary artery disease. *Circulation.* (2005) 111:3481–8. doi: 10.1161/CIRCULATIONAHA.105.537878

36. Taylor AJ, Kent SM, Flaherty PJ, Coyle LC, Markwood TT, Vernalis MN. Arbiter: arterial biology for the investigation of the treatment effects of reducing cholesterol: a randomized trial comparing the effects of atorvastatin and pravastatin on carotid intima medial thickness. *Circulation.* (2002) 106:2055–60. doi: 10.1161/01.CIR.0000034508.55617.65

37. Tonkin AM, Blankenberg S, Kirby A, Zeller T, Colquhoun DM, Funke-Kaiser A, et al. Biomarkers in stable coronary heart disease, their modulation and cardiovascular risk: the lipid biomarker study. *Int J Cardiol.* (2015) 201:499–507. doi: 10.1016/j.ijcard.2015.07.080

38. Yu CM, Zhang Q, Lam L, Lin H, Kong SL, Chan W, et al. Comparison of intensive and low-dose atorvastatin therapy in the reduction of carotid intimal-medial thickness in patients with coronary heart disease. *Heart.* (2007) 93:933–9. doi: 10.1136/hrt.2006.102848

39. Ran D, Nie HJ, Gao YL, Deng SB, Du JL, Liu YJ, et al. A randomized, controlled comparison of different intensive lipid-lowering therapies in Chinese patients with Non-St-Elevation Acute Coronary Syndrome (Nste-Acs): ezetimibe and rosuvastatin versus high-dose rosuvastatin. *Int J Cardiol.* (2017) 235:49–55. doi: 10.1016/j.ijcard.2017.02.099

40. Guo J, Zhang WZ, Zhao Q, Wo JS, Cai SL. Study on the effect of different doses of rosuvastatin on ventricular remodeling in patients with acute coronary syndrome after emergency percutaneous coronary intervention. *Eur Rev Med Pharmacol Sci.* (2017) 21:4457–63. https://www.europeanreview.org/article/13522

41. Qu HY, Xiao YW, Jiang GH, Wang ZY, Zhang Y, Zhang M. Effect of atorvastatin versus rosuvastatin on levels of serum lipids, inflammatory markers and adiponectin in patients with hypercholesterolemia. *Pharm Res.* (2009) 26:958–64. doi: 10.1007/s11095-008-9798-6

42. Hiro T, Kimura T, Morimoto T, Miyauchi K, Nakagawa Y, Yamagishi M, et al. Effect of intensive statin therapy on regression of coronary atherosclerosis in patients with acute coronary syndrome: a multicenter randomized trial evaluated by volumetric intravascular ultrasound using pitavastatin versus atorvastatin (Japan-Acs [Japan Assessment of Pitavastatin and Atorvastatin in Acute Coronary Syndrome] Study). *J Am Coll Cardiol.* (2009) 54:293–302. doi: 10.1016/j.jacc.2009.04.033

43. Lim JW, Jeong HS, Hong SJ, Kim HJ, Kim YC, Kang BG, et al. Effects of lowest-dose vs. highest-dose pitavastatin on coronary neointimal hyperplasia at 12-month follow-up in type 2 diabetic patients with non-ST elevation acute coronary syndrome: an optical coherence tomography analysis. *Heart Vessels.* (2019) 34:62–73. doi: 10.1007/s00380-018-1227-0

44. Komukai K, Kubo T, Kitabata H, Matsuo Y, Ozaki Y, Takarada S, et al. Effect of atorvastatin therapy on fibrous cap thickness in coronary atherosclerotic plaque as assessed by optical coherence tomography: the easy-fit study. *J Am Coll Cardiol.* (2014) 64:2207–17. doi: 10.1016/j.jacc.2014.08.045

45. Chan KC, Chou HH, Huang CN, Chou MC. Atorvastatin administration after percutaneous coronary intervention in patients with coronary artery disease and normal lipid profiles: impact on plasma adiponectin level. *Clin Cardiol.* (2008) 31:253–8. doi: 10.1002/clc.20181

46. Koh KK, Son JW, Ahn JY, Jin DK, Kim HS, Choi YM, et al. Vascular effects of diet and statin in hypercholesterolemic patients. *Int J Cardiol.* (2004) 95:185–91. doi: 10.1016/j.ijcard.2003.05.018

47. Koh KK, Quon MJ, Han SH, Lee Y, Ahn JY, Kim SJ, et al. Simvastatin improves flow-mediated dilation but reduces adiponectin levels and insulin sensitivity in hypercholesterolemic patients. *Diabetes Care.* (2008) 31:776–82. doi: 10.2337/dc07-2199

48. Koh KK, Quon MJ, Sakuma I, Lee Y, Lim S, Han SH, et al. Effects of simvastatin therapy on circulating adipocytokines in patients with hypercholesterolemia. *Int J Cardiol.* (2011) 146:434–7. doi: 10.1016/j.ijcard.2010.10.103

49. Koh KK, Oh PC, Sakuma I, Kim EY, Lee Y, Hayashi T, et al. Vascular and metabolic effects of ezetimibe combined with simvastatin in patients with hypercholesterolemia. *Int J Cardiol.* (2015) 199:126–31. doi: 10.1016/j.ijcard.2015.07.016

50. Koh KK, Oh PC, Sakuma I, Lee Y, Han SH, Shin EK. Rosuvastatin dose-dependently improves flow-mediated dilation, but reduces adiponectin levels and insulin sensitivity in hypercholesterolemic patients. *Int J Cardiol.* (2016) 223:488–93. doi: 10.1016/j.ijcard.2016.08.051

51. Kanadaşi M, Cayli M, Demirtaş M, Inal T, Demir M, Koç M, et al. The effect of early statin treatment on inflammation and cardiac events in acute coronary syndrome patients with low-density lipoprotein cholesterol. *Heart Vessels.* (2006) 21:291–7. doi: 10.1007/s00380-005-0901-1

52. Nakagomi A, Shibui T, Kohashi K, Kosugi M, Kusama Y, Atarashi H, et al. Differential effects of atorvastatin and pitavastatin on inflammation, insulin resistance, and the carotid intima-media thickness in patients with dyslipidemia. *J Atheroscler Thromb.* (2015) 22:1158–71. doi: 10.5551/jat.29520

53. Kitagawa K, Hosomi N, Nagai Y, Kagimura T, Ohtsuki T, Origasa H, et al. Reduction in high-sensitivity C-reactive protein levels in patients with ischemic stroke by statin treatment: Hs-CRP sub-study in J-STARS. *J Atheroscler Thromb.* (2017) 24:1039–47. doi: 10.5551/jat.39354

54. Chen Q, Shang X, Yuan M, Liang L, Zhong X. Effect of atorvastatin on serum omentin-1 in patients with coronary artery disease. *Coron Artery Dis.* (2017) 28:44–51. doi: 10.1097/MCA.0000000000000435

55. Werida R, Khairat I, Khedr NF. Effect of atorvastatin versus rosuvastatin on inflammatory biomarkers and lv function in type 2 diabetic patients with dyslipidemia. *Biomed Pharmacother.* (2021) 135:111179. doi: 10.1016/j.biopha.2020.111179

56. Krysiak R, Gdula-Dymek A, Okopien B. Effect of simvastatin and fenofibrate on cytokine release and systemic inflammation in type 2 diabetes mellitus with mixed dyslipidemia. *Am J Cardiol.* (2011) 107:1010–8.e1. doi: 10.1016/j.amjcard.2010.11.023

57. Krysiak R, Okopien B. The effect of ezetimibe and simvastatin on monocyte cytokine release in patients with isolated hypercholesterolemia. *J Cardiovasc Pharmacol.* (2011) 57:505–12. doi: 10.1097/FJC.0b013e318211703b

58. Kinlay S, Schwartz GG, Olsson AG, Rifai N, Leslie SJ, Sasiela WJ, et al. High-dose atorvastatin enhances the decline in inflammatory markers in patients with acute coronary syndromes in the miracl study. *Circulation.* (2003) 108:1560–6. doi: 10.1161/01.CIR.0000091404.09558.AF

59. Park SJ, Kang SJ, Ahn JM, Chang M, Yun SC, Roh JH, et al. Effect of statin treatment on modifying plaque composition: a double-blind, randomized study. *J Am Coll Cardiol.* (2016) 67:1772–83. doi: 10.1016/j.jacc.2016.02.014

60. Tani S, Takahashi A, Nagao K, Hirayama A. Contribution of apolipoprotein A-I to the reduction in high-sensitivity C-reactive protein levels by different statins: comparative study of pitavastatin and atorvastatin. *Heart Vessels.* (2015) 30:762–70. doi: 10.1007/s00380-014-0554-z

61. Nicholls SJ, Brewer HB, Kastelein JJ, Krueger KA, Wang MD, Shao M, et al. Effects of the CETP inhibitor evacetrapib administered as monotherapy or in combination with statins on HDL and LDL cholesterol: a randomized controlled trial. *JAMA.* (2011) 306:2099–109. doi: 10.1001/jama.2011.1649

62. Nicholls SJ, Ballantyne CM, Barter PJ, Chapman MJ, Erbel RM, Libby P, et al. Effect of two intensive statin regimens on progression of coronary disease. *N Engl J Med.* (2011) 365:2078–87. doi: 10.1056/NEJMoa1110874

63. Nissen SE, Tuzcu EM, Schoenhagen P, Brown BG, Ganz P, Vogel RA, et al. Effect of intensive compared with moderate lipid-lowering therapy on progression of coronary atherosclerosis: a randomized controlled trial. *JAMA.* (2004) 291:1071–80. doi: 10.1001/jama.291.9.1071

64. Nozue T, Yamamoto S, Tohyama S, Fukui K, Umezawa S, Onishi Y, et al. Effects of statins on serum n-3 to n-6 polyunsaturated fatty acid ratios in patients with coronary artery disease. *J Cardiovasc Pharmacol Ther.* (2013) 18:320–6. doi: 10.1177/1074248412473202

65. Zhang X, Wang H, Liu S, Gong P, Lin J, Lu J, et al. Intensive-dose atorvastatin regimen halts progression of atherosclerotic plaques in new-onset unstable angina with borderline vulnerable plaque lesions. *J Cardiovasc Pharmacol Ther.* (2013) 18:119–25. doi: 10.1177/1074248412465792

66. Zamani B, Saatlo BB, Naghavi-Behzad M, Taqizadeh-Jahed M, Alikhah H, Abbasnezhad M. Effects of high versus low-dose atorvastatin on high sensitive C-reactive protein in acute coronary syndrome. *Niger Med J.* (2014) 55:490–4. doi: 10.4103/0300-1652.144704

67. Zhao Z, Geng J, Ge ZM, Wang W, Zhang Y, Kang WQ. Efficacy and safety of atorvastatin during early hospitalization in elderly patients with unstable angina. *Clin Exp Pharmacol Physiol.* (2009) 36:554–8. doi: 10.1111/j.1440-1681.2008.05110.x

68. Peters SA, Lind L, Palmer MK, Grobbee DE, Crouse JR III, O'Leary DH, et al. Increased age, high body mass index and low HDL-C levels are related to an echolucent carotid intima-media: the METEOR study. *J Intern Med.* (2012) 272:257–66. doi: 10.1111/j.1365-2796.2011.02505.x

69. Peng M, Dong H, Jiang X, Che W, Zou Y, Zhang Y, et al. A randomized unblinded trial to compare effects of intensive versus conventional lipid-lowering therapy in patients undergoing renal artery stenting. *J Cardiol.* (2019) 74:443–50. doi: 10.1016/j.jjcc.2019.04.010

70. Wang X, Li J, Ju J, Fan Y, Xu H. Effect of different types and dosages of statins on plasma lipoprotein(a) levels: a network meta-analysis. *Pharmacol Res.* (2021) 163:105275. doi: 10.1016/j.phrs.2020.105275

71. Lu G, Ades AE. Assessing evidence inconsistency in mixed treatment comparisons. *J Am Stat Assoc.* (2006) 101:447–59. doi: 10.1198/016214505000001302

72. Ridker PM, Danielson E, Fonseca FA, Genest J, Gotto AM Jr, Kastelein JJ, et al. Rosuvastatin to prevent vascular events in men and women with elevated C-reactive protein. *N Engl J Med.* (2008) 359:2195–207. doi: 10.1056/NEJMoa0807646

73. Yusuf S, Bosch J, Dagenais G, Zhu J, Xavier D, Liu L, et al. Cholesterol lowering in intermediate-risk persons without cardiovascular disease. *N Engl J Med.* (2016) 374:2021–31. doi: 10.1056/NEJMoa1600176

74. Kandelouei T, Abbasifard M, Imani D, Aslani S, Razi B, Fasihi M, et al. Effect of statins on serum level of Hs-CRP and CRP in patients with cardiovascular diseases: a systematic review and meta-analysis of randomized controlled trials. *Mediators Inflamm.* (2022) 2022:8732360. doi: 10.1155/2022/8732360

75. Alikiaii B, Heidari Z, Bagherniya M, Askari G, Sathyapalan T, Sahebkar A. The effect of statins on C-reactive protein in stroke patients: a systematic review of clinical trials. *Mediators Inflamm.* (2021) 2021:7104934. doi: 10.1155/2021/7104934

76. Milajerdi A, Larijani B, Esmaillzadeh A. Statins influence biomarkers of low grade inflammation in apparently healthy people or patients with chronic diseases: a systematic review and meta-analysis of randomized clinical trials. *Cytokine.* (2019) 123:154752. doi: 10.1016/j.cyto.2019.154752

77. Jia J, Zhang L, Wang L, Ji C, Xia R, Yang Y. A systematic review and meta-analysis on the efficacy of statins in the treatment of atherosclerosis. *Ann Palliat Med.* (2021) 10:6793–803. doi: 10.21037/apm-21-1243

78. Tuñón J, Bäck M, Badimón L, Bochaton-Piallat ML, Cariou B, Daemen MJ, et al. Interplay between hypercholesterolaemia and inflammation in atherosclerosis: translating experimental targets into clinical practice. *Eur J Prev Cardiol.* (2018) 25:948–55. doi: 10.1177/2047487318773384

79. Labos C, Brophy JM, Smith GD, Sniderman AD, Thanassoulis G. Evaluation of the pleiotropic effects of statins: a reanalysis of the randomized trial evidence using egger regression-brief report. *Arterioscler Thromb Vasc Biol.* (2018) 38:262–5. doi: 10.1161/ATVBAHA.117.310052

80. Hartwig FP, Borges MC, Lawlor DA. Letter by Hartwig et al. regarding article, "Evaluation of the pleiotropic effects of statins: a reanalysis of the randomized trial evidence using egger regression". *Arterioscler Thromb Vasc Biol.* (2018) 38:e85–6. doi: 10.1161/ATVBAHA.118.310897

81. Ridker PM, Rifai N, Pfeffer MA, Sacks FM, Moye LA, Goldman S, et al. Inflammation, pravastatin, and the risk of coronary events after myocardial infarction in patients with average cholesterol levels. Cholesterol and Recurrent Events (CARE) investigators. *Circulation.* (1998) 98:839–44. doi: 10.1161/01.CIR.98.9.839

82. Ridker PM, Rifai N, Clearfield M, Downs JR, Weis SE, Miles JS, et al. Measurement of C-reactive protein for the targeting of statin therapy in the primary prevention of acute coronary events. *N Engl J Med.* (2001) 344:1959–65. doi: 10.1056/NEJM200106283442601

83. Albert MA, Danielson E, Rifai N, Ridker PM. Effect of statin therapy on C-reactive protein levels: the pravastatin inflammation/CRP evaluation (PRINCE): a randomized trial and cohort study. *JAMA.* (2001) 286:64–70. doi: 10.1001/jama.286.1.64

84. Vlachopoulos C, Xaplanteris P, Aboyans V, Brodmann M, Cífková R, Cosentino F, et al. The role of vascular biomarkers for primary and secondary prevention. A position paper from the European Society of Cardiology Working Group on peripheral circulation: Endorsed by the Association for Research into Arterial Structure and Physiology (ARTERY) Society. *Atherosclerosis.* (2015) 241:507–32. doi: 10.1016/j.atherosclerosis.2015.05.007

85. Ridker PM, Rifai N, Rose L, Buring JE, Cook NR. Comparison of C-reactive protein and low-density lipoprotein cholesterol levels in the prediction of first cardiovascular events. *N Engl J Med.* (2002) 347:1557–65. doi: 10.1056/NEJMoa021993

86. Ridker PM, Hennekens CH, Buring JE, Rifai N. C-reactive protein and other markers of inflammation in the prediction of cardiovascular disease in women. *N Engl J Med.* (2000) 342:836–43. doi: 10.1056/NEJM200003233421202

87. Plosker GL, McTavish D. Simvastatin. A reappraisal of its pharmacology and therapeutic efficacy in hypercholesterolaemia. *Drugs.* (1995) 50:334–63. doi: 10.2165/00003495-199550020-00009

88. Qi YY, Yan L, Wang ZM, Wang X, Meng H, Li WB, et al. Comparative efficacy of pharmacological agents on reducing the risk of major adverse cardiovascular events in the hypertriglyceridemia population: a network meta-analysis. *Diabetol Metab Syndr.* (2021) 13:15. doi: 10.1186/s13098-021-00626-7

89. Abbasifard M, Kandelouei T, Aslani S, Razi B, Imani D, Fasihi M, et al. Effect of statins on the plasma/serum levels of inflammatory markers in patients with cardiovascular disease; a systematic review and meta-analysis of randomized clinical trials. *Inflammopharmacology.* (2022) 30:369–83. doi: 10.1007/s10787-022-00926-y

90. Stone NJ, Robinson JG, Lichtenstein AH, Bairey Merz CN, Blum CB, Eckel RH, et al. 2013 ACC/AHA guideline on the treatment of blood cholesterol to reduce atherosclerotic cardiovascular risk in adults: a report of the American College of Cardiology/American Heart Association Task Force on Practice Guidelines. *J Am Coll Cardiol.* (2014) 63:2889–934. doi: 10.1016/j.jacc.2013.11.002

91. Tramacere I, Boncoraglio GB, Banzi R, Del Giovane C, Kwag KH, Squizzato A, et al. Comparison of statins for secondary prevention in patients with ischemic stroke or transient ischemic attack: a systematic review and network meta-analysis. *BMC Med.* (2019) 17:67. doi: 10.1186/s12916-019-1298-5

92. Chen X, Wang DD, Li ZP. Analysis of time course and dose effect of tacrolimus on proteinuria in lupus nephritis patients. *J Clin Pharm Ther.* (2021) 46:106–13. doi: 10.1111/jcpt.13260

frontiers | Frontiers in Cardiovascular Medicine

TYPE Original Research
PUBLISHED 12 August 2022
DOI 10.3389/fcvm.2022.935185

OPEN ACCESS

EDITED BY
Wen-Jun Tu,
Chinese Academy of Medical Sciences and Peking Union Medical College, China

REVIEWED BY
Yanhui Dong,
Peking University, China
Yoshiharu Fukuda,
Teikyo University, Japan

*CORRESPONDENCE
Yinglong Duan
yinglongduan@outlook.com
Jianfei Xie
xiejianfei007@163.com

†These authors share first authorship

SPECIALTY SECTION
This article was submitted to Atherosclerosis and Vascular Medicine, a section of the journal Frontiers in Cardiovascular Medicine

RECEIVED 03 May 2022
ACCEPTED 18 July 2022
PUBLISHED 12 August 2022

CITATION
Zhang C, Wang J, Ding S, Gan G, Li L, Li Y, Chen Z, Duan Y, Xie J and Cheng ASK (2022) Relationship between lifestyle and metabolic factors and carotid atherosclerosis: A survey of 47,063 fatty and non-fatty liver patients in China. *Front. Cardiovasc. Med.* 9:935185. doi: 10.3389/fcvm.2022.935185

Relationship between lifestyle and metabolic factors and carotid atherosclerosis: A survey of 47,063 fatty and non-fatty liver patients in China

Chun Zhang[1,2†], Jiangang Wang[1†], Siqing Ding[3], Gang Gan[2], Lijun Li[2], Ying Li[3], Zhiheng Chen[3], Yinglong Duan[3*], Jianfei Xie[3*] and Andy S. K. Cheng[4]

[1]Health Management Center, The Third Xiangya Hospital, Central South University, Changsha, China, [2]Xiangya Nursing School, Central South University, Changsha, China, [3]The Third Xiangya Hospital, Central South University, Changsha, China, [4]Department of Rehabilitation Sciences, The Hong Kong Polytechnic University, Hong Kong, Hong Kong SAR, China

Background and aims: Carotid atherosclerosis and stenosis are common lesions of the artery wall that form the basis of cardiovascular events. Compared with coronary atherosclerosis, few studies have explored the influencing factors of carotid atherosclerosis. The aim of this study was to explore the influencing factors of carotid atherosclerosis and carotid stenosis without and with fatty liver disease (FLD).

Methods: A total of 47,063 adults were recruited for this cross-sectional study. The color Doppler ultrasound, including metabolic factors and lifestyle surveys, was used to determine whether the participants had FLD and carotid artery disease. Multiple logistic regression was used to investigate the influencing factors of lifestyle and metabolism of carotid atherosclerosis and stenosis in the participants with and without FLD.

Results: In participants without FLD, current alcohol consumption (OR: 0.749, 95% CI: 0.588) and hip circumference (OR: 0.970, 95% CI: 0.961, 0.979) were the main protective factors for carotid atherosclerosis. Systolic blood pressure (OR: 1.022, 95% CI: 1.019, 1.025) and diastolic blood pressure (OR: 1.005, 95% CI: 1.001, 1.010), elevated fasting blood glucose (OR: 1.012, 95% CI: 1.005, 1.019), and non-sedentary behavior (OR: 1.084, 95% CI: 1.014, 1.160) were the main risk factors for carotid atherosclerosis. Hip circumference (OR: 0.932, 95% CI: 0.910, 0.954) and low-density lipoprotein (OR: 0.979, 95% CI: 0.964, 0.994) were protective factors for carotid stenosis. Smoking (OR: 3.525, 95% CI: 1.113, 11.169) and unqualified exercise (OR: 1.402, 95% CI: 1.083, 1.815) were risk factors for carotid stenosis. In participants with FLD, smoking (OR: 0.827, 95% CI: 0.703, 0.973) and hip circumference (OR: 0.967, 95% CI: 0.958, 0.977) were the main protective factors for carotid atherosclerosis. BMI 18.5–23.9 (OR: 1.163, 95% CI: 1.002, 1.351), non-sedentary behavior (OR: 1.086, 95% CI: 1.009, 1.168), and waist circumference (OR: 1.030, 95% CI: 1.022, 1.038) were the main risk factors for carotid atherosclerosis.

Conclusion: Based on a large-sample check-up population in China, this study investigated the influencing factors of carotid atherosclerosis and carotid stenosis in fatty liver and non-fatty liver patients and explored the influencing factors of metabolism and lifestyle, which were mainly focused on exercise, sedentary behavior, smoking, alcohol consumption, hip circumference, and blood pressure.

KEYWORDS

lifestyle, metabolic factors, carotid atherosclerosis, fatty liver, large sample

Introduction

Fatty liver disease (FLD) is a common chronic disease that is a pathological process of excessive accumulation of fat in liver cells caused by various factors, such as disease or drugs (1). With the development of the disease, fatty liver can progress from simple steatosis to steatohepatitis and can develop into cirrhosis in serious cases. FLD is becoming the most common liver disease in the world and is not only associated with significant morbidity but also leads to higher socioeconomic costs and impaired health-related quality of life (2). Previous studies have shown that fatty liver is often affected by lifestyle factors, such as diet and exercise (3). Hepatic steatosis has also been found to be associated with individual metabolic factors, including diabetes, hypertension, impaired fasting glucose, high-density lipoprotein cholesterol (HDL-C), and hypertriglyceridemia (4).

Cardiovascular disease (CVD) is one of the major public health problems threatening the health of Chinese people (5). Prevention of CVD risk factors and early diagnosis and treatment of high-risk groups can effectively reduce mortality. Carotid atherosclerosis and stenosis are common lesions of the artery wall that form the basis of CVD, which may lead to narrowing and occlusion of the arteries (6).

Studies have explored the relationship between FLD and coronary atherosclerosis and found that people with FLD have a higher probability of coronary atherosclerosis than those without FLD (4). Other studies have also found that the increased risk of FLD was associated with cardiovascular risk factors and persisted after adjustment for overall obesity or visceral adipose tissue, suggesting a bidirectional relationship between fatty liver and cardiovascular risk factors (7). Moreover, in a study of 265 patients with early liver disease, carotid intima–media thickness (cIMT) was higher in patients with fatty liver than in those without fatty liver (8), and fatty liver was associated with increased cIMT, artery calcification, and endothelial dysfunction (9).

However, compared with coronary atherosclerosis, few studies have explored the influencing factors of carotid atherosclerosis among fatty and non-fatty liver patients. In our study, we conducted a large-sample survey to explore the lifestyle and metabolic factors affecting carotid atherosclerosis and stenosis in both participants with and without FLD to provide evidence for targeted prevention of carotid artery disease and further reduce the risk of CVD.

Materials and methods

Study design and participants

The study was a cross-sectional survey, and we recruited participants from two health management centers of general hospitals located in China. From 1 January 2017 to 31 December 2019, a total of 53,657 people aged ≥18 years underwent a color Doppler ultrasound of the liver and carotid artery. The following participants were excluded: participants who lacked sociodemographic data (n=1511) and metabolism-related indicators (n = 530) and participants lacking data on smoking, alcohol consumption, physical activity (n = 1,840), and diet-related information (n = 2,713). As a result, 47,063 participants were assessed in further data analysis. All the institutions involved in this study have given their approval. Informed consent was obtained from each participant in this study, and participation was voluntary without any reward (see Figure 1).

Measures

Demographic and lifestyle characteristics

We collected the following data for each participant through questionnaires: sex, age, and body mass index (BMI), which was categorized as lean, normal weight, overweight, and obese for BMI < 18.5, 18.5–23.9, 24–27.9, and ≥28 kg/m^2, respectively. Smoking was classified as a non-smoker, current smoker, and ex-smoker, while alcohol consumption was classified as none, yes, and abstinent from alcohol. Based on the American College of Sports Medicine's standards (10), physical activity standards were judged based on whether the amount of activity in the previous month was more than 12 times per month, including the intensity, duration, and frequency. The Dietary Diversity Scale (DDS) was used to evaluate dietary diversity, which was divided into nine categories according to the 2016 Edition of

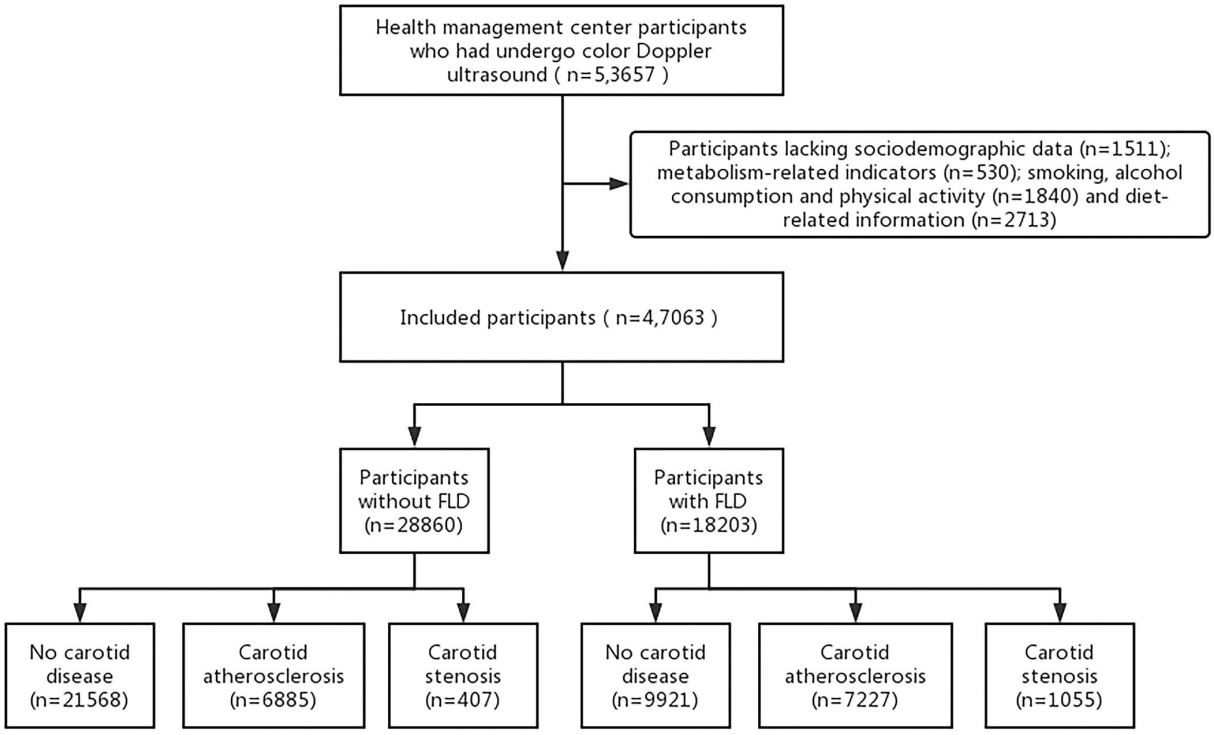

FIGURE 1
Flowchart of this study.

Chinese Residents' Balanced Diet Pagoda (11), including cereals, vegetables, fruits, livestock and poultry meat, fish and shrimp, eggs, milk, beans, and oil. According to the total number of types of food consumed by the subjects in a week, the consumption score is 1, and the non-consumption score is 0. The level of dietary diversification was divided into three grades: 1 to 3 was insufficient, 4 to 6 was moderate, and 7 to 9 was sufficient (12). Sedentary behavior was defined as waking, using the equivalent of 1.5 MET while sitting or lying down (13), and a metabolic equivalent was defined as the amount of energy expended while sitting at rest. According to the relevant literature (14), with 5 h/d as the cutoff, sedentary behavior was defined as $\geq$5 h/d, and non-sedentary behavior was defined as $<$ 5 h/d.

Common metabolic risk factors

According to the standard of waist and hip circumference unique to Asia, waist circumference (WC) was measured by trained researchers at the midpoint between the base of the thoracic cage and the top of the iliac crest, and hip circumference was measured at the symphysis pubis and the most convex part of the posterior gluteus maximus while the subjects were standing. Blood pressure was measured by a trained nurse using a sphygmomanometer while subjects sat in a seated position with their arms supported at the heart level. Blood lipid examination results included fasting blood glucose, total cholesterol (TC), triglyceride (TG), HDL-C, and low-density lipoprotein cholesterol (LDL-C).

Statistical analysis

All data in this study were collated and analyzed using SPSS 25.0. Demographic and lifestyle data were described by frequencies, and metabolic indicators were described by mean (M) $\pm$ standard deviation (SD). Multiple logistic regression was used to investigate the influencing factors of carotid atherosclerosis and stenosis in participants without and with fatty liver. Odds ratios (ORs) and 95% confidence intervals (CIs) were reported, with a test level of $\alpha = 0.05$.

Results

Demographic characteristics and the prevalence of carotid atherosclerosis and stenosis

Of 47,063 participants, 28,860 (61.3%) had no FLD and 18,203 (38.7%) had FLD. The demographic characteristics and lifestyle characteristics of the participants are listed in Table 1, and metabolic factors are listed in Table 2. Among the people without FLD, 21,568 (74.7%) did not have carotid artery

TABLE 1 Demographic characteristics and lifestyle factors.

Variable		Without FLD		With FLD	
		N	Percentage (%)	N	Percentage (%)
Sex	Men	14,634	50.7%	13,132	72.1%
	Female	14,226	49.3%	5,071	27.9%
Age	≤30	3,604	12.5%	1,253	6.9%
	31–49	14,377	49.8%	8,843	48.6%
	50–64	9,025	31.3%	6,924	38.0%
	≥65	1,854	6.4%	1,183	6.5%
BMI	<18.5	1,134	3.9%	106	0.6%
	18.5–23.9	16,743	58.0%	4,274	23.5%
	24–27.9	9,123	31.6%	9,575	52.6%
	≥28	1,860	6.4%	4,248	23.3%
Smoking	Non-smoker	19,512	67.6%	9,592	52.7%
	Current	8,570	29.7%	7,771	42.7%
	Ex-smoker	778	2.7%	840	4.6%
Alcohol	Never	19,321	66.9%	9,185	50.5%
	Current	9,158	31.7%	8,665	47.6%
	Abstinent from alcohol	381	1.3%	353	1.9%
Physical activity	Unqualified	22,246	77.1%	14,222	78.1%
	Qualified	6614	22.9%	3,981	21.9%
Sedentary behavior	Yes	18,473	64.0%	11,107	61.0%
	None	10,387	36.0%	7,096	39.0%
Dietary diversity	Insufficient	2,187	7.6%	1,578	8.7%
	Moderate	6,344	22.0%	3,778	20.8%
	Sufficient	20,329	70.4%	12,847	70.6%
Carotid artery Disease	None	21,568	74.7%	9,921	54.5%
	Carotid atherosclerosis	6,885	23.9%	7,227	39.7%
	Carotid stenosis	407	1.4%	1055	5.8%

disease, 6,885 (23.9%) suffered from carotid atherosclerosis, and 407 (1.4%) suffered from carotid stenosis. There were 3,604 participants ≤ 30 years, accounting for 12.5%; 14,377 participants were 31–49 years old, accounting for 49.8%; 9,025 participants were 50–64 years old, accounting for 31.3%; and 1,854 participants were ≥ 65 years old, accounting for 6.4%. Among participants with FLD, there were 9,921 (54.5%) participants without carotid artery disease, 7,227 participants (39.7%) with carotid atherosclerosis, and 1,055 participants (5.8%) with carotid stenosis. There were 13,132 male (72.1%) and 5,071 female participants (27.9%). A total of 1,253 (6.9%) participants were ≤ 30 years, 8,843 participants (48.6%) were 31–49 years, 6,924 participants (38.0%) were 50–64 years, and 1,183 (6.5%) participants were ≥ 65 years.

Factors influencing carotid disease in participants without FLD

The results of multiple logistic regression analysis in participants without FLD are shown in Table 3.

Influencing factors of carotid atherosclerosis without FLD

Compared with participants of age ≥65 years, participants whose age ≤30 years (OR: 0.076, 95% CI: 0.063, 0.092, $p < 0.000$) and 31-49 years (OR: 0.218, 95% CI: 0.194, 0.244, $p<0.000$) were considered protective factors. Compared with participants of BMI ≥ 28, participants with BMI < 18.5 was a protective factor (OR: 0.594, 95% CI: 0.448, 0.788, $p < 0.000$). Non-smoking was a protective factor compared with smoking cessation (OR: 0.726, 95% CI: 0.608, 0.866, $p < 0.000$). Current drinkers were less likely to develop carotid atherosclerosis than former drinkers who abstained (OR: 0.749, 95% CI: 0.588, 0.953, $p = 0.019$). Hip circumference was a protective factor, and greater hip circumference was associated with the likelihood of developing carotid atherosclerosis (OR: 0.970, 95% CI: 0.961, 0.979, $p < 0.000$). Both systolic blood pressure (OR: 1.022, 95% CI: 1.019, 1.025, $p < 0.000$) and diastolic blood pressure (OR: 1.005, 95% CI: 1.001, 1.010, $p = 0.024$) were risk factors. Elevated fasting blood glucose was a risk factor (OR: 1.012, 95% CI: 1.005, 1.019, $p = 0.001$). Being male was a greater risk factor than being female (OR: 1.104, 95% CI: 1.024, 1.189, $p = 0.009$); unqualified exercise

TABLE 2 Metabolic related factors.

Variable	Without FLD		With FLD	
	M	SD	M	SD
Waistline	79.26	9.322	87.896	8.9884
Hip circumference	95.77	553.457	96.466	10.0494
Systolic pressure	120.28	15.911	127.68	15.720
Diastolic pressure	73.07	10.884	79.42	11.177
FBG	5.57	3.977	6.24275	6.494533
Total cholesterol	6.18	6.892	6.0780	5.74361
TG	2.92	5.631	4.4457	7.81684
HDL-C	2.75	4.534	3.2967	5.11097
LDL-C	5.48	8.765	5.4248	8.68359

was a risk factor compared with qualified exercise (OR: 1.316, 95% CI: 1.218, 1.422, $p < 0.000$); and non-sedentary behavior was a risk factor compared with sedentary behavior (OR: 1.084, 95% CI: 1.014, 1.160, $p = 0.019$).

Influencing factors of carotid artery stenosis without FLD

Smoking was a risk factor compared with smoking cessation (OR: 3.525, 95% CI: 1.113, 11.169, $p = 0.032$); unqualified exercise was a risk factor compared with qualified exercise (OR: 1.402, 95% CI: 1.083, 1.815, $p = 0.010$). Hip circumference was a protective factor (OR: 0.932, 95% CI: 0.910, 0.954, $p = 0.000$), and LDL-C was a protective factor (OR: 0.979, 95% CI: 0.964, 0.994, $p = 0.006$).

Influencing factors of carotid disease in participants with FLD

The results of multiple logistic regression analysis in participants with FLD are given in Table 3.

Factors influencing carotid atherosclerosis with FLD

Participants of age ≤30 years (OR: 0.087, 95% CI: 0.068, 0.112, $p < 0.000$) and 31-49 years (OR: 0.257, 95% CI: 0.223, 0.296, $p < 0.000$) were protective factors compared with participants of age ≥65 years. Non-smoking was a protective factor compared with smoking cessation (OR: 0.818, 95% CI: 0.695, 0.962, $p = 0.015$), and smoking was also a protective factor (OR: 0.827, 95% CI: 0.703, 0.973, $p = 0.022$). Hip circumference was a protective factor (OR: 0.967, 95% CI: 0.958, 0.977, $p < 0.000$); WC was a risk factor (OR: 1.030, 95% CI: 1.022, 1.038, $p < 0.000$); elevated systolic blood pressure was a risk factor (OR: 1.013, 95% CI: 1.010, 1.017, $p < 0.000$); elevated blood glucose was a risk factor (OR: 1.010, 95% CI: 1.004, 1.015, $p = 0.001$); compared with participants with BMI≥28, people with BMI 18.5–23.9 (OR: 1.163, 95% CI: 1.002, 1.351, $p = 0.047$) and BMI 24–27.9 (OR: 1.112, 95% CI: 1.004, 1.232, $p = 0.041$) were more likely to develop carotid atherosclerosis; unqualified exercise was a risk factor (OR: 1.280, 95% CI: 1.177, 1.392, $p < 0.000$); and non-sedentary behavior was also a risk factor (OR: 1.086, 95%CI: 1.009, 1.168, $p = 0.028$).

Factors influencing carotid artery stenosis with FLD

Waist circumference was a protective factor (OR: 0.916, 95% CI: 0.904, 0.927, $p < 0.000$); systolic blood pressure was also a protective factor (OR: 0.992, 95% CI: 0.985, 1.000, $p = 0.047$); and elevated TG was a protective factor (OR: 0.981, 95% CI: 0.970, 0.992, $p = 0.001$). Compared to participants with a BMI ≥ 28, participants with BMI < 18.5 (OR: 0.492, 95% CI: 0.273, 0.887, $p = 0.018$), 18.5–23.9 (OR: 0.585, 95% CI: 0.438, 0.781, $p < 0.000$), and 24–27.9 (OR: 0.558, 95% CI: 0.448, 0.695, $p < 0.000$) were risk factors. Men were more at risk than women (OR: 1.424, 95% CI: 1.194, 1.700, $p < 0.000$), and age ≤30 years was a risk factor (OR: 1.778, 95% CI: 1.187, 2.663, $p = 0.005$).

Discussion

To investigate the influencing factors of carotid atherosclerosis and stenosis in participants with and without FLD, we investigated the presence of carotid atherosclerosis and stenosis identified in subjects in a large sample of people at health management centers in China. Relevant lifestyle and metabolic factors were also explored. In this study of 47,063 participants, there were 2,8,860 (61.3%) without FLD and 18,203 (38.7%) with FLD. Among the participants without FLD, 23.9% had carotid atherosclerosis and 1.4% had carotid artery stenosis. In participants with FLD, 39.7% had carotid atherosclerosis and 5.8% had carotid artery stenosis.

Influencing factors of carotid atherosclerosis in participants without FLD

We found that age ≤30 years and 31–49 years were protective factors for carotid atherosclerosis compared with age ≥65 years. With increasing age, the prevalence of carotid atherosclerosis increases gradually (15), which may be related to the aging of blood vessels in elderly individuals and the reduction in vascular elasticity in vascular calcification (16). Although the results were statistically significant, the OR value of the factor was very small, which may lead to weak convincing results. In our study, participants with a BMI ≤18.5

TABLE 3 Multivariate logistic regression of influencing factors of carotid artery disease.

			Without FLD					With FLD				
			B	SE	Wald	P	OR(95%CI)	B	SE	Wald	P	OR(95%CI)
Carotid arteriosclerosis	Intercept		−0.237	0.446	0.283	0.594		−1.009	0.487	4.283	0.038	
	Waistline		−0.001	0.003	0.125	0.724	0.999 (0.992, 1.006)	0.029	0.004	57.766	0.000	1.030 (1.022, 1.038)
	Hip circumference		−0.030	0.005	41.355	0.000	0.970 (0.961,0.979)	−0.033	0.005	43.090	0.000	0.967 (0.958,0.977)
	Systolic pressure		0.022	0.002	189.298	0.000	1.022 (1.019, 1.025)	0.013	0.002	52.115	0.000	1.013 (1.010, 1.017)
	Diastolic pressure		0.005	0.002	5.125	0.024	1.005 (1.001, 1.010)	0.005	0.003	3.487	0.062	1.005 (1.000, 1.010)
	FBG		0.012	0.004	10.361	0.001	1.012 (1.005, 1.019)	0.010	0.003	11.874	0.001	1.010 (1.004, 1.015)
	Total cholesterol		−0.002	0.002	0.506	0.477	0.998 (0.994, 1.003)	−0.005	0.003	3.152	0.076	0.995 (0.989, 1.001)
	TG		−0.003	0.003	1.272	0.259	0.997 (0.992, 1.002)	−0.002	0.002	1.154	0.283	0.998 (0.993, 1.002)
	HDL-C		−0.005	0.003	2.065	0.151	0.995 (0.988, 1.002)	0.002	0.003	0.249	0.618	1.002 (0.995, 1.008)
	LDL-C		0.002	0.002	1.194	0.274	1.002 (0.999, 1.005)	−0.003	0.002	1.782	0.182	0.997 (0.994, 1.001)
	Gender	Men	0.099	0.038	6.740	0.009	1.104 (1.024, 1.189)	−0.080	0.048	2.843	0.092	0.923 (0.840, 1.013)
		Female	0[b]					0[b]				
	Age	≤30	−2.579	0.096	720.595	0.000	0.076 (0.063,0.092)	−2.442	0.128	366.548	0.000	0.087 (0.068,0.112)
		31–49	−1.526	0.058	694.794	0.000	0.218 (0.194,0.244)	−1.359	0.072	359.836	0.000	0.257 (0.223,0.296)
		50–64	−0.061	0.055	1.250	0.264	0.940 (0.845, 1.047)	0.098	0.070	1.974	0.160	1.103 (0.962, 1.265)
		≥65	0[b]					0[b]				
	BMI	<18.5	−0.520	0.144	13.108	0.000	0.594 (0.448,0.788)	−0.040	0.316	0.016	0.898	0.960 (0.517, 1.785)
		18.5–23.9	−0.019	0.085	0.051	0.821	0.981 (0.830, 1.160)	0.151	0.076	3.945	0.047	1.163 (1.002, 1.351)
		24–27.9	−0.003	0.072	0.002	0.968	0.997 (0.865, 1.149)	0.107	0.052	4.156	0.041	1.112 (1.004, 1.232)
		≥28	0[b]					0[b]				
	Smoking	Non-smoker	−0.320	0.090	12.624	0.000	0.726 (0.608,0.866)	−0.201	0.083	5.918	0.015	0.818 (0.695,0.962)
		Current	−0.156	0.091	2.911	0.088	0.856 (0.716, 1.023)	−0.190	0.083	5.245	0.022	0.827 (0.703,0.973)
		Ex-smoker	0[b]					0[b]				
	Alcohol	Never	−0.221	0.122	3.268	0.071	0.802 (0.631, 1.019)	−0.197	0.123	2.548	0.110	0.821 (0.645, 1.046)
		Current	−0.289	0.123	5.536	0.019	0.749 (0.588,0.953)	−0.187	0.123	2.308	0.129	0.829 (0.652, 1.056)
		Abstinent from alcohol	0[b]					0[b]			.	
	Physical activity	Unqualified	0.275	0.039	48.487	0.000	1.316 (1.218, 1.422)	0.247	0.043	33.182	0.000	1.280 (1.177, 1.392)

(Continued)

10.3389/fcvm.2022.935185

TABLE 3 Continued

			Without FLD					With FLD				
			B	SE	Wald	P	OR(95%CI)	B	SE	Wald	P	OR(95%CI)
		Qualified	0[b]					0[b]				
	Sedentary behavior	Yes	0.081	0.034	5.538	0.019	1.084 (1.014, 1.160)	0.082	0.037	4.813	0.028	1.086 (1.009, 1.168)
		None	0[b]					0[b]				
	Dietary diversity	Insufficient	0.019	0.061	0.097	0.756	1.019 (0.904, 1.149)	0.097	0.068	2.040	0.153	1.101 (0.965, 1.257)
		Moderate	0.003	0.037	0.008	0.928	1.003 (0.933, 1.080)	0.066	0.043	2.416	0.120	1.069 (0.983, 1.162)
		Sufficient	0[b]					0[b]			.	
Carotid stenosis	Intercept		0.961	1.548	0.386	0.535		6.604	0.784	70.911	0.000	
	Waistline		0.007	0.011	0.431	0.511	1.007 (0.986, 1.029)	−0.088	0.007	183.349	0.000	0.916 (0.904,0.927)
	Hip circumference		−0.071	0.012	34.274	0.000	0.932 (0.910,0.954)	0.002	0.002	1.757	0.185	1.002 (0.999, 1.006)
	Systolic pressure		−0.001	0.006	0.008	0.927	0.999 (0.988, 1.011)	−0.008	0.004	3.956	0.047	0.992 (0.985, 1.000)
	Diastolic pressure		−0.005	0.008	0.395	0.530	0.995 (0.979, 1.011).	−0.007	0.005	2.002	0.157	0.993 (0.982, 1.003)
	FBG		−0.133	0.070	3.631	0.057	0.875 (0.763, 1.004)	−0.004	0.009	0.208	0.648	0.996 (0.979, 1.013)
	Total cholesterol		0.009	0.006	2.369	0.124	1.009 (0.997, 1.021)	0.000	0.005	0.000	0.989	1.000 (0.989, 1.011)
	TG		0.003	0.008	0.093	0.760	1.003 (0.986, 1.019)	−0.019	0.006	11.076	0.001	0.981 (0.970,0.992)
	HDL-C		0.004	0.011	0.106	0.745	1.004 (0.982, 1.025)	−0.014	0.007	3.707	0.054	0.987 (0.973, 1.000)
	LDL-C		−0.022	0.008	7.613	0.006	0.979 (0.964,0.994)	−0.007	0.004	2.600	0.107	0.993 (0.985, 1.001)
	Gender	Men	−0.085	0.129	0.434	0.510	0.919 (0.714, 1.182)	0.354	0.090	15.387	0.000	1.424 (1.194, 1.700)
		Female	0[b]					0[b]				
	Age	≤30	0.045	0.279	0.027	0.871	1.047 (0.606, 1.808)	0.575	0.206	7.791	0.005	1.778 (1.187, 2.663)
		31–49	−0.075	0.255	0.086	0.769	0.928 (0.563, 1.529)	−0.077	0.194	0.159	0.690	0.926 (0.633, 1.353)
		50–64	0.171	0.258	0.438	0.508	1.186 (0.715, 1.967)	0.292	0.196	2.208	0.137	1.339 (0.911, 1.967)
		≥65	0[b]					0[b]				
	BMI	<18.5	0.490	0.489	1.001	0.317	1.632 (0.625, 4.259)	−0.708	0.300	5.569	0.018	0.492 (0.273,0.887)
		18.5–23.9	0.552	0.408	1.831	0.176	1.737 (0.781, 3.864)	−0.537	0.148	13.225	0.000	0.585 (0.438,0.781)
		24–27.9	0.708	0.382	3.430	0.064	2.030 (0.960, 4.292)	−0.584	0.112	27.114	0.000	0.558 (0.448,0.695)
		≥28	0[b]					0[b]				
	Smoking	Non-smoker	0.987	0.588	2.821	0.093	2.683 (0.848, 8.487)	0.077	0.186	0.173	0.677	1.080 (0.750, 1.556).
		Current	1.260	0.588	4.587	0.032	3.525 (1.113, 11.169)	−0.154	0.188	0.671	0.413	0.857 (0.593, 1.239)
		Ex-smoker	0[b]					0[b]				

(Continued)

10.3389/fcvm.2022.935185

10.3389/fcvm.2022.935185

TABLE 3 Continued

		Without FLD					With FLD				
		B	SE	Wald	P	OR(95%CI)	B	SE	Wald	P	OR(95%CI)
Alcohol	Never	0.197	0.590	0.112	0.738	1.218 (0.383, 3.867)	0.161	0.282	0.325	0.569	1.175 (0.675, 2.043)
	Current	0.362	0.591	0.376	0.540	1.437 (0.451, 4.575)	−0.027	0.283	0.009	0.924	0.973 (0.559, 1.695)
	Abstinent from alcohol	0[b]					0[b]				
Physical activity	Unqualified	0.338	0.132	6.572	0.010	1.402 (1.083, 1.815)	0.076	0.080	0.897	0.344	1.079 (0.922, 1.262)
	Qualified	0[b]					0[b]			.	
Sedentary behavior	Yes	0.030	0.112	0.072	0.789	1.030 (0.828, 1.282)	0.084	0.073	1.317	0.251	1.087 (0.942,1.255)
	None	0[b]					0[b]				
Dietary diversity	Insufficient	0.216	0.189	1.309	0.253	1.242 (0.857, 1.799)	0.244	0.146	2.796	0.095	1.277 (0.959, 1.700)
	Moderate	−0.144	0.129	1.249	0.264	0.866 (0.672, 1.115)	0.055	0.082	0.442	0.506	1.056 (0.899, 1.241)
	Sufficient	0[b]					0[b]				

[b] is the symbol of the statistical result derived from the system.

were less likely to develop carotid atherosclerosis than those with a BMI of ≥28. A cohort study (15) found that long-term high BMI was associated with a carotid atherosclerosis index and plaque volume. The participants without FLD did not necessarily have a lower BMI, so the possibility that a high BMI may increase the risk of carotid atherosclerosis should be considered. Non-smoking was a protective factor for carotid atherosclerosis compared with previous smoking. Studies have shown that active and passive smoking may lead to an increased carotid artery calcification index in patients with essential hypertension (17), and exposure to cigarette smoke appears to be a contributing factor to atherosclerosis. We also found that current drinkers were less likely to develop carotid atherosclerosis than previous drinkers. Previous studies have shown (18) that moderate alcohol consumption was inversely associated with carotid atherosclerosis among Han, Uighur, and Kazakh populations in China. Moreover, compared with the non-drinking elderly, drinking one to six cups per week was negatively correlated with carotid atherosclerosis (19). Therefore, most of the non-fatty liver patients in our study may be moderate drinkers. Compared with women without FLD, men were more likely to develop carotid atherosclerosis. Studies have shown (20) that reduced social support and lack of awareness of the disease and physiological differences between the sexes contribute to differences in the prevalence of carotid atherosclerosis. Therefore, we should not only be aware of the differences between men and women in carotid artery disease but also provide different treatment measures. We also found that, compared with qualified exercise, unqualified exercise was a risk factor for carotid atherosclerosis; however, non-sedentary behavior was a risk factor for carotid atherosclerosis compared with sedentary behavior. Physical activity levels were significantly and negatively correlated with cIMT (21). The risk of the carotid artery and carotid plaque (CP) abnormalities decreased significantly with increased exercise levels, and the negative correlation was stronger among participants aged ≥60 years. However, sedentary leisure time was not associated with cIMT or CP. Physical activity is important for carotid artery health, especially in the elderly. Research has shown that self-reporting can underestimate the actual amount of time taken by some sedentary behaviors and thus cannot be considered the gold standard, while a combination of self-reporting and usage of devices that objectively assess sedentary behavior may be more accurate (22, 23).

The results showed that the larger the hip circumference, the less likely the carotid atherosclerosis development. Hassinen et al. (24) found that the smaller the hip circumference, the faster the progression of carotid atherosclerosis. We found that higher systolic and diastolic blood pressure were associated with a greater risk of carotid atherosclerosis in participants without FLD. Studies suggested that the brachial muscle and systolic blood pressure index were associated with increased cIMT (25). The target organ damage and incidence of cardiovascular and

cerebrovascular events significantly increase in hypertensive patients with abnormal blood pressure rhythm (26), which increased the risk of carotid atherosclerosis. Therefore, blood pressure should be controlled at not only a normal level but also at the morning peak of blood pressure. Elevated fasting glucose was a risk factor for carotid atherosclerosis, which was consistent with the results of previous studies (27). Although participants did not have FLD, elevated fasting glucose may represent endocrine disorders, resulting in the decreased metabolic function of individuals and an increased possibility of atherosclerosis.

Influencing factors of carotid artery stenosis in participants without FLD

Our results found that smoking and unqualified exercise were risk factors for carotid artery stenosis, which was identical to carotid atherosclerosis, suggesting that smoking and lack of exercise may be risk factors for carotid disease. Hip circumference was a protective factor for carotid stenosis in patients without FLD. Earlier studies (28, 29) have shown that hip circumference was negatively associated with type 2 diabetes and CVD morbidity and mortality. We found that low-density lipoprotein was a protective factor for carotid atherosclerosis in patients without FLD. However, studies (30) showed that increased LDL-C levels were an independent risk factor for carotid artery stenosis. The difference may be due to the difference in subjects.

Factors influencing carotid atherosclerosis in patients with FLD

Patients with age ≤30 and 31–49 years were protective factors for carotid atherosclerosis compared with patients with age ≥65 years. Young and middle-aged people were less likely to develop carotid atherosclerosis, which was consistent with participants without FLD. The possible reason may be that aging is a process characterized by progressive loss of tissue and organ functions (31), ROS-induced damage causes age-related functional loss, and this oxidative stress is also involved in age-related diseases. Compared with those who had quit smoking, non-smoking was a protective factor, which was consistent with those without FLD. However, smoking was also a protective factor. The possible reason may be that smoking was a risk factor for carotid artery abnormalities, but there exists a dose-dependent relationship (32, 33). Therefore, it is necessary to further explore the specific amount of smoking, such as the number of carotid artery influences, to better guide smokers to gradually change their smoking habits. We also found that those with BMI of 18.5–23.9 and 24–27.9 were more likely to develop carotid atherosclerosis. In a cohort study of NAFLD patients in the United States (34), more than 10% of participants were thin, and Asians made up almost half of the thin people with FLD. The possible reason may be that Asians with fatty liver may be more emaciated due to physical differences, so participants with FLD with a lower BMI may be more prone to carotid atherosclerosis. We also found that unqualified exercise and sedentary time of up to 5 h were risk factors. A large study of Lavie et al. (35) sedentary times revealed that 49,493 adults living in 20 countries sat for an average of 5 h a day, and studies of older adults found that 59% sat for 4 h a day, and 27% sat for 6 h a day (13). In this study, according to self-reports, sedentary behavior time ≤5 h was a risk factor for carotid atherosclerosis in participants with FLD. Self-reported assessments of sitting time may vary across fields, backgrounds, and countries.

In participants with FLD, the greater the hip circumference, the less likely carotid atherosclerosis development, which was consistent with the participants without FLD, suggesting that hip circumference may be a protective factor for carotid atherosclerosis, regardless of whether participants had FLD. WC was a risk factor for carotid atherosclerosis, which was not found in people without FLD. Studies have shown that in diabetic patients (36), a larger WC increases the burden of carotid atherosclerosis. It may also be that WC was generally larger in people with FLD than in people without FLD. In a Chinese cohort study (37), increased WC and sustained high WC were found to be associated with increased cIMT. Therefore, maintaining normal WC may be important to promote vascular health. Studies (38) have shown that curcumin supplementation may have a positive effect on visceral fat and abdominal obesity associated with FLD. Therefore, curcumin supplementation may be considered for people with large abdominal fatty liver. Elevated systolic blood pressure and elevated blood sugar levels were risk factors for carotid atherosclerosis, similar to participants without FLD. A 5-year follow-up of a Korean male occupational population showed that the incidence of hypertension in moderate and severe fatty liver patients was 1.60 times and 2.22 times higher than that in the control group (8). After adjusting for age, BMI, liver function, blood lipids, smoking and other factors, FLD was still correlated with hypertension.

Influencing factors of carotid stenosis in patients with FLD

People with BMI<18.5, 18.5–23.9, and 24–27.9 were less likely to have carotid artery stenosis, which was consistent with previous studies (39, 40). Men were more likely to develop carotid artery stenosis than women, which was consistent with the influencing factors of carotid atherosclerosis. In patients with fatty liver, those aged ≤30 years were more likely to develop carotid artery stenosis than those aged ≥65 years, and increasing age was an independent risk factor for carotid artery stenosis

(30). Studies have shown that (4) FLD may be a more important contributor to subclinical atherosclerosis in younger, rather than older, populations. In our study, the possible reason may be that among the participants with FLD, the elderly died due to carotid artery stenosis. This may also be due to the small proportion of the two age-groups.

We found that the larger the WC, the less likely the carotid stenosis development. There was a statistically significant difference in the prevalence of high cIMT between WC 79 cm and WC < 79 cm (41), and the optimal WC cutoff currently used to diagnose carotid artery disease may be lower than Japan's current diagnostic criteria. Other studies (42) have shown that WC in Shanghai women was significantly correlated with cIMT, and WC ≥85 cm can be used as a risk indicator for subclinical carotid artery disease. Therefore, more evidence should be compiled to determine the most reliable thresholds for carotid atherosclerosis risk. The higher the systolic blood pressure, the less likely the presence of carotid stenosis, which was not found in participants without FLD. The prevalence of baseline characteristics and vascular risk factors in our study population differs from previous studies (43). Elevated TG was a protective factor for carotid artery stenosis. The relationship between TG and CVD risk factors has been controversial. Hypertriglyceridemia was often associated with lipoprotein changes, such as decreased HDL and HDL-C levels and increased non-HDL-C levels, all of which were associated with increased cardiovascular risk (44). Therefore, more studies are needed to explore the mechanism between elevated TG levels and carotid artery disease.

There were several limitations in our study. First, lifestyle characteristics were collected through questionnaires. Although self-report can help judge the background status of an individual at that time, the form of self-report may lead to information bias. Therefore, a combination of objective instrument-based measurements and self-reporting may lead to more accurate results. Second, the influencing factors of carotid atherosclerosis and stenosis in patients with and without fatty liver were only discussed through cross-sectional investigation, but the comparison between the two groups and the discussion on the longitudinal influence of carotid artery disease were lacking, which should be remedied in future to better prevent and control the occurrence and development of carotid artery disease. Third, this study only discussed the influencing factors of carotid artery disease in participants with and without FLD but did not discuss the type and severity of fatty liver; therefore, the type and severity of fatty liver should be further clarified to further explore the risk factors for carotid artery disease.

Conclusion

The prevalence of FLD was 38.7% in the health check-up population in China. In participants without FLD, 6,885 (23.9%) suffered from carotid atherosclerosis and 407 (1.4%) suffered from carotid artery stenosis. In participants with FLD, 7,227 participants (39.7%) had carotid atherosclerosis and 1,055 participants (5.8%) had carotid stenosis. The lifestyle and metabolic factors of carotid atherosclerosis and carotid stenosis were different in the patients without and with FLD and mainly focused on exercise, sedentary behavior, smoking, alcohol consumption, hip circumference, and blood pressure. Our study investigated lifestyle and metabolic factors in a large sample of participants without and with FLD, which can provide a basis for the targeted prevention of carotid disease risk and lay a foundation for the study of CVD risk factors.

Data availability statement

The original contributions presented in the study are included in the article/supplementary material, further inquiries can be directed to the corresponding author/s.

Ethics statement

The studies involving human participants were reviewed and approved by research and development of the health coaching technology intervention decision support system on residents healthy lifestyle self-reporting (No: 2020-S587). Written informed consent was obtained from all participants for their participation in this study.

Author contributions

CZ: conceptualization. CZ, JW, SD, GG, LL, YL, AC, and ZC: funding acquisition. CZ, JW, SD, GG, LL, YL, ZC, YD, JX, and AC: writing—review and editing and investigation. JW and YD: formal analysis. YD and JX: writing—original draft. All authors contributed to the article and approved the submitted version.

Funding

This work was supported by the Special Funding for the Construction of Innovative Provinces in Hunan (No. 2020SK53618).

Acknowledgments

Author grateful to two health management centers of general hospitals and 47063 participants for their

voluntary participation and all the members of our research team.

Conflict of interest

The authors declare that the research was conducted in the absence of any commercial or financial relationships that could be construed as a potential conflict of interest.

Publisher's note

References

1. Asrani SK, Devarbhavi H, Eaton J, Kamath PS. Burden of liver diseases in the world. *J Hepatol.* (2019) 70:151–71. doi: 10.1016/j.jhep.2018.09.014

2. Younossi Z, Henry L. Contribution of alcoholic and nonalcoholic fatty liver disease to the burden of liver-related morbidity and mortality. *Gastroenterology.* (2016) 150:1778–85. doi: 10.1053/j.gastro.2016.03.005

3. Younossi ZM, Corey KE, Lim JK. AGA clinical practice update on lifestyle modification using diet and exercise to achieve weight loss in the management of nonalcoholic fatty liver disease: expert review. *Gastroenterology.* (2021) 160:912–8. doi: 10.1053/j.gastro.2020.11.051

4. Chang Y, Ryu S, Sung KC, Cho YK, Sung E, Kim HN, et al. Alcoholic and non-alcoholic fatty liver disease and associations with coronary artery calcification: evidence from the Kangbuk Samsung Health Study. *Gut.* (2019) 68:1667–75. doi: 10.1136/gutjnl-2018-317666

5. Zhou M, Wang H, Zeng X, Yin P, Zhu J, Chen W, et al. Mortality, morbidity, and risk factors in China and its provinces, 1990-2017: a systematic analysis for the Global Burden of Disease Study 2017. *Lancet.* (2019) 394:1145–58. doi: 10.1016/S0140-6736(19)30427-1

6. Hong H, Wang MS, Liu Q, Shi JC, Ren HM, Xu ZM. Angiographically evident atherosclerotic stenosis associated with myocardial bridging and risk factors for the artery stenosis located proximally to myocardial bridging. *Anadolu Kardiyol Derg.* (2014) 14:40–7. doi: 10.5152/akd.2013.4702

7. Ma J, Hwang SJ, Pedley A, Massaro JM, Hoffmann U, Chung RT, et al. Bi-directional analysis between fatty liver and cardiovascular disease risk factors. *J Hepatol.* (2017) 66:390–7. doi: 10.1016/j.jhep.2016.09.022

8. Kim JH, Kim SY, Jung ES, Jung SW, Koo JS, Kim JH, et al. Carotid intima-media thickness is increased not only in non-alcoholic fatty liver disease patients but also in alcoholic fatty liver patients. *Digestion.* (2011) 84:149–55. doi: 10.1159/000326854

9. Oni ET, Agatston AS, Blaha MJ, Fialkow J, Cury R, Sposito A, et al. A systematic review: burden and severity of subclinical cardiovascular disease among those with nonalcoholic fatty liver; should we care? *Atherosclerosis.* (2013) 230:258–67. doi: 10.1016/j.atherosclerosis.2013.07.052

10. American College of Sports Medicine position stand. Exercise for patients with coronary artery disease. *Med Sci Sports Exerc.* (1994) 26:i–v. doi: 10.1249/00005768-199403000-00024

11. Chinese Nutrition Society. *Dietary Guidelines for Chinese Residents.* (2016). Beijing: People's Medical Publishing House (2016).

12. Jin Y. *Study on the Relationship Between Dietary Diversity and Nutritional Status and Chronic Diseases in Chinese Residents.* Chinese Center for Disease Control and Prevention. Full text Database of Excellent Master's Dissertations in China. (2011). p. 18–20. Available online at: https://kns.cnki.net/KCMS/detail/detail.aspx?dbname=CDFD1214&filename=1011211180.nh

13. Young DR, Hivert MF, Alhassan S, Camhi SM, Ferguson JF, Katzmarzyk PT, et al. Physical activity committee of the council on lifestyle and cardiometabolic health; council on clinical cardiology; council on epidemiology and prevention; council on functional genomics and translational biology; and stroke council. Sedentary behavior and cardiovascular morbidity and mortality: a science advisory from the American Heart Association. *Circulation.* (2016) 134:e262–79. doi: 10.1161/CIR.0000000000000440

14. Werneck AO, Oyeyemi AL, Szwarcwald CL, Vancampfort D, Silva DR. Associations between TV viewing and depressive symptoms among 60,202 Brazilian adults: The Brazilian National health survey. *J Affect Disord.* (2018) 236:23–30. doi: 10.1016/j.jad.2018.04.083

15. Preventive Services Task US. Davidson KW, Mangione CM, Barry MJ, Cabana M, Caughey AB, Donahue K, et al. Screening for asymptomatic carotid artery stenosis: US preventive services task force recommendation statement. *JAMA.* (2021) 325:476–81. doi: 10.1001/jama.2020.26988

16. Pei F, Wang X, Chen P, Yue R, Chen C, Zeng C. Expression and methylation of angiotensin II1a receptor in blood vessels of spontaneous hypertension rats. *Chin J Hypertension.* (2015) 23:231–7. doi: 10.16439/j.cnki.1673-7245.2015.03.012

17. Gać P, Jazwiec P, Mazur G, Poreba R. Exposure to cigarette smoke and the carotid arteries calcification index in patients with essential hypertension. *Cardiovasc Toxicol.* (2017) 17:335–43. doi: 10.1007/s12012-016-9391-x

18. Xie X, Ma YT, Yang YN, Fu ZY, Ma X, Huang D, et al. Alcohol consumption and carotid atherosclerosis in China: the cardiovascular risk survey. *Eur J Prev Cardiol.* (2012) 19:314–21. doi: 10.1177/1741826711404501

19. Mukamal KJ, Kronmal RA, Mittleman MA, O'Leary DH, Polak JF, Cushman M, et al. Alcohol consumption and carotid atherosclerosis in older adults: the Cardiovascular Health Study. *Arterioscler Thromb Vasc Biol.* (2003) 23:2252–9. doi: 10.1161/01.ATV.0000101183.58453.39

20. Gasbarrino K, Di Iorio D, Daskalopoulou SS. Importance of sex and gender in ischaemic stroke and carotid atherosclerotic disease. *Eur Heart J.* (2022) 43:460–73. doi: 10.1093/eurheartj/ehab756

21. Chen L, Bi Y, Su J, Cui L, Han R, Tao R, et al. Physical activity and carotid atherosclerosis risk reduction in population with high risk for cardiovascular diseases: a cross-sectional study. *BMC Public Health.* (2022) 22:250. doi: 10.1186/s12889-022-12582-6

22. Healy GN, Clark BK, Winkler EA, Gardiner PA, Brown WJ, Matthews CE. Measurement of adults' sedentary time in population-based studies. *Am J Prev Med.* (2011) 41:216–27. doi: 10.1016/j.amepre.2011.05.005

23. Troiano RP, Pettee Gabriel KK, Welk GJ, Owen N, Sternfeld B. Reported physical activity and sedentary behavior: why do you ask? *J Phys Act Health.* (2012) (suppl 1):S68–S75. doi: 10.1123/jpah.9.s1.s68

24. Hassinen M, Lakka TA, Komulainen P, Haapala I, Nissinen A, Rauramaa R. Association of waist and hip circumference with 12-year progression of carotid intima-media thickness in elderly women. *Int J Obes (Lond).* (2007) 31:1406–11. doi: 10.1038/sj.ijo.0803613

25. Cheng G, Fan F, Zhang Y, Qi L, Jia J, Liu Y, et al. Different associations between blood pressure indices and carotid artery damages in a community-based population of China. *J Hum Hypertens.* (2016) 30:750–4. doi: 10.1038/jhh.2016.36

26. Pierdomenico SD, Pierdomenico AM, Cuccurullo F. Morning blood pressure surge, dipping, and risk of ischemic stroke in elderly patients treated for hypertension. *Am J Hypertens.* (2014) 27:564—70. doi: 10.1093/ajh/hpt170

27. Wang J, Wu J, Zhang S, Zhang L, Wang C, Gao X, et al. Elevated fasting glucose as a potential predictor for asymptomatic cerebral artery stenosis: a cross-sectional study in Chinese adults. *Atherosclerosis.* (2014) 237:661–5. doi: 10.1016/j.atherosclerosis.2014.10.083

28. Seidell JC, Perusse L, Despres JP, Bouchard C. Waist and hip circumferences have independent and opposite effects on cardiovascular disease risk factors: the Quebec Family Study. *Am J Clin Nutr.* (2001) 74:315–21. doi: 10.1093/ajcn/74.3.315

29. Heitmann BL, Frederiksen P, Lissner L. Hip circumference and cardiovascular morbidity and mortality in men and women. *Obes Res.* (2004) 12:482–7. doi: 10.1038/oby.2004.54

30. Yi L, Tang J, Shi C, Zhang T, Li J, Guo F, et al. Pentraxin 3, TNF-α, and LDL-C are associated with carotid artery stenosis in patients with ischemic stroke. *Front Neurol.* (2020) 10:1365. doi: 10.3389/fneur.2019.01365

31. Liguori I, Russo G, Curcio F, Bulli G, Aran L, Della-Morte D, et al. Oxidativestress, aging, and diseases. *Clin Interv Aging.* (2018) 13:757–72. doi: 10.2147/CIA.S158513

32. Kweon SS, Lee YH, Shin MH, Choi JS, Rhee JA, Choi SW, et al. Effects of cumulative smoking exposure and duration of smoking cessation on carotid artery structure. *Circ J.* (2012) 76:2041–7. doi: 10.1253/circj.CJ-11-1353

33. Siasos G, Tsigkou V, Kokkou E, Oikonomou E, Vavuranakis M, Vlachopoulos C, et al. Smoking and atherosclerosis: mechanisms of disease and new therapeutic approaches. *Curr Med Chem.* (2014) 21:3936–48. doi: 10.2174/092986732134141015161539

34. Weinberg EM, Trinh HN, Firpi RJ, Bhamidimarri KR, Klein S, Durlam J, et al. Lean Americans with nonalcoholic fatty liver disease have lower rates of cirrhosis and comorbid diseases. *Clin Gastroenterol Hepatol.* (2021) 19:996–1008.e6. doi: 10.1016/j.cgh.2020.06.066

35. Lavie CJ, Ozemek C, Carbone S, Katzmarzyk PT, Blair SN. Sedentary behavior, exercise, and cardiovascular health. *Circ Res.* (2019) 124:799–815. doi: 10.1161/CIRCRESAHA.118.312669

36. Kim SK, Choi YJ, Huh BW, Kim CS, Park SW, Lee EJ, et al. Ratio of waist-to-calf circumference and carotid atherosclerosis in Korean patients with type 2 diabetes. *Diabetes Care.* (2011) 34:2067–71. doi: 10.2337/dc11-0743

37. Wang H, Sun J, Zhang Z, Yang L, Zhao M, Bovet P, et al. Waist circumference change and risk of high carotid intima-media thickness in a cohort of Chinese children. *J Hypertens.* (2021) 39:1901–7. doi: 10.1097/HJH.0000000000002881

38. Baziar N, Parohan M. The effects of curcumin supplementation on body mass index, body weight, and waist circumference in patients with nonalcoholic fatty liver disease: a systematic review and dose-response meta-analysis of randomized controlled trials. *Phytother Res.* (2020) 34:464–74. doi: 10.1002/ptr.6542

39. Strazzullo P, D'Elia L, Cairella G, Garbagnati F, Cappuccio FP, Scalfi L. Excess body weight and incidence of stroke: meta-analysis of prospective studies with 2 million participants. *Stroke.* (2010) 41:e418–e426. doi: 10.1161/STROKEAHA.109.576967

40. Chen CY, Weng WC, Wu CL, Huang WY. Association between gender and stoke recurrence in ischemic stroke patients with high-grade carotid artery stenosis. *J Clin Neurosci.* (2019) 67:62–7. doi: 10.1016/j.jocn.2019.06.021

41. Kamon T, Kaneko H, Itoh H, Kiriyama H, Mizuno Y, Morita H, et al. Association between waist circumference and carotid intima-media thickness in the general population. *Int Heart J.* (2020) 61:103–8. doi: 10.1536/ihj.19-470

42. Shen Y, Zhang L, Zong WH, Wang Z, Zhang Y, Yang MJ, et al. Correlation between waist circumference and carotid intima-media thickness in women from Shanghai, China. *Biomed Environ Sci.* (2013) 26:531–8. doi: 10.3967/0895-3988.2013.07.003

43. Guan X, Zhang Q, Xing J, Chen S, Wu S, Sun X. Systolic blood pressure mediates body mass index and non-alcoholic fatty liver disease: a population-based study. *Turk J Gastroenterol.* (2021) 32:458–65. doi: 10.5152/tjg.2021.20641

44. Sandesara PB, Virani SS, Fazio S, Shapiro MD. The forgotten lipids: triglycerides, remnant cholesterol, and atherosclerotic cardiovascular disease risk. *Endocr Rev.* (2019) 40:537–57. doi: 10.1210/er.2018-00184

frontiers | Frontiers in Cardiovascular Medicine

TYPE Original Research
PUBLISHED 18 August 2022
DOI 10.3389/fcvm.2022.907665

OPEN ACCESS

EDITED BY
Mark Slevin,
Manchester Metropolitan University,
United Kingdom

REVIEWED BY
Sakir Ahmed,
Kalinga Institute of Medical Sciences (KIMS), India
Erkan Cüre,
Bagcilar Medilife Hospital, Turkey

*CORRESPONDENCE
Liming Zhang
zlmlimingzz@163.com

SPECIALTY SECTION
This article was submitted to Atherosclerosis and Vascular Medicine, a section of the journal Frontiers in Cardiovascular Medicine

RECEIVED 30 March 2022
ACCEPTED 11 July 2022
PUBLISHED 18 August 2022

CITATION
Zhang J and Zhang L (2022) Bioinformatics approach to identify the influences of SARS-COV2 infections on atherosclerosis. *Front. Cardiovasc. Med.* 9:907665. doi: 10.3389/fcvm.2022.907665

Bioinformatics approach to identify the influences of SARS-COV2 infections on atherosclerosis

Jiuchang Zhang and Liming Zhang*

Department of Neurology, The First Affiliated Hospital of Harbin Medical University, Harbin, China

Coronavirus disease (COVID-19), caused by severe acute respiratory syndrome coronavirus 2 (SARS-CoV-2), has been a global pandemic since early 2020. Understanding the relationship between various systemic disease and COVID-19 through disease ontology (DO) analysis, an approach based on disease similarity studies, has found that COVID-19 is most strongly associated with atherosclerosis. The study provides new insights for the common pathogenesis of COVID-19 and atherosclerosis by looking for common transcriptional features. Two datasets (GSE152418 and GSE100927) were downloaded from GEO database to search for common differentially expressed genes (DEGs) and shared pathways. A total of 34 DEGs were identified. Among them, ten hub genes with high degrees of connectivity were picked out, namely C1QA, C1QB, C1QC, CD163, SIGLEC1, APOE, MS4A4A, VSIG4, CCR1 and STAB1. This study suggests the critical role played by Complement and coagulation cascades in COVID-19 and atherosclerosis. Our findings underscore the importance of C1q in the pathogenesis of COVID-19 and atherosclerosis. Activation of the complement system can lead to endothelial dysfunction. The DEGs identified in this study provide new biomarkers and potential therapeutic targets for the prevention of atherosclerosis.

KEYWORDS

COVID-19, atherosclerosis, C1q, SARS-CoV-2, immune

Introduction

Coronavirus disease (COVID-19), caused by severe acute respiratory syndrome coronavirus 2 (SARS-CoV-2), has been a global pandemic since early 2020. According to the WHO, until March 9, 2022, the number of confirmed cases worldwide was 448,313,293, including 6,011,482 deaths (1). In response to the COVID-19 pandemic, a global effort is in progress to develop a vaccine against SARS-CoV-2. Vaccination can help control SARS-CoV-2 outbreaks by preventing infection, reducing disease severity, and blocking transmission (2). COVID-19 is typically characterized by upper respiratory symptoms, including fever, cough, and fatigue, and it is often accompanied by pulmonary infection (3). In addition to typical symptoms, some patients have serious cardiovascular damage, or even the first symptoms. (4) Except for the traditional established risk factors for atherosclerosis, such as age, smoking, hyperlipidemia, and hypertension, viral infection has been supposed to be a potential implication in atherosclerosis (5). SARS-CoV-2 binds to ACE2 to gain intracellular entry, leading to endothelial dysfunction (6). SARS-CoV-2

also promotes the accumulation of perivascular adipose tissue (7). These may exacerbate the underlying pathology of cardiovascular disease, leading to accelerated progression of atherosclerosis.

The purpose of this study was to explore the pathophysiological association between SARS-CoV-2 and atherosclerosis, and to better understand the underlying mechanisms, so as to facilitate early detection and prevention of atherosclerosis. Two gene expression datasets (GSE152418 and GSE100927) were downloaded from Gene Expression Omnibus (GEO) database. We used bioinformatics and enrichment analysis to determine the common DEGs and their functions for COVID-19 and atherosclerosis. In addition, protein protein interaction (PPI) networks were established to reveal hub genes. These data can better understand the potential link between the two diseases and provide evidence for therapeutic targets.

Materials and methods

Microarray data

The GSE152418 and GSE100927 gene expression profile were obtained from the GEO database (https://www.ncbi.nlm.nih.gov/geo) [Illumina NovaSeq 6000 (Homo sapiens)] platform was used for the GSE152418 dataset where samples were got from seventeen COVID-19 patients, and seventeen healthy people. On the contrary, for the GSE100927 dataset, GPL17077 [Agilent-039494 SurePrint G3 Human GE v2 8x60K Microarray 039381 (Probe Name version)] platform was adopted where samples were collected from sixty-nine atherosclerotic patients and thirty-five control subjects (Table 1).

Disease ontology (DO) analysis

Firstly, the "edgeR" package was applied to screen Differentially Expressed Genes (DEGs) from the GSE152418 dataset and a adjusted *P* less than 0.05, and |log2 Fold change (FC)| more than or equal to 1 was set as a cut-off point for selecting DEGs. The "DOSE" (8). and "ClusterProfiler" (9). packages were then used for DO analysis to study the disease mechanism by looking for disease correlation. DO analysis is a method based on the study of disease similarity, and it plays a vital role in understanding the pathogenesis of complex diseases, the early prevention and diagnosis of major diseases, new drug development, and drug safety evaluation.

Acquisition of common genes

The LIMMA package was used to detect the DEGs between atherosclerotic patients and healthy control from the GSE100927 dataset, and the adjusted P-value and |log2FC| were calculated. Genes that met the cutoff criteria, adjusted $P < 0.05$ and |log2FC| more than or equal to 1.0, were considered as DEGs. Then the common genes of the GSE152418 and GSE100927 sets were identified by using the Venn diagram webtool (bioinformatics.psb.ugent.be/webtools/Venn/).

Enrichment analysis of common genes

To further analyze biological processes of common DEGs, GO annotation analysis and KEGG pathway enrichment analysis were carried out through the Database for Annotation, Visualization and Integrated Discovery [DAVID (2021 Update), https://david.ncifcrf.gov/]. *P*-Value <0.05 was used as the enrichment screening condition.

Construction PPI network and selection hub genes

The PPI network was predicted using Search Tool for the Retrieval of Interacting Genes (STRING, version 11.5, http://string-db.org/) online database. The PPI pairs were extracted with a interaction score more than or equal to 0.15, and then the PPI network was visualized by Cytoscape software (www.cytoscape.org/). Here, we used Degree to evaluate and select hub genes.

Results

DO analysis

Based on the cut-off criteria of adjusted $P < 0.05$ and |log2FC| more than or equal to 1, a total of 2080 DEGs were identified from GSE152418, including 1905 upregulated genes and 175 downregulated genes. p.adjust <0.05 and gene counts more than or equal to 20 were used as the DO screening condition. Figure 1 shows the top ten most significantly enriched diseases, coronary artery disease, atherosclerosis, arteriosclerotic cardiovascular disease, arteriosclerosis, myocardial infarction, congestive heart failure, acute myocardial infarction, pulmonary hypertension, focal epilepsy and temporal lobe epilepsy. The enrichment results of other diseases by DO analysis are shown in Table 2.

Identification of common DEGs

From GSE100927, 418 DEGs including 295 upregulated genes and 123 downregulated genes were identified. We analyzed the intersection of the DEG profiles using Venn

TABLE 1 Basic information of the two microarray databases derived from the GEO database.

Disease name	Dataset ID	Subjects	GEO platform	Number of samples(control/disease)
COVID-19	GSE152418	Peripheral blood mononuclear cell	GPL24676	17/17
Atherosclerosis	GSE100927	Carotid, femoral and infra-popliteal arteries	GPL17077	35/69

GEO, Gene Expression Omnibus; COVID-19, Coron a Virus Disease 2019.

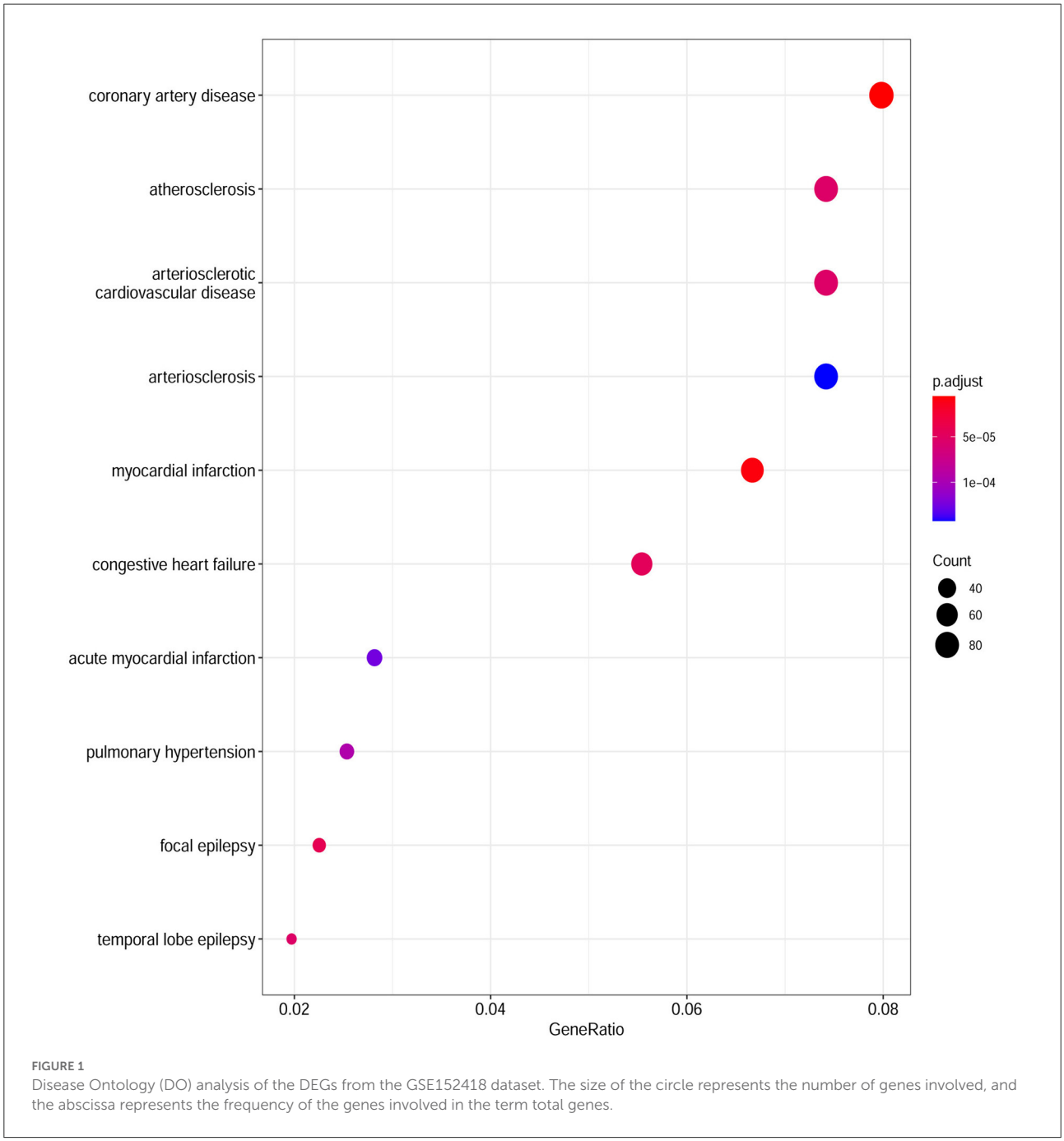

FIGURE 1
Disease Ontology (DO) analysis of the DEGs from the GSE152418 dataset. The size of the circle represents the number of genes involved, and the abscissa represents the frequency of the genes involved in the term total genes.

TABLE 2 Significantly enriched DO terms of DEGs.

DO ID	Description	Count	*P*-Value	*P*-Adjust
DOID:3393	Coronary artery disease	85	6.97E−09	5.83E−06
DOID:5844	Myocardial infarction	71	2.17E−08	9.07E−06
DOID:2234	Focal epilepsy	24	1.52E−07	4.24E−05
DOID:6000	Congestive heart failure	59	2.20E−07	4.59E−05
DOID:3328	Temporal lobe epilepsy	21	3.18E−07	5.32E−05
DOID:1936	Atherosclerosis	79	3.97E−07	5.38E−05
DOID:2348	Arteriosclerotic cardiovascular disease	79	4.50E−07	5.38E−05
DOID:6432	Pulmonary hypertension	27	9.09E−07	9.50E−05
DOID:9408	Acute myocardial infarction	30	1.34E−06	0.000124898
DOID:2349	Arteriosclerosis	79	1.70E−06	0.000142212
DOID:5679	Retinal disease	77	7.92E−06	0.000601666
DOID:1168	Familial hyperlipidemia	26	1.20E−05	0.000834386
DOID:3146	Lipid metabolism disorder	28	1.34E−05	0.00085861
DOID:1793	Pancreatic cancer	69	1.94E−05	0.00115929
DOID:850	Lung disease	98	2.75E−05	0.001532539
DOID:4450	Renal cell carcinoma	72	3.34E−05	0.001746893
DOID:8466	Retinal degeneration	58	3.98E−05	0.001958846
DOID:6364	Migraine	23	4.23E−05	0.00196426
DOID:3324	Mood disorder	45	5.17E−05	0.00227529
DOID:0080000	Muscular disease	82	5.54E−05	0.002316532
DOID:263	Kidney cancer	86	8.04E−05	0.003053437
DOID:3459	Breast carcinoma	77	9.26E−05	0.003364892
DOID:0060037	Developmental disorder of mental health	75	0.000113602	0.003794572
DOID:1826	Epilepsy syndrome	46	0.000118977	0.003794572
DOID:4451	Renal carcinoma	76	0.000122552	0.003794572
DOID:1686	Glaucoma	29	0.00014554	0.004217764
DOID:2355	Anemia	53	0.0001587	0.004416723
DOID:2742	Auditory system disease	27	0.000187263	0.00470284
DOID:936	Brain disease	87	0.000192221	0.00470284
DOID:15	Reproductive system disease	76	0.000205883	0.00470284
DOID:120	Female reproductive organ cancer	87	0.000207772	0.00470284
DOID:74	Hematopoietic system disease	90	0.00020814	0.00470284
DOID:3996	Urinary system cancer	94	0.000217288	0.00473576
DOID:4074	Pancreas adenocarcinoma	38	0.000234928	0.00473576
DOID:0060040	Pervasive developmental disorder	45	0.000239673	0.00473576
DOID:0060116	Sensory system cancer	34	0.000241385	0.00473576
DOID:2174	Ocular cancer	34	0.000241385	0.00473576
DOID:0060041	Autism spectrum disorder	43	0.000254915	0.00473576
DOID:12849	Autistic disorder	43	0.000254915	0.00473576
DOID:18	Urinary system disease	90	0.000280864	0.005097229
DOID:3083	Chronic obstructive pulmonary disease	48	0.000286567	0.005097229
DOID:423	Myopathy	77	0.00033099	0.005647089
DOID:66	Muscle tissue disease	77	0.00033099	0.005647089
DOID:374	Nutrition disease	67	0.000399054	0.006672186
DOID:0050700	Cardiomyopathy	35	0.000449318	0.007240401
DOID:6713	Cerebrovascular disease	29	0.000459021	0.007240401
DOID:654	Overnutrition	64	0.000496562	0.007574304
DOID:4905	Pancreatic carcinoma	50	0.000498309	0.007574304

(Continued)

TABLE 2 Continued

DO ID	Description	Count	*P*-Value	*P*-Adjust
DOID:557	Kidney disease	86	0.000522392	0.007798559
DOID:4645	Retinal cancer	29	0.000620866	0.008650729
DOID:9970	Obesity	62	0.000663498	0.008946528
DOID:1115	Sarcoma	42	0.000711231	0.009147531
DOID:229	Female reproductive system disease	42	0.000711231	0.009147531
DOID:2320	Obstructive lung disease	61	0.000734442	0.009302929
DOID:10534	Stomach cancer	55	0.000950468	0.011515815
DOID:768	Retinoblastoma	28	0.001033977	0.012138426
DOID:771	Retinal cell cancer	28	0.001033977	0.012138426
DOID:3312	Bipolar disorder	35	0.001091638	0.012501503
DOID:9352	Type 2 diabetes mellitus	45	0.001110794	0.012548966
DOID:5041	Esophageal cancer	33	0.001158125	0.012909231
DOID:3770	Pulmonary fibrosis	29	0.001261354	0.013519123
DOID:403	Mouth disease	40	0.001484673	0.015136423
DOID:26	Pancreas disease	37	0.001605415	0.015977706
DOID:633	Myositis	21	0.001648237	0.016210895
DOID:0060085	Organ system benign neoplasm	52	0.00167946	0.01632591
DOID:4607	Biliary tract cancer	38	0.001807765	0.017371169
DOID:0060084	Cell type benign neoplasm	85	0.002061029	0.019359779
DOID:657	Adenoma	64	0.002109774	0.019597453
DOID:1074	Kidney failure	34	0.002145424	0.019709612
DOID:48	Male reproductive system disease	30	0.002200606	0.019996808
DOID:865	Vasculitis	28	0.002325529	0.020904752
DOID:8398	Osteoarthritis	39	0.002473537	0.021998689
DOID:0060100	Musculoskeletal system cancer	79	0.002508247	0.022023954
DOID:299	Adenocarcinoma	34	0.002676763	0.022177269
DOID:5223	Infertility	42	0.002695257	0.022177269
DOID:3082	Interstitial lung disease	36	0.00271993	0.022177269
DOID:1575	Rheumatic disease	39	0.002732367	0.022177269
DOID:418	Systemic scleroderma	39	0.002732367	0.022177269
DOID:419	Scleroderma	39	0.002732367	0.022177269
DOID:2394	Ovarian cancer	59	0.002780859	0.022331756
DOID:201	Connective tissue cancer	68	0.002894952	0.022331756
DOID:10952	Nephritis	32	0.002911676	0.022331756
DOID:3620	Central nervous system cancer	28	0.002988188	0.022505631
DOID:0080015	Physical disorder	30	0.003147388	0.023285098
DOID:4960	Bone marrow cancer	61	0.003537522	0.025494557
DOID:0070004	Myeloma	60	0.003905917	0.026264796
DOID:2621	Autonomic nervous system neoplasm	68	0.004049339	0.026264796
DOID:769	Neuroblastoma	68	0.004049339	0.026264796
DOID:1091	Tooth disease	34	0.004084239	0.026264796
DOID:10825	Essential hypertension	27	0.004708132	0.028812356
DOID:289	Endometriosis	21	0.00483272	0.029276479
DOID:854	Collagen disease	40	0.005216331	0.03128014
DOID:1107	Esophageal carcinoma	27	0.005290025	0.031364972
DOID:0050737	Autosomal recessive disease	61	0.005365584	0.031588932
DOID:0060036	Intrinsic cardiomyopathy	29	0.00544447	0.03160817
DOID:127	Leiomyoma	22	0.005828457	0.032922905

(Continued)

TABLE 2 Continued

DO ID	Description	Count	*P*-Value	*P*-Adjust
DOID:37	Skin disease	63	0.00656053	0.035847078
DOID:1192	Peripheral nervous system neoplasm	70	0.006679809	0.036261818
DOID:552	Pneumonia	24	0.007057917	0.037823198
DOID:4766	Embryoma	63	0.007450764	0.039423029
DOID:3388	Periodontal disease	29	0.008300314	0.04322301
DOID:16	Integumentary system disease	69	0.008758512	0.044109131
DOID:0060038	Specific developmental disorder	42	0.009006264	0.044816886
DOID:12930	Dilated cardiomyopathy	21	0.009380129	0.04640111
DOID:230	Lateral sclerosis	24	0.009987727	0.047987012

DEG, Differentially Expressed Gene; DO, Disease Ontology; ID, Identity Document.

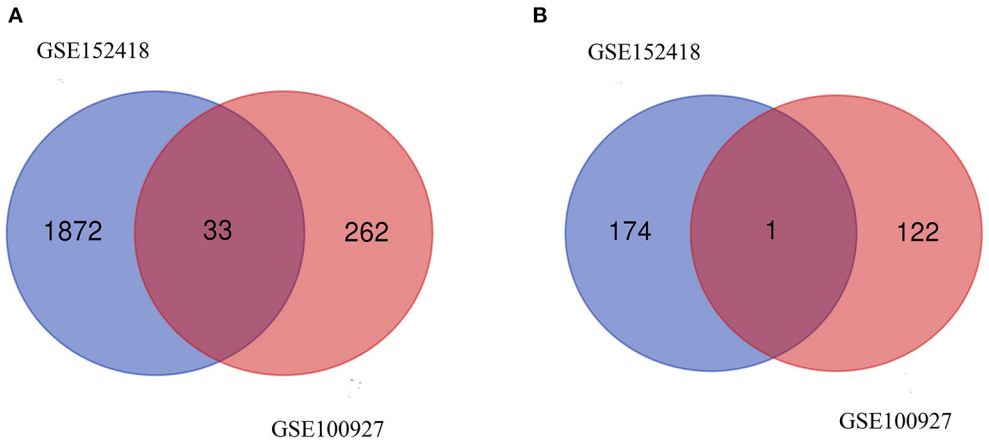

FIGURE 2
Venn diagram. **(A)** Upregulated common DEGs of the GSE152418 and GSE100927 datasets. **(B)** Downregulated common DEGs of the GSE152418 and GSE100927 datasets.

(Figure 2). Ultimately, 34 DEGs were significantly differentially expressed in two datasets, of which 33 were significantly upregulated genes and 1 was downregulated gene.

Gene ontology and pathway enrichment analysis

GO and KEGG pathway analyses for DEGs were performed using the DAVID. The biological processes of DEGs were primarily associated with synapse disassembly, complement activation and innate immune response. For the cell component, the DEGs were enriched in extracellular region, blood microparticle, hemoglobin complex, collagen trimer, and so on. Molecular functions analysis showed that the DEGs were significantly enriched in oxygen transporter activity, oxygen binding, scavenger receptor activity, voltagE–gated potassium channel activity involved in atrial cardiac muscle cell action potential repolarization, phosphatidylcholinE–sterol O-acyltransferase activator activity, haptoglobin binding, organic acid binding and heme binding (Table 3). In addition, the KEGG pathway analysis showed that the DEGs were significantly enriched in Complement and coagulation cascades, Pertussis, Coronavirus disease—COVID-19, Staphylococcus aureus infection, Chagas disease, Systemic lupus erythematosus and Alcoholic liver disease (Table 4).

PPI network construction and hub gene identification

Using STRING tools, we predicted protein interactions among DEGs. The PPI network presented in Figure 3 consists of 34 nodes and 209 edges. Based on the PPI network, we identified 10 genes with the highest connectivity degree (Table 5). The results showed that C1QA was the most outstanding gene with

TABLE 3 Significantly enriched GO terms of DEGs.

GO ID	Description	Count	*P*-Value	Genes
Biological process				
GO:0098883	Synapse disassembly	3	6.04E−05	C1QB, C1QA, C1QC
GO:0006958	Complement activation, classical pathway	5	8.67E−05	C1QB, C1QA, IGLL5, IGLL1, C1QC
GO:0045087	Innate immune response	7	2.32E−04	C1QB, C1QA, IGLL5, VNN1, IGLL1, C1QC, OASL
GO:0006898	Receptor-mediated endocytosis	4	0.001825851	CD163, STAB1, HBA2, APOE
GO:0006954	Inflammatory response	5	0.002915761	CCR1, VNN1, STAB1, SPP1, SIGLEC1
GO:0098869	Cellular oxidant detoxification	3	0.00591978	HBA2, HBD, APOE
GO:0042159	Lipoprotein catabolic process	2	0.007472267	APOE, CTSD
GO:0098914	Membrane repolarization during atrial cardiac muscle cell action potential	2	0.007472267	KCNJ5, KCNA5
GO:0006956	Complement activation	3	0.008884327	C1QB, C1QA, C1QC
GO:0034447	Very-low-density lipoprotein particle clearance	2	0.008960238	APOC1, APOE
GO:0034382	Chylomicron remnant clearance	2	0.010446055	APOC1, APOE
GO:0030449	Regulation of complement activation	3	0.012175792	C1QB, C1QA, C1QC
GO:0010873	Positive regulation of cholesterol esterification	2	0.013411239	APOC1, APOE
GO:0033700	Phospholipid efflux	2	0.017842935	APOC1, APOE
GO:0044267	Cellular protein metabolic process	3	0.021136392	MMP1, SPP1, APOE
GO:0015671	Oxygen transport	2	0.022255408	HBA2, HBD
GO:0015909	Long-chain fatty acid transport	2	0.025186416	FABP5, APOE
GO:0034375	High-density lipoprotein particle remodeling	2	0.026648738	APOC1, APOE
GO:0042157	Lipoprotein metabolic process	2	0.032476871	APOC1, APOE
GO:0033344	Cholesterol efflux	2	0.036825845	APOC1, APOE
GO:0045671	Negative regulation of osteoclast differentiation	2	0.039714668	MAFB, LILRB4
GO:0032703	Negative regulation of interleukin-2 production	2	0.041155941	VSIG4, LILRB4
GO:0042744	Hydrogen peroxide catabolic process	2	0.041155941	HBA2, HBD
GO:0010033	Response to organic substance	2	0.042595125	AQP9, KCNA5
GO:0007267	Cell-cell signaling	3	0.045927718	CCR1, C1QA, STAB1
GO:0042742	Defense response to bacterium	3	0.046288292	IGLL5, IGLL1, STAB1
Cellular component				
GO:0005576	Extracellular region	17	2.40E−08	C1QB, C1QA, CD163, CD163L1, MMP1, HBA2, VNN1, FNDC1, FABP5, IGLL1, APOC1, SPP1, PLBD1, SIGLEC1, APOE, CTSD, C1QC
GO:0072562	Blood microparticle	5	7.68E−05	C1QB, HBA2, HBD, APOE, C1QC
GO:0005833	Hemoglobin complex	3	2.19E−04	HBA2, HBD
GO:0005581	Collagen trimer	4	4.28E−04	C1QB, C1QA, MMP1, C1QC
GO:0009897	External side of plasma membrane	6	6.43E−04	CCR1, KCNJ5, IGLL5, CD163, CD163L1, IGLL1
GO:0005602	Complement component C1 complex	2	0.003171533	C1QB, C1QA
GO:0098794	Postsynapse	3	0.012921039	C1QB, C1QA, C1QC
GO:0031838	Haptoglobin-hemoglobin complex	2	0.017323254	HBA2, HBD
GO:0042627	Chylomicron	2	0.021997095	APOC1, APOE
GO:0071682	Endocytic vesicle lumen	2	0.028195396	HBA2, APOE
GO:0016021	Integral component of membrane	15	0.028427769	PTCRA, CCR1, KCNJ5, CD163, CD163L1, AQP9, KCNA5, HBD, LILRB4, MS4A4A, VNN1, SLCO2B1, STAB1, SIGLEC1, VSIG4

(Continued)

TABLE 3 Continued

GO ID	Description	Count	*P*-Value	Genes
GO:0034361	Very-low-density lipoprotein particle	2	0.03281913	APOC1, APOE
GO:0045202	Synapse	4	0.041387143	C1QB, C1QA, FABP5, C1QC
GO:0034364	High-density lipoprotein particle	2	0.042002749	APOC1, APOE
Molecular function				
GO:0005344	Oxygen transporter activity	3	3.12E−04	HBA2, HBD
GO:0019825	Oxygen binding	3	0.001605913	HBA2, HBD
GO:0005044	Scavenger receptor activity	3	0.002957949	CD163, CD163L1, STAB1
GO:0086089	Voltage–gated potassium channel activity involved in atrial cardiac muscle cell action potential repolarization	2	0.006590464	KCNJ5, KCNA5
GO:0060228	Phosphatidylcholine–sterol O-acyltransferase activator activity	2	0.009869914	APOC1, APOE
GO:0031720	Haptoglobin binding	2	0.016397412	HBA2, HBD
GO:0043177	Organic acid binding	2	0.018022768	HBA2, HBD
GO:0020037	Heme binding	3	0.025666884	HBA2, HBD

DEG, Differentially Expressed Gene; GO, Gene Ontology; ID, Identity Document.

TABLE 4 Significantly enriched KEGG terms of DEGs.

KEGG ID	Description	Count	*P*-Value	Genes
hsa04610	Complement and coagulation cascades	4	0.001112855	C1QB, C1QA, VSIG4, C1QC
hsa05133	Pertussis	3	0.014757214	C1QB, C1QA, C1QC
hsa05171	Coronavirus disease—COVID-19	4	0.018374812	C1QB, C1QA, MMP1, C1QC
hsa05150	Staphylococcus aureus infection	3	0.022928086	C1QB, C1QA, C1QC
hsa05142	Chagas disease	3	0.02567277	C1QB, C1QA, C1QC
hsa05322	Systemic lupus erythematosus	3	0.043532485	C1QB, C1QA, C1QC
hsa04936	Alcoholic liver disease	3	0.047059029	C1QB, C1QA, C1QC

KEGG, Kyoto Encyclopedia of Genes and Genomes; ID, Identity Document; DEG, Differentially Expressed Gene.

connectivity degree = 24, followed by C1QB (degree = 23), C1QC (degree = 22), CD163 (degree = 22), SIGLEC1 (degree = 21), APOE (degree = 19), MS4A4A (degree = 19), VSIG4 (degree = 18), CCR1 (degree = 18), STAB1 (degree = 18).

Discussion

Some diseases, thought to be unrelated, share the same biological processes (10). We conducted the DO analysis on the GSE152418 dataset to find the similarity between diseases and COVID-19, and found that COVID-19 was most significantly associated with atherosclerosis among various diseases. Our results suggest that COVID-19 will lead to faster atherosclerosis. Then, we took the intersection of two datasets, GSE152418 and GSE100927, to identify common genes between COVID-19 and atherosclerosis. After obtaining 34 common genes, the GO, pathway, PPI networks were further analyzed.

GO enrichment analysis showed that C1QA, C1QB, C1QC were significantly enriched in synapse disassembly, complement activation, and innate immune response. Complement 1q (C1q) is composed of six subunits, which form a molecule containing 18 polypeptide chains, while C1qA, C1qB, and C1qC genes encode three types of polypeptide chains, A, B, and C of the subunit of C1q, respectively (11). C1q is an important recognition molecule to initiate the classical pathway involved in the complement activation and function, playing a major role in the connection between innate and specific immunity. (12, 13). After identifying the complement binding site on the antibody Fc segment of the IgM or IgG immune complex, the complement cascade will be activated to clear the antigen-antibody complexes (14). Complement proteins specifically locate apoptotic, immature or weak developing synapses in the central nervous system (15). The number of those apoptotic markers in the synapse is equal to the localization of C1q, which promotes synaptic pruning (16). A study found that of 281 patients diagnosed with COVID-19, 21.1% had dementia and 8.9% had mild cognitive impairment (MCI) (17). Moreover, high activation of C1q leads to a large number of synaptic loss which is associated with the development of Alzheimer's disease

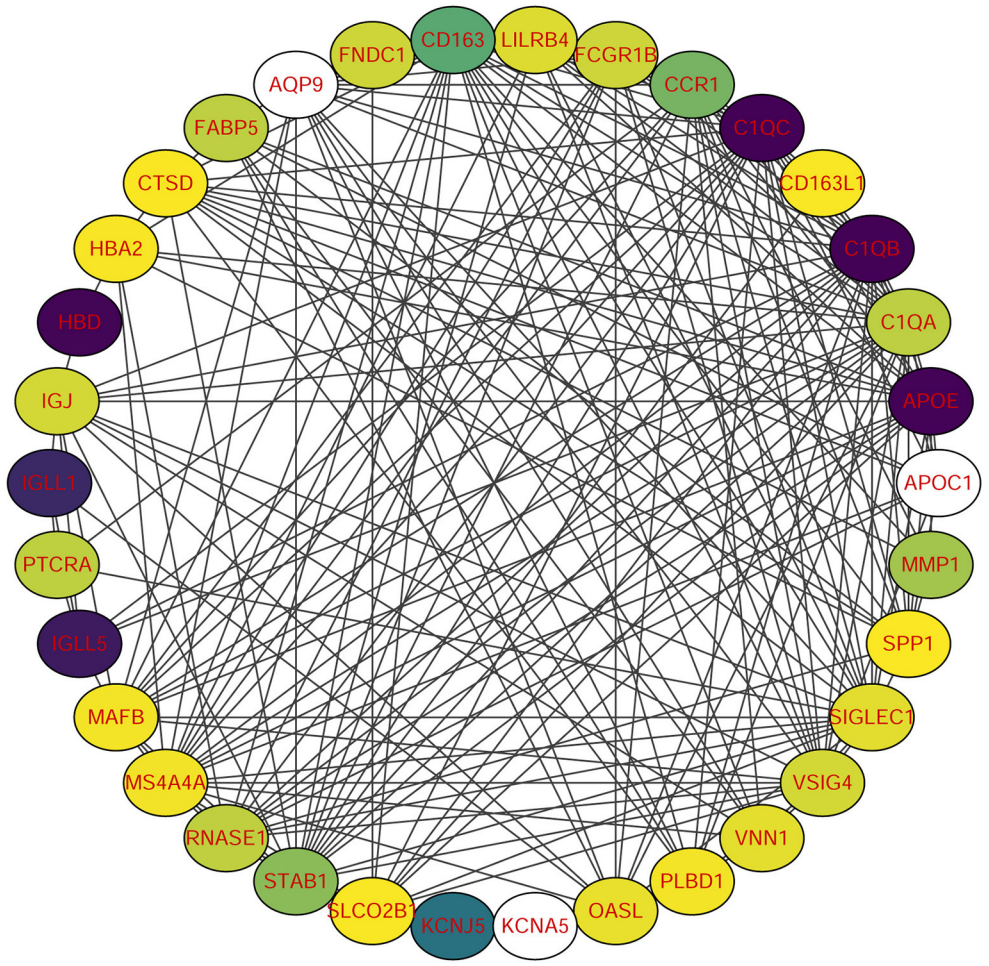

FIGURE 3
Protein-protein interaction (PPI) network of common DEGs among SRAS-CoV-2 and atherosclerosis. In the figure, the circle nodes represent DEGs and edges represent interactions between nodes.

(18). Then, does the activation of complement system C1q cause cognitive impairment in COVID-19 patients?

KEGG enrichment analysis is the best way to reflect the changes of pathways in organisms. Those results indicate that complement and coagulation cascades change most significantly in atherosclerosis and COVID-19. Macor et al. found positive lung C1q staining which suggests that the classical pathway is important for complement activation which may be triggered by IgG, antibodies widely distributed in patients' lungs (19). In atherosclerosis plaques, C1q activates the classical complement pathway by recognizing oxidized low-density lipoprotein auto-antibodies or directly binding modified lipoprotein and cholesterol crystal (20). Endothelial dysfunction, an important mechanism for the formation and development of atherosclerosis, can be caused by the activation of the complement system can lead to (20). Gao et al. demonstrated that subsequent endothelial dysfunction persisted in COVID-19 survivors even 327 days after diagnosis (6). The activated fragments generated after the activation of the complement system may be closely related to the coagulation and fibrinolytic system and inflammation in COVID-19 patients, so additional studies on the changes in the number of fragments and tissue distribution are needed.

The 10 hub genes selected by PPI were C1QA, C1QB, C1QC, CD163, SIGLEC1, APOE, MS4A4A, VSIG4, CCR1, and STAB1. The C1QA, C1QB, and C1QC genes had the highest degree in the PPI networks. Then v-set and immunoglobulin domain containing 4 (VSIG4) is the receptor of complement component 3 fragments C3b and iC3b, which activates macrophage immunity through C3b/iC3b binding (21). VSIG4 may be involved in lung injury through induction of phagocytosis (22). VSIG4 activate macrophages, through induction of chemokines, promote the migration of inflammatory cells to the lesion area, and participate in the pathogenesis of arteriosclerosis

TABLE 5 Top ten hub genes with higher degree of connectivity.

Gene symbol	Gene description	Degree
C1QA	Complement C1q A chain	24
C1QB	Complement C1q B chain	23
C1QC	Complement C1q C chain	22
CD163	CD163 molecule	22
SIGLEC1	Sialic acid binding Ig like lectin 1	21
APOE	Apolipoprotein E	19
MS4A4A	Membrane spanning 4-domains A4A	19
VSIG4	V-set and immunoglobulin domain containing 4	18
CCR1	C-C motif chemokine receptor 1	18
STAB1	Stabilin 1	18

(23). Increased expressions of C1QA, C1QB, C1QC, and VSIG4 all relate to enhanced complement system. CD163, a scavenger receptor, is a major component of inflammation and the immune response. Among plasmacytoid dendritic cells, type I interferon is induced with the appearance of CD163+ SIGLEC1+ macrophages with increased angiotensin converting enzyme 2 (ACE2) levels (24). Macrophages are highly enriched in the lungs of macaques at peak viremia and harbor the SARS-CoV-2 virus while also expressing an interferon-driven innate antiviral gene signature (25). CD163(+) macrophages promote angiogenesis, vascular permeability and inflammation in atherosclerosis via the CD163/HIF1α/VEGF-A pathway. The increased expression of CD163 was revealed in ruptured coronary plaques (26). There are three APOE isoforms, namely APOE epsilon2 (APOE2), APOE epsilon3 (APOE3) and APOE epsilon4 (APOE4) located on chromosome 19q13.2 (27). APOE can function as an endogenous, concentration-dependent pulmonary danger signal that primes and activates the NLPR3 inflammasome in bronchoalveolar lavage fluid macrophages from asthmatic subjects to secrete IL-1β (28). A recent study in the UK Biobank Cohort, APOE4 has been shown to associate with increased susceptibility to SARS-CoV-2 infection and COVID-19 mortality (29). APOE is a therapeutic target for statins that inhibit inflammation in patients with atherosclerotic vascular disease.

Statins possess antiviral, immunomodulatory, antithrombotic, and anti-inflammatory properties, which may improve short- and long-term outcomes in COVID-19 patients.

STAB1 encodes an unusual type of multifunctional scavenger receptor that causes increased lipid uptake and transient lipid depletion in virus-infected areas and is associated with poor prognosis for COVID-19 (30). STAB1 expression may contribute to foam cell formation, monocyte adhesion/migration, and regulation of inflammation in atherosclerotic lesions (31). Lectins such as sialic acid-binding Ig-like lectin 1 (SIGLEC1/CD169) mediate the attachment of viruses to Antigen-presenting cells (APCs) (32). SIGLEC1 expression is induced on APCs upon IFN-α or LPS exposure and increased in myeloid cells of COVID-19 patients (33) Inhibition of Siglec-1 prevents monocytes from adhering to vascular endothelial cells in the early stage of atherosclerosis, and reduces lipid phagocytosis and chemokine secretion of macrophages, alleviating the inflammatory response of established fat streaking lesions (34). CCR1 is critical mediators of monocyte/macrophage polarization and tissue infiltration, which are pathogenic hallmarks of severe COVID-19 (35). The use of monocyte CCR1 in arterial recruitment is due in part to activated chemokines of platelet deposition, which is important in the early stages of atherosclerosis (36). MS4A4A is a novel M2 macrophage cell surface marker, which is essential for dectin-1-dependent activation of NK cell-mediated anti-metastatic properties (37). Silva-Gomes et al. found MS4A4A was expressed by MΦs or alveolar MΦs in COVID-19 bronchoalveolar lavage fluid (38).

Through DO analysis, we also found several neurological disorders associated with COVID-19, such as focal epilepsy, temporal lobe epilepsy, migraine, epilepsy syndrome, neuroblastoma, and lateral sclerosis. There have been a large number of reported cases of these conditions, with a seizure prevalence ranging from 0 to 26% in COVID-19 patients (39, 40). Moreover, seizures may be related to cerebrovascular disease and central nervous system infection. Vascular endothelial injury leads to hypercoagulability and microembolism, resulting in reduced cortical blood flow accompanied by hypoxia. Vascular endothelial dysfunction can lead to changes in the nervous system, resulting in neurological sequelae (41). The Atherosclerosis Risk in Communities (ARIC) study also revealed that migraine patients were more susceptible to retinopathy (retinal hemorrhage, macular oedema, retinal microvascular abnormalities, venous bleeding, etc.) than non-migraine patients, and retinopathy was more strongly associated with migraine in people without a history of diabetes or hypertension (42). Interestingly, we also discovered DEGs enrichment in retinopathy. Besides, previous animal-based experimental studies of the coronavirus infection reported retinal diseases such as retinal vasculitis and retinal degeneration. Moreover, blood-retinal barrier breakdown revealed the possibility of immune-privileged site infectivity by SARS-CoV-2 (43). We believe that SARS-CoV-2 causes vascular injury and may lead to retinal degeneration. Results also revealed different types of cancer, such as pancreatic cancer, kidney cancer, breast carcinoma, stomach cancer, esophageal cancer, and ovarian cancer. In patients with COVID19, severe illness and mortality are closely related to cancer. SARS CoV 2 may promote tumor progression and stimulate metabolic switching in tumor cells to initiate tumor metabolic modes with higher production efficiency, such as glycolysis, for facilitating the replication of SARS CoV 2 (44). Meanwhile, we also established that muscular disease, such as myositis, is

associated with COVID-19. Previous studies have demonstrated that patients with dermatomyositis have three immunogenic linear epitopes with a high degree of sequence identity to the SARS-CoV-2 protein, so potential exposure to the coronavirus family may lead to the development of dermatomyositis (45). Effective Janus kinase (JAK) inhibitors for dermatomyositis, including tofacitinib, ruxolitinib, and baricitinib, may provide new directions for COVID-19 treatment.

In conclusion, the study provides new insights for the common pathogenesis of COVID-19 and atherosclerosis by looking for common transcriptional features. The DEGs identified by bioinformatics data analysis, including C1QA, C1QB, C1QC, CD163, SIGLEC1, APOE, MS4A4A, VSIG4, CCR1, and STAB1, may be therapeutic targets for the atherosclerosis caused by COVID-19. However, more wet lab-based studies are required to validate the impact of COVID-19 severity on atherosclerosis. Studies on the long-term effects of SARS-CoV-2 infection, the effect of persistent endothelial dysfunction on atherosclerosis, and the role of preventive therapy are also needed.

Data availability statement

The datasets presented in this study can be found in online repositories. The names of the repository/repositories and accession number(s) can be found in the article/supplementary material.

Author contributions

JZ performed the data analyses and wrote the manuscript. LZ helped perform the analysis with constructive discussions. Both authors approved the final version of the manuscript.

Acknowledgments

We acknowledge GEO database for providing their platforms and contributors for uploading their meaningful datasets.

Conflict of interest

The authors declare that the research was conducted in the absence of any commercial or financial relationships that could be construed as a potential conflict of interest.

Publisher's note

References

1. WHO COVID-19 Dashboard (2020). Geneva: World Health Organization. Available online: https://covid19.who.int/ (accessed March 9, 2022).

2. Callaway E. The race for coronavirus vaccines: a graphical guide. *Nature.* (2020) 580:576–7. doi: 10.1038/d41586-020-01221-y

3. Zheng Y, Xu H, Yang M, Zeng Y, Chen H, Liu R, et al. Epidemiological characteristics and clinical features of 32 critical and 67 noncritical cases of COVID-19 in Chengdu. *J Clin Virol.* (2020) 127:104366. doi: 10.1016/j.jcv.2020.104366

4. Huang C, Wang Y, Li X, Ren L, Zhao J, Hu Y, et al. Clinical features of patients infected with 2019 novel coronavirus in Wuhan, China. *Lancet (London, England).* (2020) 395:497–506. doi: 10.1016/S0140-6736(20)30183-5

5. Gao YP, Zhou W, Huang PN, Liu HY, Bi XJ, Zhu Y, et al. Persistent Endothelial dysfunction in coronavirus diseasE—2019 survivors late after recovery. *Front. Med.* (2022) 9:809033. doi: 10.3389/fmed.2022.809033

6. Robson A. Preventing cardiac damage in patients with COVID-19. *Nat Rev Cardiol.* (2021) 18:387. doi: 10.1038/s41569-021-00550-3

7. Mester A, Benedek I, Rat N, Tolescu C, Polexa SA, Benedek T, et al. Imaging cardiovascular inflammation in the COVID-19 era. *Diagnostics (Basel, Switzerland).* (2021) 11:1114. doi: 10.3390/diagnostics11061114

8. Yu G, Wang LG, Yan GR, He QY. DOSE: an R/Bioconductor package for disease ontology semantic and enrichment analysis. *Bioinformatics (Oxford, England).* (2015) 31:608–9. doi: 10.1093/bioinformatics/btu684

9. Wu T, Hu E, Xu S, Chen M, Guo P, Dai Z, et al. clusterProfiler 4.0: A universal enrichment tool for interpreting omics data. *Innovation (New York. NY).* (2021) 2:100141. doi: 10.1016/j.xinn.2021.100141

10. Butte AJ, Kohane IS. Creation and implications of a phenomE–genome network. *Nat Biotechnol.* (2006) 24:55–62. doi: 10.1038/nbt1150

11. Lu JH, Teh BK, Wang LD, Wang YN, Tan YS, Lai MC, et al. The classical and regulatory functions of C1q in immunity and autoimmunity. *Cell Mol Immunol.* (2008) 5:9–21. doi: 10.1038/cmi.2008.2

12. Tenner AJ. C1q interactions with cell surface receptors. *Behring Institute Mitteilungen.* (1989) 84:220–9.

13. Mortensen SA, Sander B, Jensen RK, Pedersen JS, Golas MM, Jensenius JC, et al. Structure and activation of C1, the complex initiating the classical pathway of the complement cascade. *Proc Natl Acad Sci USA.* (2017) 114:986–91. doi: 10.1073/pnas.1616998114

14. Sjöberg AP, Trouw LA, Blom AM. Complement activation and inhibition: a delicate balance. *Trends Immunol.* (2009) 30:83–90. doi: 10.1016/j.it.2008.11.003

15. Cornell J, Salinas S, Huang HY, Zhou M. Microglia regulation of synaptic plasticity and learning and memory. *Neural Regener Res.* (2022) 17:705–16. doi: 10.4103/1673-5374.322423

16. Györffy BA, Kun J, Török G, Bulyáki É, Borhegyi Z, Gulyássy P, et al. Local apoptotic-like mechanisms underlie complement-mediated synaptic pruning. *Proc Natl Acad Sci USA.* (2018) 115:6303–8. doi: 10.1073/pnas.1722613115

17. Martín-Jiménez P, Muñoz-García MI, Seoane D, Roca-Rodríguez L, García-Reyne A, Lalueza A, et al. Cognitive impairment is a common comorbidity

in deceased covid-19 patients: a hospital-based retrospective cohort study. *J Alzheimer's Dis.* (2020) 78:1367–72. doi: 10.3233/JAD-200937

18. Stephan AH, Barres BA, Stevens B. The complement system: an unexpected role in synaptic pruning during development and disease. *Annu Rev Neurosci.* (2012) 35:369–89. doi: 10.1146/annurev-neuro-061010-113810

19. Macor P, Durigutto P, Mangogna A, Bussani R, De Maso L, D'Errico PL, et al. MultiplE–organ complement deposition on vascular endothelium in COVID-19 patients. *Biomedicines.* (2021) 9:1003. doi: 10.3390/biomedicines9081003

20. Samstad EO, Niyonzima N, Nymo S, Aune MH, Ryan L, Bakke SS, et al. Cholesterol crystals induce complement-dependent inflammasome activation and cytokine release. *J Immunol (Baltimore, Md. : 1950).* (2014) 192:2837–45. doi: 10.4049/jimmunol.1302484

21. Hertle E, Stehouwer CD, van Greevenbroek MM. The complement system in human cardiometabolic disease. *Mol Immunol.* (2014) 61:135–48. doi: 10.1016/j.molimm.2014.06.031

22. Helmy KY, Katschke KJ, Gorgani NN, Kljavin NM, Elliott JM, Diehl L, et al. CRIg: a macrophage complement receptor required for phagocytosis of circulating pathogens. *Cell.* (2006) 124:915–27. doi: 10.1016/j.cell.2005.12.039

23. Zhao C, Mo J, Zheng X, Wu Z, Li Q, Feng J, et al. Identification of an alveolar macrophagE–related core gene set in acute respiratory distress syndrome. *J Inflamm Res.* (2021) 14:2353–61. doi: 10.2147/JIR.S306136

24. Lee MY, Kim WJ, Kang YJ, Jung YM, Kang YM, Suk K, et al. Z39Ig is expressed on macrophages and may mediate inflammatory reactions in arthritis and atherosclerosis. *J Leukoc Biol.* (2006) 80:922–8. doi: 10.1189/jlb.0306160

25. Singh DK, Aladyeva E, Das S, Singh B, Esaulova E, Swain A, et al. Myeloid cell interferon responses correlate with clearance of SARS-CoV-2. *Nat Commun.* (2022) 13:679. doi: 10.1038/s41467-022-28315-7

26. Guo L, Akahori H, Harari E, Smith SL, Polavarapu R, Karmali V, et al. CD163+ macrophages promote angiogenesis and vascular permeability accompanied by inflammation in atherosclerosis. *J Clin Invest.* (2018) 128:1106–24. doi: 10.1172/JCI93025

27. Weisgraber KH, Rall SC, Mahley RW. Human E apoprotein heterogeneity. CysteinE–arginine interchanges in the amino acid sequence of the apo-E isoforms. *J Biol Chem.* (1981) 256:9077–83. doi: 10.1016/S0021-9258(19)52510-8

28. Gordon EM, Yao X, Xu H, Karkowsky W, Kaler M, Kalchiem-Dekel O, et al. Apolipoprotein E is a concentration-dependent pulmonary danger signal that activates the NLRP3 inflammasome and IL-1β secretion by bronchoalveolar fluid macrophages from asthmatic subjects. *J Allerg Clin Immunol.* (2019) 144:426–441.e3. doi: 10.1016/j.jaci.2019.02.027

29. Kuo CL, Pilling LC, Atkins JL, Masoli J, Delgado J, Kuchel GA, et al. ApoE e4e4 genotype and mortality with COVID-19 in UK Biobank. *J Gerontol Ser A, Biol Sci Med Sci.* (2020) 75:1801–3. doi: 10.1093/gerona/glaa169

30. Vlasov I, Panteleeva A, Usenko T, Nikolaev M, Izumchenko A, Gavrilova E, et al. Transcriptomic profiles reveal downregulation of low-density lipoprotein particle receptor pathway activity in patients surviving severe COVID-19. *Cells.* (2021) 10:3495. doi: 10.3390/cells10123495

31. Brochériou I, Maouche S, Durand H, Braunersreuther V, Le Naour G, Gratchev A, et al. Antagonistic regulation of macrophage phenotype by M-CSF and GM-CSF: implication in atherosclerosis. *Atherosclerosis.* (2011) 214:316–24. doi: 10.1016/j.atherosclerosis.2010.11.023

32. Perez-Zsolt D, Muñoz-Basagoiti J, Rodon J, Elosua-Bayes M, Raïch-Regué D, Risco C, et al. SARS-CoV-2 interaction with Siglec-1 mediates trans-infection by dendritic cells. *Cell Mol Immunol.* (2021) 18:2676–8. doi: 10.1038/s41423-021-00794-6

33. Bedin AS, Makinson A, Picot MC, Mennechet F, Malergue F, Pisoni A, et al. Monocyte CD169 expression as a biomarker in the early diagnosis of coronavirus disease 2019. *J Infect Dis.* (2021) 223:562–7. doi: 10.1093/infdis/jiaa724

34. Xiong YS, Wu AL, Mu D, Yu J, Zeng P, Sun Y, et al. Inhibition of siglec-1 by lentivirus mediated small interfering RNA attenuates atherogenesis in apoE–deficient mice. *Clin Immunol (Orlando, Fla).* (2017) 174:32–40. doi: 10.1016/j.clim.2016.11.005

35. Stikker B, Stik G, Hendriks RW, Stadhouders R. Severe COVID-19 associated variants linked to chemokine receptor gene control in monocytes and macrophages. *bioRxiv : the preprint server for biology.* (2021) 01, 22.427813. doi: 10.1101/2021.01.22.427813

36. Drechsler M, Megens RT, van Zandvoort M, Weber C, Soehnlein O. Hyperlipidemia-triggered neutrophilia promotes early atherosclerosis. *Circulation.* (2010) 122:1837–45. doi: 10.1161/CIRCULATIONAHA.110.961714

37. Huo Q, Li Z, Chen S, Wang J, Li J, Xie N, et al. VWCE as a potential biomarker associated with immune infiltrates in breast cancer. *Cancer Cell Int.* (2021) 21:272. doi: 10.1186/s12935-021-01955-3

38. Silva-Gomes R, Mapelli SN, Boutet MA, Mattiola I, Sironi M, Grizzi F, et al. Differential expression and regulation of MS4A family members in myeloid cells in physiological and pathological conditions. *J leukocyte Biol.* (2021) 111:817–36. doi: 10.1002/JLB.2A0421-200R

39. Pellinen J, Holmes MG. Evaluation and treatment of seizures and epilepsy during the COVID-19 pandemic. *Curr Neurol Neurosci Rep.* (2022) 1–7. doi: 10.1007/s11910-022-01174-x

40. Danoun OA, Zillgitt A, Hill C, Zutshi D, Harris D, Osman G, et al. Outcomes of seizures, status epilepticus, and EEG findings in critically ill patient with COVID-19. *Epilepsy Behav: EandB.* (2021) 118:107923. doi: 10.1016/j.yebeh.2021.107923

41. Qin Y, Wu J, Chen T, Li J, Zhang G, Wu D, et al. Long-term microstructure and cerebral blood flow changes in patients recovered from COVID-19 without neurological manifestations. *J Clin Invest.* (2021) 131:e147329. doi: 10.1172/JCI147329

42. Rose KM, Wong TY, Carson AP, Couper DJ, Klein R, Sharrett AR, et al. Migraine and retinal microvascular abnormalities: the atherosclerosis risk in communities study. *Neurology.* (2007) 68:1694–700. doi: 10.1212/01.wnl.0000261916.42871.05

43. Zhou X, Zhou YN, Ali A, Liang C, Ye Z, Chen X, et al. Case report: a rE–positive case of SARS-CoV-2 Associated With Glaucoma. *Front Immunol.* (2021) 12:701295. doi: 10.3389/fimmu.2021.701295

44. Li YS, Ren HC, Cao JH. Correlation of SARS-CoV-2 to cancer: Carcinogenic or anticancer? (Review). *Int J Oncol.* (2022) 60:42. doi: 10.3892/ijo.2022.5332

45. Megremis S, Walker T, He X, Ollier W, Chinoy H, Hampson L, et al. Antibodies against immunogenic epitopes with high sequence identity to SARS-CoV-2 in patients with autoimmune dermatomyositis. *Ann Rheum Dis.* (2020) 79:1383–6. doi: 10.1136/annrheumdis-2020-217522

frontiers | Frontiers in Cardiovascular Medicine

TYPE Review
PUBLISHED 26 August 2022
DOI 10.3389/fcvm.2022.959955

OPEN ACCESS

EDITED BY
Wen-Jun Tu,
Chinese Academy of Medical Sciences and Peking Union Medical College, China

REVIEWED BY
Beatrice Charreau,
Université de Nantes, France
Madeline Nieves-Cintron,
University of California, Davis, United States

*CORRESPONDENCE
Fei Lin
linfeixixi@aliyun.com
Guo-An Zhao
guoanzhao@xxmu.edu.cn

†These authors share first authorship

SPECIALTY SECTION
This article was submitted to Atherosclerosis and Vascular Medicine, a section of the journal Frontiers in Cardiovascular Medicine

RECEIVED 02 June 2022
ACCEPTED 01 August 2022
PUBLISHED 26 August 2022

CITATION
Lu B-H, Liu H-B, Guo S-X, Zhang J, Li D-X, Chen Z-G, Lin F and Zhao G-A (2022) Long non-coding RNAs: Modulators of phenotypic transformation in vascular smooth muscle cells.
Front. Cardiovasc. Med. 9:959955.
doi: 10.3389/fcvm.2022.959955

Long non-coding RNAs: Modulators of phenotypic transformation in vascular smooth muscle cells

Bing-Han Lu[1,2†], Hui-Bing Liu[1,2,3†], Shu-Xun Guo[1,2], Jie Zhang[1,2], Dong-Xu Li[1,2], Zhi-Gang Chen[1,2], Fei Lin[1,2*] and Guo-An Zhao[1,2*]

[1]Department of Cardiology, Life Science Center, The First Affiliated Hospital of Xinxiang Medical University, Weihui, China, [2]Key Laboratory of Cardiovascular Injury and Repair Medicine of Henan, Weihui, China, [3]Henan Normal University, Xinxiang, China

Long non-coding RNA (lncRNAs) are longer than 200 nucleotides and cannot encode proteins but can regulate the expression of genes through epigenetic, transcriptional, and post-transcriptional modifications. The pathophysiology of smooth muscle cells can lead to many vascular diseases, and studies have shown that lncRNAs can regulate the phenotypic conversion of smooth muscle cells so that smooth muscle cells proliferate, migrate, and undergo apoptosis, thereby affecting the development and prognosis of vascular diseases. This review discusses the molecular mechanisms of lncRNA as a signal, bait, stent, guide, and other functions to regulate the phenotypic conversion of vascular smooth muscle cells, and summarizes the role of lncRNAs in regulating vascular smooth muscle cells in atherosclerosis, hypertension, aortic dissection, vascular restenosis, and aneurysms, providing new ideas for the diagnosis and treatment of vascular diseases.

KEYWORDS

long non-coding RNAs, vascular smooth muscle cells, phenotypic transformation, vascular disease, atherosclerosis

Introduction

Phenotype transformation of vascular smooth muscle cells (VSMCs) is an important cause of vascular dysfunction, capable of inducing vascular diseases, such as atherosclerosis (AS), hypertension, vascular stenosis, and diabetic vascular complications (1–6), and mature smooth muscle cells are widely distributed in the walls of blood vessels and internal organs, and normal VSMCs have no significant function in proliferating, migrating, and secreting the extracellular matrix, called constrictive VSMCs, which maintain vascular elasticity and ensure vasoconstriction (7). VSMCs exhibit significant proliferation and migration under immature or pathological conditions, such as inflammation, hypertension, and diabetes, and they synthesize large amounts of extracellular matrix, which are called synthetic VSMCs (8). After the phenotypic transformation occurs in smooth muscle cells, they change from "contractile type" to "synthetic type," causing changes in vascular function and playing an important role in the development of vascular remodeling, and increasing evidence is emerging that the

phenotype of VSMCs can develop fibroblastic, osteoblastic, and even macrophage-like cell characteristics (9, 10). Thus, understanding the pathophysiological changes in muscle cells is essential for diagnosing and treating vascular diseases. For a better understanding, we have made a graph, as shown in Figure 1.

Long non-coding RNAs (lncRNAs) are longer than 200 nucleotides and cannot code for proteins (11); according to the genome and the location relationship between adjacent genes, lncRNAs can be divided into sense, antisense, bidirectional, intronic, and intergenic lncRNA (12), and lncRNA expression has the spatial specificity of tissue expression. They play important roles in disease development, such as regulating transcription, epigenetic modifications, protein, and RNA stability, and translation and post-translational modifications, by interacting with DNA, RNA, and proteins, which are closely related to their intracellular localization, lncRNAs localized in the nucleus play several roles: (1) regulate chromatin remodeling, induce histone modifications to regulate downstream gene expression; (2) act as enhancer RNAs to regulate transcription; and (3) interfere with pre-mRNA processing to regulate mRNA splicing. LncRNAs localized in the cytoplasm can play several roles: (1) act as decoys that can regulate specific transcription factors and inhibit their function (13, 14); (2) act as sponges to adsorb miRNAs, regulate their stability and reduce their bioavailability (15); (3) act as molecular scaffolds that can bring two or more proteins into complex transcriptional or post-transcriptional complexes regulating gene expression; and (4) binding to specific proteins to affect protein translation and post-translational modifications, or as a precursor molecule for small molecule RNAs (16). The specific functions are shown in Figure 2 (17).

LncRNAs regulate smooth muscle cell phenotypic transition (18) and play a key role in related diseases, but the molecular mechanisms are not fully understood. In this review, we briefly outline the effect of the regulation of lncRNAs on differentiation and phenotypic transition in VSMCs during pathological remodeling. We also focus on how lncRNAs play a regulatory role in various conditions and their contribution to vascular diseases.

Role of LncRNA in smooth muscle cell phenotypic transformation

This review focuses on the mechanisms by which LncRNAs are known to play a regulatory role in various conditions and their contribution to vascular diseases. Table 1 shows the lncRNAs implicated in the regulation of VSMC phenotype and their validated targets.

LncRNA and atherosclerosis

Dysfunction of smooth muscle cells can trigger plaque formation, which is an important link in the pathogenesis of atherosclerosis, namely, the phenotypic transformation of proliferation, migration, and apoptosis. Platelet-derived growth factor-BB (PDGF-BB), oxidized low-density lipoprotein (ox-LDL), interleukin-6 (IL-6), and tumor necrosis factor-α (TNF-α) can change the phenotypic transformation of VSMCs from a contractile to a synthetic phenotype, promote smooth muscle cell proliferation and migration, and inhibit apoptosis. Matrix metalloprotein 2 (MMP-2) and matrix metalloprotein 9 (MMP-9) are important VSMC migration regulators. B cell lymphoma-2 (Bcl-2) and BCL2-Associated X (Bax) are apoptosis-related proteins. LncRNAs play various roles in regulating smooth muscle cell phenotypic transformation, as well as cell proliferation and migration. Detection of smooth muscle cell phenotypic transformation-related markers, cell proliferation, apoptosis-related proteins, and other clear regulatory roles implies that the effective control of smooth muscle cell phenotypic transformation may be an important therapeutic measure to prevent and treat AS.

The lncRNA SMILR can act as an enhancer or molecular scaffold to promote the proliferation of VSMCs by interacting with the promoter region of hyaluronidase 2 (HAS2), an important component of the extracellular matrix deposited in AS lesions, which promotes vessel wall thickening and reflects the degree of AS disease progression (19). Animal studies show that VSMC-specific HAS2 overexpression in transgenic mice increases susceptibility to AS and promoted vessel wall thickening. The investigators found increased expression of lncRNA SMILR in unstable AS plaques, which was detectable in the plasma of patients. These results confirmed that lncRNA SMILR is a driver of VSMC proliferation (20). However, it has been shown that lincRNA-p21 can also act as an enhancer partially bound to mouse double minutes2 (MDM2), enhancing the transcriptional activity of p53 and enabling p53 to interact with protein 300 (p300) and bind to the promoter/enhancer of its target gene, thereby inhibiting cell proliferation and inducing apoptosis in VSMCs (21). Another study showed that under ox-LDL stimulation, lncRNA antisense non-coding RNA in the INK4 locus (ANRIL) can act as a molecular scaffold to promote the binding of WD-40 repeat-containing protein 5(WDR5) and histone deacetylase 3 (HDAC3), thus, forming a WDR5/HDAC3 complex that regulates the expression of the target gene NADPH oxidase 1 (NOX1) through histone modifications, upregulates reactive oxygen species (ROS) levels, promotes phenotypic transition in HASMCs, and is a potential scaffolding protein (23).

LncRNAs can exert a role by directly binding to proteins and participating in protein phosphorylation and the activation of signaling pathways. lncRNAs are required to localize specific protein complexes, which can interact with DNA or mRNA

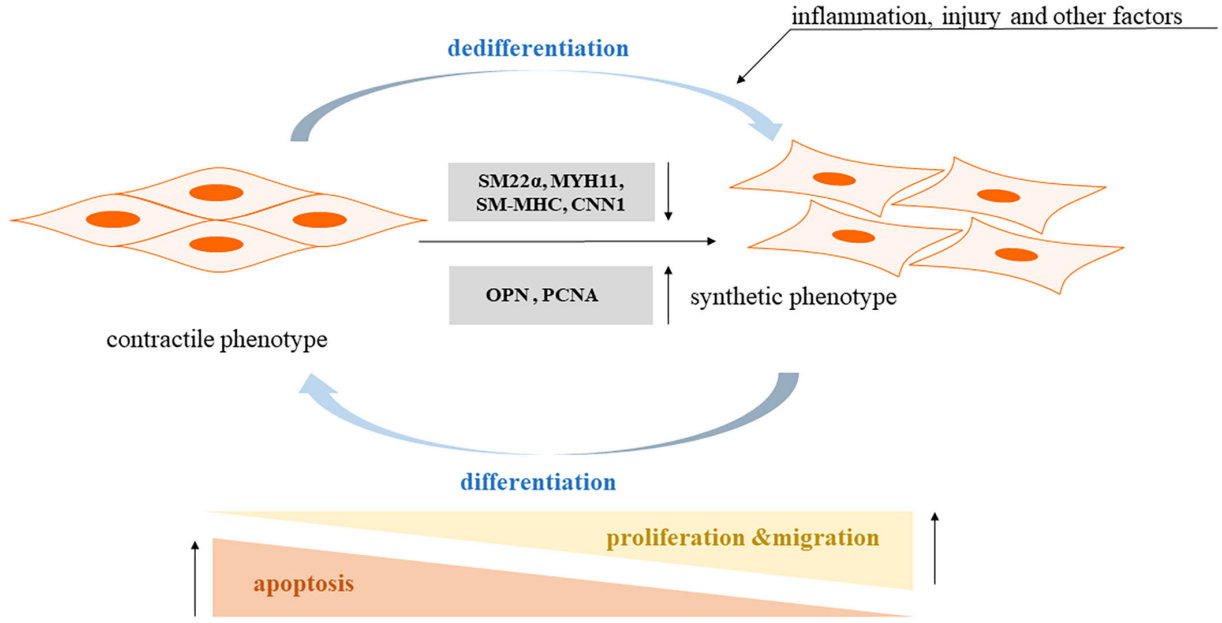

FIGURE 1
The pathophysiological mechanism of smooth muscle cells phenotypic transformation. Contractile phenotype markers: SM22a: smooth muscle 22a; SM-MHC: smooth muscle myosin heavy chain; MYH11: myosin heavy chain 11; CNN1: calponin 1. Synthetic phenotype markers: OPN: osteopontin; PCNA: proliferating cell nuclear antigen.

and inhibit their expression or translation through methylation. In AS plaques, lncRNA ZNF800 expression is upregulated by directly binding to phosphatase and tensin homolog deleted on chromosome 10 (PTEN), thereby blocking the AKT (also known as protein kinase B PKB)/mammalian target of rapamycin (mTOR) pathway to inhibit PDGF-BB-mediated proliferation and migration of VSMCs. MMP1 promotes cell migration by degrading ECM components, and vascular endothelial growth factor-α (VEGF-α) can also lead to cell proliferation and migration. LncRNA ZNF800 regulates the hypoxia-inducible factor-1α (HIF-1α)-mediated VEGF-α or MMP1 pathway through the PTEN-activated AKT/mTOR signaling pathway to inhibit VSMC proliferation and migration (26). Similarly, the inhibition of lncRNA myocardial infarction-associated transcript (MIAT) limits the phosphorylation of extracellular signal-regulated kinase (p-ERK), increases the phosphorylation of ETS transcription factor (p-ELK1) accumulation in the nucleus, and subsequently decreases early growth response 1 (EGR1) expression, thereby regulating the proliferation of smooth muscle cells (SMCs) through the EGR1-ELK1-ERK pathway. The lncRNA MIAT also binds to the promoter region of Krüppel-like factor 4 (KLF4) and enhances its transcription, participating in the phenotypic transformation of SMCs to pro-inflammatory macrophage-like cells. *In vivo* studies have shown that SMCs in mouse and minipig models of AS display changes similar to those of HASMCs, thus confirming that lncRNA MIAT plays a regulatory role in advanced AS lesion formation by inducing the differentiation and dedifferentiation of SMCs (27). Another study showed that lncRNA 430945 is highly expressed in human AS tissues, which in turn promotes the angiotensin II (AngII)-induced proliferation of VSMCs. The upregulation of lncRNA 430945 expression activates signaling pathways associated with receptor tyrosine kinase-like orphan receptor 2 (ROR2) and Ras homolog gene family member A (RhoA), promoting AngII-induced proliferation and migration of VSMCs (29). In contrast, metformin exerts an anti-AS effect by activating AMP-activated protein kinase (AMPK), increasing the expression of lncRNA ANRIL, enhancing the affinity of lncRNA ANRIL to the AMPKγ subunit, increasing the catalytic activity of AMPK, and increasing its phosphorylation level, thereby inhibiting the phenotypic transition of VSMCs (88). The downregulation of miR-34c expression may be owing to the demethylation associated with lncRNA BRAF-activated non-coding RNA (BANCR). High mobility group protein B1 (HMGB1) is a pro-inflammatory mediator that upregulates the expression of cytokines, chemokines, and adhesion molecules, thereby enhancing macrophage infiltration, leading to AS. miR-34c overexpression inhibits the expression of HMGB1, TNF-α, and Bcl-2. LncRNA BANCR overexpression induces HASMC proliferation by downregulating miR-34c methylation and reversing the effect of miR-34c on HMGB1, TNF-α, and Bcl-2 expression, thereby promoting HASMCs proliferation and inhibiting apoptosis (30). The expression of LncRNA RP11-531A24.3 is reduced in advanced AS lesions;

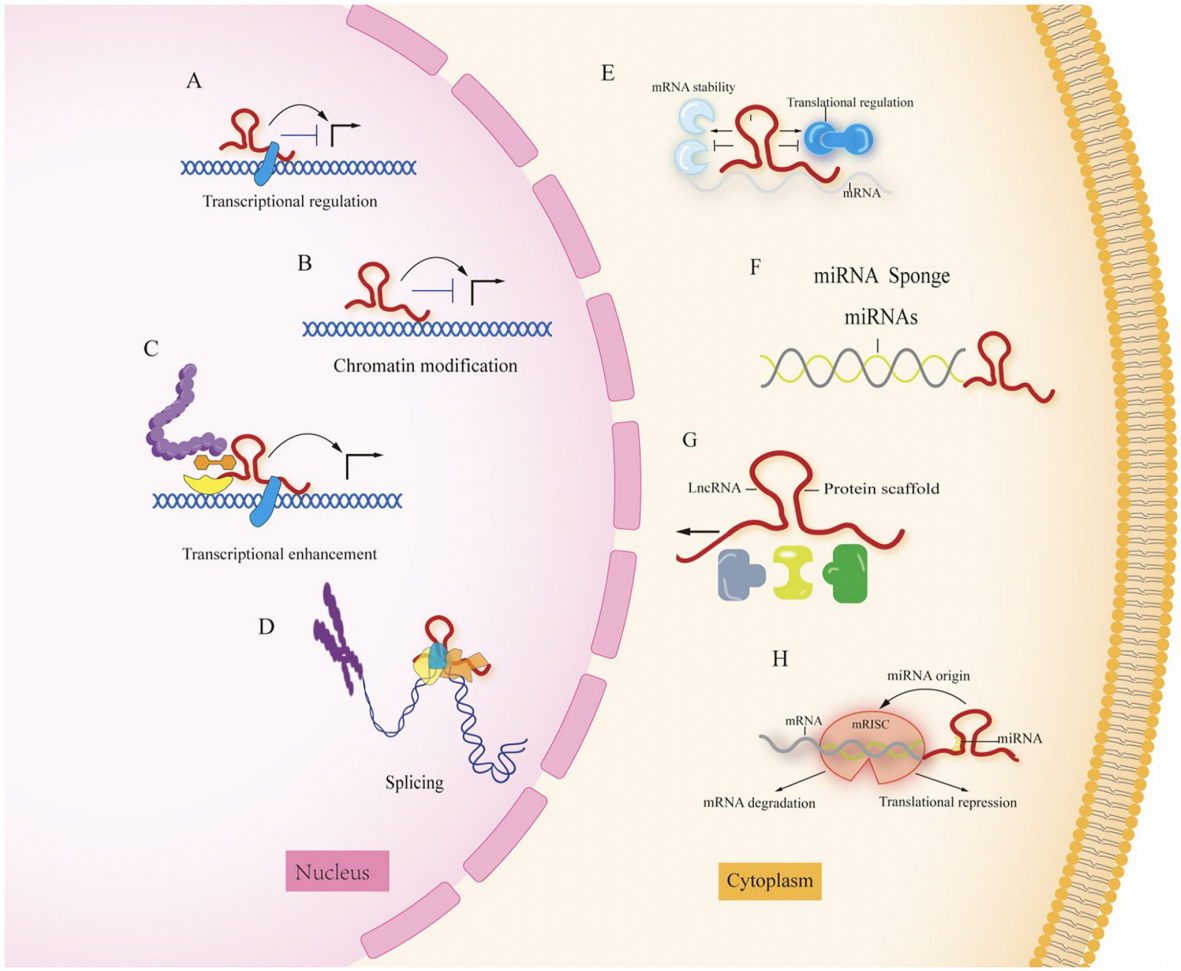

FIGURE 2
The different roles of LncRNA in the nucleus and cytoplasm. **(A)** Transcriptional regulation; **(B)** chromation modification; **(C)** transcriptional enhancement; **(D)** splicing; **(E)** regulation of mRNA stability; **(F)** miRNA sponge; **(G)** protein scaffold; **(H)** LncRNAs can function as miRNA host transcripts (miRNA origin). Mature single-stranded miRNA is derived from lncRNA transcripts and loaded into RNA induced silencing complex (RISC) by repressing translation or inducing mRNA degradation.

in cells overexpressing it, lncRNA RP11-531A24.3 inhibits the migration and proliferation of HA-VSMCs by binding directly to the RNA-binding protein annexin 2 (ANXA2) in the cytoplasm to reduce its expression at the mRNA and protein levels (31).

The cardiac mesoderm enhancer-associated non-coding RNA (CARMN) regulates specific transcription factors, and serum response factor (SRF), a transcription factor that binds to CArG elements, plays an important role in regulating the VSMC phenotype by interacting with multiple cofactors (32). Myocardin (MYOCD) is a specific transcriptional co-activator involved in the differentiation of cardiomyocytes and VSMCs. MYOCD enhances the binding of SRF to the CArG box and transcriptionally activates a variety of downstream VSMC contractile genes, representing the contractile and differentiated VSMC phenotype (33). The lncRNA CARMN enhances trans-MYOCD function by directly binding to MYOCD to maintain the contractile phenotype of VSMCs in healthy arteries. In contrast, in diseased arteries, lncRNA CARMN expression is downregulated, thereby attenuating the trans-activating activity of the MYOCD/SRF complex on SMC-specific gene expression and triggering the dedifferentiation of VSMCs, leading to increased neointimal formation (34). Another transcriptional regulator, cyclin-dependent kinase 9 (CDK9), was shown to be a direct target of lncRNA PEBP1P2, and overexpression of lncRNA PEBP1P2 significantly inhibited proliferation, migration, and dedifferentiation during PDGF-BB-induced phenotypic transformation of VSMCs by directly binding to CDK9 to downregulate its expression. This idea was similarly validated in animal experiments, where lncRNA PEBP1P2 overexpression attenuated neointima formation and VSMC phenotypic transformation induced in a balloon-injured carotid artery model (35). LncRNA LIPCAR accelerates the cell cycle by

TABLE 1 Long non-coding RNA with functional relevance in different vascular diseases.

LncRNA	Regulation	Related target	The function in the VSMCs	Disease	References	Genbank accession numbers
SMILR	Promote	HAS2	Proliferation	Atherosclerosis	Zhang et al. (19), Ballantyne et al. (20)	105375734
P21	Inhibit	p53, p300, miR-17-5p	Proliferation, apoptosis	Atherosclerosis	Wu et al. (21), Wang et al. (22)	102800311
ANRIL	Inhibit	AMPK, WDR5, HDAC3, miR-126-5p	Proliferation, apoptosis	Atherosclerosis, PAH	Zhang et al. (23), Li et al. (24), Wang et al. (25)	100048912
ZNF800	Inhibit	PTEN, AKT/mTOR	Proliferation, migration	Atherosclerosis	Lu et al. (26)	168850
MIAT	Promote	EGR1-ELK1-ERK, miR-641	Proliferation, migration, invade	Atherosclerosis	Fasolo et al. (27), Ma et al. (28)	440823
430945	Promote	RhoA	Proliferation, migration	Atherosclerosis	Cui et al. (29)	23569
BANCR	Promote	miR-34c	Proliferation, apoptosis	Atherosclerosis	Jiang et al. (30)	100885775
RP11-531A24.3	Inhibit	ANXA2	Proliferation, migration	Atherosclerosis	Wu et al. (31)	26121
CARMN	Inhibit	MYOCD	Proliferation, migration	Atherosclerosis	Onuh et al. (32), Miano, (33), Dong et al. (34).	728264
PEBP1P2	Inhibit	CDK9	Proliferation, migration	Atherosclerosis	He et al. (35)	647307
LIPCAR	Promote	P21, CDK2	Proliferation, migration	Atherosclerosis	Hung et al. (36), Wang et al. (37)	103504742
H19	Promote	miR-675, miR-599, miR-148b, miR-193b-3p	Proliferation, migration, apoptosis	Atherosclerosis, AD	Cai et al. (38), Sun et al. (39), Lu et al. (40), Zhang et al. (41), Lv et al. (42), Ren et al. (43)	283120
AC105942.1	Inhibit	hnRNPA2/ B1	Proliferation	Atherosclerosis	Zhang et al. (44)	2157
TUG1	Promote	miR-21	Proliferation	Atherosclerosis	Li et al. (45)	55000
FOXC2-AS1	Promote	miR-1253	Proliferation, apoptosis	Atherosclerosis	Wang et al. (46)	103752587
HCG11	Promote	miR-144	Proliferation, apoptosis	Atherosclerosis	Liu et al. (47)	493812
CTB P1-AS2	Inhibit	miR-195-5p	Migration	Atherosclerosis	Wang et al. (48)	92070
XIST	Promote	miR-539-5p, miR-17	Proliferation, migration, invade	Atherosclerosis, TAAD	Wang et al. (48), Zhang et al. (49)	7503
CASC2	Inhibit	miR-532-3p	Proliferation, apoptosis	Atherosclerosis,PAH	Wang et al. (50), Gong et al. (51)	255082
MEG3	Promote	miR-361-5p	Proliferation, apoptosis	Atherosclerosis	Wang et al. (52)	55384
MEG8	Inhibit	miR-181a-5p, miR-195-5p	Proliferation, migration, apoptosis	Atherosclerosis	Zhang et al. (53), Xu et al. (54)	79104
MALAT1	Inhibit	miR-124-3p	Proliferation, apoptosis	Atherosclerosis	Cheng et al. (55)	378938
SNHG7-003	Inhibit	miR-1306-5p	Proliferation, migration, invade	Atherosclerosis	Zheng et al. (56)	84973

(Continued)

10.3389/fcvm.2022.959955

TABLE 1 (Continued)

LncRNA	Regulation	Related target	The function in the VSMCs	Disease	References	Genbank accession numbers
C2dat1	Promote	miR-34a	Proliferation, migration	Atherosclerosis	Wang et al. (57)	107980436
SNHG12	Inhibit	miR-7665p, miR-199a-5p	Proliferation, migration	Atherosclerosis	Liu et al. (58), Sun et al. (59)	85028
LEF1-AS1	Promote	miR-544	Proliferation, migration, invade	Atherosclerosis	Zhang et al. (60)	641518
01123	Promote	miR-1277-5p	Proliferation, migration	Atherosclerosis	Weng et al. (61)	440894
00341	Promote	miR-214	Proliferation, migration	Atherosclerosis	Liu et al. (62)	79686
ES3	Promote	miR-95-5p, miR-6776-5p, miR-3620-5p and miR-4747-5p,	Osteoblast-like cells	Diabetes	Zhong et al. (63)	100507428
EPS	Inhibit	Wnt/β-catenin	Migration,osteoblast-like cells	Diabetes	Li et al. (64)	102635290
UCA1	Promote	miR582-5p, hnRNP I	Proliferation, apoptosis, invade	Diabetes, PAH	Yang et al. (65), Zhu et al. (66)	652995
HCG18	Inhibit	fused in sarcoma (FUS)	Proliferation, apoptosis	Hypertension	Lu et al. (67)	414777
GAS5	Inhibit	miR-21, p53, NOXA	Proliferation, migration	Hypertension, restenosis,	Liu et al. (68), Tang et al. (69).	60674
MRAK048635_P1	Inhibit	Rb,E2F	Proliferation, migration, apoptosis	Hypertension	Fang et al. (70)	25102670
AK098656	Promote	MYH11/ FN1	Proliferation	Hypertension	Jin et al. (71).	831169
CDKN2B-AS1	Promote	miR-143-3p	Proliferation, migration	Restenosis	Ma et al. (72).	100048912
CRNDE	Promote	smad3	Proliferation, migration	Restenosis, AAA	Zhou et al. (73), Li et al. (74).	643911
NEAT1	Promote	WDR5,miR-34a-5p, KLF4	Proliferation, migration	Restenosis, PAH	Ahmed et al. (75), Dou et al. (76).	283131
Hoxaas3	Inhibit	H3K9,Hoxa3	proliferation	PAH	Zhang et al. (77).	72628
TCONS_00034812	Inhibit	STOX1	Proliferation	PAH	Liu et al. (78).	100506542
Rps4l	Inhibit	ILF3	Proliferation, migration	PAH	Liu et al. (79)	66184
AC068039.4	Promote	miR-26a-5p	Proliferation, migration	PAH	Qin et al. (80)	10982
MYOSLID	Inhibit	Smad2,MKL1	Proliferation, migration	PAH	Zhao et al. (81)	105373853
01278	Inhibit	miR- 500b-5p	Proliferation, migration	AD	Wang et al. (82)	92249
PVT1	Promote	miR-27b-3p,miR-3127-5p	Proliferation, migration	AD, AAA	Li et al. (83), Huang et al. (84)	5820
LUCAT1	Inhibit	miR-199a-5p	Proliferation, apoptosis	AAA	Xia et al. (85)	100505994
SNHG5	Promote	miR-205-5p	Proliferation, migration, apoptosis	AAA	Nie et al. (86)	387066
00473	Inhibit	miR-212-5p	Proliferation, apoptosis	AAA	Tian et al. (87)	90632

LncRNAs and their regulation (promote or inhibit) under vascular disease-relevant conditions. Further depicted in the table are the downstream targets of lncRNAs, their main function in VSMC dynamics, the respective references, and the GenBank accession numbers. Abbreviations of target genes are explained in the text.

10.3389/fcvm.2022.959955

inhibiting the expression of the anti-proliferative gene P21 and activating the transcriptional regulator CDK2, decreasing the expression of α-SMA, and increasing the expression of MMP-2 and MMP-9 to promote VSMC proliferation, migration, and ultimately endothelial hyperplasia and AS plaque formation (36, 37). In another study, lncRNA H19 was expressed in the neoplastic endothelium of a mouse balloon injury model as well as in the VSMCs of human plaques (38), and knockdown of lncRNA H19 enhanced the interaction between Bax and p53 proteins by increasing p53-regulated transcription, leading to the proliferation of VSMCs and a reduction in plaque size, and mediated VSMC apoptosis to delay the development of AS (39). In AS plaques, lncRNA AC105942.1 expression was downregulated and hnRNPA2/B1 expression was upregulated, whereas hnRNPA2/B1 functions in the cell cycle by regulating the transcriptional levels of cell cycle protein kinase (CDK4) and p27. When lncRNA AC105942.1 expression was upregulated, the proliferation of AngII-treated VSMCs was reduced, CDK4 expression was decreased, and p27 was upregulated, whereas heterogeneous nuclear ribonucleoprotein A2/B1 (hnRNPA2/B1) expression was reduced. hnRNPA2/B1 knockdown also significantly reduced CDK4 expression and upregulated p27 levels, and the results suggest that lncRNA AC105942.1 acts by downregulating hnRNPA2/B1 expression to regulate the transcriptional levels of CDK4 and p27, thereby inhibiting the proliferative effects of AngII on VSMCs (44).

However, in ox-LDL-induced HA-VSMCs, knockdown of lncRNA H19 also acts as a sponge to adsorb miR-599 to reduce pappalysin 1 (PAPPA) to inhibit the increase in cyclin D1 and N-cadherin in HA-VSMCs and decrease E-cadherin to promote proliferation, migration, and invasion of HA-VSMCs (40). H19 also acts as a competitive endogenous RNA (ceRNA) for miR-148b to enhance the expression of wnt family member 1 (WNT1). Moreover, miR-148 inhibitors exert their pro-proliferative and anti-apoptotic effects by activating ox-LDL-stimulated Wnt/β-catenin signaling in HA-VSMCs (41). LncRNA taurine upregulated gene 1 (TUG1) expression was also upregulated in VSMCs induced by hypoxia or TNF-α in patients with AS. In established injury models, lncRNA TUG1 promotes VSMC proliferation and AS by targeting miRNA-21 to downregulate PTEN expression, decrease PTEN activity, and increase cyclin D1 expression (45). Another lncRNA, ANRIL, also called cyclin-dependent kinase inhibitor 2B antisense RNA 1 (CDKN2B-AS1), acts as a ceRNA to competitively bind miR-126-5p to upregulate protein tyrosine phosphatase non-receptor type 7 (PTPN7) expression and inhibit the phosphatidylinositide 3-kinases (PI3K)-AKT pathway, thereby hindering ox-LDL-induced proliferation and accelerating apoptosis (24). LncRNA forkhead box protein C2-AS1 (FOXC2-AS1) expression was significantly upregulated in VSMCs induced by ox-LDL and IL-6. LncRNA FOXC2-AS1 binds to miR-1253 as a ceRNA, causing miR-1253 to target forkhead box protein F1 (FOXF1), increasing the levels of Bcl-2 and significantly decreasing Bax and caspase-3, thereby regulating cell proliferation and the development of AS (46). Similarly, overexpression of lncRNA HLA complex group 11 (HCG11) can act as a sponge to negatively regulate miR-144 while increasing FOXF1 expression, resulting in increased Bcl-2 and decreased Bax expression, thereby promoting proliferation and inhibiting apoptosis in VSMCs (47). Silencing the lncRNA MIAT acts as a sponge for miR-641, induces stromal interaction molecule 1 (STIM1), attenuates the protein expression of proliferating cell nuclear antigen (PCNA), and Ki-67, and thus inhibits ox-LDL-induced proliferation, migration, and invasion (28). Likewise, overexpression of lncRNA C-terminal binding protein 1-antisense RNA 2 (CTBP1-AS2) acts as a ceRNA for miR-195-5p to promote autophagy-related 14 (ATG14) expression and decrease PCNA and Ki-67 expression levels, thereby inhibiting HAVSMC proliferation (48). Downregulation of lncRNA X-inactive-specific transcript (XIST), as a competitive endogenous RNA for miR-539-5p to enhance the expression of secreted phosphoprotein 1, inhibited the upregulation of PCNA and Ki-67 expression, as well as the expression of MMP-2 and MMP-9, thereby suppressing the proliferation, migration, and invasion of VSMCs by ox-LDL stimulation (89). Similarly, overexpression of another lncRNA, cancer susceptibility candidate 2 (CASC2), can act as a sponge to negatively regulate the expression of miR-532-3p, upregulate the expression of non-canonical poly (A) polymerase 5 (PAPD5), and inhibit the expression of PCNA, α-SMA, MMP-2, and MMP-9. LncRNA CASC2 inhibits the proliferation of VSMCs and promotes apoptosis by regulating the miR-532-3p/PAPD5 axis (50). miR-361-5p targets the 3′-UTR of ATP-binding cassette transporter A1 (ABCA1) mRNA and downregulates lncRNA maternally expressed gene 3 (MEG3), possibly by binding miR-361-5p to act as an endogenous "sponge," thereby abolishing the miRNA-mediated inhibitory activity on the 3′-UTR of ABCA1 and promoting the proliferation and slowing the apoptosis of VSMCs (52). Likewise, overexpression of lncRNA maternally expressed gene 8 (MEG8) indirectly targets peroxisome proliferator-activated receptor α (PPARα) by adsorbing miR-181a-5p at the 3′-UTR and positively regulating its expression, thereby inhibiting the proliferation and migration of VSMCs and promoting their apoptosis (53). Another study indicated that lncRNA MEG8 as a ceRNA targeting the miR-195-5p/RECK (reversion inducing cysteine-rich protein with kazal motifs) axis attenuated the hypoxia-induced overproliferation, inflammation, and migration of VSMCs (54). However, overexpression of metastasis associated with lung adenocarcinoma transcript 1 (MALAT1) can also sponge miRNA-124-3p to positively regulate PPARα levels, inhibit proliferation, and promote apoptosis of VSMCs (55). Another study showed that the expression of p53, lincRNA-p21, and sirtuin 7(SIRT7)was downregulated, whereas that of miR-17-5p was upregulated in carotid tissue from AS mice and peripheral blood from patients with AS. p53-dependent

lincRNA-p21 could increase SIRT7 expression by binding to miR-17-5p, thereby inhibiting VSMC proliferation and promoting apoptosis, while reducing AS-vulnerable plaques and lipid accumulation in mice (22). Similarly, overexpression of lncRNA small nucleolar RNA host gene 7-003 (SNHG7-003) inhibited the proliferation, migration, and invasion of VSMCs by suppressing miR-1306-5p, which directly binds SIRT7, upregulates its expression, and downregulates the contractile marker α-SMA in VSMCs (56). In contrast, overexpression of lncRNA CAMK2D associated transcript 1 (C2dat1) promoted the proliferation and migration of VSMCs by repressing miR-34a, another member of the SIRT family, by detecting the expression of PCNA, and by wound healing to detect migration (57). LncRNA small nucleolar RNA host gene 12 (SNHG12) was significantly upregulated in ox-LDL-treated hVSMCs. Moreover, SNHG12 acts as a sponge for miR-7665p. Eukaryotic translation initiation factor 5A(EIF5A)is a direct target gene of miR-766-5, and EIF5A promotes the proliferation and migration of ox-LDL-induced hVSMCs. However, silencing lncRNA SNHG12 counteracts the effect of EIF5A. This demonstrates that silencing lncRNA SNHG12 blocks the proliferation and migration of hVSMCs by targeting the miR-766-5p/EIF5A axis (58). In another study, knockdown of lncRNA SHNG12 targeting miR-199a-5p/HIF-1α was shown to be involved in the pathophysiological process of AS by regulating the phenotype of VSMCs (59). LncRNA lymph enhancer-binding factor 1-antisense RNA 1 (LEF1-AS1) regulates the PTEN/PI3K/AKT signaling pathway in VSMCs by targeting miR-544 (60). LINC01123 is highly expressed in patients with carotid atherosclerosis and promotes cell proliferation and migration by regulating the miR-1277-5p/KLF5 axis in ox-LDL-induced VSMCs (61). Similarly, investigators found that in ox-LDL-induced VSMCs, LINC00341 expression was increased, whereas miR-214 expression was significantly decreased. LINC00341 promoted FOXO4 protein expression by adsorbing miR-214, and forkhead box O4 (FOXO4) protein could counteract the promoter region of LINC00341 binding to promote its transcription, and LINC00341 promoted the proliferation and migration of VSMCs by regulating the miR-214/FOXO4 axis (62).

LncRNA and diabetes

It is well known that diabetes can cause extensive damage to the macrovascular and microvascular systems in different organs and tissues, resulting in macrovascular complications like atherosclerosis, hypertension and stroke, and microvascular complications like diabetic nephropathy, diabetic retinopathy, and diabetic neuropathy (90). Therefore, it is important to understand that diabetes-related LncRNAs affect the development of diabetes by regulating smooth muscle cell phenotypic transition.

VSMCs are the main cells involved in the process of medial membrane vascular calcification. Calcified vascular smooth muscle cells can change from a contractile phenotype to a bone/chondrogenic phenotype (91). High glucose induces severe calcification/senescence in HA-VSMCs, a process that is exacerbated by lncRNA-ES3 (LINC00458) expression. Investigators found that lncRNA-ES3 acts as a ceRNA for miR-95-5p, miR-6776-5p, miR-3620-5p, and miR-4747-5p, exacerbating calcification/senescence in HA-VSMCs. Basic helix-loop-helix family member e40 (Bhlhe40) attenuates high glucose-induced calcification/senescence in HA-VSMCs by binding to the promoter region of the lncRNA-ES3 and subsequently regulating its expression in HA-VSMCs (63). Another study showed that lncRNA erythroid pro-survival (lincRNA EPS) could regulate the Wnt/β-catenin pathway by promoting TGF-β expression and interfering with Wnt3 and β-catenin expression, thereby inhibiting the differentiation to osteogenesis and migration of VSMCs and thereby reducing diabetes-related vascular calcification (64).

A study showed that lncRNA urothelial carcinoma associated 1 (UCA1) was significantly downregulated and miR-582-5p was upregulated in VSMCs and serum exosomes of patients with T2DM. There was a negative correlation between them and miR582-5p was a direct target of lncRNA UCA1. Downregulation of lncRNA UCA1 attenuated the proliferation and invasion of VSMCs induced by increasing glucose dose. However, these inhibited trends were partially abolished by co-transfection of miR582-5p inhibitor; therefore, the authors concluded that miR-582-5p was engaged in the repair of VSMCs induced by lncRNA UCA1 in the hyperglycemic state (65).

LncRNA and hypertension

AngII is an active downstream peptide of the renin–angiotensin system that promotes the proliferation and migration of VSMCs by binding to its receptor (92). VSMCs are the major cellular components of the arterial mesothelium, and their proliferation promotes vascular remodeling in hypertension (93). Vascular remodeling caused by essential hypertension is a major cause of death in patients. Therefore, inhibiting cellular dysfunction and phenotypic transition in VSMCs may be a novel therapeutic strategy for essential hypertension.

The expression of serum lncRNA HLA complex group 18 (HCG18) was reduced in hypertensive patients and PDGF-BB-treated VSMCs. After knockdown of HCG18, the expression levels of contractile phenotypic markers, α-SMA, SM22α, and smoothelin, were significantly reduced in VSMCs, whereas synthetic markers, such as OPN, were increased; that is, knockdown of lncRNA HCG18 promoted the proliferation of VSMCs (67). In PDGF-BB-treated VSMCs, lncRNA growth

arrest-specific transcript 5 (GAS5) blocked the PDGF-BB-induced proliferation and migration of VSMCs by competitively binding to miR-21, thereby attenuating its inhibitory effect on programmed cell death 4 (PDCD4). Thus, the lncRNA GAS5/miR-21/PDCD4 axis may be a potential target for hypertension treatment (68).

AngII-treated VSMCs were very close to the *in vitro* hypertensive state, and the apoptosis rate of VSMCs increased significantly after H_2O_2 treatment. Knockdown of lncRNA MRAK048635_P1 reversed this change. α-SMA, SM22α, and calponin expression levels were significantly reduced, while OPN expression levels were enhanced. VSMC proliferation and migration also increased. Knockdown of lncRNA MRAK048635_P1 in VSMCs also resulted in the overexpression of cyclin D1, cyclin E, CDK2, and CDK4. In the G1 phase, CDK phosphorylates the Rb protein and activates transcription factor E2F, which regulates the cell cycle and thus promotes the transcription of proliferation-related genes. Therefore, downregulation of lncRNA MRAK048635_P1 expression induces a phenotypic shift from contractile to synthetic VSMCs, promotes VSMC proliferation and migration, and inhibits apoptosis (70).

lncRNA AK098656 is mainly expressed in HASMCs, and lncRNA AK098656 overexpression promotes the proliferation of HASMCs by downregulating α-SMA and upregulating the expression of OPN and collagen-I. LncRNA AK098656 binds directly to both MYH11/FN1 (fibronectin-1) proteins, which can act as a scaffold to drag MYH11 closer to the proteasome to promote its degradation, and it can also mediate MYH11/FN1 degradation through the lysosomal pathway. Expression of MYH11, FN1, and α-SMA was also lower in the thoracic aorta, left renal artery, and superior mesenteric artery of rats overexpressing the lncRNA AK098656 gene, while collagen-I deposition increased, arterial lumen narrowing increased intima-media thickness and intima-media/lumen ratio and reduced vasodilation, which induced resistance to vascular arterial remodeling. LncRNA AK098656 can promote hypertension by accelerating contractile protein degradation, increasing VSMC synthetic markers, and, ultimately, antiatherogenic narrowing (71).

LncRNA and revascularization, vascular remodeling

In a rat balloon injury model of restenosis, the expression of lncRNA H19 and miR-675 increased significantly in the neoplastic endothelium. The lncRNA H19-derived miR-675 was found to regulate PTEN and promote the proliferation of VSMCs by directly targeting the 3′-UTR of PTEN (42). In in-stent restenosis patient sera, lncRNA cyclin-dependent protein kinase inhibitors antisense RNA 1 (CDKN2B-AS1) levels were elevated, and miR-143-3p levels were decreased. In human carotid artery smooth muscle cells (hHCtASMCs), knockdown of lncRNA CDKN2B-AS1 resulted in the inhibition of cell proliferation and migration. miR-143-3p is a target of lncRNA CDKN2B-AS1. The results of *in vitro* studies suggest that the lncRNA CDKN2B-AS1/miR-143-3p axis may regulate the proliferation and migration of hHCtASMCs (72). Similarly, knockdown of lncRNA colorectal neoplasia differentially expressed (CRNDE] significantly inhibited PDGF-BB-induced proliferation and migration of VSMCs (73).

LncRNA GAS5 expression was reduced in PDGF-BB-induced VSMCs, but lncRNA GAS5 overexpression inhibited VSMC proliferation, blocked the cell cycle in the G1/G0 phase, and enhanced caspase-3 cleavage, promoting cell cycle arrest and apoptosis. Overexpression of lncRNA GAS5 increases the expression of the transcriptional regulator p53 and its downstream genes NOXA and p21. This hypothesis was supported by animal experiments. LncRNA GAS5 inhibited neoplastic endothelial formation by increasing the expression of p53 and its downstream genes NOXA and p21 to suppress VSMC proliferation and induce their apoptosis (69). LncRNA nuclear paraspeckle assembly transcript 1 (NEAT1) expression was elevated in PDGF-BB-induced VSMCs, and knockdown of lncRNA NEAT1 decreased the proliferation and migration ability of VSMCs and significantly reduced neoplastic endosomes, with similar changes in the proliferation markers Ki-67 and SM α-actin. PDGF-BB can also promote the binding of lncRNA NEAT1 to WDR5 to activate gene transcription and shift the SM-specific gene promoter from "open" to "closed" to suppress the expression of specific genes in SMCs, thereby regulating their phenotypic transition (75).

LncRNA and pulmonary arterial hypertension

Pulmonary arterial hypertension (PAH) is a refractory cardiovascular disease characterized mainly by increased pulmonary vascular resistance and pulmonary artery pressure, resulting in vascular remodeling, leading to right ventricular hypertrophy, and eventually right heart failure. Hypoxia is a major factor in PAH pathogenesis. During hypoxic exposure, pulmonary artery smooth muscle cells (PASMCs) undergo excessive proliferation and migration, leading to hypertrophy of PASMCs and narrowing of the pulmonary vascular lumen, resulting in pulmonary hypertension (94).

In hypoxic PASMCs, lncRNA hoxa cluster antisense RNA 3 (Hoxaas3) affects transcriptional regulation by regulating histone H3K9 acetylation, which activates Hoxaas3 upregulation in PASMCs and increases the percentage of cells in the S + G2/M phase. In contrast, knockdown of Hoxaas3 reduces the number of cells in the S + G2/M phase and

downregulates PCNA, Ki-67, cyclin A, D, and E expression, thereby inhibiting the proliferation of PASMCs under hypoxic conditions. Overexpression of Hoxa3 can reverse these changes. These results suggest that under hypoxia, Hoxaas3 regulates cell cycle changes by interacting with Homeobox a3 (Hoxa3) to allow PASMCs to proliferate (77). In hypoxia-induced PASMCs, the expression of another lncRNA, ANRIL, is significantly downregulated. The downregulation of lncRNA ANRIL expression caused more PASMCs to move from the G0/G1 phase into the G2/M+S phase, with increased expression of the cell cycle-related proteins, cyclin A, D, and E, and enhanced cell proliferation. In addition, the Transwell migration assay confirmed that the downregulation of ANRIL expression increased the migration of PASMCs under hypoxic conditions (25). A novel LncRNA TCONS_00034812 expression was significantly downregulated in PAH rats and hypoxic pulmonary artery SMCs. LncRNA TCONS_00034812 knockdown similarly increased the percentage of G2/M+S phase cells in PASMCs, ultimately leading to thickening of the pulmonary vascular mesoderm. Storkhead box 1 (STOX1) factor is a downstream lncRNA TCONS_00034812 target, and lncRNA TCONS_00034812 negatively regulates STOX1 to affect the proliferation of PASMCs (78). LncRNA Rps4l expression was downregulated in both hypoxia-induced PH tissues and PASMCs, and hypoxia increased the proportion of cells in the G2/M+S phase. In contrast, overexpression of lncRNA Rps4l inhibited the proliferation of PASMCs and attenuated hypoxia-induced cell cycle progression, causing PASMCs to stagnate in the G0/G1 phase. The increased expression levels of cyclins A, D, and E under hypoxic conditions were reversed by overexpression of lncRNA Rps4l. Upregulation of lncRNA Rps4l expression results in a significant reduction in the migratory capacity of PASMCs under hypoxic conditions by regulating the interleukin enhancer-binding factor 3 (ILF3)/HIF-1α axis (79). The expression of LncRNA AC068039.4, which functions in the same way, is significantly upregulated in hypoxia-induced PASMCs, and knockdown of lncRNA AC068039.4 reduced hypoxia-induced G2/M and S-phase cell percentages and attenuated PASMCs proliferation and migration. LncRNA AC068039.4 also binds miR-26a-5p through the ceRNA pattern to regulate the downstream target gene transient receptor potential canonical 6 (TRPC6) to promote PASMCs proliferation, migration, and cell cycle progression, thereby promoting pulmonary vascular remodeling (80).

The smad pathway is important for the vascular development and differentiation of VSMCs, which requires the phosphorylation of smad transcription factors for its subsequent nuclear translocation, DNA binding, and eventual transcriptional activation. Investigators found that the downregulation of lncRNA MYOSLID attenuates TGF-β1-induced Smad2 phosphorylation, disrupts F-actin formation, and blocks TGF-β1-induced megakaryoblastic leukemia 1 [MKL1) nuclear translocation, suggesting that lncRNA MYOSLID plays a key role in SMAD activation and subsequent transcription of VSMCs, and this study shows that lncRNA MYOSLID promotes the expression of contractile markers by inhibiting the proliferation and migration of VSMCs, but its effect on contractile gene expression in VSMCs is cellular context-dependent and may be restricted to VSMCs (81).

In hypoxia-treated PASMCs and PAH patient sera, investigators found a higher expression level of lncRNA NEAT1, which targets miR-34a-5p, while miR-34a-5p targets KLF4. Hypoxia significantly decreased αSMA and caspase-3 expression and increased PCNA and MMP-2 levels. In contrast, the knockdown of lncRNA NEAT1 reversed these alterations by the adsorption of miR-34a-5p and downregulation of KLF4, thereby slowing the progression of PAH (76).

LncRNA UCA1 was overexpressed in hypoxic HPASMCs, and overexpression of the inhibitor of growth proteins5 (ING5) reduced PCNA expression, inhibited cell viability, and promoted apoptosis in hypoxic HPASMCs, which was reversed by lncRNA UCA1 overexpression. LncRNA UCA1 competes with ING5 for heterogeneous nuclear ribonucleoprotein I, a protein that binds RNA and splice mRNA, and promotes proliferation and inhibit apoptosis (66). In PASMCs of hypoxia-induced rats, the expression of lncRNA CASC2 was significantly reduced and the expression of phenotypic transition markers troponin and α-SMA was reduced, while the amount of syndecan-1 and PCNA was significantly increased, and overexpression of lncRNA CASC2 resulted in opposite changes in the above markers. Therefore, overexpression of lncRNA CASC2 alleviated hypoxia-induced cell proliferation and migration, thereby regulating phenotype transition in PASMCs to partially restore hypoxia (51).

LncRNA and aneurysm

Aortic aneurysms are usually defined as localized dilatations larger than 50% of the normal diameter and can occur in the thorax, but have the highest incidence in the abdominal aorta (95). Many inflammatory factors, such as CC chemokine ligand 2 (CCL2), IL-6, IL-1β, and TNFα, induce a chronic inflammatory response, inflammatory cell infiltration accompanied by elastin disruption and degeneration, and loss of mesangial SMCs. The pathophysiological process of aortic aneurysms is characterized by inflammatory cell infiltration, elastic and collagen fiber degradation, smooth muscle cell death, arterial wall defects, and increased oxidative stress (96). There is growing evidence that lncRNA promotes the proliferation of VSMCs or inhibiting apoptosis can prevent aneurysm progression.

In the thoracic aortic tissue of patients with aortic dissection (AD), lncRNA H19 was highly expressed, which competitively bound and inhibited the expression of miR-193b-3p. Upon

PDGF-BB induction, the expression of lncRNA H19, MMP-2, and MMP-9 was upregulated; the expression of miR-193b-3p, α-SMA, and SM22α was downregulated; and the proliferation and migration rates of HASMCs were increased. However, silencing lncRNA H19 reversed the change induced by PDGF-BB. These results were consistently validated in animal experiments, indicating that silencing lncRNA H19 significantly attenuated PDGF-BB-induced proliferation and migration of HASMCs through the upregulation of miR-193b-3p, thereby reducing pathological injury in the thoracic aorta of AD mice (43). LncRNA X-inactive-specific transcript (XIST] is upregulated in the aortic wall tissue of patients with Stanford type A aortic dissection (TAAD) and correlates with the prognosis of TAAD. Knockdown of lncRNA XIST regulates downstream PTEN by inhibiting miR-17, which increases PCNA expression, accelerates Bcl-2 expression, and suppresses the levels of Bax and caspase-3, thereby promoting VSMC proliferation and inhibiting apoptosis to slow TAAD progression (49). Tissues near endothelial tears in patients with AD were proliferating; the expression of linc01278 and ACTG2 was downregulated; miR-500b-5p expression was upregulated; VSMC differentiation markers SMA, SM22α, calponin, and MYH11 were decreased. Silencing linc01278 targeted miR-500b-5p and ACTG2 in the three untranslated regions decreased the expression of SMA, SM22α, calponin, and MYH1; promoted the phenotypic conversion of aortic VSMCs from contractile to synthetic phenotypes; and promoted VSMC proliferation and migration. Thus, the linc01278/miR-500b-5p/ACTG2 axis may provide novel molecular mechanisms for diagnostic markers and therapeutic targets of AD (82). In AD, another lncRNA, PVT1 expression was upregulated, while the downregulation of lncRNA plasmacytoma variant translocation 1 (PVT1) expression led to an increase in α-SMA and SM22α expression and decreased MMP-2 and MMP-9 expression by targeting miR-27b-3p, which inhibited phenotypic transition and suppressed proliferation and migration in PDGF-BB-treated HASMCs (83).

In SMCs, the lncRNA lung cancer-associated transcript 1 (LUCAT1) exhibits anti-proliferative and pro-apoptotic effects, and knockdown of LUCAT1 leads to decreased caspase-3 activity and recovery after myelin regulatory factor (MYRF) overexpression. LUCAT1 acts as a decoy for miR-199a-5p and promotes MYRF expression, and lncRNA LUCAT1/miR-199a-5p/MYRF regulates the proliferation and apoptosis of SMCs in abdominal aortic aneurysms (85). In abdominal aortic aneurysm (AAA) tissues, lncRNA PVT1, and NCK-associated protein 1-like (NCKAP1L) expression was elevated and induced *in vitro* in AAA models, while miR-3127-5p showed the opposite trend, and lncRNA PVT1 acted as a sponge for miR-3127-5p to regulate NCKAP1L expression, inhibit VSMC proliferation, and induce apoptosis (84). In contrast, in AAA tissue, lncRNA SNHG5 was downregulated; overexpression of lncRNA SNHG5 could act as a molecular sponge for miR-205-5p and downregulate its expression, but upregulate the expression of SMAD4, thus increasing proliferation and migration and decreasing apoptosis in abdominal aortic aneurysm VSMCs (86). Another study found that H_2O_2 inhibited the activity of VSMCs, thus mimicking the AAA model. After H_2O_2 treatment, LINC00473 expression was upregulated, Bax expression was enhanced, and Bcl-2 expression was decreased. In AAA, brain acid-soluble protein 1 (BASP1) expression was inversely correlated with miR-212-5p expression but positively correlated with LINC00473 levels. These results suggest that LINC00473 competitively interacts with miR-212-5p to promote BASP1 expression and VSMC apoptosis, ultimately leading to AAA exacerbation (87). In AAA tissues and AngII-stimulated VSMCs, the expression of lncRNA CRNDE was downregulated, and the data suggest that overexpression of lncRNA CRNDE can promote VSMC proliferation and inhibit apoptosis by upregulating Bcl-3 ubiquitination of Smad3 protein and upregulating smad3 expression, thereby inhibiting mouse AAA growth (74).

Conclusion and perspectives

LncRNAs are relatively newly discovered RNA molecules with important regulatory functions. These findings suggest that lncRNAs may have profound effects on the regulation of VSMCs and are regulators of gene expression and vascular function. Although our knowledge of lncRNAs is limited, their emergence may further our understanding of the complex regulatory network of cellular function in clinical vascular diseases. Targeting lncRNAs may be an extremely promising modality of governance not only in tumors but also in cardiac or vascular diseases, and thus, they are regulators of smooth muscle cell phenotypic transition.

Author contributions

B-HL and H-BL: original draft writing and manuscript revision. D-XL and Z-GC: manuscript revision. S-XG and JZ: graphic design. G-AZ and FL: manuscript design and revision.

Funding

This work was supported by the Research Projects of Higher Education Institutions in Henan Province of China (Nos: 21A320012 and 22A360017), Key Specialized Research and Development Breakthrough in Henan Province of China (Nos: 212102310350, 222102310442, and 222102310631), Graduate Student Research Innovation Support Program of Xinxiang Medical University in Henan Province of China (YJSCX202174Y), and The First Affiliated Hospital of

Xinxiang Medical University Youth Foundation (Grant Nos. QN-2017-B026 and QN-2021-B15).

Acknowledgments

We would like to thank Editage (www.editage.cn) for English language editing.

Conflict of interest

The authors declare that the research was conducted in the absence of any commercial or financial relationships that could be construed as a potential conflict of interest.

Publisher's note

All claims expressed in this article are solely those of the authors and do not necessarily represent those of their affiliated organizations, or those of the publisher, the editors and the reviewers. Any product that may be evaluated in this article, or claim that may be made by its manufacturer, is not guaranteed or endorsed by the publisher.

References

1. Brunner AL, Beck AH, Edris B, Sweeney RT, Zhu SX, Li R, et al. Transcriptional profiling of long non-coding RNAs and novel transcribed regions across a diverse panel of archived human cancers. *Genome Biol.* (2012) 13:1–13. doi: 10.1186/gb-2012-13-8-r75

2. Scheuermann JC, Boyer LA. Getting to the heart of the matter: long non-coding RNAs in cardiac development and disease. *EMBO J.* (2013) 32:1805–16. doi: 10.1038/emboj.2013.134

3. Herring BP, Hoggatt AM, Burlak C, Offermanns S. Previously differentiated medial vascular smooth muscle cells contribute to neointima formation following vascular injury. *Vasc Cell.* (2014) 6:21. doi: 10.1186/2045-824X-6-21

4. Shi N, Chen SY. Mechanisms simultaneously regulate smooth muscle proliferation and differentiation. *J Biomed Res.* (2014) 28:40–46. doi: 10.7555/JBR.28.20130130

5. Uchida S, Dimmeler S. Long non-coding RNAs in cardiovascular diseases. *Circ Res.* (2015) 116:737–50. doi: 10.1161/CIRCRESAHA.116.302521

6. Leeper NJ, Maegdefessel L. Non-coding RNAs: key regulators of smooth muscle cell fate in vascular disease. *Cardiovasc Res.* (2018) 114:611–21. doi: 10.1093/cvr/cvx249

7. Basatemur GL, Jørgensen HF, Clarke MCH, Bennett MR, Mallat Z. Vascular smooth muscle cells in atherosclerosis. *Nat Rev Cardiol.* (2019) 16:727–44. doi: 10.1038/s41569-019-0227-9

8. Dobnikar L, Taylor AL, Chappell J, Oldach P, Harman JL, Oerton E, et al. Disease-relevant transcriptional signatures identified in individual smooth muscle cells from healthy mouse vessels. *Nat Commun.* (2018) 9:4567. doi: 10.1038/s41467-018-06891-x

9. Wang G, Jacquet L, Karamariti E, Xu Q. Origin and differentiation of vascular smooth muscle cells. *J Physiol.* (2015) 593:3013–30. doi: 10.1113/JP270033

10. Allahverdian S, Chaabane C, Boukais K, Francis GA, Bochaton-Piallat ML. Smooth muscle cell fate and plasticity in atherosclerosis. *Cardiovasc Res.* (2018)**0.1**14:540–50. doi: 10.1093/cvr/cvy022

11. Wang KC, Chang HY. Molecular mechanisms of long noncoding RNAs. *Mol Cell.* (2011) 43:904–14. doi: 10.1016/j.molcel.2011.08.018

12. Jian L, Jian D, Chen Q, Zhang L. Long Noncoding RNAs in Atherosclerosis. *J Atheroscler Thromb.* (2016) 23:376–84. doi: 10.5551/jat.33167

13. Kallen AN, Zhou XB, Xu J, Qiao C, Ma J, Yan L, et al. The imprinted H19 lncRNA antagonizes let-7 microRNAs. *Mol Cell.* (2013) 52:101–12. doi: 10.1016/j.molcel.2013.08.027

14. Ferre F, Colantoni A, Helmer-Citterich M. Revealing protein-lncRNA interaction. *Brief Bioinform.* (2016)17:106–16. doi: 10.1093/bib/bbv031

15. Imig J, Brunschweiger A, Brümmer A, Guennewig B, Mittal N, Kishore S, et al. miR-CLIP capture of a miRNA targetome uncovers a lincRNA H19-miR-106a interaction. *Nat Chem Biol.* (2015) 11:107–14. doi: 10.1038/nchembio.1713

16. Kung JTY, Colognori D, Lee JT. Long noncoding RNAs: past, present, and future. *Genetics.* (2013) 193:651–69. doi: 10.1534/genetics.112.146704

17. Deng L, Bradshaw AC, Baker AH. Role of non-coding RNA in vascular remodelling. *Curr Opin Lipidol.* (2016) 27:439–48. doi: 10.1097/MOL.0000000000000336

18. Miano JM, Long X. The short and long of noncoding sequences in the control of vascular cell phenotypes. *Cell Mol Life Sci.* (2015) 72:3457–88. doi: 10.1007/s00018-015-1936-9

19. Zhang M, He J, Jiang C, Zhang W, Yang Y, Wang Z, et al. Plaque-hyaluronidase-responsive high-density-lipoprotein-mimetic nanoparticles for multistage intimal-macrophage-targeted drug delivery and enhanced anti-atherosclerotic therapy. *Int J Nanomed.* (2017) 12:533–58. doi: 10.2147/IJN.S124252

20. Ballantyne MD, Pinel K, Dakin R, Vesey AT, Diver L, Mackenzie R, et al. Smooth Muscle Enriched Long Non-coding RNA (SMILR) regulates cell proliferation. *Circulation.* (2016) 133:2050–65. doi: 10.1161/CIRCULATIONAHA.115.021019

21. Wu G, Cai J, Han Y, Chen J, Huang ZP, Chen C, et al. LincRNA-p21 regulates neointima formation, vascular smooth muscle cell proliferation, apoptosis, and atherosclerosis by enhancing p53 activity. *Circulation.* (2014) 130:1452–65. doi: 10.1161/res.115.suppl_1.32

22. Wang H, He F, Liang B, Jing Y, Zhang P, Liu W, et al. p53-dependent LincRNA-p21 protects against proliferation and anti-apoptosis of vascular smooth muscle cells in atherosclerosis by upregulating SIRT7 *via* microRNA-17-5p. *J Cardiovasc Transl Res.* (2021) 14:426–40. doi: 10.1007/s12265-020-10074-9

23. Zhang C, Ge S, Gong W, Xu J, Guo Z, Liu Z, et al. LncRNA ANRIL acts as a modular scaffold of WDR5 and HDAC3 complexes and promotes alteration of the vascular smooth muscle cell phenotype. *Cell Death Dis.* (2020) 11:435. doi: 10.1038/s41419-020-2645-3

24. Li J, Chen J, Zhang F, Li J, An S, Cheng M, et al. LncRNA CDKN2B-AS1 hinders the proliferation and facilitates apoptosis of ox-LDL-induced vascular smooth muscle cells via the ceRNA network of CDKN2B-AS1/miR-126-5p/PTPN7. *Int J Cardiol.* (2021) 340:79–87. doi: 10.1016/j.ijcard.2021.08.009

25. Wang S, Zhang C, Zhang X. Downregulation of long non-coding RNA ANRIL promotes proliferation and migration in hypoxic human pulmonary artery smooth muscle cells. *Mol Med Rep.* (2020) 21:589–96. doi: 10.3892/mmr.2019.10887

26. Lu YB, Shi C, Yang B, Lu ZF, Wu YL, Zhang RY, et al. Long non-coding RNA ZNF800 suppresses proliferation and migration of vascular smooth muscle cells by upregulating PTEN and inhibiting AKT/mTOR/HIF-1α signaling. *Atherosclerosis.* (2020) 312:43–53. doi: 10.1016/j.atherosclerosis.2020.09.007

27. Fasolo F, Jin H, Winski G, Chernogubova E, Pauli J, Winter H, et al. Long non-coding rna controls advanced atherosclerotic lesion formation and plaque destabilization. *Circulation.* (2021) 144:1567–83. doi: 10.1161/CIRCULATIONAHA.120.052023

28. Ma G, Bi S, Zhang P. Long non-coding RNA MIAT regulates ox-LDL-induced cell proliferation, migration and invasion by miR-641/STIM1 axis in human vascular smooth muscle cells. *BMC Cardiovasc Disord.* (2021) 21:248. doi: 10.1186/s12872-021-02048-9

29. Cui C, Wang X, Shang XM, Li L, Ma Y, Zhao GY, et al. lncRNA 430945 promotes the proliferation and migration of vascular smooth muscle cells via the ROR2/RhoA signaling pathway in atherosclerosis. *Mol Med Rep*. (2019) 19:4663–72. doi: 10.3892/mmr.2019.10137

30. Jiang X, Liu Z, Qi X. LncRNA BANCR induced vascular smooth muscle cell proliferation by downregulating miR-34c methylation in atherosclerosis. *J Thromb Thrombolysis*. (2021) 51:924–32. doi: 10.1007/s11239-020-02314-1

31. Wu Y, Cai F, Lu Y, Hu Y, Wang Q. lncRNA RP11-531A243 inhibits the migration and proliferation of vascular smooth muscle cells by downregulating ANXA2 expression. *Exp Ther Med*. (2021) 22:1439. doi: 10.3892/etm.2021.10874

32. Onuh JO, Qiu H. Serum response factor-cofactor interactions and their implications in disease. *FEBS J*. (2021) 288:3120–34. doi: 10.1111/febs.15544

33. Miano JM. Myocardin in biology and disease. *J Biomed Res*. (2015) 29:3–19. doi: 10.7555/JBR.29.20140151

34. Dong K, Shen J, He X, Hu G, Wang L, Osman I, et al. Is an Evolutionarily Conserved Smooth Muscle Cell-Specific LncRNA That Maintains Contractile Phenotype by Binding Myocardin. *Circulation*. (2021) 144:1856–75. doi: 10.1161/CIRCULATIONAHA.121.055949

35. He X, Lian Z, Yang Y, Wang Z, Fu X, Liu Y, et al. Long non-coding RNA PEBP1P2 Suppresses Proliferative VSMCs Phenotypic Switching and Proliferation in Atherosclerosis. *Mol Ther Nucleic Acids*. (2020) 22:84–98. doi: 10.1016/j.omtn.2020.08.013

36. Hung J, Miscianinov V, Sluimer JC, Newby DE, Baker AH. Targeting non-coding RNA in vascular biology and disease. *Front Physiol*. (2018) 9:1655. doi: 10.3389/fphys.2018.01655

37. Wang X, Li D, Chen H, Wei X, Xu X. Expression of long non-coding RNA LIPCAR promotes cell proliferation, cell migration, and change in phenotype of vascular smooth muscle cells. *Med Sci Monit*. (2019) 25:7645–51. doi: 10.12659/MSM.915681

38. Cai X, Cullen BR. The imprinted H19 non-coding RNA is a primary microRNA precursor. *RNA*. (2007) 13:313–6. doi: 10.1261/rna.351707

39. Sun H, Jiang Q, Sheng L, Cui K. Downregulation of lncRNA H19 alleviates atherosclerosis through inducing the apoptosis of vascular smooth muscle cells. *Mol Med Rep*. (2020) 22:3095–102. doi: 10.3892/mmr.2020.11394

40. Lu G, Chu Y, Tian P. Knockdown of H19 Attenuates Ox-LDL-induced vascular smooth muscle cell proliferation, migration, and invasion by regulating miR-599/PAPPA axis. *J Cardiovasc Pharmacol*. (2021) 77:386–96. doi: 10.1097/FJC.0000000000000959

41. Zhang L, Cheng H, Yue Y, Li S, Zhang D, He R, et al. H19 knockdown suppresses proliferation and induces apoptosis by regulating miR-148b/WNT/β-catenin in ox-LDL -stimulated vascular smooth muscle cells. *J Biomed Sci*. (2018) 25:11. doi: 10.1186/s12929-018-0418-4

42. Lv J, Wang L, Zhang J, Lin R, Wang L, Sun W, et al. Long noncoding RNA H19-derived miR-675 aggravates restenosis by targeting PTEN. *Biochem Biophys Res Commun*. (2018) 497:1154–61. doi: 10.1016/j.bbrc.2017.01.011

43. Ren M, Wang T, Wei X, Wang Y, Ouyang C, Xie Y, et al. LncRNA H19 regulates smooth muscle cell functions and participates in the development of aortic dissection through sponging miR-193b-3p. *Biosci Rep*. (2021) 41. doi: 10.1042/BSR20202298

44. Zhang RY, Wu CM, Hu XM, Lin XM, Hua YN, Chen JJ, et al. LncRNA AC105942.1 downregulates hnRNPA2/B1 to attenuate vascular smooth muscle cells proliferation. *DNA Cell Biol*. (2021) 40:652–61. doi: 10.1089/dna.2020.6451

45. Li FP, Lin DQ, Gao LY. LncRNA TUG1 promotes proliferation of vascular smooth muscle cell and atherosclerosis through regulating miRNA-21/PTEN axis. *Eur Rev Med Pharmacol Sci*. (2018) 22:7439–47. doi: 10.26355/eurrev_201811_16284

46. Wang YQ, Xu ZM, Wang XL, Zheng JK, Du Q, Yang JX, et al. LncRNA FOXC2-AS1 regulated proliferation and apoptosis of vascular smooth muscle cell through targeting miR-1253/FOXF1 axis in atherosclerosis. *Eur Rev Med Pharmacol Sci*. (2020) 24:3302–14.

47. Liu Y, Cui X, Wang C, Zhao S. LncRNA HCG11 regulates proliferation and apoptosis of vascular smooth muscle cell through targeting miR-144-3p/FOXF1 axis in atherosclerosis. *Biol Res*. (2020) 53:44. doi: 10.1186/s40659-020-00306-2

48. Wang Y, Zhang CX, Ge SL, Gong WH. CTBP1-AS2 inhibits proliferation and induces autophagy in ox-LDL-stimulated vascular smooth muscle cells by regulating miR-195-5p/ATG14. *Int J Mol Med*. (2020) 46:839–48. doi: 10.3892/ijmm.2020.4624

49. Zhang X, Wu H, Mai C, Qi Y. Long non-coding RNA XIST/miR-17/PTEN axis modulates the proliferation and apoptosis of vascular smooth muscle cells to affect stanford Type A aortic dissection. *J Cardiovasc Pharmacol*. (2020) 76:53–62. doi: 10.1097/FJC.0000000000000835

50. Wang C, Zhao J, Nan X, Guo Z, Huang S, Wang X, et al. Long noncoding RNA CASC2 inhibits ox-LDL-mediated vascular smooth muscle cells proliferation and migration via the regulation of miR-532-3p/PAPD5. *Mol Med*. (2020) 26:74. doi: 10.1186/s10020-020-00200-3

51. Gong J, Chen Z, Chen Y, Lv H, Lu H, Yan F, et al. Long non-coding RNA CASC2 suppresses pulmonary artery smooth muscle cell proliferation and phenotypic switch in hypoxia-induced pulmonary hypertension. *Respir Res*. (2019) 20:53. doi: 10.1186/s12931-019-1018-x

52. Wang M, Li C, Zhang Y, Zhou X, Liu Y, Lu C, et al. LncRNA MEG3-derived miR-361-5p regulate vascular smooth muscle cells proliferation and apoptosis by targeting ABCA1. *Am J Transl Res*. (2019) 11:3600–9.

53. Zhang B, Dong Y, Zhao Z. LncRNA MEG8 regulates vascular smooth muscle cell proliferation, migration and apoptosis by targeting PPARα. *Biochem Biophys Res Commun*. (2019) 510:171–6. doi: 10.1016/j.bbrc.2019.01.074

54. Xu D, Dai R, Chi H, Ge W, Rong J. Long non-coding RNA MEG8 suppresses hypoxia-induced excessive proliferation, migration and inflammation of vascular smooth muscle cells by regulation of the miR-195-5p/RECK axis. *Front Mol Biosci*. (2021) 8:697273. doi: 10.3389/fmolb.2021.697273

55. Cheng C, Xu BL, Sheng JL, He F, Yang T, Shen SC, et al. LncRNA MALAT1 regulates proliferation and apoptosis of vascular smooth muscle cells by targeting miRNA-124-3p/PPARα axis. *Eur Rev Med Pharmacol Sci*. (2019) 23:9025–32.

56. Zheng J, Tan Q, Chen H, Chen K, Wang H, Chen Z, et al. lncRNA-SNHG7-003 inhibits the proliferation, migration and invasion of vascular smooth muscle cells by targeting the miR-1306-5p/SIRT7 signaling pathway. *Int J Mol Med*. (2021) 47:741–50. doi: 10.3892/ijmm.2020.4821

57. Wang H, Jin Z, Pei T, Song W, Gong Y, Chen D, et al. Long non-coding RNAs C2dat1 enhances vascular smooth muscle cell proliferation and migration by targeting MiR-34a-5p. *J Cell Biochem*. (2019) 120:3001–8. doi: 10.1002/jcb.27070

58. Liu W, Che J, Gu Y, Song L, Jiao Y, Yu S, et al. Silencing of lncRNA SNHG12 inhibits proliferation and migration of vascular smooth muscle cells via targeting miR-766-5p/EIF5A axis. *Adv Clin Exp Med*. (2021) 30:591–8. doi: 10.1007/978-981-16-0267-2

59. Sun Y, Zhao JT, Chi BJ, Wang KF. Long non-coding RNA SNHG12 promotes vascular smooth muscle cell proliferation and migration via regulating miR-199a-5p/HIF-1α. *Cell Biol Int*. (2020) 44:1714–26. doi: 10.1002/cbin.11365

60. Zhang L, Zhou C, Qin Q, Liu Z, Li P. LncRNA LEF1-AS1 regulates the migration and proliferation of vascular smooth muscle cells by targeting miR-544a/PTEN axis. *J Cell Biochem*. (2019) 120:14670–8. doi: 10.1002/jcb.28728

61. Weng G, Gu M, Zhang Y, Zhao G, Gu Y. LINC01123 promotes cell proliferation and migration *via* regulating miR-1277-5p/KLF5 axis in ox-LDL-induced vascular smooth muscle cells. *J Mol Histol*. (2021) 52:943–53. doi: 10.1007/s10735-021-10010-4

62. Liu X, Ma BD, Liu S, Liu J, Ma BX. Long noncoding RNA LINC00341 promotes the vascular smooth muscle cells proliferation and migration via miR-214/FOXO4 feedback loop. *Am J Transl Res*. (2019) 11:1835–42.

63. Zhong JY, Cui XJ, Zhan JK, Wang YJ, Li S, Lin X, et al. LncRNA-ES3 inhibition by Bhlhe40 is involved in high glucose-induced calcification/senescence of vascular smooth muscle cells. *Ann N Y Acad Sci U.S.A*. (2020) 1474:61–72. doi: 10.1111/nyas.14381

64. Li Y, Xi Z, Yu Z, Yang C, Tan C. LincRNA-EPS increases TGF-β expression to inhibit the Wnt/β-catenin pathway, VSMC osteoblastic differentiation and vascular calcification in diabetic mice. *Exp Ther Med*. (2022) 23:425. doi: 10.3892/etm.2022.11352

65. Yang JL, Han NH. LncRNA UCA1 stimulates the repair of hyperglycemic vascular smooth muscle cells through targeting miR-582-5p. *Eur Rev Med Pharmacol Sci*. (2020) 24:12859–66. doi: 10.26355/eurrev_202012_24188

66. Zhu TT, Sun RL, Yin YL, Quan JP, Song P, Xu J, et al. Long noncoding RNA UCA1 promotes the proliferation of hypoxic human pulmonary artery smooth muscle cells. *Pflugers Arch*. (2019) 471:347–55. doi: 10.1007/s00424-018-2219-8

67. Lu Y, Guo J, Zhu S, Zhang H, Zhu Q, Li Y, et al. LncRNA HCG18 is critical for vascular smooth muscle cell proliferation and phenotypic switching. *Hum Cell*. (2020) 33:537–44. doi: 10.1007/s13577-020-00366-2

68. Liu K, Liu C, Zhang Z. lncRNA GAS5 acts as a ceRNA for miR-21 in suppressing PDGF-bb-induced proliferation and migration in vascular smooth muscle cells. *J Cell Biochem*. (2019) 120:15233–40. doi: 10.1002/jcb.28789

69. Tang R, Mei X, Wang YC, Cui XB, Zhang G, Li W, et al. LncRNA GAS5 regulates vascular smooth muscle cell cycle arrest and apoptosis via p53 pathway. *Biochim Biophys Acta Mol Basis Dis*. (2019) 1865:2516–25. doi: 10.1016/j.bbadis.2019.05.022

70. Fang G, Qi J, Huang L, Zhao X. LncRNA MRAK048635_P1 is critical for vascular smooth muscle cell function and phenotypic switching in essential hypertension. *Biosci Rep*. (2019) 39. doi: 10.1042/BSR20182229

71. Jin L, Lin X, Yang L, Fan X, Wang W, Li S, et al. AK098656 a novel vascular smooth muscle cell-dominant long non-coding RNA, promotes hypertension. *Hypertension*. (2018) 71:262–72. doi: 10.1161/HYPERTENSIONAHA.117.09651

72. Ma H, Dong A. Long non-coding RNA cyclin-dependent kinase inhibitor 2B antisense ribonucleic acid 1 is associated with in-stent restenosis and promotes human carotid artery smooth muscle cell proliferation and migration by sponging miR-143-3p. *Exp Ther Med*. (2021) 21:234. doi: 10.3892/etm.2021.9665

73. Zhou Y, He X, Liu R, Qin Y, Wang S, Yao X, et al. LncRNA CRNDE regulates the proliferation and migration of vascular smooth muscle cells. *J Cell Physiol*. (2019) 23:16205-14 doi: 10.1002/jcp.28284

74. Li K, Cui M, Zhang K, Wang G, Zhai S. LncRNA CRNDE affects the proliferation and apoptosis of vascular smooth muscle cells in abdominal aortic aneurysms by regulating the expression of Smad3 by Bcl-3. *Cell Cycle*. (2020) 19:1036–47. doi: 10.1080/15384101.2020.1743915

75. Ahmed ASI, Dong K, Liu J, Wen T, Yu L, Xu F, et al. Long noncoding RNA (nuclear paraspeckle assembly transcript 1) is critical for phenotypic switching of vascular smooth muscle cells. *Proc Natl Acad Sci U.S.A*. (2018) 115:E8660–7. doi: 10.1073/pnas.1803725115

76. Dou X, Ma Y, Qin Y, Dong Q, Zhang S, Tian R, et al. NEAT1 silencing alleviates pulmonary arterial smooth muscle cell migration and proliferation under hypoxia through regulation of miR-34a-5p/KLF4. *Mol Med Rep*. (2021) 24. doi: 10.3892/mmr.2021.12389

77. Zhang H, Liu Y, Yan L, Wang S, Zhang M, Ma C, et al. Long noncoding RNA Hoxaas3 contributes to hypoxia-induced pulmonary artery smooth muscle cell proliferation. *Cardiovasc Res*. (2019) 115:647–57. doi: 10.1093/cvr/cvy250

78. Liu Y, Sun Z, Zhu J, Xiao B, Dong J, Li X, et al. LncRNA-TCONS_00034812 in cell proliferation and apoptosis of pulmonary artery smooth muscle cells and its mechanism. *J Cell Physiol*. (2018) 233:4801–14. doi: 10.1002/jcp.26279

79. Liu Y, Zhang H, Li Y, Yan L, Du W, Wang S, et al. Long non-coding RNA Rps4l mediates the proliferation of hypoxic pulmonary artery smooth muscle cells. *Hypertension*. (2020) 76:1124–33. doi: 10.1161/HYPERTENSIONAHA.120.14644

80. Qin Y, Zhu B, Li L, Wang D, Qiao Y, Liu B, et al. Overexpressed lncRNA AC068039.4 contributes to proliferation and cell cycle progression of pulmonary artery smooth muscle cells *via* sponging miR-26a-5p/TRPC6 in hypoxic pulmonary arterial hypertension. *Shock*. (2021) 55:244–55. doi: 10.1097/SHK.0000000000001606

81. Zhao J, Zhang W, Lin M, Wu W, Jiang P, Tou E, et al. MYOSLID Is a Novel Serum Response Factor-Dependent Long Noncoding RNA That Amplifies the Vascular Smooth Muscle Differentiation Program. *Arterioscler Thromb Vasc Biol*. (2016) 36:2088–99. doi: 10.1161/ATVBAHA.116.307879

82. Wang W, Liu Q, Wang Y, Piao H, Zhu Z, Li D, et al. LINC01278 Sponges miR-500b-5p to regulate the expression of ACTG2 to control phenotypic switching in human vascular smooth muscle cells during aortic dissection. *J Am Heart Assoc*. (2021) 10:e018062. doi: 10.1161/JAHA.120.018062

83. Li S, Zhao X, Cheng S, Li J, Bai X, Meng X, et al. Downregulating long non-coding RNA PVT1 expression inhibited the viability, migration and phenotypic switch of PDGF-BB-treated human aortic smooth muscle cells via targeting miR-27b-3p. *Hum Cell*. (2021) 34:335–48. doi: 10.1007/s13577-020-00452-5

84. Huang Y, Ren L, Li J, Zou H. Long non-coding RNA PVT1/microRNA miR-3127-5p/NCK-associated protein 1-like axis participates in the pathogenesis of abdominal aortic aneurysm by regulating vascular smooth muscle cells. *Bioengineered*. (2021) 12:12583–96. doi: 10.1080/21655979.2021.2010384

85. Xia Q, Zhang L, Yan H, Yu L, Shan W, Jiang H, et al. LUCAT1 contributes to MYRF-dependent smooth muscle cell apoptosis and may facilitate aneurysm formation via the sequestration of miR-199a-5p. *Cell Biol Int*. (2020) 44:755–63. doi: 10.1002/cbin.11270

86. Nie H, Zhao W, Wang S, Zhou W. Based on bioinformatics analysis lncrna SNHG5 modulates the function of vascular smooth muscle cells through mir-205-5p/SMAD4 in abdominal aortic aneurysm. *Immun Inflamm Dis*. (2021) 9:1306–20. doi: 10.1002/iid3.478

87. Tian Z, Sun Y, Sun X, Wang J, Jiang T. LINC00473 inhibits vascular smooth muscle cell viability to promote aneurysm formation via miR-212-5p/BASP1 axis. *Eur J Pharmacol*. (2020) 873:172935. doi: 10.1016/j.ejphar.2020.172935

88. Hu DJ, Li ZY, Zhu YT, Li CC. Overexpression of long noncoding RNA ANRIL inhibits phenotypic switching of vascular smooth muscle cells to prevent atherosclerotic plaque development. *Aging*. (2020) 13:4299–316. doi: 10.18632/aging.202392

89. Zhang Y, Tang Y, Yan J. LncRNA-XIST Promotes Proliferation and Migration in ox-LDL Stimulated Vascular Smooth Muscle Cells through miR-539-5p/SPP1 Axis. *Oxid Med Cell Longev*. (2022) 2022:9911982. doi: 10.1155/2022/9911982

90. Feng SD, Yang JH, Yao CH, Yang SS, Zhu ZM, Wu D, et al. Potential regulatory mechanisms of lncRNA in diabetes and its complications. *Biochem Cell Biol*. (2017) 95:361–7. doi: 10.1139/bcb-2016-0110

91. Shi J, Yang Y, Cheng A, Xu G, He F. Metabolism of vascular smooth muscle cells in vascular diseases. *Am J Physiol Heart Circ Physiol*. (2020) 319:H613–31. doi: 10.1152/ajpheart.00220.2020

92. Montezano AC, Nguyen Dinh Cat A, Rios FJ, Touyz RM. Angiotensin II and vascular injury. *Curr Hypertens Rep*. (2014) 16:431. doi: 10.1007/s11906-014-0431-2

93. Brown IA, Diederich L, Good ME, DeLalio LJ, Murphy SA, Cortese-Krott MM, et al. Vascular smooth muscle remodeling in conductive and resistance arteries in hypertension. *Arterioscler Thromb Vasc Biol*. (2018) 38:1969–85. doi: 10.1161/ATVBAHA.118.311229

94. Galie N, Hoeper MM, Humbert M, Torbicki A, Vachiery JL, Barbera JA, et al. 2015 ESC/ERS Guidelines for the diagnosis and treatment of pulmonary hypertension: the joint task force for the diagnosis and treatment of pulmonary hypertension of the European Society of Cardiology (ESC) and the European Respiratory Society (ERS): Endorsed by: association for European Paediatric and Congenital Cardiology (AEPC), International Society for Heart and Lung Transplantation (ISHLT). *Eur Heart J*. 37 doi: 10.1093/eurheartj/ehv317

95. Kuivaniemi H, Elmore JR. Opportunities in abdominal aortic aneurysm research: epidemiology, genetics, and pathophysiology. *Ann Vasc Surg*. (2012) 26:862–70. doi: 10.1016/j.avsg.2012.02.005

96. Shimizu K, Mitchell RN, Libby P. Inflammation and cellular immune responses in abdominal aortic aneurysms. *Arterioscler Thromb Vasc Biol*. (2006) 26:987–94. doi: 10.1161/01.ATV.0000214999.12921.4f

frontiers | Frontiers in Cardiovascular Medicine

TYPE Original Research
PUBLISHED 14 September 2022
DOI 10.3389/fcvm.2022.950961

OPEN ACCESS

EDITED BY
Mark Slevin,
Manchester Metropolitan University,
United Kingdom

REVIEWED BY
Ting Zhou,
University of Wisconsin-Madison,
United States
Matthew Dale Woolard,
Louisiana State University,
United States

*CORRESPONDENCE
Shijie Xin
xinsj@cmu1h.com

SPECIALTY SECTION
This article was submitted to Atherosclerosis and Vascular Medicine, a section of the journal Frontiers in Cardiovascular Medicine

RECEIVED 23 May 2022
ACCEPTED 25 August 2022
PUBLISHED 14 September 2022

CITATION
Cheng S, Liu Y, Jing Y, Jiang B, Wang D, Chu X, Jia L and Xin S (2022) Identification of key monocytes/macrophages related gene set of the early-stage abdominal aortic aneurysm by integrated bioinformatics analysis and experimental validation. *Front. Cardiovasc. Med.* 9:950961. doi: 10.3389/fcvm.2022.950961

Identification of key monocytes/macrophages related gene set of the early-stage abdominal aortic aneurysm by integrated bioinformatics analysis and experimental validation

Shuai Cheng[1,2,3], Yuanlin Liu[1,2,3], Yuchen Jing[1,2,3], Bo Jiang[1,2,3], Ding Wang[1,2,3], Xiangyu Chu[1,2,3], Longyuan Jia[1,2,3] and Shijie Xin[1,2,3]*

[1]Department of Vascular and Thyroid Surgery, The First Hospital, China Medical University, Shenyang, China, [2]Key Laboratory of Pathogenesis, Prevention, and Therapeutics of Aortic Aneurysm in Liaoning Province, Shenyang, China, [3]Regenerative Medicine Research Center of China Medical University, Shenyang, China

Objective: Abdominal aortic aneurysm (AAA) is a lethal peripheral vascular disease. Inflammatory immune cell infiltration is a central part of the pathogenesis of AAA. It's critical to investigate the molecular mechanisms underlying immune infiltration in early-stage AAA and look for a viable AAA marker.

Methods: In this study, we download several mRNA expression datasets and scRNA-seq datasets of the early-stage AAA models from the NCBI-GEO database. mMCP-counter and *CIBERSORT* were used to assess immune infiltration in early-stage experimental AAA. The scRNA-seq datasets were then utilized to analyze AAA-related gene modules of monocytes/macrophages infiltrated into the early-stage AAA by Weighted Correlation Network analysis (WGCNA). After that, Gene Ontology (GO) and Kyoto Encyclopedia of Genes and Genomes (KEGG) functional enrichment analysis for the module genes was performed by ClusterProfiler. The STRING database was used to create the protein-protein interaction (PPI) network. The Differentially Expressed Genes (DEGs) of the monocytes/macrophages were explored by Limma-Voom and the key gene set were identified. Then We further examined the expression of key genes in the human AAA dataset and built a logistic diagnostic model for distinguishing AAA patients and healthy people. Finally, real-time quantitative polymerase chain reaction (RT-qPCR) and Enzyme Linked Immunosorbent Assay (ELISA) were performed to validate the gene expression and serum protein level between the AAA and healthy donor samples in our cohort.

Results: Monocytes/macrophages were identified as the major immune cells infiltrating the early-stage experimental AAA. After pseudocell construction of monocytes/macrophages from scRNA-seq datasets and WGCNA analysis, four gene modules from two datasets were identified positively related to AAA, mainly enriched in Myeloid Leukocyte Migration, Collagen-Containing Extracellular matrix, and PI3K-Akt signaling pathway by functional enrichment analysis. *Thbs1*, *Clec4e*, and *Il1b* were identified as key genes among the hub genes in the modules, and the high expression of *Clec4e*, *Il1b*, and *Thbs1* was confirmed in the other datasets. Then, in human AAA transcriptome datasets, the high expression of *CLEC4E*, *IL1B* was confirmed and a logistic regression model based on the two gene expressions was built, with an AUC of 0.9 in the train set and 0.79 in the validated set. Additionally, in our cohort, we confirmed the increased serum protein levels of IL-1β and CLEC4E in AAA patients as well as the increased expression of these two genes in AAA aorta samples.

Conclusion: This study identified monocytes/macrophages as the main immune cells infiltrated into the early-stage AAA and constructed a logistic regression model based on monocytes/macrophages related gene set. This study could aid in the early diagnostic of AAA.

KEYWORDS

bioinformatics, abdominal aortic aneurysm, macrophage, single-cell RNA sequencing, WGCNA

Introduction

Abdominal aortic aneurysm (AAA) was defined as having diameters 1.5 times greater than normal (or which measure > 3 cm), which is a life-threatening aortic disease characterized by permanent, localized dilations of the abdominal aorta. AAA is an important cause of morbidity and mortality in developed countries (1). AAA rupture is a leading cause of death, an AAA might be asymptomatic until it ruptures (2). Early detection of AAA is therefore critical. Currently, ultrasonography is the most effective method of choice for early diagnosis of AAA (3). Given the cost-effectiveness of screening, the development of novel biomarkers for the detection of early AAA appears to be a viable future undertaking (4). In this context, understanding the molecular mechanism of early AAA pathogenesis is crucial.

Generally, apoptosis of smooth muscle cells, degradation of the extracellular matrix, infiltration of inflammatory cells, and increase of oxidative stress were considered to be central parts of AAA pathogenesis (5). With the deepening of research, growing evidence emerged indicating the invasion of diverse immune cells, such as macrophages, $CD4^+$ T cells, NK cells, and others, played a significant role in the development of AAA (6). Furthermore, the infiltration of immune cells into the aortic wall was discovered to occur early in the development of AAA (7). Understanding the process of immune infiltration is therefore critical for devising AAA medication therapy and developing early diagnostic methods.

Several animal models have been established in recent decades to examine the mechanisms involved in the formation and progression of AAA, and each animal model has its own benefits in reflecting distinct aspects of AAA (8). Angiotensin II infusion model, elastase perfusion model, and $CaCl_2$ perivascularly application model were the three most widely used AAA animal models as they were stable, easily accessible, and can reflect representative features of AAA pathogenesis, including early-stage inflammatory response and apoptosis of smooth muscle cells (9). Experimental animal models are of great significance for understanding the pathogenesis of early AAA.

With the advancement of high throughput sequencing technology, increasing amounts of biological data have been generated, and recently, scRNA-sequence was applied to study the mechanism of AAA progress, providing new insights into the disease's etiology (10). Based on the large scale of data and various bioinformatic methodologies, several studies investigated the differential gene expression pattern and immune infiltration pattern of AAA. However, few studies focus on the early stage of AAA growth. In the present study, we download several scRNA-seq datasets and

microarray datasets from the early stage of experimental AAA to screen for potential biomarkers by various bioinformatics analysis methods.

Materials and methods

Data collection and processing

In our study, we downloaded scRNA-seq dataset GSE152583, GSE164678, GSE166676 and mRNA expression dataset GSE51227, GSE109639, GSE17901, GSE57691, GSE47472 from Gene Expression Omnibus (GEO)[1] database. **Table 1** showed the details of the datasets used.

For datasets GSE152583 and GSE164678, R package "Seurat" v4.0 was used for quality control, normalization, CCA integration, and TSNE dimensional reduction. Cells were filtered out by nFeature_RNA < 200, nFeature_RNA > 4,000, nCount_RNA > 25,000, and percent. mt > 10. After dimensional reduction, marker genes for different cell types were used for cluster identification, and the marker genes used were consistent with the original publications (**Supplementary Figures 1A–D**). For GSE152583, data from days 0 and 7 samples were subset for further analysis. For dataset GSE166676, cells were filtered out by nFeature_RNA < 200, nFeature_RNA > 2,500, and percent.mt > 25. After dimensional reduction, we just examined the expression pattern of four genes using Featureplot function, and no further step was carried out.

For datasets GSE51227, GSE109639, GSE17091, GSE57691, and GSE47472, R package "Limma" was used for data normalization. Samples from AOD patients in GSE57691 were excluded as those samples were not relevant to the purpose of our study. Boxplots were generated to confirm the normalization effect by R package "ggplot2" (**Supplementary Figures 1E–G**).

Immune cell infiltration analysis

Two methods were used to evaluated the infiltration of immune cells. One was Microenvironment Cell Population counter (mMCP-counter), a method developed recently to quantify immune cell populations for the mouse, was employed to evaluate infiltration of immune cells for the mouse aorta samples by using R package "mMCPcounter" (11). The other method used was *CIBERSORT*, with a reference gene set came from ImmuCC (12, 13). Then the results were visualized by a box plot generated by R package "ggplot2."

The Weighted gene coexpression network analysis

R package "WGCNA" was used for the Weighted Gene coexpression Network Analysis of monocytes/macrophages populations from datasets GSE152583 and GSE164678. Firstly, monocytes/macrophages populations gene expression matrices were subset, and then we constructed pseudo cells by combining cells in the same sample and clusters. Ten cells were combined as one pseudo cell. After that, high variable genes were selected for further analysis.

Functional enrichment analysis and protein-protein interaction network construction

The R package "clusterProfiler" (version 4.0.2) was adopted for the Kyoto Encyclopedia of Genes and Genomes (KEGG) pathway enrichment analysis and Gene Ontology (GO) functional annotation to explore the biological functions of genes in the modules that were associated with the disease. By setting up cor.geneModuleMembership > 0.8 and cor.geneTraitSignificance > 0.4 for dataset GSE152583, cor.geneModuleMembership > 0.8 and cor.geneTraitSignificance > 0.3 for dataset GSE164678, hub gene in the modules were selected. Then the PPI network of hub genes was constructed by the STRING database[2] with a confidence score of 0.4, and the disconnected nodes in the network were hidden.

Differential gene expression analysis

According to previous comparative analysis, Limma-voom was an ideal method for DEG analysis of scRNA-seq data (14). Thus, the Differentially Expressed Genes (DEGs) of the monocytes/macrophages population in GSE152583 and GSE164678 datasets were explored by the Limma-voom method using R package "edgeR." $\log_2 |FC| \geq 1$ and $P < 0.05$ were set as cut-offs for GSE152583, while $FC \geq 1.3$, $FC \leq 0.7$ and $P < 0.05$ were set as cut-offs for GSE164678, and the results were visualized by volcano map using R package "ggscatter."

Logistic regression model

Multivariate logistic regression analysis was performed using the glm function in R package "stats." AAA samples and control samples were used as categorical responsive

1 https://www.ncbi.nlm.nih.gov/geo/

2 http://string-db.org

TABLE 1 Details of the datasets used in this study.

Dataset	Type	Platform	Sample species	Samples included and stage
GSE152583 (35)	scRNA-seq	Illumina HiSeq 4000	Mouse [Elastase-induced AAA model, peri-adventitial elastase incubation)]	Control (N = 1, 5 pooled aortas); AAA (N = 1, 5 pooled aortas, days 7 post induced)
GSE164678 (36)	scRNA-seq	Illumina NovaSeq 6000	Mouse ($CaCl_2$-induced AAA model)	Control (N = 1, 4 pooled aortas); AAA (N = 1, 4 pooled aortas, days 4 post induced)
GSE51227 (37)	Microarray	Agilent-028005 SurePrint G3 Mouse GE 8 × 60 K Microarray	Mouse (Elastase-induced AAA model, intraluminal perfusion)	Control (N = 5); AAA (N = 5, days 7 post induced)
GSE109639 (38)	Microarray		Mouse ($CaCl_2$-induced AAA model)	Control (N = 3); AAA (N = 3, days 7 post induced)
GSE17901 (39)	Microarray	Agilent-014868 Whole Mouse Genome Microarray 4 × 44K G4122F	Mouse (AngII-induced AAA model)	Control (N = 6); AAA (N = 7, days 7 post induced)
GSE166676 (10)	scRNA-seq	Illumina NovaSeq 6000	Human	Control (N = 2); AAA (N = 4)
GSE57691 (40)	Microarray	Illumina HumanHT-12 V4.0 expression bead chip	Human	Control (N = 10); AAA (N = 49)
GSE47472 (41)	Microarray		Human (AAA neck)	Control(N = 8); AAA (N = 14)

values, and gene expression values were used as continuous predictive variables. Visualization of logistic regression analysis by dynamic nomogram was constructed through R package "DynNom." Hosmer-Lemeshow goodness-of-fit test was used for calibration examination. Receiver operating characteristic (ROC) curve analysis was generated to evaluate the model to distinguish AAA and normal aorta samples by R package "pROC."

Sample collection

For the protein-specific enzyme-linked immunosorbent assay (ELISA), a total of 38 patients diagnosed as AAA and 18 age and gender matched healthy controls were enrolled in the study from the First Hospital of China Medical University. The diagnosis of all patients was confirmed by computed tomography angiography (CTA), The exclusion criteria included subjects with chronic aortic dissection, congenital heart disease, severe vascular stenosis, autoimmune diseases, infectious diseases, malignant tumors, hematological system diseases, previous aortic surgery or received non-steroidal anti-inflammatory drugs or steroids. Approximately 5 mL fasting blood sample was collected from each participant using standardized sterile tubes. All samples were centrifuged immediately at 3,000 r/min for 10 min at 4°C, and the serum was separated, and stored at −80°C until analysis.

For the mRNA expression detection, 10 patients diagnosed as AAA and 10 age and gender matched healthy controls were enrolled in the study. Fresh infrarenal AAA wall tissue samples were collected from patients undergoing open elective aneurysmectomy, and control infrarenal aortas were obtained from organ donors. All the aortic tissues were put into liquid nitrogen in 30 min after collection and stored at −80°C.

Written and informed consent to participate in this study was obtained from all subjects. The baseline characteristic data of the subject involved are presented in **Supplementary Table 1**. Ethical approval was obtained from the ethical committee of the hospital. The patients/participants provided their written informed consent to participate in this study.

Real-time quantitative polymerase chain reaction and enzyme linked immunosorbent assay

Aortic specimens were ground in liquid nitrogen, and *RNAiso Plus* reagent (Takara 9109, Shiga, Japan) was used to extract total RNAs, and the concentration and purity of total RNA were detected by a nanometer photometer (IMPLEN). After that, reverse transcription was performed using PrimeScript RT reagent Kit with gDNA Eraser (TaKaRa RR047A, Shiga, Japan). Real-time quantitative polymerase chain reaction (RT-qPCR) was conducted using TB Green® Premix Ex Taq (TaKaRa RR420A, Shiga, Japan) on an ABI Q3 7500 Real-Time PCR System (ABI). *ACTB* was used as internal controls, and the relative expression level of the target gene was calculated as $2-\Delta Ct$, where $-\Delta Ct$ = (Ct, target gene − Ct, *ACTB*). Statistical analysis was conducted with GraphPad Primer 8.0 (GraphPad Software Inc., GraphPad Prism 8.0.1.2). Primer sequences used in the study were listed in **Supplementary Table 3**.

IL-1β and CLEC4E concentrations in the serum were measured using a commercial ELISA kit according to the

manufacturer's instructions (#KET6013, EliKine Human IL-1β ELISA Kit; Abbkine Scientific Co., Ltd., Wuhan, China; # EK3805, Human C-type lectin domain family 4 member E ELISA Kit; Sabbiotech, College Park, MD, United States).

Statistical analyses

All statistical analyses were completed in the R language (Version 4.0.2). The continuous variables were presented as means ± standard deviations. The Shapiro-Wilk normality test was used to test whether the continuous variables conformed to a normal distribution. The Mann–Whitney *U*-test was used for pairwise comparison of data that did not followed a normal distribution, while the Student's *t*-test was used to evaluate normally distributed data. Correlation analyses were performed by the Spearman test and visualized by R package "corrplot." $P < 0.05$ was considered statistically significant.

Results

Monocytes/macrophages are the main infiltrating immune cells in the early stages of experimental abdominal aortic aneurysms

After data-processing, we clustered all the cells into 17 cell clusters from the peri-adventitial elastase incubation induced AAA dataset (GSE152583), then we identified these clusters by marker genes and classified them into 10 different cell types, which were monocytes/macrophages (4 clusters), smooth muscle cells (4 clusters), fibroblasts (2 clusters), NK-T cells (2 clusters), endothelial cells (1 cluster), dendritic cells (1 cluster), B cells (1 cluster), erythrocytes (1 cluster) and neural cells (1 cluster). Similarly, from the $CaCl_2$ induced AAA dataset (GSE164678), we got 15 cell clusters and classified them as monocytes/macrophages (4 clusters), fibroblasts (4 clusters), smooth muscle cells (2 clusters), B cells (1 cluster), endothelial cells (1 cluster), dendritic cells (1 cluster), NK-T cells (1 cluster), and neutrophils (1 cluster) (**Figures 1A,B**). Despite the different methods of inducing the AAA model, in both datasets, the TSNE plot showed that monocytes/macrophages accounted for the majority of immune cells infiltrating the aorta.

At the same time, deconvolution algorithms were used to evaluate the immune infiltration landscape from three bulk RNA-seq datasets that contain early-stage AAA samples (day 7) created by three different methods. Microenvironment Cell Population counter (mMCP-counter) immune infiltration analysis was used to analyze the differences of the immune cell infiltration levels between different early-stage AAA and control samples. As shown in **Figures 1C,E,G**, monocytes/macrophages cells got much higher enrichment scores in the early stage AAA samples than that in the control aorta for the three datasets. Moreover, *CIBERSORT* was used to estimate the immune cell composition in the sample, among the various immune cell types, monocytes and macrophages got the most enrichment ratios in the early stage AAA samples (**Figures 1D,F,H**). All the results above highlighted the vital role of monocytes/macrophages in the early stage of AAA.

Weighted gene coexpression network analysis

To further investigate the gene expression patterns of monocytes/macrophages between the early-stage AAA and control aorta, we extracted the expression matrix of monocytes/macrophages populations from the two scRNA-seq datasets and then constructed pseudo cells with highly variant genes to perform WGCNA analysis. After the combination of cells, 98 pseudocells with 1,891 high variable genes were developed from 1,093 monocytes/macrophages cells for the $CaCl_2$ induced AAA dataset (GSE164678), while for the peri-adventitial elastase incubation induced AAA dataset (GSE152583), 84 pseudocells with 1,960 high variable genes were generated from 938 monocytes/macrophages cells. Sample clustering dendrogram for the pseudocells generated from the two datasets was shown in **Figures 2A,E**. After that, step by step process was used to generate a co-expression network. For the elastase induced AAA dataset, β was chosen to be 3 ($R^2 = 0.9$) to comply with the scale-free network, and β = 6 was used for the $CaCl_2$ induced AAA dataset (**Figures 2B,F**). The genes were grouped into 11 modules in the macrophage gene expression matrix of the elastase induced AAA dataset and 9 modules in the $CaCl_2$ induced AAA dataset by setting the Cut-off value to 0.25 and the minModuleSize to 30 **Figures 2C,G**). The Spearman correlation between the module eigen gene and the traits was calculated in a subsequent phase to investigate module-trait correlations. As shown in **Figures 2D,H**, the blue, brown, and yellow modules were positively correlated with aneurysms in the elastase induced AAA dataset, whereas only the yellow gene module was positively correlated with AAA development in the $CaCl_2$ induced AAA dataset.

Functional enrichment analysis and protein-protein interaction analysis of gene module

To understand the function of the modules, GO, and KEGG functional annotation analyses were performed using genes in the modules. For the brown module in the elastase induced AAA dataset (GSE152583), GO analysis revealed that genes within the module are associated with the following BPs including "response to interferon-beta," "defense

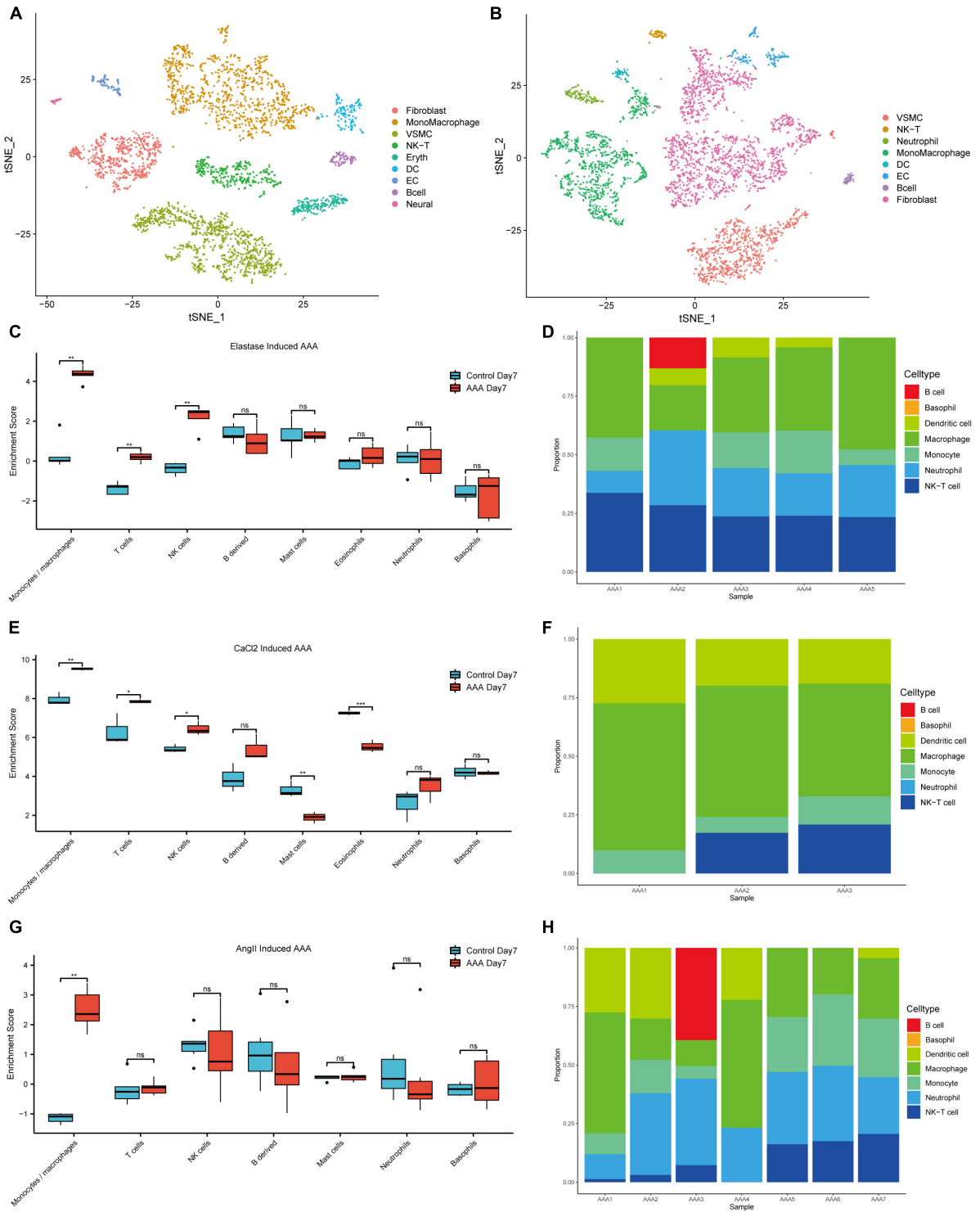

FIGURE 1
Immune cell infiltration analysis of the early-stage experimental AAA models. The t-SNE plot for peri-adventitial elastase incubation induced AAA scRNA-seq dataset (GSE152583) which contains elastase-induced AAA samples on day 7 and control aortas **(A)**. The t-SNE plot for $CaCl_2$ induced AAA scRNA-seq dataset (GSE164678) which contains $CaCl_2$-induced AAA samples on day 4 and control aortas **(B)**. Boxplot of the mMCP-counter enrichment score of microarray dataset **(C)** GSE51227 which contains AAA samples induced by intraluminal elastase perfusion on day 7 and control aortas **(E)** GSE109639 which contains $CaCl_2$-induced AAA samples on day 7 and control aortas **(G)** GSE17901 which contains AAA samples from AngII treated $ApoE^{-/-}$ mice on day 7 and control aortas. Bar graph of the CIBERSORT enrichment ratio of microarray dataset GSE51227 **(D)**, GSE109639 **(F)**, GSE17901 **(H)** (*$P < 0.05$, **$P < 0.01$, ***$P < 0.001$, ns, not significant).

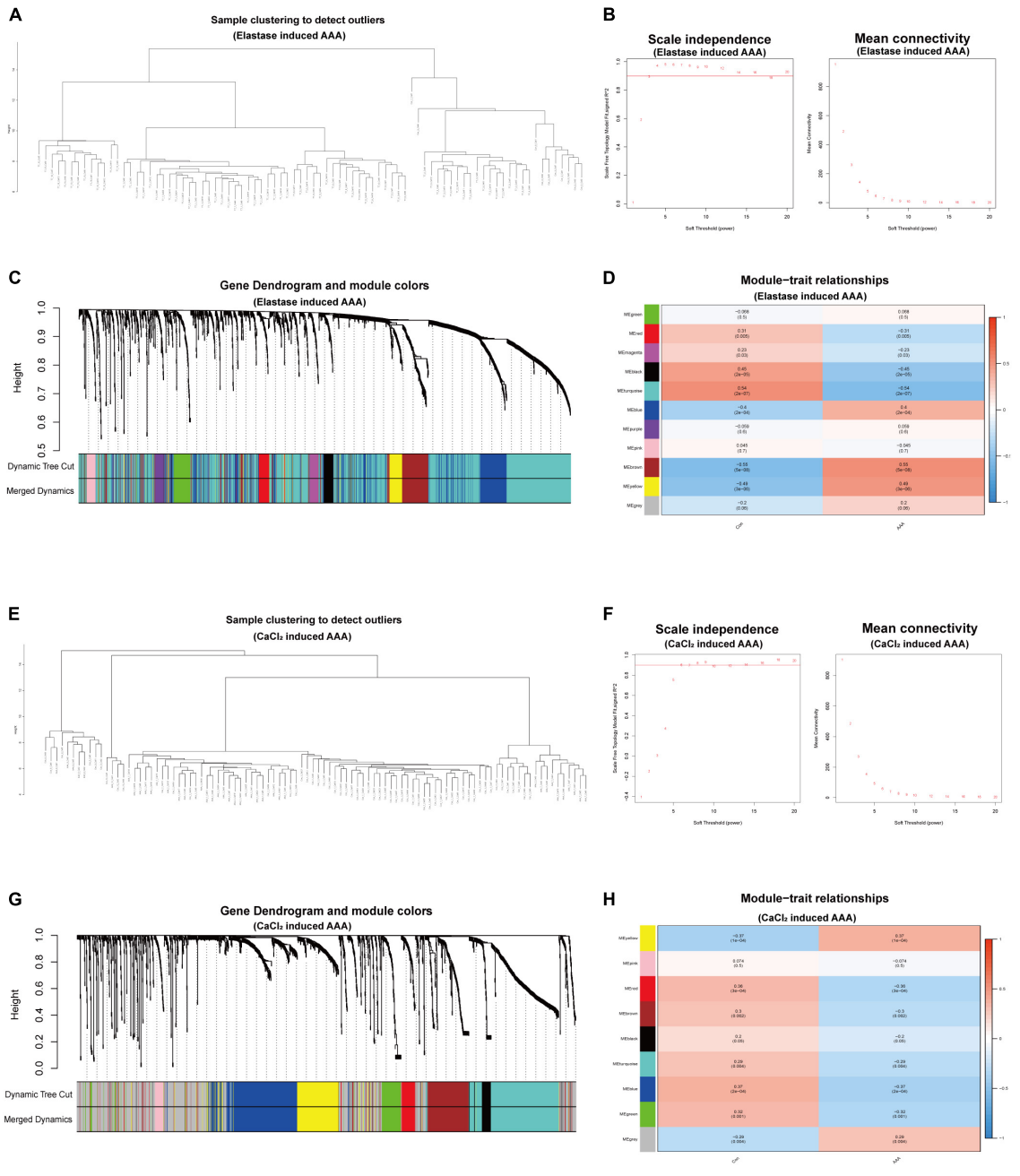

FIGURE 2
WGCNA for monocytes/macrophages populations of scRNA-seq datasets. WGCNA for monocytes/macrophages populations from peri-adventitial elastase incubation induced AAA dataset (GSE152583) **(A–D)** and $CaCl_2$ induced AAA dataset (GSE164678) **(E–H)**. Sample clustering dendrogram for the pseudocells **(A,E)**. Topology network analysis of the scale-free fit index for various soft-thresholding powers (β) and the mean connectivity for various soft-thresholding powers **(B,F)**. The cluster dendrograms represented the co-expression modules **(C,G)**. Heatmap exhibited the relationships between gene modules and clinical traits (Con and AAA) by Spearman correlation **(D,H)**.

response to virus," and "response to Virus"; the following CCs including "extracellular Matrix," "collagen-containing extracellular matrix" and "extracellular matrix component"; the following MFs including "protein kinase regulator activity," "heparin binding" and "kinase regulator activity." While, KEGG enrichment analysis revealed genes in the module were associated with "PI3K-Akt signaling pathway," "Epstein-Barr virus infection" and "Viral protein interaction with cytokine and cytokine receptor" (Figure 3A). In addition, there are 13 hub genes identified in the brown module, including *Xaf1*, *Bst2*,

Irf7, *Ms4a6c*, *Mnda*, *Ms4a4c*, *Fcgr1*, *Phf11b*, *Zbp1*, *Psmb8*, *Isg20*, *Rtp4*, *Fcgr4,* and the PPI network of those genes was shown in **Figure 3B**.

As for the yellow module in the elastase induced AAA dataset, genes in this module were involved in "myeloid leukocyte migration," "leukocyte migration" and "leukocyte chemotaxis" for BPs; "lysosome," "extracellular matrix" and "collagen-containing extracellular matrix" for CCs; "chemokine receptor binding," "chemokine activity" for MFs. What's more, KEGG enrichment analysis revealed genes in the module were associated with "NF-Kappa B Signaling Pathway," "Chemokine Signaling Pathway" and "TNF signaling pathway" (**Figure 3C**). *Cxcl16*, *Ifi30*, *AF251705*, *Ctss*, *Cd72*, *Fcgr4* were identified as hub genes for the yellow module. **Figure 3D** showed the PPI network of hub genes in the yellow module.

In terms of genes within the blue module, "positive regulation of cytokine production," "leukocyte migration," "extracellular structure organization" were the most enriched pathways for BPs; "extracellular matrix structural constituent," "receptor ligand activity," and "cell adhesion molecule binding" were the most enriched for CCs; while "extracellular matrix," "collagen-containing extracellular matrix" and "receptor complex" were the most enriched pathways for MFs. Meanwhile, "PI3K-Akt signaling pathway," "Focal adhesion" and "Cytokine-cytokine receptor interaction" were the most enriched pathways for KEGG analysis (**Figure 3E**). Hub genes in this module included *Thbs1*, *Csf2rb*, *Il1b*, *Cd44*, *Clec4d*, *Adam8*, *and Clec4e*. PPI network of hub genes in this module is shown in **Figure 3F**.

As mentioned above, for the $CaCl_2$ induced AAA dataset (GSE164678), only the yellow module was positively associated with AAA development. GO enrichment analysis revealed that genes in this module were associated with "cell Chemotaxis," "myeloid leukocyte migration," and "leukocyte migration" for BPs; "lysosome," "lytic vacuole," and "cell-cell junction" for CCs, "cell adhesion molecule binding," "integrin binding" and "cytokine receptor binding" for MFs. KEGG enrichment analysis revealed "Rap1 signaling pathway," "Osteoclast differentiation" and "Leukocyte transendothelial migration" pathways were related to genes in this module (**Figure 3G**). 12 hub genes meeting our criterion were selected, including *Cd244*, *Gngt2*, *Thbs1*, *Chil3*, *Srgn*, *Itgax*, *Ltb4r1*, *Spint1*, *Il1b*, *Clec4e*, *Ncf4*, *Trem3,* and PPI network of hub genes in the gene module was shown in **Figure 3H**.

Identification of key monocytes/macrophages related gene set

As we can observe, the gene expression patterns of monocytes/macrophages in AAA models built using various approaches varied significantly. Next, we wanted to see if, despite diverse AAA models, monocytes/macrophages share changed genes throughout the early stages of AAA onset. So, firstly, differential gene expression analysis between the monocytes/macrophages populations of the control aorta and AAA was performed in the two datasets. As shown in **Figures 4A,B**, 67 up-regulated DEGs and 41 downregulated DEGs were identified in elastase induced AAA dataset (GSE152583), while 88 up-regulated DEGs and 17 downregulated DEGs were identified in $CaCl_2$ induced AAA dataset (GSE164678) (**Figures 4A,B** and **Supplementary Table 2**). Then we took the intersection of the hub genes identified above and the DEGs in the two datasets. Finally, three genes, *Thbs1*, *Il1b*, and *Clec4e*, were chosen (**Figure 4C**). After that, we looked at how the three genes were expressed in distinct cell groups. For the peri-adventitial elastase incubation induced AAA dataset, these three genes were mostly expressed in monocytes/macrophages, while for the $CaCl_2$ induced AAA dataset, they were mostly expressed in neutrophils and monocytes/macrophages (**Figure 4D**). The elevated expression of the three genes was then validated in other datasets (**Figures 4E–G**). Furthermore, it is worth mentioning that the high expression of the three genes persist until day 42 following $CaCl_2$ induction (**Figure 4G**).

Logistic regression model for prediction of abdominal aortic aneurysm

Going a step further, the expression of the three genes in the human AAA dataset was inspected, and all three genes were found to be up-regulated, as shown in **Figure 5A**. We also discovered that the three genes colocalized with CD68, a common macrophage marker, using the human AAA scRNA-seq dataset (**Figure 5B**). Next, we wanted to know if these three genes had potential diagnostic value for AAA in humans. So, we built a logistic regression model employing the gene expression in the GSE57691 dataset as continuous predictive variables and sample type (AAA and control aorta) as categorical responsive values. The *P*-values of *IL1B* and *CLEC4E* were < 0.05 in the logistic regression model. **Figure 5C** shows the dynamic nomogram of the logistic regression model. The calibration curve of the model showed that the predicted probability and the observed probability were generally fitting (**Figure 5D**), and the *P*-values of the Hosmer-Lemeshow test were > 0.05. The area under the curve (AUC) value was used to assess the discrimination of the models. As a result, the AUC of the combined diagnostic method was 0.9 (**Figure 5E**). In addition, the GSE47472 dataset, which includes AAA neck samples with less severe lesions, was used to evaluate the effectiveness of this logistic regression model. The AUC value of 0.79 demonstrated the model's superior ability to distinguish between AAA and control aorta (**Figure 5F**).

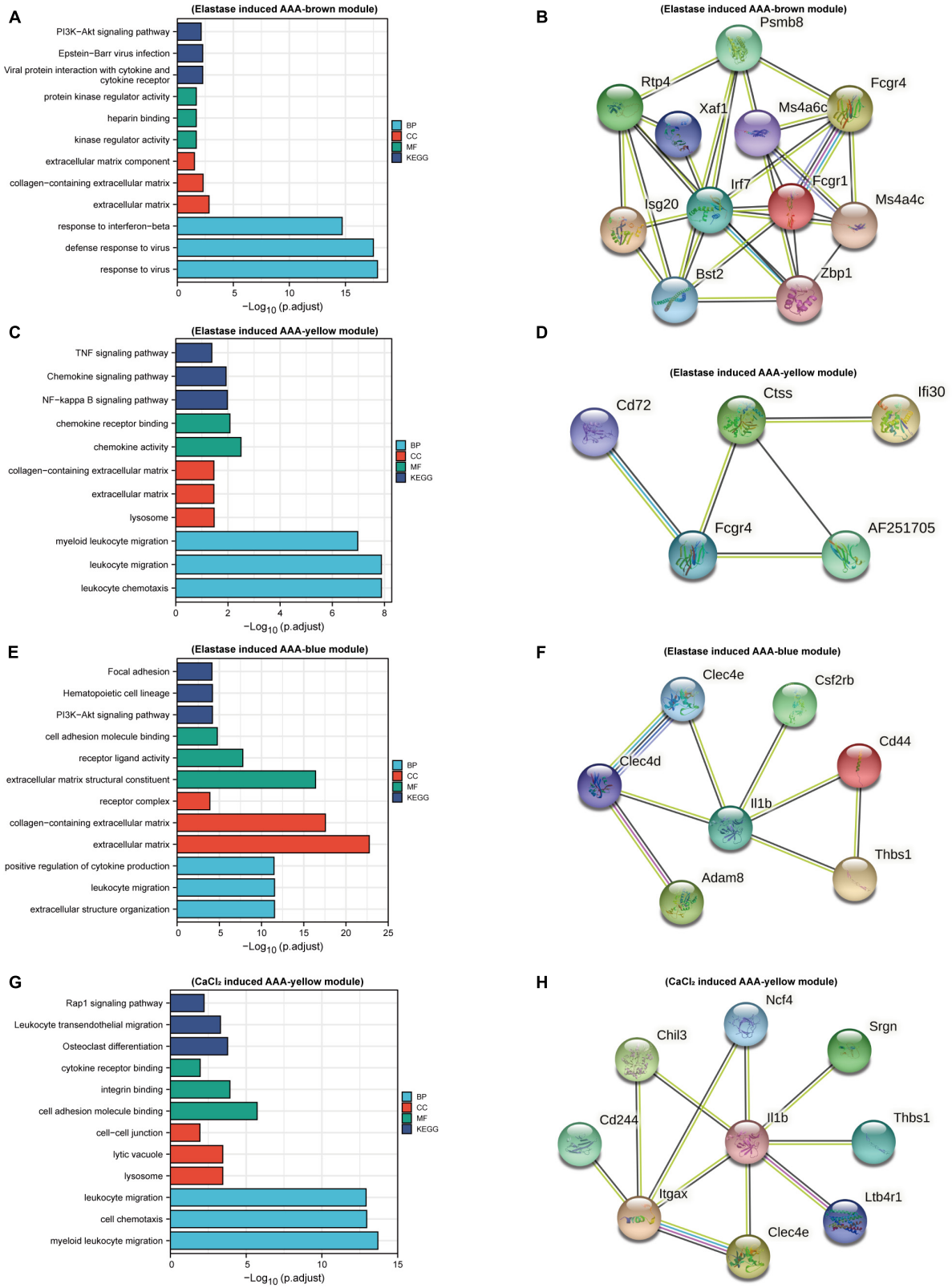

FIGURE 3
Function enrichment and PPI analysis. Bar plots of GO and KEGG function enrichment results for genes in brown module **(A)**, yellow module **(C)**, and blue module **(E)** of peri-adventitial elastase incubation induced AAA dataset (GSE152583) and genes in blue module **(G)** of $CaCl_2$ induced AAA dataset (GSE164678). PPI network for hub genes in brown module **(B)**, yellow module **(D)**, and blue module **(F)** of elastase induced AAA dataset and for hub genes in blue module **(H)** of $CaCl_2$ induced AAA dataset.

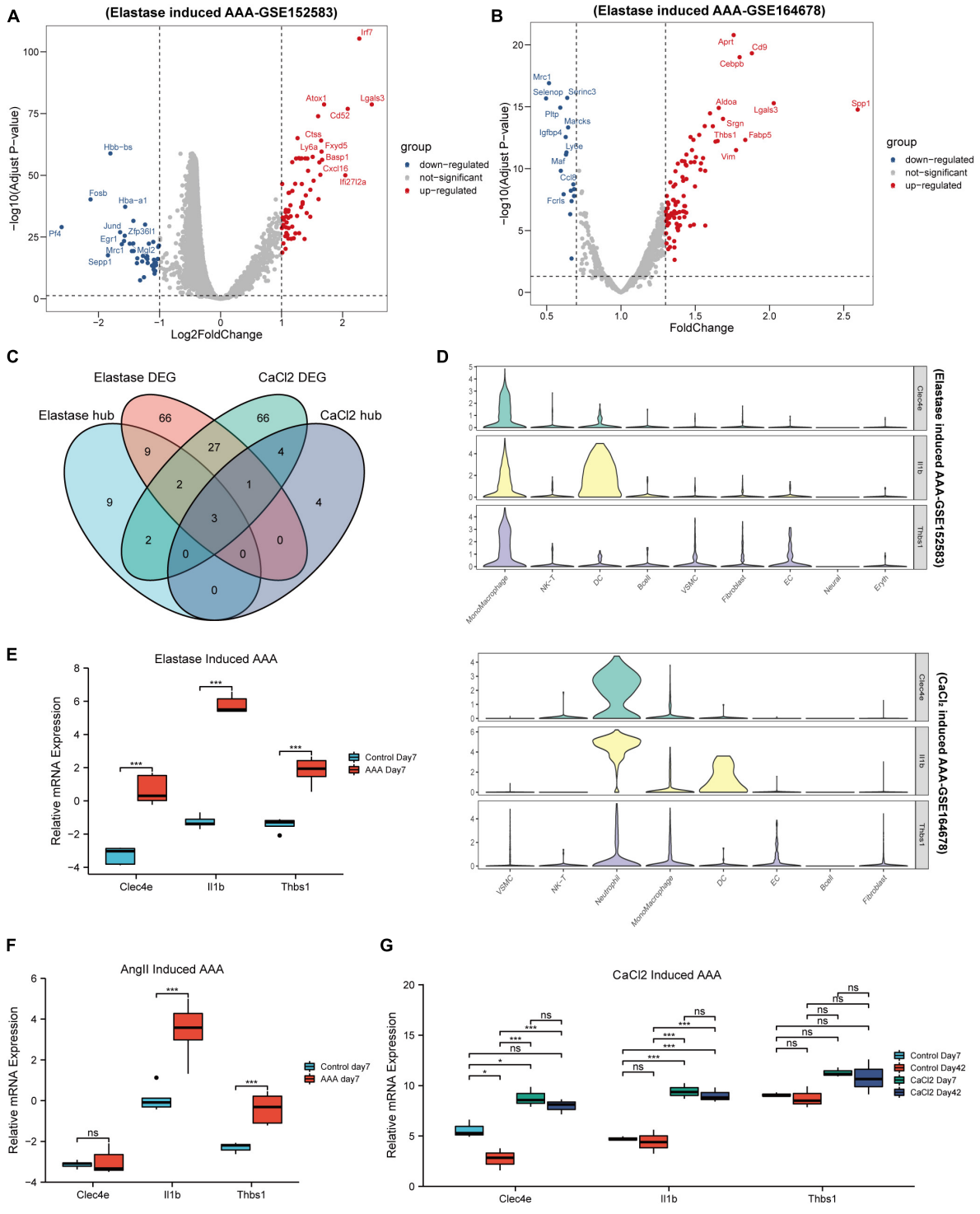

FIGURE 4
Identification of key genes. Volcano map of differential genes for monocytes/macrophages populations between control and AAA model group in peri-adventitial elastase incubation induced AAA dataset (GSE152583) **(A)** and $CaCl_2$ induced AAA dataset (GSE164678) **(B)**. Veen diagrams of DEGs and hub genes for monocytes/macrophages populations between elastase induced AAA dataset and $CaCl_2$ induced AAA dataset **(C)**. Violin plots of *Clec4e*, *Il1b*, and *Thbs1* expression in different cell types from peri-adventitial elastase incubation induced AAA dataset and $CaCl_2$ induced AAA dataset **(D)**. Boxplot showing the relative expression of *Clec4e*, *Il1b*, and *Thbs1* in the early stage AAA and control aortas for intraluminal elastase perfusion induced AAA microarray dataset (GSE51227) **(E)** and AngII induced AAA dataset (GSE17091) **(F)**. Boxplot showing the relative expression of *Clec4e*, *Il1b*, and *Thbs1* in AAA and control aortas of day 7 and 42 for $CaCl_2$ induced AAA microarray dataset (GSE109639) **(G)**. $^*P < 0.05$, $^{****}P < 0.0001$.

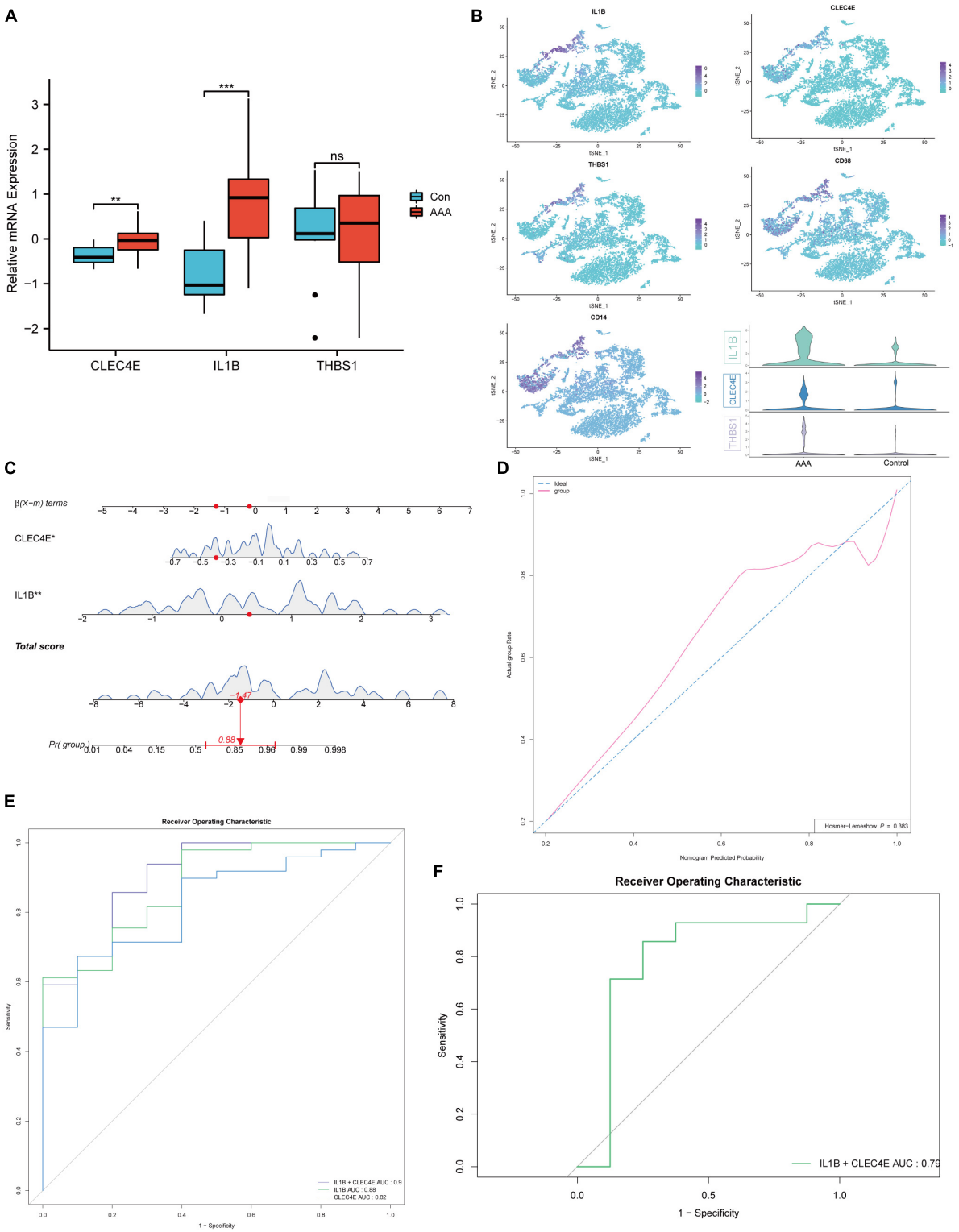

FIGURE 5
Construction of the logistic regression diagnostic model. Boxplot showing the relative expression of *CLEC4E*, *IL1B*, and *THBS1* in AAA and control aortas for human AAA dataset (GSE57691) **(A)**. *CLEC4E*, *IL1B*, *THBS1,* and *CD68* expression in different cell types of human AAA scRNA-seq dataset (GSE166676) **(B)**. Dynamic nomogram of the two-gene-based model for predicting patients with AAA **(C)**. Dynamic nomogram of the two-gene-based model for predicting patients with AAA **(C)**. The calibration curve of the model **(D)**. ROC curves for the train dataset GSE57691 **(E)** and the validation dataset GSE47472 (human AAA neck) **(F)**. $^{**}P < 0.01$, $^{***}P < 0.001$.

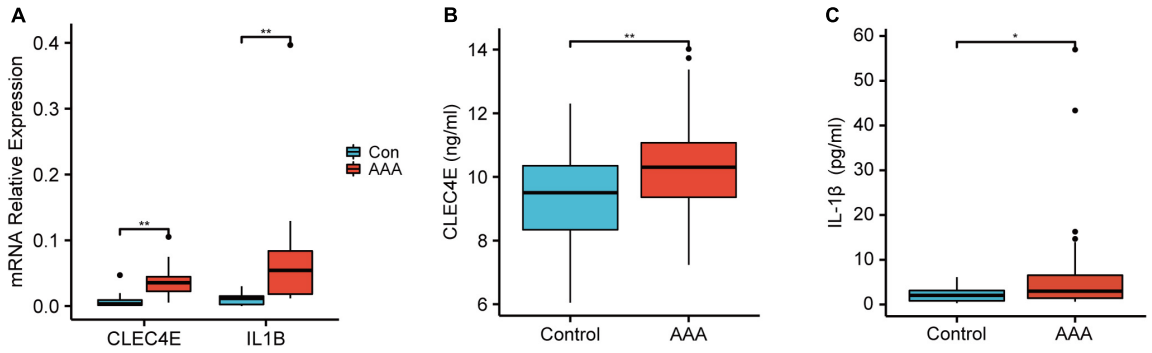

FIGURE 6
Validation of the gene expression and serum protein level. Boxplot showing the relative expression of *CLEC4E* and *IL1B* in AAA (N = 10) and control aortas (N = 10) **(A)**. Boxplot showing the protein level of CLEC4E **(B)** and IL-1β **(C)** in AAA (N = 30) and control serum (N = 10). *P < 0.05, **P < 0.01.

Validation of key monocytes/macrophages related gene set in human abdominal aortic aneurysm aorta and serum

To further validate the high expression of the two genes in human AAA samples, we collected aortic tissues from AAA patients (n = 10) and non-AAA aortas from healthy donors (n = 10). Patients and the control group were age and sex-matched (**Supplementary Table 1**). As shown in **Figure 6**, *IL1B* and *CLEC4E* were highly expressed in the AAA sample. Next, we further detected the proteins expression levels of IL-1β and CLEC4E in the serum of patients. IL-1β expression was detectable in 32 of 38 AAA patients and in 10 of 18 control samples (P = 0.044). *IL1B* was increased in AAA patients (7.532 ± 12.529, Mean ± SD, pg/mL) compared with controls (2.234 ± 1.792, Mean ± SD,pg/mL). To our surprise, CLEC4E protein was detectable in the serum of all the participants with a high level of expression. Also, the expression of CLEC4E protein was higher in AAA serum than that in control serum (10.428 ± 1.55 vs. 9.224 ± 1.553, Mean ± SD, ng/mL).

Discussion

AAA can be asymptomatic in the early stages, but if they reach a late stage, they can rupture and cause abrupt mortality. However, surgical intervention is the only effective method for AAA, and there is no effective medical therapy for patients who do not have surgical indications (15, 16). Understanding the pathology of an AAA in its early stages is critical for early diagnosis, prevention, and therapy.

Previous studies have identified multiple immune cell types in human AAA tissues. To assess the immune infiltration of the early-stage experimental AAA, we employed a deconvolution algorithm based on transcriptome data and cell identification based on single-cell sequencing data. Although some immune cell types, including mast cells, eosinophils, and basophils, had a certain enrichment score through deconvolution evaluation, these cells could not be well identified in the single-cell sequencing data from the same AAA model. This inconsistency may be due to sample variances and single-cell sequencing dropout. In any case, there was good consistency between the main immune cell types that can be identified by single-cell sequencing and the enrichment results of the transcriptome data, including T cells, NK cells, and monocytes/macrophages. Regrettably, no single-cell sequencing data of the early-stage AAA model generated by Ang II is currently available, however, the current study highlighted the importance of monocytes/macrophages in the early stages of AAA. What's more, several recent studies evaluated the immune infiltration landscape in human AAA samples by *CIBERSORTx*, and the results showed that compared to the control aortas, monocytes and macrophages are the main types of immune cells infiltrated in AAA (17, 18). Hence, the infiltration of monocytes/macrophages may be an event that started in the early stage of AAA and existed through the development of AAA.

WGCNA is one of the most used methods for inferencing gene networks from transcriptomic data. Previous studies have used WGCNA to identify hub genes for AAA based on bulk transcriptomic data (19, 20). But the same gene may have different effects on AAA progression in different cell types. Several studies have shown that WGCNA can be applied to single-cell sequencing data by constructing pseudocells (21, 22). Given the vital role of monocytes/macrophages in AAA immune infiltration, we constructed pseudocells and performed WGCNA based on the monocytes/macrophages expression profile in two different AAA model scRNA-seq datasets. Correlation analysis showed that three gene modules were involved in the early stage AAA induced by elastase.

KEGG pathway enrichment analysis showed that the three gene modules were related to virus infection (brown), leukocyte chemotaxis (yellow), and cytokine release (blue), respectively. GO pathway enrichment analysis highlighted the role of "PI3K-Akt signaling pathway," "NF-Kappa B Signaling Pathway," "TNF Signaling Pathway" and the importance of extracellular matrix components. Prior studies have noted the vital role of macrophages in ECM degradation, while our study is consistent with this and suggests that this process may be occurring in the early stage of AAA (23). Compared to the elastase-induced AAA model, only one gene module (yellow) was identified as being positively associated with AAA in $CaCl_2$ induced AAA, of which pathway enrichment analysis emphasized the role of leukocyte adhesion and Rap1 signaling pathway. DEG analysis of monocytes/macrophages in the $CaCl_2$ induced AAA model also showed much less genetic alternations than that induced by elastase, so much so that we had to relax the logFC selection criteria to get the same number of differential expression genes. It is worth mentioning that although $CaCl_2$ induced AAA models are widely used, the researchers found that the expansion of AAA was not significant compared to that induced by AngII and elastase, while the aortic calcification was more predominant (24, 25). In line with this, GO pathway enrichment analysis of the yellow gene module in the $CaCl_2$ induced AAA model also highlighted the role of osteogenic differentiation, which is a similar physiological process to vascular calcification. Anyway, three genes were identified in both models, including *Thbs1*, *Il1b,* and *Clec4e*. Furthermore, the expression of the three genes in human AAA samples was examined, and a logistic regression diagnostic model was built based on *IL1B* and *CLEC4E*.

CLEC4E, also called MINCLE (Macrophage-Inducible C-Type Lectin), is a pattern recognition receptor that belongs to the C-type lectin receptor family. Antigen-presenting cells such as macrophages, neutrophils, DCs, and B cells express MINCLE, which can bind a variety of PAMPs generated from the fungal microbiome, including -mannose, lipidic species, and certain endogenous self-ligands such Sin3A-associated protein 130 (SAP130) (26, 27). In the present study, *CLEC4E* is principally expressed on monocytes/macrophages in elastase-induced AAA model and human AAA samples. As far as we know, there were no studies have investigated the role of MINCLE in the formation of AAA. According to a recent study, Clec4e expressed on macrophages can detect necrotic cells and promote local inflammation, which promotes atherosclerosis (28). Hence, in the early stage of AAA development, MINCLE may be activated by necrotic cells and initiate the early stage inflammatory response.

IL1B, which encoded interleukin-1, is a well-known inflammatory gene involved in various diseases. Due to ROS-mediated inflammasome activation, Il-1 was observed to be increased in the early stages of experimental AAA (29, 30). Some researchers suggest that macrophages and vascular smooth muscle cells are the main sources of Il-1β (31). Consistent with the literature, in our study, Il-1β was most expressed on monocytes/macrophages and dendritic cells in elastase-induced AAA model while in $CD68^+$ monocytes/macrophages-like cells in human AAA samples. However, though we observed the high expression on monocytes/macrophages in $Cacl_2$ induced AAA model, more prominent *IL1B* mRNA expression was observed to express in the neutrophils. Researcher has found that IL-1β expression in neutrophils could contributed to AAA by promoting NETosis during an earlier stage on day 3. Since AAA samples used for sc-RNA sequence by $Cacl_2$-induced were taken much earlier (day 4) than that by elastase induced AAA (day 7), we suggest that the difference in *IL1B* expression pattern stems from the different timing of sampling. In AAA patients, elevated plasma and aortic wall Il-1β levels were reported in the previous studies (32, 33). It also has been reported that the Il-1β levels were the same in the AAA patients with small and large aneurysms (maximal diameter $>$ or $<$ 45 mm), highlighting the diagnostic value of Il-1β for AAA in the early stage (34).

There were several limits to our study. First of all, although we used datasets from different AAA models, there was still a certain difference between the pathology of the early-stage experimental AAA and that of human AAA. Secondly, Due to the lack of clinical information in the dataset, risk factors such as gender and smoking status were not considered. Lastly, because it didn't meet the surgical indications, it was difficult for us to obtain blood and tissue samples from early-stage AAA patients. Thus, we couldn't evaluate the diagnostic performance of *IL1B* and *CLEC4E* in the early-stage AAA patient cohorts.

Conclusion

This study downloaded scRNA-seq data and transcriptome data of experimental AAA and human AAA samples from the GEO database. Through multiple bioinformatics analysis methods based on the data, we identified macrophages as the main immune cells infiltrated in the early stage AAA. Moreover, we identified *Clec4e*, *Il1b,* and *Thbs1* as key monocytes/macrophages related genes. After that, a logistic regression diagnostic model was established based on *CLEC4E* and *IL1B*, which can distinguish AAA patients from the control group well.

Data availability statement

The datasets presented in this study can be found in online repositories. The names of the repository and accession numbers can be found below: https://www.ncbi.nlm.nih.gov/geo/, GSE152583, GSE164678, GSE166676, GSE51227, GSE109639, GSE17091, GSE57691, and GSE47472.

Ethics statement

The studies involving human participants were reviewed and approved by Ethics Committee at the Chinese Medical University, The First Affiliated Hospital of China Medical University. The patients/participants provided their written informed consent to participate in this study.

Author contributions

SC and SX designed the study. YL collected the data and materials. SC and YL performed the data analysis. SC wrote the manuscript. YJ and BJ contributed to essential reagents and tools. BJ and SX revised the manuscript. All authors contributed to the article and approved the submitted version.

Funding

This work was supported by the National Natural Science Foundation of China (Grant nos. 81974049 and 81770488).

Acknowledgments

We thank Yunlai Zhou, Jianming Zeng (University of Macau) and all the members of his bioinformatics team, biotrainee, for generously sharing their experience and codes.

Conflict of interest

The authors declare that the research was conducted in the absence of any commercial or financial relationships that could be construed as a potential conflict of interest.

Publisher's note

Supplementary material

The Supplementary Material for this article can be found online at: https://www.frontiersin.org/articles/10.3389/fcvm.2022.950961/full#supplementary-material

SUPPLEMENTARY FIGURE 1
Cell marker used for scRNA-seq datasets processing and boxplots of mRNA seq datasets following normalization.

SUPPLEMENTARY TABLE 1
The baseline characteristic data of the subject involved in our cohort.

SUPPLEMENTARY TABLE 2
DEGs list of **Figure 4**.

SUPPLEMENTARY TABLE 3
Primer sequences used in the work.

References

1. Golledge J, Muller J, Daugherty A, Norman P. Abdominal aortic aneurysm: pathogenesis and implications for management. *Arterioscler Thromb Vasc Biol.* (2006) 26:2605–13.

2. Sprynger M, Willems M, Van Damme H, Drieghe B, Wautrecht JC, Moonen M. Screening program of abdominal aortic aneurysm. *Angiology.* (2019) 70:407–13. doi: 10.1177/0003319718824940

3. Schäberle W, Leyerer L, Schierling W, Pfister K. Ultrasound diagnostics of the abdominal aorta: english version. *Gefasschirurgie.* (2015) 20(Suppl. 1):22–7. doi: 10.1007/s00772-014-1411-1

4. Moris D, Mantonakis E, Avgerinos E, Makris M, Bakoyiannis C, Pikoulis E, et al. Novel biomarkers of abdominal aortic aneurysm disease: identifying gaps and dispelling misperceptions. *Biomed Res Int.* (2014) 2014:925840. doi: 10.1155/2014/925840

5. Zhang S-L, Du X, Chen Y-Q, Tan Y-S, Liu L. Potential medication treatment according to pathological mechanisms in abdominal aortic aneurysm. *J Cardiovasc Pharmacol.* (2018) 71:46–57. doi: 10.1097/FJC.0000000000000540

6. Yuan Z, Lu Y, Wei J, Wu J, Yang J, Cai Z. Abdominal aortic aneurysm: roles of inflammatory cells. *Front Immunol.* (2020) 11:609161. doi: 10.3389/fimmu.2020.609161

7. Meher AK, Spinosa M, Davis JP, Pope N, Laubach VE, Su G, et al. Novel role of IL (interleukin)-1β in neutrophil extracellular trap formation and abdominal aortic aneurysms. *Arterioscler Thromb Vasc Biol.* (2018) 38:843–53. doi: 10.1161/ATVBAHA.117.309897

8. Golledge J, Krishna SM, Wang Y. Mouse models for abdominal aortic aneurysm. *Br J Pharmacol.* (2020) 5:792–810. doi: 10.1111/bph.15260

9. Patelis N, Moris D, Schizas D, Damaskos C, Perrea D, Bakoyiannis C, et al. Animal models in the research of abdominal aortic aneurysms development. *Physiol Res.* (2017) 66:899–915. doi: 10.33549/physiolres.933579

10. Davis FM, Tsoi LC, Melvin WJ, denDekker A, Wasikowski R, Joshi AD, et al. Inhibition of macrophage histone demethylase JMJD3 protects against abdominal aortic aneurysms. *J Exp Med.* (2021) 218:e20201839. doi: 10.1084/jem.20201839

11. Petitprez F, Levy S, Sun CM, Meylan M, Linhard C, Becht E, et al. The murine microenvironment cell population counter method to estimate abundance of tissue-infiltrating immune and stromal cell populations in murine samples using gene expression. *Genome Med.* (2020) 12:86. doi: 10.1186/s13073-020-00783-w

12. Chen Z, Huang A, Sun J, Jiang T, Qin FX, Wu A. Inference of immune cell composition on the expression profiles of mouse tissue. *Sci Rep.* (2017) 7:40508. doi: 10.1038/srep40508

13. Newman AM, Liu CL, Green MR, Gentles AJ, Feng W, Xu Y, et al. Robust enumeration of cell subsets from tissue expression profiles. *Nat Methods.* (2015) 12:453–7. doi: 10.1038/nmeth.3337

14. Soneson C, Robinson MD. Bias, robustness and scalability in single-cell differential expression analysis. *Nat Methods.* (2018) 15:255–61. doi: 10.1038/nmeth.4612

15. Chaikof EL, Dalman RL, Eskandari MK, Jackson BM, Lee WA, Mansour MA, et al. The society for vascular surgery practice guidelines on the care of patients with an abdominal aortic aneurysm. *J Vasc Surg.* (2018) 67:2–77.e2. doi: 10.1016/j.jvs.2017.10.044

16. Golledge J, Moxon JV, Singh TP, Bown MJ, Mani K, Wanhainen A. Lack of an effective drug therapy for abdominal aortic aneurysm. *J Intern Med.* (2020) 288:6–22. doi: 10.1111/joim.12958

17. Lei C, Yang D, Chen S, Chen W, Sun X, Wu X, et al. Patterns of immune infiltration in stable and raptured abdominal aortic aneurysms: a gene-expression-based retrospective study. *Gene.* (2020) 762:145056. doi: 10.1016/j.gene.2020.145056

18. Nie H, Qiu J, Wen S, Zhou W. Combining bioinformatics techniques to study the key immune-related genes in abdominal aortic aneurysm. *Front Genet.* (2020) 11:579215. doi: 10.3389/fgene.2020.579215

19. Kan KJ, Guo F, Zhu L, Pallavi P, Sigl M, Keese M. Weighted gene co-expression network analysis reveals key genes and potential drugs in abdominal aortic aneurysm. *Biomedicines.* (2021) 9:546. doi: 10.3390/biomedicines9050546

20. Chen S, Yang D, Liu B, Chen Y, Ye W, Chen M, et al. Identification of crucial genes mediating abdominal aortic aneurysm pathogenesis based on gene expression profiling of perivascular adipose tissue by WGCNA. *Ann Transl Med.* (2021) 9:52. doi: 10.21037/atm-20-3758

21. Tosches MA, Yamawaki TM, Naumann RK, Jacobi AA, Tushev G, Laurent G. Evolution of pallium, hippocampus, and cortical cell types revealed by single-cell transcriptomics in reptiles. *Science.* (2018) 360:881–8. doi: 10.1126/science.aar4237

22. Han X, Zhou Z, Fei L, Sun H, Wang R, Chen Y, et al. Construction of a human cell landscape at single-cell level. *Nature.* (2020) 581:303–9. doi: 10.1038/s41586-020-2157-4

23. Pyo R, Lee JK, Shipley JM, Curci JA, Mao D, Ziporin SJ, et al. Targeted gene disruption of matrix metalloproteinase-9 (gelatinase b) suppresses development of experimental abdominal aortic aneurysms. *J Clin Invest.* (2000) 105:1641–9. doi: 10.1172/jci8931

24. Golledge J. Abdominal aortic aneurysm: update on pathogenesis and medical treatments. *Nat Rev Cardiol.* (2019) 16:225–42. doi: 10.1038/s41569-018-0114-9

25. Wang Y, Krishna S, Golledge J. The calcium chloride-induced rodent model of abdominal aortic aneurysm. *Atherosclerosis.* (2013) 226:29–39. doi: 10.1016/j.atherosclerosis.2012.09.010

26. Drouin M, Saenz J, Chiffoleau EC-. Type lectin-like receptors: head or tail in cell death immunity. *Front Immunol.* (2020) 11:251. doi: 10.3389/fimmu.2020.00251

27. Li TH, Liu L, Hou YY, Shen SN, Wang TT. C-Type lectin receptor-mediated immune recognition and response of the microbiota in the gut. *Gastroenterol Rep.* (2019) 7:312–21. doi: 10.1093/gastro/goz028

28. Clément M, Basatemur G, Masters L, Baker L, Bruneval P, Iwawaki T, et al. Necrotic cell sensor clec4e promotes a proatherogenic macrophage phenotype through activation of the unfolded protein response. *Circulation.* (2016) 134:1039–51. doi: 10.1161/circulationaha.116.022668

29. Usui F, Shirasuna K, Kimura H, Tatsumi K, Kawashima A, Karasawa T, et al. Inflammasome activation by mitochondrial oxidative stress in macrophages leads to the development of angiotensin ii-induced aortic aneurysm. *Arterioscler Thromb Vasc Biol.* (2015) 35:127–36. doi: 10.1161/atvbaha.114.303763

30. Sun W, Pang Y, Liu Z, Sun L, Liu B, Xu M, et al. Macrophage inflammasome mediates hyperhomocysteinemia-aggravated abdominal aortic aneurysm. *J Mol Cell Cardiol.* (2015) 81:96–106. doi: 10.1016/j.yjmcc.2015.02.005

31. Johnston WF, Salmon M, Su G, Lu G, Stone ML, Zhao Y, et al. genetic and pharmacologic disruption of interleukin-1β signaling inhibits experimental aortic aneurysm formation. *Arterioscler Thromb Vasc Biol.* (2013) 33:294–304. doi: 10.1161/atvbaha.112.300432

32. Wu X, Cakmak S, Wortmann M, Hakimi M, Zhang J, Böckler D, et al. Sex- and disease-specific inflammasome signatures in circulating blood leukocytes of patients with abdominal aortic aneurysm. *Mol Med.* (2016) 22:505–18. doi: 10.2119/molmed.2016.00035

33. Newman KM, Jean-Claude J, Li H, Ramey WG, Tilson MD. Cytokines that activate proteolysis are increased in abdominal aortic aneurysms. *Circulation.* (1994) 90:II224–7.

34. Juvonen J, Surcel HM, Satta J, Teppo AM, Bloigu A, Syrjälä H, et al. Elevated circulating levels of inflammatory cytokines in patients with abdominal aortic aneurysm. *Arterioscler Thromb Vasc Biol.* (1997) 17:2843–7. doi: 10.1161/01.atv.17.11.2843

35. Zhao G, Lu H, Chang Z, Zhao Y, Zhu T, Chang L, et al. Single-cell RNA sequencing reveals the cellular heterogeneity of aneurysmal infrarenal abdominal aorta. *Cardiovasc Res.* (2021) 117:1402–16. doi: 10.1093/cvr/cvaa214

36. Yang H, Zhou T, Stranz A, DeRoo E, Liu B. Single-cell RNA sequencing reveals heterogeneity of vascular cells in early stage murine abdominal aortic aneurysm-brief report. *Arterioscler Thromb Vasc Biol.* (2021) 41:1158–66. doi: 10.1161/atvbaha.120.315607

37. Maegdefessel L, Spin JM, Raaz U, Eken SM, Toh R, Azuma J, et al. Mir-24 limits aortic vascular inflammation and murine abdominal aneurysm development. *Nat Commun.* (2014) 5:5214. doi: 10.1038/ncomms6214

38. Furusho A, Aoki H, Ohno-Urabe S, Nishihara M, Hirakata S, Nishida N, et al. Involvement of B cells, immunoglobulins, and syk in the pathogenesis of abdominal aortic aneurysm. *J Am Heart Assoc.* (2018) 7:e007750. doi: 10.1161/jaha.117.007750

39. Spin JM, Hsu M, Azuma J, Tedesco MM, Deng A, Dyer JS, et al. Transcriptional profiling and network analysis of the murine angiotensin II-induced abdominal aortic aneurysm. *Physiol Genomics.* (2011) 43:993–1003. doi: 10.1152/physiolgenomics.00044.2011

40. Biros E, Gäbel G, Moran CS, Schreurs C, Lindeman JH, Walker PJ, et al. Differential gene expression in human abdominal aortic aneurysm and aortic occlusive disease. *Oncotarget.* (2015) 6:12984–96. doi: 10.18632/oncotarget.3848

41. Biros E, Moran CS, Rush CM, Gäbel G, Schreurs C, Lindeman JH, et al. Differential gene expression in the proximal neck of human abdominal aortic aneurysm. *Atherosclerosis.* (2014) 233:211–8. doi: 10.1016/j.atherosclerosis.2013.12.017

frontiers | Frontiers in Cardiovascular Medicine

TYPE Review
PUBLISHED 20 September 2022
DOI 10.3389/fcvm.2022.988266

OPEN ACCESS

EDITED BY
Mark Slevin,
Manchester Metropolitan University, United Kingdom

REVIEWED BY
Preetha Shridas,
University of Kentucky, United States
Richard Austin,
McMaster University, Canada

*CORRESPONDENCE
Liqun Jiao
liqunjiao@sina.cn
Tao Wang
wangtao_dr@sina.com
Ge Yang
Ge.yang@ia.ac.cn

†These authors have contributed equally to this work

SPECIALTY SECTION
This article was submitted to Atherosclerosis and Vascular Medicine, a section of the journal Frontiers in Cardiovascular Medicine

RECEIVED 07 July 2022
ACCEPTED 30 August 2022
PUBLISHED 20 September 2022

CITATION
Li W, Jin K, Luo J, Xu W, Wu Y, Zhou J, Wang Y, Xu R, Jiao L, Wang T and Yang G (2022) NF-κB and its crosstalk with endoplasmic reticulum stress in atherosclerosis.
Front. Cardiovasc. Med. 9:988266.
doi: 10.3389/fcvm.2022.988266

NF-κB and its crosstalk with endoplasmic reticulum stress in atherosclerosis

Wenjing Li[1,2†], Kehan Jin[3†], Jichang Luo[4,5†], Wenlong Xu[4,5†], Yujie Wu[1], Jia Zhou[3], Yilin Wang[6], Ran Xu[4,5], Liqun Jiao[4,5,7*], Tao Wang[4,5*] and Ge Yang[1,2*]

[1]Laboratory of Computational Biology and Machine Intelligence, National Laboratory of Pattern Recognition, Institute of Automation, Chinese Academy of Sciences, Beijing, China, [2]School of Artificial Intelligence, University of Chinese Academy of Sciences, Beijing, China, [3]Peking Union Medical College Hospital, Peking Union Medical College, Chinese Academy of Medical Sciences, Beijing, China, [4]Department of Neurosurgery, Xuanwu Hospital, Capital Medical University, Beijing, China, [5]China International Neuroscience Institute (China-INI), Beijing, China, [6]Institute of Cerebrovascular Disease Research and Department of Neurology, Xuanwu Hospital of Capital Medical University, Beijing, China, [7]Department of Interventional Radiology, Xuanwu Hospital, Capital Medical University, Beijing, China

Atherosclerosis (AS) is a common cardiovascular disease with complex pathogenesis, in which multiple pathways and their interweaving regulatory mechanism remain unclear. The primary transcription factor NF-κB plays a critical role in AS *via* modulating the expression of a series of inflammatory mediators under various stimuli such as cytokines, microbial antigens, and intracellular stresses. Endoplasmic reticulum (ER) stress, caused by the disrupted synthesis and secretion of protein, links inflammation, metabolic signals, and other cellular processes *via* the unfolded protein response (UPR). Both NF-κB and ER stress share the intersection regarding their molecular regulation and function and are regarded as critical individual contributors to AS. In this review, we summarize the multiple interactions between NF-κB and ER stress activation, including the UPR, NLRP3 inflammasome, and reactive oxygen species (ROS) generation, which have been ignored in the pathogenesis of AS. Given the multiple links between NF-κB and ER stress, we speculate that the integrated network contributes to the understanding of molecular mechanisms of AS. This review aims to provide an insight into these interactions and their underlying roles in the progression of AS, highlighting potential pharmacological targets against the atherosclerotic inflammatory process.

KEYWORDS

NF-κB, endoplasmic reticulum stress, atherosclerosis, unfolded protein response, NLRP3 inflammasome, reactive oxygen species

Introduction

The transcription factor NF-κB regulates immunity by controlling the expression of genes associated with inflammation. In mammals, five proteins belonging to the NF-κB family have been identified, NF-κB1 (p50), NF-κB2 (p52), RelA (p65), RelB, and cRel (**Table 1**). NF-κB exists in the cytoplasm in the form of homodimer (e.g., p50) or heterodimer (e.g., p50/p65) as a family of structurally related proteins (1, 2). It moves into the nucleus to transcribe target genes upon activation. Highly conservative NF-κB plays critical and stable roles in the immune response or embryonic development of many species (3). Recently, some studies have found that the NF-κB signaling pathway is associated with therapy resistance in breast and ovarian cancer (4, 5). On the other hand, accumulating evidence has proved that the NF-κB signaling pathway plays a key role in the development of many inflammatory metabolic diseases such as obesity, insulin resistance, and atherosclerosis (AS) (6).

The endoplasmic reticulum (ER) is an organelle responsible for protein folding. In the ER, unfolded or misfolded proteins are detected and retained until they are properly folded or degraded. Disturbance in ER protein homeostasis leads to ER stress, activating a specific signaling pathway termed the unfolded protein response (UPR). The UPR is initiated by activation of three ER membrane-bound transducers including inositol requiring enzyme 1 (IRE1), activating transcription factor 6 (ATF6), and protein kinase-RNA like ER kinase (PERK), which alleviates ER stress and helps cells adapt to and survive from ER stress caused by various stimuli (7). However, if the ER stress cannot be resolved, the UPR initiates programmed cell death.

Atherosclerosis is a chronic inflammatory disease contributing to the main pathological basis of ischemic heart disease, myocardial infarct and stroke (8, 9). Increasing evidence has documented that both NF-κB and ER stress closely affect the course of AS, and targeting those pathways may provide new approaches for the treatments against it (10). Herein, some interesting crosstalk in the molecular signaling pathways between NF-κB and ER stress in AS has been reviewed. In this regard, it is reasonable that these links may also be related to AS, which may offer promising opportunities for new strategies against AS.

Composition and regulation of NF-κB

The NF-κB signaling

NF-κB activation is initiated from extracellular stimulation signals and is precisely regulated. NF-κB1 (p50) and NF-κB2 (p52) are produced by cleavage of precursors p105 and p100, respectively. In resting cells, NF-κB is kept in the cytosol in its inactive form by binding to IκB (inhibitor of NF-κB) molecule (11). This binding prevents its nuclear localization and transcriptional function by masking the nuclear localization sequence (NLS) at the C-terminus of Rel Homology Region (RHR) (12). RelA (p65), RelB, and cRel contain a transactivation domain (TAD) at the C-terminal end which is responsible for transcribing target genes (**Table 1**) (13). Thereby, NF-κB dimer consisting of at least one of these three subunits is an active transcription factor, whereas NF-κB containing only p50 and p52 suppresses transcription due to lack of TAD, despite being able to bind to DNA (14).

IκB proteins consist of three groups: the classical IκB proteins, the precursor proteins, and the atypical (nuclear) IκB proteins (14) (**Table 1**). All of them have an ankyrin repeat sequence (AnkR) for interaction with Rel proteins (2, 15). IκBα, IκBβ, and IκBε belong to the typical group and share the conserved two serine residues at the N-terminal whose phosphorylation regulates the ubiquitination of itself (11). IκBα is associated with dimers of p50-RelA or p50-cRel. It keeps NF-κB in the cytoplasm through an exclusive nuclear export sequence that is exposed when bound to NF-κB. In contrast, NF-κB with IκBβ can locate in the nucleus stably. IκBε and IκBα are found to be the negative feedback regulators of NF-κB back to the cytoplasm (16, 17). NF-κB precursors, p100 (IκBδ) and p105 (IκBγ), also inhibit NF-κB by assembling into high-molecular-weight complexes (18). Phosphorylation of p105 targets it for complete degradation, but it may also promote p105 to be processed into p50 in some cell types (19–21), forming p50-RelA, p50-cRel, or p50 homodimers. Atypical IκB proteins include IκBζ, BCL-3, and IκBNS (**Table 1**). The most distinct feature of classical IκBs is their extra functions to positively regulate NF-κB (22).

When cells are stimulated by cytokines or pathogen-associated molecular patterns (PAMPs) binding to membrane receptors, signaling cascades initiate and finally converge on the activation of the IκB kinase (IKK) complex (23). The IKK complex consists of three subunits, the catalytic subunits IKKα (IKK1) and IKKβ (IKK2), and the regulatory subunit NF-κB essential modulator (NEMO or IKKγ) (**Table 1**). IκBs are phosphorylated by the IKK complex, then selectively ubiquitinated by E3 ubiquitin ligase (24), and finally degraded by the proteasome, thus allowing NF-κB translocation to the nucleus. In the nucleus, it is bound to the coactivator molecule to have optimal transcriptional activity (25), leading to gene transcription of growth factors, cytokines, chemokines, adhesion molecules, and other immunoregulatory molecules (**Figure 1**).

The activation of NF-κB signaling

Under various stimuli like cytokines, lipopolysaccharide (LPS), UV irradiation, intracellular stresses, and autoantibodies,

TABLE 1 Components and characteristics of the NF-κB signaling pathway.

Components	Subunits/Precursors	Functions	Structure
NF-κB	NF-κB1 (p50)/p105	Nuclear localization and DNA binding activity; inhibition of transcription	
	NF-κB2 (p52)/p100		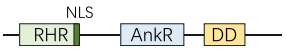
	RelA (p65)	Transcription activity for NF-κB target genes	
	RelB		
	cRel		
IκB	IκBα	Releasing NF-κB dimer by poly-ubiquitination and degradation	
	IκBβ		
	IκBε		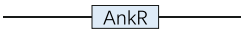
	p100 (IκBδ)	Inhibition of NF-κB by assembling into high-molecular-weight complexes; or being processed into NF-κB subunits	
	p105 (IκBγ)		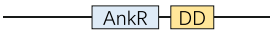
	IκBζ	Modulating NF-κB transcription either positively or negatively	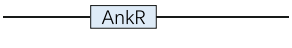
	BCL-3		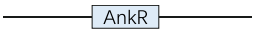
	IκBNS		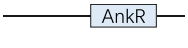
IKK complex	IKKα (IKK1)	Kinase activity	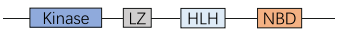
	IKKβ (IKK2)	Kinase activity	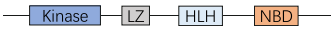
	NEMO (IKKγ)	Regulatory and non-enzymatic	

RHR, Rel homology region; NLS, nuclear localization sequence; AnkR, ankyrin repeats; DD, death domain; TAD, transactivation domain; PEST, region rich in proline, glutamate, serine, and threonine; LZ, leucine zipper; Kinase, kinase domain; HLH, helix-loop-helix region; NBD, NEMO-binding domain; CC, coiled-coil domain; Zn, zinc-finger.

NF-κB is activated and triggers modification signals. The activation involves two signaling pathways: the canonical and the non-canonical (alternative) pathway (26).

The canonical pathway is initiated by tumor necrosis factor receptor (TNFR), T cell receptor (TCR), Toll-like receptor (TLR), and interleukin 1 receptor (IL-1R), leading to rapid but transient NF-κB activation (23, 27). Upon TNF-α binding, TNFR1 drives the assembly of the E3 ubiquitin ligases cellular inhibitor of apoptosis (cIAP) as well as TNFR-associated factor (TRAF) 2 with the protein kinase receptor-interacting protein 1 (RIP1) (28). RIP1 is then ubiquitinated and bound to NEMO (29), forming TGF-β activated kinase 1 (TAK1)-IKK complex. TAK1 phosphorylates and activates IKKβ as well as modification signals. TCR activates NF-κB through the recruitment of CARD11/Bcl10/MALT1 (CBM) complex (30, 31), which is then ubiquitinated by recruiting TRAF6, resulting in the activation of TAK1 as well as IKK (32). TLR and IL-1R initiate signaling through recruiting myeloid differentiation primary response gene 88 (MyD88) directly (33) or indirectly (34) which induces the recruitment of IL-1 receptor-associated kinase (IRAK) 1/4, followed by TRAF6 to activate TAK complex and intracellular signaling cascades (35, 36) (**Figure 1**). Sequentially, variant modification signals are converged on the activation of TAK1, which activates the IKK complex *via* phosphorylation of IKKβ. IκB family members phosphorylated by IKK undergo ubiquitin-dependent degradation, releasing the canonical NF-κB dimers, predominantly the p50-RelA and p50-cRel (**Figure 1**). The regulation of the canonical NF-κB pathway occurs at different levels to maintain homeostasis. Firstly, NF-κB transcribes IκBα and IκBε genes to form negative feedback (37). NF-κB activity is also controlled at the transcriptional factor level. For example, IKKα and ubiquitin ligase complex mediate the turnover of RelA (38) and impede its binding to DNA (39). In addition, deubiquitylation of

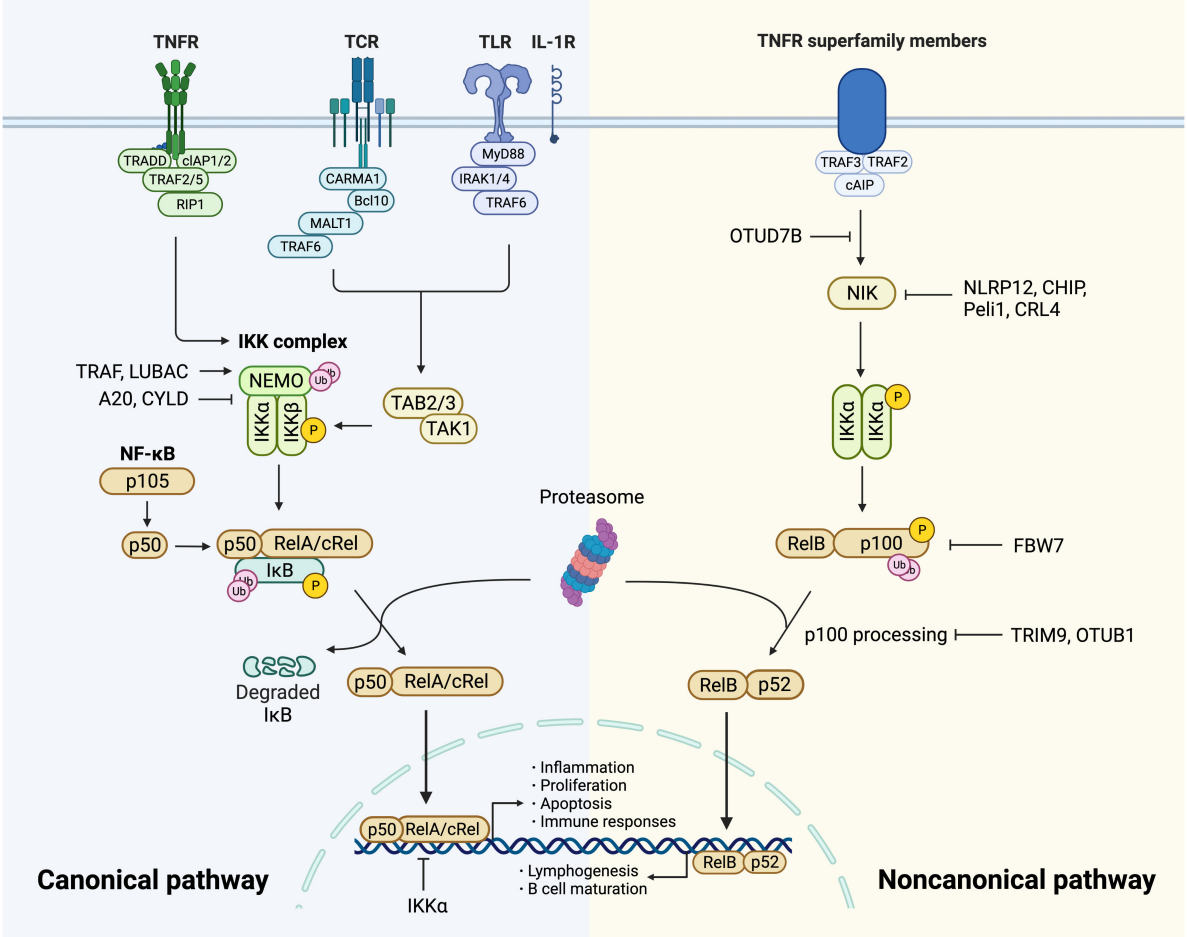

FIGURE 1
Canonical and non-canonical NF-κB pathway. *The canonical pathway* is induced *via* activation of receptors like TNFR, TCR, TLR, and IL-1R. When TNFR is activated by ligands, it recruits TRADD and drives the assembly of cIAP, TRAF, and RIP1 which is then recruited to NEMO and subsequent formation of IKK complex. TCR recruits CBM complex which is then ubiquitinated by TRAF6, resulting in the activation of TAK1. TLR and IL-1R recruits MyD88 and IRAK1/4, followed by TRAF6 to activate TAK and then IKK complex. TAK1 phosphorylates and activates IKK complex *via* phosphorylation of IKKβ. Then IκB family members phosphorylated by IKK undergo ubiquitin-dependent degradation, resulting in the release of NF-κB dimers. The canonical NF-κB pathway is regulated precisely. IKKα impedes RelA binding to DNA in nucleus. A20 and CYLD destabilize IKK complex *via* their deubiquitination activities. The activity of NF-κB is increased by TRAF- and LUBAC-mediated ubiquitination of NEMO. *The non-canonical NF-κB pathway* is initiated from the stimulation of specific TNFRs, which triggers the recruitment of TRAF3-TRAF2-cIAP and eventually results in stabilization and accumulation of NIK, which is impeded by deubiquitinase OTUD7B. Degradation of NIK is promoted by NLRP12, CHIP, Peli1, and CRL4. NIK phosphorylates and activates IKKα, triggering phosphorylation and ubiquitylation of p100. RelB and p52 generated from p100 constitute NF-κB heterodimer that conducts nuclear translocation and gene transcription. TRIM9 and OTUB1 inhibit p100 processing and FBW7 mediates p100 destruction.

signal molecules upstream of IKK is important in the negative regulation. A20 modifies signaling molecules, especially NEMO to destabilize the IKK complex and down-regulate inflammatory response (40). Tumor suppressor protein cylindromatosis (CYLD) also inhibits the activation of IKK by a similar mechanism (41). IKK inhibitors suppress thrombosis by blocking soluble N-ethylmaleimide-sensitive factor attached protein receptor (SNARE) complex formation and platelet secretion, thus mitigating late-stage plaque development (42). Lastly, canonical NF-κB is positively regulated by ubiquitination of NEMO through TRAF and linear ubiquitin chain assembly complex (LUBAC), which is crucial for IKK activation (43) (**Figure 1**).

The non-canonical pathway is activated slowly and persistently compared to the canonical one. It has a central signaling component, NF-κB-inducing kinase (NIK), equivalent to TAK1 in the canonical pathway. The signaling cascade is based on the stimulation of specific TNFRs by CD40 ligand, B cell-activating factor (BAFF), and lymphotoxin-β (14). The process initiates from TRAF3-TRAF2-cIAP recruitment and ends up with NIK activation (44). NIK phosphorylates and activates IKKα (23, 45, 46), which mediates phosphorylation

of p100, triggering its ubiquitylation *via* recruitment of the E3 ubiquitin ligase βTrCP (47–49). The processing of p100 generates p52, resulting in the nuclear translocation of p52-RelB heterodimer. Since the non-canonical activation relies on the generation of p52 from p100, the processing of p100 lies in the key position of regulation. This process is dependent on ubiquitination and phosphorylation, which are regulated by specific ubiquitin E3 ligase and NIK-IKKα axis, respectively. The former includes tripartite motif family 9 (TRIM9) which inhibits NIK-induced and β-TrCP-dependent p100 processing (50). FBW7, also an E3 ligase, exclusively interacts with glycogen synthase kinase 3β (GSK3β) phosphorylated p100 and mediates its destruction (51). OTUB1 is a deubiquitinase that stabilizes p100. As a pivotal node in the non-canonical pathway, NIK has a significant role in NF-κB regulation. Its degradation is promoted by NOD-like receptors family pyrin domain-containing (NLRP) 12 and E3 ligases, CHIP, Peli1, and CRL4 (14). Additionally, OTUD7B, an A20-like protein, deubiquitinates TRAF3 and thus negatively regulates signal-induced non-canonical NF-κB (52) (**Figure 1**).

Notably, apart from those pathways mentioned above, ER stress has emerged as an important trigger upstream of NF-κB. NF-κB activation mediated by ER stress is dependent on Ca^{2+} efflux and subsequent production of reactive oxygen species (ROS) (13). More mechanisms and interactions will be discussed in detail later in this review.

The NF-κB and ER stress in atherosclerosis

Three stages of atherosclerosis progression

Atherosclerosis is a common chronic inflammatory disease characterized by the accumulation of fibrin and lipids in subendothelial space, being a leading cause of cardiovascular diseases, including heart failure, stroke, and claudication (53, 54). AS dominantly occurs in the intima of middle and large-sized arteries, where endothelial cells are exposed to excessive shear stress. Vessel stenosis resulting from atherosclerotic plaque could induce CVD by abolishing blood flow. However, the dominant mechanism linking AS and CVD appears to be the vulnerability of plaque (55). Vulnerable plaque rupture exposes prothrombotic components, triggers the clotting cascade, and leads to atherothrombosis (56). Notably, inflammation is the pivotal cause of plaque progression and vulnerability.

Loss of intact endothelial functions occurs at the earliest in atherogenesis, followed by lipid accumulation and fatty streak formation under the endothelial cells. Fatty streak is a reversible lesion that can appear as early as childhood. In this process, multiple molecules mediate leukocyte adhesion, extravasation, migration, chemotaxis, activation, and the formation of foam cells from macrophages by uptake of lipids. Then the nascent plaque generally develops and forms a complex lesion with migration and proliferation of vascular smooth muscle cells (VSMCs), which secrete extracellular matrix such as collagen accumulated in the plaque (57) (**Figure 2A**). As plaque progresses, a necrotic core containing necrotic material, foam cells, cholesterol crystals, and lipids is formed and developed. Necrotic cores are considered to further promote inflammation, plaque rupture, and thrombosis by storing inflammatory mediators, matrix proteases, and thrombotic molecules (**Figure 2B**). A fissure of the fibrous cap eliminates the barrier between the tissue factor rich in the lipid core and the coagulation factors in the bloodstream, which triggers a clotting reaction and leads to thrombosis in advanced atherosclerotic lesions (58–61). Finally, the rupture of advanced plaque from the instability of the fibrous cap is primarily determined by the level of interstitial collagen (62). In addition, the disruption of fragile neovasculature in atherosclerotic plaques provides a possibility of sudden plaque progression (63) (**Figure 2C**).

NF-κB has been regarded as a critical player in atherogenesis over the past decades partly because the genes it transcribed mediate all three phases of AS (64–66). Studies have revealed that IKK/NF-κB signaling promotes atherogenesis and that targeting NF-κB is a treatment strategy against AS and CVDs (67). Nevertheless, sufficient evidence proves that NF-κB activation leads to both protective and destructive outcomes (68). Research suggests that ER stress is associated with various lesions during AS and affects the disease course, which occurs in endothelial cells, VSMCs, and macrophages by integrating protein and lipid metabolism, cell death, and inflammatory responses (69).

Taken together, it is important to figure out how the NF-κB, ER stress-related molecules, and their functional crosstalk intervene in three stages of AS, including atherogenesis (plaque formation), plaque progression, and plaque instability.

NF-κB and ER stress in early atherosclerotic lesion formation

Endothelial dysfunction, an initial factor in early atherosclerotic lesion formation, is induced by NF-κB and downstream production of inflammatory cytokines, such as IL-6 and TNF-α (70). Regenerated endothelial cells produce a large amount of NO and aggravate inflammatory response, leading to the formation of plaque (71). A recent study found that RIP1 primarily drives inflammatory cells toward activation in early atherosclerotic lesion formation in an NF-κB-dependent manner (10). Moreover, inhibiting cyclooxygenase-2 (COX-2) expression, a downstream gene of NF-κB, dramatically impedes the early evolution of AS (72). CCL20, a chemokine exerting selective attraction to lymphocytes, is upregulated

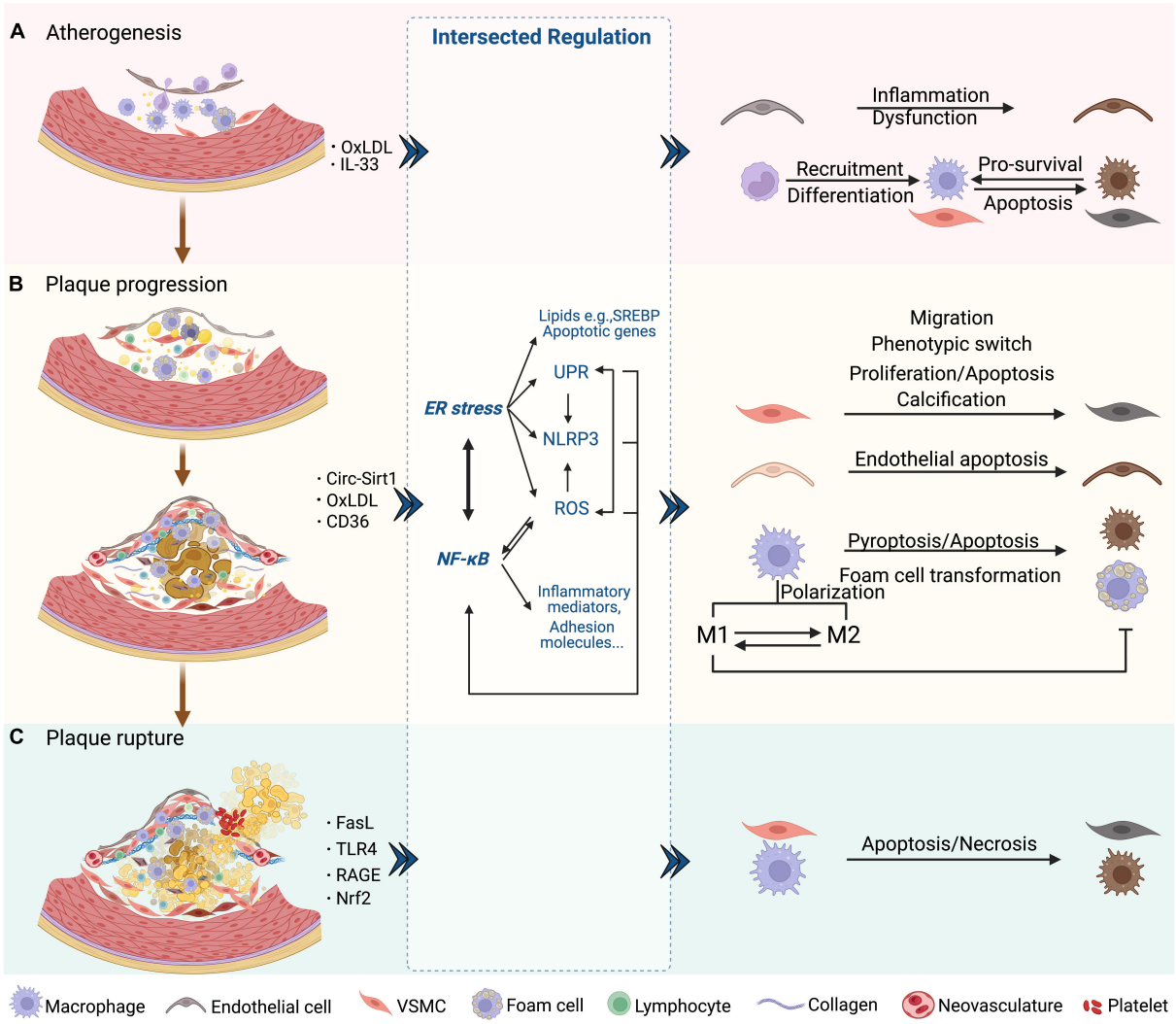

FIGURE 2

NF-κB and ER stress in three phases of AS. **(A)** Atherogenesis. Endothelial dysfunction as an initial event in atherogenesis is induced by NF-κB and downstream inflammatory mediators. The SREBP pathway is induced by ER stress and aggravates endothelial dysfunction. SREBP- and NF-κB-induced NLRP3 inflammasome contributes to atherogenesis. Chemokines induced by NF-κB attract lymphocytes and trigger endothelial inflammation. NF-κB also promotes the recruitment and differentiation of monocytes by increasing the levels of adhesion molecules and M-CSF of endothelial cells. After differentiated into macrophages, UPR markers are activated, which protects macrophages from ER stress-induced apoptosis. **(B)** Plaque progression. This phase is characterized by foam cell formation, VSMC migration and proliferation, ECM accumulation, and NC formation. ROS/NF-κB regulates the migration and phenotypic switch of VSMCs. Circ-Sirt1 inhibits NF-κB and thus alleviates the progression of AS. Macrophages uptake oxLDL *via* CD36 and this triggers the NF-κB signaling pathways, which promotes the transformation into foam cells. XBP-1 also regulates foam cell formation, endothelial apoptosis and VSMC calcification. Inhibition of ER stress promotes the formation of M1 subtype and subsequent foam cell formation. In macrophages, activated NLRP3 inflammasome causes pyroptosis and apoptosis *via* caspase. **(C)** Plaque rupture. This phase is characterized by less SMCs and collagen, and more lipids and macrophages, which could involve NF-κB-FasL pathway. Macrophages induce plaque rupture by secreting MMPs, which is regulated by TLR4/NF-κB and RAGE/NF-κB signaling. Apoptosis of macrophages and VSMCs is induced by the prolonged ER stress, including PERK and IRE-XBP1. CHOP is also a mediator of apoptosis, vascular remodeling and plaque necrosis, whose expression is promoted by UPR signaling. Nrf2, as a synergistic mediator between NF-κB and ER stress, has an athero-protective role by upregulating some antioxidant enzymes. Additionally, NLRP3 inflammasome-mediated up-regulation of MMPs predisposes plaque to rupture.

by NF-κB and is strongly associated with vascular endothelial inflammation (73). At this early stage, NF-κB also participates in the production of adhesion molecules in the endothelium, including E-selectin, VCAM-1, and intercellular adhesion molecule-1 (ICAM-1), promoting the recruitment of monocytes (**Figure 2A**). The effects of NF-κB activation in the early stage of AS are not limited to endothelial cells but also occur in various cell types within the plaque (57). CCL20 is overexpressed

in VSMCs of atherosclerotic lesions from coronary artery patients, triggers the inflammatory response, and significantly induces human lymphocyte migration (74). Besides, IL-33 upregulates the macrophage-colony stimulating factor (M-CSF) of endothelial cells through the NF-κB pathway, promoting the differentiation of monocytes (75).

Unfolded protein response activation in endothelial cells can be observed at the very beginning of AS. In athero-susceptible regions, activation of IRE1α and ATF6 is consistent with a high expression of molecular chaperones in ER. Additionally, ATF4 and CCAAT/enhancer-binding protein (CEBP) homologous protein (CHOP) mRNA are highly expressed, along with activated PERK pathway in VSMCs and macrophages at this stage (76) (**Figure 2A**). UPR activation aims to be a protective response to harmful stress and promotes cell survival in early atherosclerotic lesion formation. For example, UPR is a vital modulator of the sterol regulatory element binding protein (SREBP) pathway to maintain lipid homeostasis and inflammatory response, which are important contributors to atherogenesis (77–79).

NF-κB and ER stress in plaque progression

NF-κB plays a considerable part in cell survival in addition to well-known pro-inflammatory functions, and the two directions may counteract each other in AS progression (80). Research has suggested that IKKβ deletion increases AS in LDLR deficient mice instead of preventing atherogenesis (68). Given the death of foam cells facilitates the necrotic core due to a defect in clearing accumulated lipids, more attention should be paid to NF-κB's roles in limiting plaque size other than in pro-inflammation.

NF-κB activation regulates the migration and proliferation of VSMCs, whereas the detailed mechanism is still controversial (81, 82). A study by Mehrhof et al. shows that in a knock-in mouse model expressing the NF-κB super repressor, the proliferation rates of VSMCs did not differ from those in wild-type when stimulated by platelet-derived growth-factor-BB (PDGF-BB) or serum. Further study indicated that VSMC proliferation is regulated by classical mitogenic signaling pathways (MAPK and PI3K pathways) rather than NF-κB (81). These results implicate that NF-κB may essentially play a role in apoptosis and inflammatory responses in VSMCs instead of pro-survival or growth signal in the progression of AS. NF-κB-mediated phenotypic switch of VSMCs involves increased synthesis capacity and decreased contraction capacity, which is closely linked with the accumulation of extracellular matrix and plaque promotion in the progression of AS (83–85). Additionally, blocking ROS/NF-κB/mTOR/P70S6K signaling pathway prevents PDGF-BB-induced VSMC phenotypic switch, multiplication, and migration (83). Circ-Sirt1, as a non-coding RNA (ncRNA) regulator of VSMC phenotype, inhibits NF-κB translocation and binding to target DNA by directly interacting with the p65 subunit in the cytoplasm and facilitating the level of SIRT1 mRNA, respectively, which alleviates neointimal hyperplasia and the progression of AS (85) (**Figure 2B**). NF-κB activated by autoantibodies is also an important mediator in atherosclerotic lesion growth. 27-kDa heat shock protein (HSP27) in the blood combines with IgG anti-HSP27 auto-antibodies to form an immune complex, which has a role in anti-inflammation and anti-atherosclerosis. HSP27 immune complex activates TLR4/NF-κB signaling and increases the level of anti-inflammatory cytokine IL-10 in macrophages. Moreover, HSP27 immune complex reduces form cell formation by inhibiting oxidized low-density lipoprotein (oxLDL) binding to scavenger receptors (86). In addition, under ER stress, chaperone protein 78 kDa glucose-regulated protein (GRP78) dissociates from ER and moves to the cell surface, resulting in the generation of anti-GRP78 autoantibodies which activate NF-κB and induce the expression of adhesion molecules in human endothelial cells (87).

Generally, macrophages are divided into M1 and M2 subtypes, which have pro-inflammatory and anti-inflammatory effects, respectively. In atherosclerotic plaques, both subtypes are identified and play important roles in plaque progression (**Table 2**). The disruption of balance is speculated to accelerate foam cell formation and be related to plaque vulnerability (88). M2 subtype is prone to apoptosis as a result of oxLDL toxicity, leading to the accumulation of necrotic material within the plaque (89). NF-κB signaling pathway affects the transition from macrophages to foam cells and its further accumulation in the subendothelial space underlying atherosclerotic disease. In macrophages, oxLDL is taken *via* CD36 and other scavenger receptors and is resistant to the lysosomal enzymes (90). It signals *via* CD36-TLR4-TLR6 and triggers the NF-κB signaling pathway to produce proinflammatory cytokines (91). MiR-216a was found to promote telomerase activation in macrophages *via* the Smad3/NF-κB pathway, contributing to the transition from M2 to M1 (92). Applying fullerene derivatives inhibits the oxLDL-induced differentiation of macrophages into lipid-laden foam cells and plaque progression of apolipoprotein (Apo) E knock-out mice arteries. Mechanically, fullerene derivatives alleviate oxidative stress, inhibit CD36 receptor expression, and reduce TRAF2/NF-κB pathway activation (93).

Endoplasmic reticulum stress is also a pivotal mechanism regulating plaque progression. Spliced X-box binding protein-1 (XBP-1), a molecule downstream of IRE1 and ATF6, modulates many aspects involved in AS progression, such as macrophage apoptosis, foam cell formation, and IL-8 and TNF-α production. Uncontrolled activation and excessive expression of splicing XBP-1 contribute to endothelial apoptosis and eventually AS evolution, as discovered in the branches and plaques of arteries in ApoE knock-out mice, which may also be related to induction of VSMC calcification (94, 95) (**Figure 2B**). ER stress is

also considered to have an important role in macrophage differentiation. Inhibition of ER stress affects lipid metabolism characterized by an increase in cholesterol efflux, which shifts the M2 subtype to M1 and reduces foam cell formation (96). These studies imply that inhibition of ER stress, which promotes transition toward M1, may decrease foam cell formation, inhibit macrophage apoptosis, and block plaque development.

NF-κB and ER stress in advanced atherosclerosis

During the last decades, people have been trying to understand the pathophysiology of atherosclerosis, though the precise mechanisms underlying plaque destabilization still remain unclear. In this phase, studies have suggested that macrophages secrete proteases, especially matrix metalloproteinase-9 (MMP-9), to destroy elastin, fibrin, and other matrix proteins that the tension of the fibrous cap comes from, making macrophages an important player in plaque destabilization (97). Several studies support that downregulation of MMP-9 expression in macrophages is mediated by suppressing TLR4/NF-κB signaling, which is associated with attenuation of plaque vulnerability (98, 99). Receptor for advanced glycation end products (RAGE) is a key factor for plaque destabilization in diabetes mellitus, where its downregulation may suppress atherosclerotic plaque development, an effect mediated by NF-κB inhibition (100, 101). Statistical analysis of atherosclerotic lesions from carotid arteries revealed colocalized NF-κB activation and FasL overexpression, and a similar result was also found in peripheral blood mononuclear cells (PBMCs), indicating the NF-κB/FasL pathway may contribute to plaque vulnerability (102) (**Figure 2C**).

Advanced atheroma provides environmental and molecular bases that trigger ER stress and the UPR. ER-resident molecular chaperone, GRP78/94, and HSP47 are predominantly localized to the VSMC-rich fibrous cap of advanced plaques, suggesting activation of the UPR in VSMCs (103). On the other hand, under prolonged and enhanced ER stress, the activated PERK pathway promotes the level of death effector, and IRE1α/XBP-1 may activate the apoptosis signaling pathway in macrophages and VSMCs at this stage (104, 105). Thin-cap atheroma and ruptured plaques display abundant dead macrophages and VSMCs featuring strongly activated PERK/CHOP which is a mediator of apoptosis on chronic ER stress and a contributor to vascular remodeling and plaque necrosis (106–108) (**Figure 2C**). The effects of ER stress on the advanced plaque in macrophages are further demonstrated in AS-prone mice lacking CHOP, which shows blockage of macrophage apoptosis and inhibition of necrotic core formation (107, 109, 110).

TABLE 2 Differences between M1 and M2 macrophages in atherosclerosis.

	M1	M2
Polarization stimuli	Cholesterol crystals; LPS; Pro-inflammatory cytokines; OxLDLs	TGF-β; IL-10; IL-4; IL-13
Activation pathway	TLR-4 or NF-κB pathway	LXR-α (liver X receptor-α)
Secretion of cytokines	TNF-α; IL-1β; IL-6; IL-12; IL-23	IL-10; TGF-β
Predominant metabolism	Aerobic glycolysis; Fatty acid synthesis; Production of mitochondrial ROS	Oxidative phosphorylation; Fatty acid oxidation (β-oxidation)
Localization	Plaque shoulder and lipid core	Adventitia and areas of neovascularization
Association with plaque stability	Abundant in symptomatic and unstable plaques	Abundant in stable zones of the plaque and asymptomatic lesions
Roles	Occurrence of postapoptotic necrosis after dead cell accumulation; Formation of a necrotic core; Contribution to plaque instability and rupture	Phagocytosis of apoptotic cells and debris; Increase of lipid degradation and prevention of foam cell formation; Resolution of inflammation

The molecular interrelated roles of ER stress and NF-κB in atherosclerosis

Various pathological factors which activate NF-κB, such as ROS, lipids, TLR ligands, and some cytokines (e.g., TNF-α and IL-1), disrupt ER homeostasis and activate the UPR, leading to the situation called ER stress (111). Of note, this relationship is not likely one-sided. There are several potential avenues through which ER function also affects inflammatory signaling. And their interplay constitutes the pathological basis of many inflammatory and metabolic diseases, including AS (112–114). The ER stress is initiated with the dissociation of chaperone proteins such as GRP78/Bip and GRP94 with the ER stress sensor proteins (IRE1α, PERK, and ATF6), which leads to UPR activation. Chaperones also directly participate in subsequential UPR and NF-κB signaling. ATF6 and IRE1α pathways promote the transcription of the ER chaperones, which is necessary for the alleviation of the misfolded proteins to restore homeostasis (115). GRP78 is a member of the chaperone HSP70 family which is closely relevant to the endothelial dysfunction in the development of AS, with a fundamental role in protecting

protein stabilization and also in anti-inflammation (116). Note that HSP70s suppress the expression of inflammatory cytokines *via* inhibiting the NF-κB. HSP70s stabilize the IκB complex through its binding and block IKK kinase activity and further NF-κB mediated transcription (117, 118).

Three branches of UPR (IRE1α, PERK, and ATF6) of ER stress have been reported to have crosstalk with many inflammation-related signaling, including the NF-κB pathway. For example, activated IRE1α and recruited TRAF2 activate JNK, inducing the production of IL-6 and TNF-α by phosphorylation of AP-1 and consequent NF-κB activation. ER stress induces TRAIL receptor activation which leads to apoptosis through the FADD/caspase-8 pathway, or alternative production of inflammatory cytokines through NF-κB activation (119–121). However, ER stress can also lead to inhibition of inflammation. The ER E3 ubiquitin ligase TRIM13 ubiquitylates the IKK regulatory subunit NEMO, blocking the degradation of IκBα, which consequently inhibits NF-κB translocation into the nucleus (122). Hence, it makes sense to unravel the exact molecular mechanisms of ER-stress-induced inflammation. Here we focus on how ER stress intersects with NF-κB through various inflammatory signaling pathways to form this integrated network (**Figure 3**).

Crosstalk through IRE1α

Several signal cascades have been discovered in the NF-κB activation *via* IRE1α kinase activity. Activated IRE1α kinase recruits TRAF2, which associates with IKK and degrades IκBα to activate NF-κB (123). It is confirmed in endothelial cells that LPS induces ER stress and overproduction of IL-6 and MCP-1 through IRE1α/NF-κB pathway, resulting in endothelial dysfunction (124). Moreover, Keestra et al. found that *Brucella abortus* infection triggered ER stress and induced inflammation and IL-6 production in a TRAF2, nucleotide-binding oligomerization domain-containing protein (NOD) 1/2, and RIP2-dependent manner, providing a novel connection between ER stress and NF-κB activation (125). IRE1α is also linked with the RIDD/RIG-I pathway upon encountering viral RNAs, which induces an inflammatory response through MAVS and downstream NF-κB (126). In addition, IRE1α oligomerization generates spliced XBP-1 mRNAs that are translated into potent transcription factors (127). Increased XBP-1 expression contributes to the secretion of myeloperoxidases, TNF-α, IL-6, and IL-1β, and is negatively correlated with NF-κB expression in the colon (128). Also, ER stress-induced IRE1α activation mediates GSK3β activation and subsequent IL-1β gene expression (129). XBP1s K60/77R mutation, preventing the ubiquitination and proteasome-degradation of XBP1s, mimics the constitutive activation of IRE1α elevated, and results in the elevated GSK3β phosphorylation (130). *In vivo* and *in vitro* studies have confirmed that GSK-3β activation is involved in NF-κB activation, suggesting crosstalk between ER stress and NF-κB through IRE1α/GSK3β pathway (131, 132).

Interestingly, GSK3β activation inhibits IRE1α-dependent XBP-1 splicing, and they differentially regulate proinflammatory cytokine gene expression, indicating complex signaling crosstalk in inflammatory pathways (**Figure 3**).

Crosstalk through PERK

Protein kinase-RNA like ER kinase branch can induce NF-κB activation essentially by translation attenuation, including the free IκBα, mediated by phosphorylated eIF2α. Zhang et al. observed that anti-dsDNA antibodies activate NF-κB and upregulate various inflammatory cytokines through PERK-eIF2α-ATF4 (133). Besides, a recent study has shown that thapsigargin-induced PERK activation along with the inositol triphosphate receptor (IP3R)-mediated calcium flux makes cells more responsive to *Salmonella typhimurium* through the NOD1-stimulated NF-κB activation and subsequent inflammatory response (134). Nuclear erythroid-related factor 2 (Nrf2), a transcription factor mainly activated by PERK and IRE1, also plays a pivotal role in the crosstalk between UPR and NF-κB. Studies on the linkage between Nrf2 and autophagy have shown that Nrf2 activates IKK and subsequent NF-κB by enhancing the expression of p62, which explains NF-κB-dependent autophagy activation (135–137). Complex interrelation indicates that Nrf2 influences NF-κB both positively and negatively due to various circumstances. For instance, studies on Nrf2 knock-out mouse embryo fibroblasts have shown increased activity of IKKβ and degradation of IκBα (138). Moreover, the increase of Nrf2 activity in patients with lupus nephritis prevents p65 activation by accumulating glutathione. Increased heme oxygenase-1 (HO-1), a product of the Nrf2 target gene, inhibits adhesion molecules such as E-selectin and vascular cell adhesion molecule-1 (VCAM-1) expressed in endothelial cells *via* NF-κB downregulation (139). Additional experiments have implicated the PERK-eIF2α signaling as a contributor to inflammation *via* the JNK and PI3K-Akt pathway, but the detailed interaction with NF-κB has not been well defined (140) (**Figure 3**).

Since Nrf2 serves as a platform of interrelation between NF-κB and ER stress (**Figure 3**), special attention has been paid to this transcription factor to better define its possible contribution to oxidative stress of the vulnerable plaque (141) (**Figure 2C**). The expansion of the necrotic core and the disruption of the plaque are largely determined by the accelerated number of apoptotic cells and phagocytic clearance defect. Nrf2 not only upregulates the expression of different antioxidant enzymes but also regulates mitochondrial ROS production through NADPH oxidase (Nox) activity. Though most studies have demonstrated the protective roles of Nrf2 against AS, several studies have

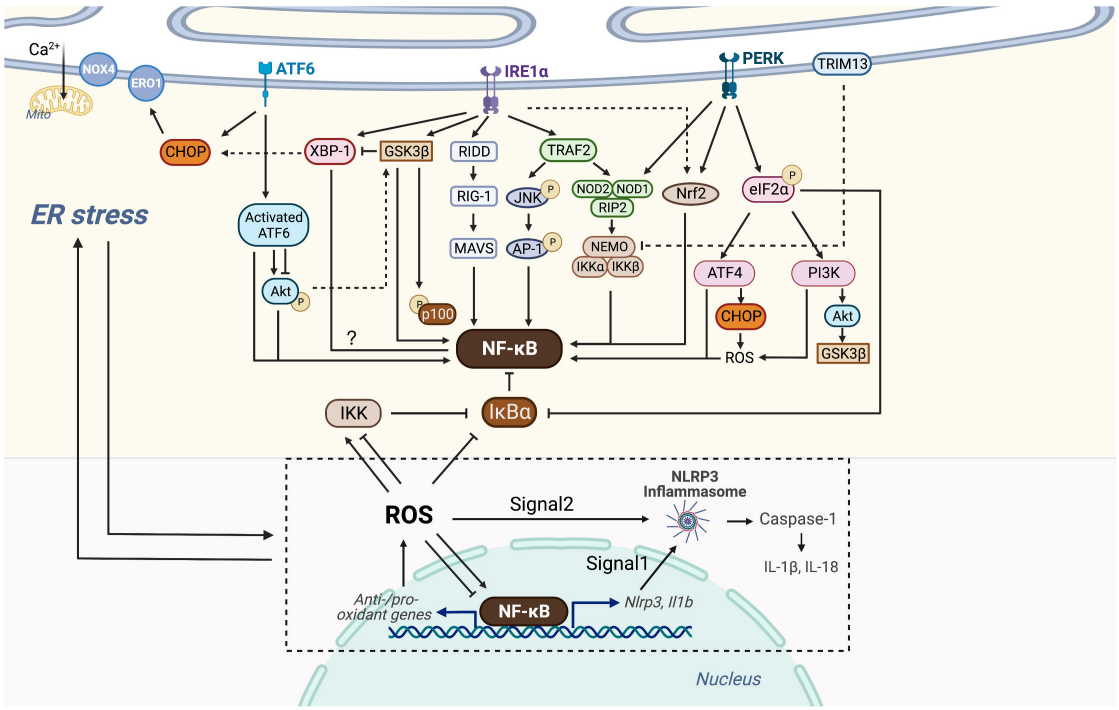

FIGURE 3
Crosstalk of NF-κB and ER stress. Three branches of UPR (IRE1α, PERK, and ATF6) of ER stress are able to intersect with NF-κB. Activated IRE1α recruits TRAF2, which activates JNK and then AP-1 or associates with IKK probably *via* NOD1/2 and RIP2. IRE1α is also linked with the RIDD/RIG-I/MAVS pathway and GSK3β to activate NF-κB. IRE1α oligomerization increases XBP-1 expression which might be associated with decreased NF-κB expression, but GSK3β activation inhibits IRE1α-dependent XBP-1 splicing. PERK branch can induce NF-κB activation essentially by translation attenuation of the free IκBα mediated by phosphorylated eIF2α. Additionally, PERK-eIF2α could also contributes to inflammation *via* ATF4 or PI3K-Akt pathway. Both of NOD1 and Nrf2 could be activated by PERK and IRE1, but Nrf2 has both positive and negative effects on NF-κB, dependent on cellular circumstances. Through the ATF6 branch transient phosphorylation of Akt activates NF-κB, whereas ATF6 activation could inhibit Akt-GSK3β and enhance NF-κB signaling. Additionally, ER E3 ubiquitin ligase, TRIM13 ubiquitylates NEMO and prevents nuclear translocation of NF-κB. CHOP could be activated by all three branches of UPR, causing ROS-mediated ER stress and NF-κB inhibition or activation. ER stress-induced NLRP3 inflammasome is dependent on NF-κB and UPR activation. Signal 1 of NLRP3 inflammasome activation is transcriptional upregulation of NLRP3 along with pro-IL-1β provided by NF-κB. Signal 2 is a posttranscriptional modification which can be provided by ROS. NF-κB controls the levels of ROS by regulating anti-oxidant and pro-oxidant genes, and ROS in turn inhibits or enhances the DNA binding activity of NF-κB itself, depending on modifications of NF-κB. ROS also regulates the IKK complex and phosphorylates IκBα. ROS produced by Nox4 transduces ER stress signals to the UPR to maintain homeostasis, whereas ROS produced by ERO1 or mitochondrial damage leads to cell death. ROS, NF-κB, NLRP3 inflammasome and the production of IL-1β and IL-18, in turn, trigger chronic ER stress.

revealed that it might play antagonistic roles, both preventing and enhancing AS. Studies found that laminar blood flow stimulates the anti-atherogenic activation of Nrf2, whereas oscillatory blood flow promotes the opposite effect (142). Nrf2 in bone marrow-derived cells promotes plaque progression in ApoE knock-out mice (143), while early AS is aggravated in LDLR knock-out mice with Nrf2-deficient macrophages (144). The positive atherogenic role of Nrf2 appears to be implemented by IL-1 release and by promoting foam cell formation through the expression of the CD36 scavenger receptor (145, 146).

Crosstalk through ATF6

As one of the UPR branches, ATF6 also plays a nonnegligible role during ER stress and in its crosstalk with NF-κB. However, Yamazaki et al. have confirmed that subtilase cytotoxin-triggered rapid cleavage of molecular chaperone GRP78/BiP (78-kD glucose-regulated protein/immunoglobulin heavy chain binding protein in pre-B cells) leads to Akt phosphorylation mediated by ATF6, contributing to downstream NF-κB activation (147). Recently, another study reported that the decrease of ATF6 expression induced by miR-149 might attenuate inflammation and apoptosis through NF-κB and Akt signaling cascades (148). In addition, *in vitro* study showed that ATF6 activation induced by chemical agents inhibits Akt/GSK3β and increases NF-κB activity, thus improving the pro-inflammatory effect of TLR4 in ER-stressed macrophages (149). Despite representing unique signaling cascades, ample evidence has indicated that the UPR and NF-κB may converge on nuclear transcription factors, such as ATF3/4/6α, CHOP, and XBP-1 (150) (**Figure 3**). Taken together,

the UPR has crosstalk with NF-κB at various levels, which offers perspectives on the adjustment of cellular stress responses and therapeutic application in the future.

Crosstalk through NLRP3

The NLRP3 inflammasome is a multi-protein complex that recognizes PAMPs or damage-related molecular patterns (DAMPs) and activates the protease caspase-1, leading to pyroptosis and the formation of mature IL-1β and IL-18 to mediate the inflammatory response (151). NLRP3 inflammasome connects lipid metabolism and inflammation because it is activated by crystalline cholesterol and oxLDL in plaques of AS, making it a possible player in the development of AS. In general, transcription and modification signals of the NLRP3 are necessary for its function. The former is provided by the binding of LPS to TLR4, resulting in NF-κB activation and consequent transcription of NLRP3 and IL-1β precursor (152). The modification signals occur after transcription, one of which is BRCA1/BRCA2-containing complex subunit 3 (BRCC3)-mediated deubiquitination (153–155). Though the exact process remains unanswered, it is considered that the activation of the NLRP3 inflammasome is possibly associated with factors such as K^+ outflow, ROS, Ca^{2+} flux, and lysosomal rupture, all of which can provide modification signal (156). Notably, these mechanisms contribute to signal one by activating NF-κB through ROS production. Hu et al. demonstrated that in LPS-induced endometritis in mice, NLRP3 inflammasome is activated *via* ER stress-associated pathway, along with increased NF-κB and ROS (157). In LPS-induced liver injury, NF-κB and the NLRP3 inflammasome activation along with cytokine production such as TNF-α, IL-1β, and IL-18, in turn, contribute to chronic ER stress to form negative feedback (158). A recent study has observed that the ER stress-induced NLRP3 inflammasome is dependent on NF-κB activation and pro-inflammatory cytokine secretion, which is linked to the pathogenesis of atrial fibrillation and can be potentially targeted in cardiac tissue (159). Nevertheless, evidence has revealed that UPR is not indispensable for inflammasome activation (160). Since UPR is involved in NF-κB activation and ROS production, which are related to the activation of the NLRP3 inflammasome, these controversial results call for further insight into UPR pathways as inflammasome mediators (**Figure 3**).

Atherosclerosis has been considered an inflammatory and lipid metabolic condition, and since the NLRP3 inflammasome is activated by lipids such as crystalline cholesterol and oxLDL, it presumably combines different pathological bases of AS. The NLRP3 inflammasome and subsequent caspase-1 activation cause pyroptosis in macrophages after uptake of oxLDL and might contribute to the progression of atheroma (161, 162). On the other hand, the NLRP3 inflammasome induces macrophage apoptosis *via* caspase-8 activation (163), though to what extent this pro-apoptotic function protects against AS development is still unanswered (**Figure 2B**). IL-1β and IL-18 produced by the NLRP3 inflammasome increase the expression of many endothelial molecules such as MCP-1, VCAM-1, and IL-8, involving inflammatory cell adhesion, chemotaxis, recruitment, and activation (164). Moreover, the NLRP3 inflammasome promotes plaque instability and subsequent thrombogenesis (165). Blocking NLRP3 signaling reduces the production of pro-inflammatory cytokines in ApoE knock-out mice and contributes to plaque stabilization by reducing macrophages and lipids as well as increasing SMCs and collagen (166).

Although numerous studies have reported the impact of NLRP3 inflammasome on the progression of AS, evidence has suggested it is not as important as we have thought. *In vivo* NLRP3 inflammasome is not critically implicated in AS progression, infiltration by macrophages, and stability of plaques (167). Research also supported that NLRP1 is more likely to be a critical factor for the initiation of endothelium inflammation (168). In addition, JNK1 and apoptosis signal-regulating kinase 1 (ASK1) contribute to inflammasome activation and caspase-8-mediated macrophage apoptosis, though whether this JNK1/ASK1/caspase-8-dependent apoptosis is directly mediated by NLRP3 inflammasome is uncertain (155). The identified pro-apoptotic activity of NLRP3 inflammasome might produce an anti-atherogenic effect, which could partly explain its controversial functions in AS.

Crosstalk through reactive oxygen species

The relationship between NF-κB and ROS is not one-sided. ROS is a key route linking the two events. Firstly, ROS activates or inactivates the IKK complex in different cell types (169). Often ROS alternatively phosphorylate IκBα, which may result in the release and activation of NF-κB (169, 170). Also, ROS may inhibit or enhance the DNA binding affinity of NF-κB itself, depending on different forms of modification in NF-κB heterodimers (171, 172). Another manner in which ROS interacts with NF-κB is the crosstalk between JNK and NF-κB, preventing persistent JNK activation and promoting cell survival (173).

As to the interactions between ER stress and ROS, it is proved that ROS plays both positive and negative roles during ER stress and in determining cell fate (174). Upon being produced by Nox4, an ER-resident oxygen-sensing enzyme, ROS acts as a signaling intermediate to transduce ER stress-related signals to the UPR, resulting in the correction of the unsteady state. However, ROS as a pro-inflammatory stimulus can further exacerbate inflammation after the UPR activation (111). On the other hand, if ER stress persists, delayed expression of the transcription factor CHOP leads to induction of ER oxidase 1 (ERO1) to produce ROS. Meanwhile,

mitochondria exaggerate ROS production stimulated by the Ca^{2+} released from ER. Both contribute to a secondary increase in ROS, generally leading to cell death. Therefore, ROS lies both upstream and downstream of the UPR, making the network composed of ER stress, ROS, and NF-κB more complex than we have imagined.

Substantial evidence indicates that ROS is a central factor through which ER stress functions cooperatively with NF-κB in inflammation and other cellular processes. Li et al. observed that recombinant *Treponema pallidum* protein regulates the ROS/NF-κB pathway through ER stress. PERK induces the activation of the NF-κB and JNK pathways, leading to the production of IL-1β, IL-6, and IL-8 by macrophages (175). In another study, NF-κB signaling is activated by phosphoinositol 3-kinase δ (PI3Kδ) through ER-associated ROS and RIDD-RIG-I activation, which may induce severe airway inflammation and hyperresponsiveness (176). In human lung cancer cells, it is observed that a CHOP activator induces necrotic cell death *via* ROS-mediated ER stress induction and unusual NF-κB inhibition (177) (**Figure 3**).

The contribution of ROS to AS has been well investigated. ROS causes endothelial dysfunction (178), atherogenesis (179), and LDL oxidation (180). OxLDL has pro-inflammatory effects and participates in the phenotype switching and apoptosis of macrophages and VSMC in the AS progression (181, 182). ROS is positively related to atherosclerotic risk factors, such as diabetes and hypertension, etc. *In vivo* studies of the animal model have also shown that anti-oxidant treatments delay or prevent AS (183), suggesting the aggravating role of ROS in AS. A recent study has demonstrated that nicotine-induced autophagy and subsequent phenotypic transition of VSMCs accelerate AS, which is partly mediated by the nAChRs/ROS/NF-κB signaling pathway (184). In addition, in cultured VSMCs, chicoric acid impeded PDGF-BB-induced VSMC phenotypic alteration, proliferation, and migration mechanistically by blocking ROS/NF-κB/mTOR/P70S6K pathway (83) (**Figure 2B**). However, the diverse effects of ROS have been reported in AS. Nox4 is a major ROS-producing NADPH oxidase and is widely expressed in VSMCs. Its endothelial-specific overexpression increases ROS level, promotes aging, and makes cells susceptible to apoptosis, resulting in aggravated AS lesions in animals (185–187). Of note, it is also found in several mice models that Nox4 knock-out promotes initial plaque formation (188). Unlike Nox4, another NADPH oxidase Nox2 overexpressing leads to atherogenic rather than protective consequences (189), highlighting the controversial roles of Nox-dependent ROS in AS. The crosstalk between ER stress and ROS may be pivotal to understanding the controversial effect of ROS. Nox4 but not Nox2 selectively phosphorylates eIF2α, the downstream PERK arm of UPR, thus providing a direct route for integrating ROS and ER stress. In addition, Nox4 is central to a signaling feedback loop of Rho/Ras GTPase and ER stress. RhoA activation occurs on ER surface in response to UPR and further promotes Nox4-dependent ROS production (190). Nox4-generated oxygen inactivates ER calcium transporter SERCA (Sarcoplasmic Reticulum Ca^{2+} ATPases) and causes calcium-calmodulin-dependent activation of RasGRF1/2, which further mediates the UPR activation (191). Thus, ROS is more than a marker of oxidative stress, but plays two opposite roles in ER stress (restoration of homeostasis or apoptosis) and involves inflammation and cell growth. These data emphasize the controversial effects of ROS and careful considerations in Nox inhibitor development aiming to reduce ROS levels. It is challenging for Nox4 inhibitor development to retain the ER stress inhibition activity and the athero-protective function of Nox4. Given the diverse signaling roles served by Nox4, more specific Nox inhibitors targeting Nox1 and Nox2 while excluding Nox4 could be an optimal treatment strategy (174).

Pharmacological targeting of NF-κB and ER stress in atherosclerosis

Innovation of prevention and treatment strategies against AS is still a pressing mission given being the leading cause of mortality and morbidity in developed and developing countries. Despite various interactions between ER stress and NF-κB, whether and to what extent these mediator molecules play a role in AS remains unanswered. Conceptually, several existing pharmacological targeting on UPR, ROS, NLRP3 inflammasome or other crossroads between ER stress and NF-κB could potentially influence both of them and impede the progression of AS. Herein, we focus on NF-κB inhibitors, UPR inhibitors, ROS-interfering molecules, natural compounds, and some ncRNAs with anti-atherogenic protective effects, targeting ER stress and/or NF-κB, which are attractive potential therapeutic strategies for AS (**Table 3**).

NF-κB inhibitors

BAY 11-7082 (BAY) inhibits IKK-mediated phosphorylation of IκBα, resulting in decreased NF-κB and decreased expression of adhesion molecules. In addition, BAY also suppresses the translocation and activation of AP-1, interferon regulatory factor-3 (IRF-3), and signal transducer and activator of transcription-1 (STAT-1) by inhibiting the phosphorylation or activation of ERK, p38, and JAK-2 (192). BAY is also an inhibitor of NLRP3 inflammasome and a modulator of apoptosis pathways shown in the management of psoriasis-like dermatitis and oral cancer (193, 194). These suggest that BAY could serve as a lead compound in developing potent anti-inflammatory drugs with multiple targets in inflammatory responses.

TABLE 3 NF-κB and/or ER stress modulators in experimental atherosclerosis and associated disease models.

Category	Modulator	Disease	Model	Pharmacological effect	References
NF-κB inhibitors	BAY 11-7082	Cancer; inflammatory diseases; neurological diseases	LPS-stimulated RAW264.7 macrophages	Inhibition on the translocation of p65, AP-1, IRF3, and STAT-1; inhibition of the phosphorylation of ERK, p38, and JAK-2	(192)
			Imiquimod cream-induced rat model of psoriasis-like dermatitis	Reduction of pNF-κB, NLRP3, TNF-α, IL-6, IL-1β, IL-23, and phosphorylated STAT3	(193)
			In vitro and *in vivo* xenograft model of oral cancer	Reduction of OSCC cell viability and of NLRP3 inflammasome, caspase-1, IL-1β, and IL-18 expression; increase of Bax, Bad, and p53 expression; reduction of Bcl-2 expression	(194)
	Pyrrolidine dithiocarbamate (PDTC)	Inflammatory disease especially AS	Rat aortic SMCs	Activation of p38 MAPK and JNK; VSMC growth inhibition	(195)
			ApoE knock-out mice	Blockade of NF-κB; down-regulation of IL-18, IL-18Rα, CD36, and MMP-9; promotion of plaque instability	(196)
	IMD-0354	Cancer; inflammatory diseases; cardiovascular diseases	Organ culture of rat mesenteric arteries with removed endothelium	Inhibition on the up-regulated ET (B2) receptor expression and NF-κB activation	(197)
			Melanoma A375 cells and skin epidermoid carcinoma A431 cells	Inhibition of glutamine uptake; attenuation of mTOR signaling; modulator of cell cycle, DNA damage response and UPR/ATF4/CHOP	(198)
UPR inhibitors	Sirtuin 1 (SIRT1)	Cardiovascular diseases	Cardiomyocytes and adult-inducible Sirtuin 1 knock-out mice	Protection against ER stress-induced apoptosis; NAD^+-dependent deacetylase, alleviating activation of the PERK/eIF2α branch of the UPR	(199)
	Irisin	Metabolic disorders and AS	OxLDL-induced RAW264.7 macrophages	Alleviation of the apoptosis by inhibiting the PERK/eIF2α/CHOP and ATF6/CHOP ER stress signaling pathways	(200)
	STF-083010 and 4μ8C	Metabolic disorders; AS; cancer	Tunicamycin-treated or high-fat diet fed BI-1 knock-out mice	Reduction of atherosclerotic plaque size; inhibition of IRE1α RNase activity, lipid-induced mtROS production, NLRP3 inflammasome activation, and consequent secretion of IL-1 and IL-18	(205)
ROS-interfering molecules	(E/Z)-BCI hydrochloride	Cancer; inflammatory diseases	LPS-activated macrophages	Inhibition on LPS-triggered inflammatory cytokine production; affecting macrophage polarization to an M1 phenotype; decrease of ROS production; inhibition on phosphorylation and nuclear expression of p65; elevation of Nrf2 levels	(206)
	Dihydrolipoic Acid	Inflammatory and neurological diseases	LPS-induced sickness behavior rat model	Increase of the expression of ERK, Nrf2, and HO-1; decrease of the ROS generation levels and the expression of NLRP3, caspase-1, and IL-1β	(207)
	LGH00168	Cancer	A549 human NSCLC xenograft mice	CHOP activator; induction of necroptosis *via* ROS-mediated ER stress and NF-κB inhibition	(177)
Natural compounds	Baicalin	Cardiovascular diseases; cancer	Neonatal rat cardiomyocytes	Protection from ER stress-induced apoptosis; targeting the CHOP/eNOS/NO pathway	(210)
	Quercetin	Cancer	Glucosamine- induced RAW264.7 macrophages	Prevention of apoptosis and lipid accumulation by inhibiting ER stress; decrease of CHOP and GRP78 expression; increase of ATF6 expression, activated JNK and caspase-12	(211)
	Resveratrol	Cancer; cardiovascular diseases; infection	Isoproterenol-induced rat cardiomyocytes	Inhibition of cardiomyocyte hypertrophy and apoptosis by suppressing ER stress; decrease of GRP78, GRP94, and CHOP expression; reversion of the expression of Bcl-2 and Bax	(215)

(Continued)

TABLE 3 (Continued)

Category	Modulator	Disease	Model	Pharmacological effect	References
			Doxorubicin-induced H9c2 cells	Protection against ER stress; downregulation of the expression of ER stress marker proteins; ER stabilization through the activation of the SIRT1 pathway	(216)
	Parthenolide	Migraine; arthritis; AS; ischemic injury in brain; cancer	Jurkat cell	Promotion of plaque stability; decrease of NF-κB activation and FasL expression	(102)
			Permanent MCAO rat model	Downregulation of NF-κB, phosho-p38 MAPK, and caspase-1 expression	(220)
	Reticuline	Cardiovascular diseases and inflammatory diseases	Xylene-induced ear edema and carrageenan-induced paw edema in mice and rats	Inhibition on the expression of pro-inflammatory cytokines, such as TNF-α and IL-6; targeting JAK2/STAT3 and NF-κB pathway	(221)
	Sappanone A	Inflammatory diseases	LPS-stimulated RAW264.7 macrophages	Induction of HO-1 expression by activating Nrf2 through the p38 MAPK pathway	(222)
	Isoliquiritigenin	Cancer; infection; inflammatory and neurological diseases	Collagenase IV-induced intracerebral hemorrhage rat model	Suppression of ROS- and/or NF-κB-mediated NLRP3 inflammasome activation by promoting Nrf2 antioxidant pathway	(223)
NcRNAs	Mir-181a-5p/3p	Vascular inflammation and AS	ApoE knock-out mice	Alleviation of atherosclerotic plaque formation; decrease of proinflammatory gene expression; decrease of infiltration of macrophage, leukocyte and T cell into the lesions; targeting TAB2 and NEMO	(224)
	LncRNA VINAS	AS	LDLR knock-out mice	VINAS knockdown reduces atherosclerotic lesion formation and expression of key inflammatory markers and leukocyte adhesion molecules; targeting MAPK and NF-κB signaling pathway	(225)
	LncRNA NORAD	Cancer; AS	OxLDL-treated HUVECs and high-fat-diet ApoE knock-out mice	Increase of endothelial viability; targeting NF-κB, p53-p21 signaling pathways and IL-8	(226)
	Circ-Sirt1	Cardiovascular diseases	HUVECs, human and rat VSMCs	Inhibition on inflammatory phenotypic switching of VSMC and neointimal hyperplasia; impeding NF-κB translocation and its binding to DNA	(85)

ERK, extracellular signal-regulated kinase; JAK, Janus kinase; OSCC, oral squamous cell carcinoma; Bax, Bcl2-Associated X; Bad, Bcl-2 associated death promoter; Bcl-2, B-cell lymphoma 2; ET, endothelin; mTOR, mammalian target of rapamycin; BI-1, Bax inhibitor-1; NSCLC, non-small-cell lung cancer; HUVEC, human umbilical vein endothelial cell; eNOS, endothelial nitric oxide synthase; MCAO, middle cerebral artery occlusion.

Pyrrolidine dithiocarbamate (PDTC), another NF-κB inhibitor, leads to PDTC-dependent VSMC growth inhibition by inducing marked activation of p38 MAPK and JNK (195). In addition, PDTC blocks IL-18 signaling in ApoE knock-out mice, thus reducing inflammation and restoring plaque instability (196). A better understanding of the molecular mechanisms of PDTC provides a theoretical basis for clinical applications of antioxidants in AS.

IMD-0354 is an IKKβ inhibitor known to exert anti-inflammatory, antitumor, and radioprotective effects. The NF-κB activation induced by TNF-α and associated up-regulation of endothelin B2 receptor could be effectively suppressed by IMD-0354 in VSMCs (197). Additionally, IMD-0354 is confirmed as a potent inhibitor of glutamine uptake that concomitantly attenuates mTOR signaling, but not IKK-NF-κB signaling, suppresses the growth of melanoma cells, and induces autophagy and apoptosis. Affected genes and molecules are implicated in ROS/UPR signaling, including ATF4 and CHOP (198). IMD-0354 has been applied in phase I clinical trials for atopic dermatitis and choroidal neovascularization, though its cardiovascular protective effect has not been verified in clinical trials.

Blockage of NF-κB alone might be insufficient for AS mitigation. Combination with NF-κB inhibitors and lipid-regulating drugs such as statins could be a feasible scheme. Considering that persistent NF-κB inhibition could cause immune deficiency, future NF-κB inhibitors for AS treatment should only be used as adjuvant and intermittent medicine. In a word, the diversity of NF-κB modification signals makes it a long way to apply NF-κB inhibitors in anti-atherosclerotic therapy.

Unfolded protein response inhibitors

Given the associations mentioned above between the UPR and NF-κB, the new functions of UPR inhibitors deserve to be reconsidered. Three representative molecules are listed in **Table 3**, with a special focus on their influences on PERK/eIF2α, ROS production, and NLRP3 inflammasome activation. Sirtuin-1 (SIRT1), an NAD^+-dependent deacetylase, protects cardiomyocytes from ER stress-induced apoptosis by attenuating PERK/eIF2α pathway activation (199). A myokine, irisin, inhibits the PERK/eIF2α/CHOP and ATF6/CHOP pathways and alleviates the apoptosis of macrophages induced by oxLDL (200). Mouse models have shown that irisin promotes endothelial cell proliferation and significantly reduces AS in mice by upregulating the expression of miRNA126-5p (201). In the last decade, abundant clinical studies on the protective functions of irisin in the cardiovascular system have made breakthroughs. A recent cohort study has indicated low serum irisin levels as biomarkers of subclinical AS (202). However, existing studies mainly focus on serum irisin level increase after beneficial interventions such as simvastatin or Omega-3 fatty acids, and direct clinical evidence is necessary before irisin application (203, 204). Still, irisin has a promising preventive and therapeutic prospect for AS. In mouse models, small molecules STF-083010 and 4μ8C have shown a role in reducing atherosclerotic plaque size by inhibiting IRE1α RNase activity, lipid-induced mtROS production, and NLRP3 inflammasome activation (205).

Although people already have much knowledge of UPR and its roles in the development of AS, clinical trials evaluating UPR inhibitors are still scanty. Considering that adaptive UPR is important for the recovery of ER homeostasis, UPR inhibition is possibly only an incidental anti-atherogenic mechanism for potential UPR inhibitor drugs. For clinical use, specific inhibition of critical interaction between NF-κB and ER stress in one checkpoint of UPR branches could be an optimal strategy.

Reactive oxygen species-interfering molecules

Many molecules present with anti-oxidant activities are promising anti-atherogenic drugs. (E/Z)-BCI hydrochloride (BCI), a small molecule inhibitor of dual-specificity phosphatase 6 (DUSP6), activates the Nrf2 signaling pathway and inhibits NF-κB activity, alleviating inflammatory response and decreasing ROS production in LPS-activated macrophages (206). Dihydrolipoic acid exhibits strong antioxidant activities in many conditions, especially neuroinflammation and provides protection *via* Nrf2/HO-1/ROS/NLRP3 signaling cascade in LPS-induced behavioral deficits in rats (207). Novel CHOP activator LGH00168 inhibits the NF-κB pathway and induces ROS-mediated ER stress, leading to necroptosis in A549 human lung cancer cells (177).

Reactive oxygen species is an identified risk factor for cardiovascular diseases. The activation of UPR branches, especially IRE1α and PERK, leads to the abrogation of ER stress-generated ROS, thus alleviating endothelial dysfunction. As discussed later, many natural compounds work by mediating ROS generation. Physical exercise is regarded as a supplement to pharmacotherapy for cardiovascular diseases by reducing ER stress and ROS (208, 209). In conclusion, numerous pathways upstream of ROS make interventions on ROS one of the most prospective strategies in extensive clinical settings more than AS. One limitation of the clinical application of ROS-interfering small molecules is toxicity.

Natural compounds

Baicalin is a primary active substance from the *Scutellaria* root and attenuates ER stress-related apoptosis *in vivo* mediated by CHOP/eNOS signaling pathway (210). Baicalin is a marketed drug in China for the treatment of hepatitis, but more convincing clinical outcomes are required to evaluate its efficacy in treating AS. Quercetin existing in the pericarp, flower, leaf, and seed of various plants has an effect on maintaining ER protein homeostasis probably by increasing ATF6 and reducing CHOP and GRP78 in glucosamine-induced macrophages (211). Quercetin has been applied in Phase 2/3 clinical trials on coronary artery disease, venous thromboembolism, hypertension, and heart failure, and assessed as disease improvement effects (212–214). Resveratrol found in red wine attenuates cardiomyocyte hypertrophy and apoptosis in isoproterenol-induced rat cardiomyocytes, characterized by a low level of GRP78, GRP94, and CHOP, and by a reversed level of Bcl-2 and Bax (215). Resveratrol also alleviates doxorubicin-induced cardiocyte apoptosis of rats by relieving ER stress-related inflammatory response and activating SIRT1 signaling (216). A series of clinical studies have shown that dietary resveratrol improves endothelial function and exerts a beneficial effect on AS (217–219). Parthenolide is demonstrated to be an anti-inflammatory mediator and an NF-κB inhibitor, which has a potential application in cardiovascular and cerebrovascular diseases. Studies have demonstrated that the NF-κB/FasL signaling contributing to plaque rupture could be inhibited by parthenolide (102). Furthermore, the neuroprotective effect of parthenolide is characterized by the downregulation of NF-κB, phospho-p38 MAPK, and caspase-1 (220). Reticuline has anti-inflammation roles in CVDs by targeting the JAK2/STAT3 and NF-κB pathway, though the specific mechanisms are still unknown and further verification in atherosclerotic models is required (221). Sappanone A increases the level of HO-1 mediated by p38/Nrf2 signaling and suppresses LPS-induced NF-κB activation by modulating

the p65 subunit, indicating its anti-inflammatory effect (222). Isoliquiritigenin from *Glycyrrhiza glabra* could reduce early neuronal degeneration after intracerebral hemorrhage, involving the NLRP3 inflammasome regulated by ROS and/or NF-κB through inducing Nrf2-mediated antioxidant activity (223).

The health effects of natural compounds in humans are limited by their purity and poor bioavailability, as they are extracted from plants and rapidly metabolized and excreted. Nevertheless, due to their easy availability from daily meals, diet change could be a simple and beneficial intervention. We can assume that natural compounds have a very high application value in AS prevention and treatment as well as improvement of general health conditions.

NcRNAs

NcRNAs have received most and more attention over the last decades for their involvement in the progression of AS. Research has identified two microRNAs, miR-181a-5p and miR-181a-3p, cooperatively recede endothelium inflammation through blockade of the NF-κB signaling pathway by post-transcriptional regulation of TAB2 and NEMO expression, respectively (224). Long ncRNA (lncRNA) VINAS is highly expressed in intimal AS lesions and promotes vascular inflammation by a possible mechanism involving MAPK and NF-κB signaling pathways. Knockdown of lncRNA VINAS decreases the expression of adhesion molecules such as E-selectin, VCAM-1, and ICAM-1 and inflammatory molecules such as MCP-1, TNF-α, IL-1β, and COX-2 (225). LncRNA NORAD (non-coding RNA activated by DNA damage) knockdown aggravates oxidative stress, increases phosphorylated IκBα level and NF-κB nuclear translocation, and directly promotes IL-8 transcription in AS model. Therefore, lncRNA NORAD has a role in attenuating endothelial cell injury and alleviating AS (226). In contrast, ncRNA circ-Sirt1 directly binds to NF-κB and inhibits its translocation (85).

A number of RNA therapeutics have been in clinical phase II or III for various diseases, but lncRNAs are not among them. Moreover, up to now, few RNA therapies have been explored for cardiovascular diseases. The application of ncRNA therapeutics in AS requires overcoming many challenges, including immunogenicity, lack of specificity, and delivery difficulty.

Conclusion

As NF-κB and ER stress are involved in many human physiological processes, such as immunity and cancer, there are certain limitations to be overcome before therapeutically targeting them in AS. Also, new drug development is limited by the complexity of intrinsic pathways and crosstalk with other pathways. Therefore, the unexpected effects should be considered with caution when evaluating the safety of NF-κB and ER stress as targets for treatment. In this regard, it is significant to further explore more specific and effective crosstalk inhibitors and/or enhancers for atherogenesis, while leaving the normal physiological functions unaffected. On the other hand, these crossover effects also mean that a single successful drug may have utility in multiple diseases.

Indeed, currently available studies provide only a theoretical prospect of targeting interactions between NF-κB and ER stress against AS, and more convincing experiments are required to come closer to the production of an effective NF-κB targeting anti-atherogenic drug. Nevertheless, a broader and deeper understanding of NF-κB signaling and recognition of the potential direct or indirect links between these divergent pathogenic processes may eventually define the value of targeting their crosstalk as a clinical application to AS.

Author contributions

WL, KJ, JL, and WX contributed to the conception, reviewed for important intellectual content, and wrote the majority of the text and created the figures. YJW, JZ, YLW, and RX provided some text. LJ, TW, and GY edited the manuscript. All authors read and approved the final manuscript.

Funding

This work was financially supported by the National Natural Science Foundation of China (Grant Nos. 82171303 and 91954201) and the Beijing Municipal Science & Technology Commission (Grant No. 5202022).

Conflict of interest

The authors declare that the research was conducted in the absence of any commercial or financial relationships that could be construed as a potential conflict of interest.

Publisher's note

References

1. Ghosh S, May MJ, Kopp EB. NF-kappa B and Rel proteins: evolutionarily conserved mediators of immune responses. *Annu Rev Immunol.* (1998) 16:225–60. doi: 10.1146/annurev.immunol.16.1.225

2. Baldwin AS Jr. The NF-kappa B and I kappa B proteins: new discoveries and insights. *Annu Rev Immunol.* (1996) 14:649–83. doi: 10.1146/annurev.immunol.14.1.649

3. Williams LM, Gilmore TD. Looking down on NF-κB. *Mol Cell Biol.* (2020) 40:e104–20. doi: 10.1128/mcb.00104-20

4. Tian M, Tian D, Qiao X, Li J, Zhang L. Modulation of Myb-induced NF-kB -STAT3 signaling and resulting cisplatin resistance in ovarian cancer by dietary factors. *J Cell Physiol.* (2019) 234:21126–34. doi: 10.1002/jcp.28715

5. Khongthong P, Roseweir AK, Edwards J. The NF-KB pathway and endocrine therapy resistance in breast cancer. *Endocr Relat Cancer.* (2019) 26:R369–80. doi: 10.1530/erc-19-0087

6. Baker RG, Hayden MS, Ghosh S. NF-κB, inflammation, and metabolic disease. *Cell Metab.* (2011) 13:11–22. doi: 10.1016/j.cmet.2010.12.008

7. Hetz C, Chevet E, Harding HP. Targeting the unfolded protein response in disease. *Nat Rev Drug Discov.* (2013) 12:703–19. doi: 10.1038/nrd3976

8. Poma P. NF-κB and Disease. *Int J Mol Sci.* (2020) 21:9181. doi: 10.3390/ijms21239181

9. DiDonato JA, Mercurio F, Karin M. NF-κB and the link between inflammation and cancer. *Immunol Rev.* (2012) 246:379–400. doi: 10.1111/j.1600-065X.2012.01099.x

10. Karunakaran D, Nguyen MA, Geoffrion M, Vreeken D, Lister Z, Cheng HS, et al. RIPK1 expression associates with inflammation in early atherosclerosis in humans and can be therapeutically silenced to reduce NF-κB activation and atherogenesis in mice. *Circulation.* (2021) 143:163–77. doi: 10.1161/circulationaha.118.038379

11. Zhang Q, Lenardo MJ, Baltimore D. 30 years of NF-κB: a blossoming of relevance to human pathobiology. *Cell.* (2017) 168:37–57. doi: 10.1016/j.cell.2016.12.012

12. Henkel T, Zabel U, van Zee K, Müller JM, Fanning E, Baeuerle PA. Intramolecular masking of the nuclear location signal and dimerization domain in the precursor for the p50 NF-kappa B subunit. *Cell.* (1992) 68:1121–33. doi: 10.1016/0092-8674(92)90083-o

13. Chaudhari N, Talwar P, Parimisetty A, Lefebvre d'Hellencourt C, Ravanan P. A molecular web: endoplasmic reticulum stress, inflammation, and oxidative stress. *Front Cell Neurosci.* (2014) 8:213. doi: 10.3389/fncel.2014.00213

14. Yu H, Lin L, Zhang Z, Zhang H, Hu H. Targeting NF-κB pathway for the therapy of diseases: mechanism and clinical study. *Signal Transduct Target Ther.* (2020) 5:209. doi: 10.1038/s41392-020-00312-6

15. Tam WF, Sen R. IkappaB family members function by different mechanisms. *J Biol Chem.* (2001) 276:7701–4. doi: 10.1074/jbc.C000916200

16. Kearns JD, Basak S, Werner SL, Huang CS, Hoffmann A. IkappaBepsilon provides negative feedback to control NF-kappaB oscillations, signaling dynamics, and inflammatory gene expression. *J Cell Biol.* (2006) 173:659–64. doi: 10.1083/jcb.200510155

17. Arenzana-Seisdedos F, Thompson J, Rodriguez MS, Bachelerie F, Thomas D, Hay RT. Inducible nuclear expression of newly synthesized I kappa B alpha negatively regulates DNA-binding and transcriptional activities of NF-kappa B. *Mol Cell Biol.* (1995) 15:2689–96. doi: 10.1128/mcb.15.5.2689

18. Savinova OV, Hoffmann A, Ghosh G. The Nfkb1 and Nfkb2 proteins p105 and p100 function as the core of high-molecular-weight heterogeneous complexes. *Mol Cell.* (2009) 34:591–602. doi: 10.1016/j.molcel.2009.04.033

19. Vallabhapurapu S, Karin M. Regulation and function of NF-kappaB transcription factors in the immune system. *Annu Rev Immunol.* (2009) 27:693–733. doi: 10.1146/annurev.immunol.021908.132641

20. Yang HT, Papoutsopoulou S, Belich M, Brender C, Janzen J, Gantke T, et al. Coordinate regulation of TPL-2 and NF-κB signaling in macrophages by NF-κB1 p105. *Mol Cell Biol.* (2012) 32:3438–51. doi: 10.1128/mcb.00564-12

21. Sriskantharajah S, Belich MP, Papoutsopoulou S, Janzen J, Tybulewicz V, Seddon B, et al. Proteolysis of NF-kappaB1 p105 is essential for T cell antigen receptor-induced proliferation. *Nat Immunol.* (2009) 10:38–47. doi: 10.1038/ni.1685

22. Schuster M, Annemann M, Plaza-Sirvent C, Schmitz I. Atypical IκB proteins - nuclear modulators of NF-κB signaling. *Cell Commun Signal.* (2013) 11:23. doi: 10.1186/1478-811x-11-23

23. Hayden MS, Ghosh S. Shared principles in NF-kappaB signaling. *Cell.* (2008) 132:344–62. doi: 10.1016/j.cell.2008.01.020

24. Libby P, Ridker PM, Maseri A. Inflammation and atherosclerosis. *Circulation.* (2002) 105:1135–43. doi: 10.1161/hc0902.104353

25. Abraham E. NF-kappaB activation. *Crit Care Med.* (2000) 28(Suppl. 4):N100–4. doi: 10.1097/00003246-200004001-00012

26. Oeckinghaus A, Ghosh S. The NF-kappaB family of transcription factors and its regulation. *Cold Spring Harb Perspect Biol.* (2009) 1:a000034. doi: 10.1101/cshperspect.a000034

27. Hu H, Sun SC. Ubiquitin signaling in immune responses. *Cell Res.* (2016) 26:457–83. doi: 10.1038/cr.2016.40

28. Hsu H, Xiong J, Goeddel DV. The TNF receptor 1-associated protein TRADD signals cell death and NF-kappa B activation. *Cell.* (1995) 81:495–504. doi: 10.1016/0092-8674(95)90070-5

29. Ea CK, Deng L, Xia ZP, Pineda G, Chen ZJ. Activation of IKK by TNFalpha requires site-specific ubiquitination of RIP1 and polyubiquitin binding by NEMO. *Mol Cell.* (2006) 22:245–57. doi: 10.1016/j.molcel.2006.03.026

30. Su TT, Guo B, Kawakami Y, Sommer K, Chae K, Humphries LA, et al. PKC-beta controls I kappa B kinase lipid raft recruitment and activation in response to BCR signaling. *Nat Immunol.* (2002) 3:780–6. doi: 10.1038/ni823

31. Bertin J, Wang L, Guo Y, Jacobson MD, Poyet JL, Srinivasula SM, et al. CARD11 and CARD14 are novel caspase recruitment domain (CARD)/membrane-associated guanylate kinase (MAGUK) family members that interact with BCL10 and activate NF-kappa B. *J Biol Chem.* (2001) 276:11877–82. doi: 10.1074/jbc.M010512200

32. Sun L, Deng L, Ea CK, Xia ZP, Chen ZJ. The TRAF6 ubiquitin ligase and TAK1 kinase mediate IKK activation by BCL10 and MALT1 in T lymphocytes. *Mol Cell.* (2004) 14:289–301. doi: 10.1016/s1097-2765(04)00236-9

33. Wesche H, Henzel WJ, Shillinglaw W, Li S, Cao Z. MyD88: an adapter that recruits IRAK to the IL-1 receptor complex. *Immunity.* (1997) 7:837–47. doi: 10.1016/s1074-7613(00)80402-1

34. Verstrepen L, Bekaert T, Chau TL, Tavernier J, Chariot A, Beyaert R. TLR-4, IL-1R and TNF-R signaling to NF-kappaB: variations on a common theme. *Cell Mol Life Sci.* (2008) 65:2964–78. doi: 10.1007/s00018-008-8064-8

35. Lamothe B, Besse A, Campos AD, Webster WK, Wu H, Darnay BG. Site-specific Lys-63-linked tumor necrosis factor receptor-associated factor 6 auto-ubiquitination is a critical determinant of I kappa B kinase activation. *J Biol Chem.* (2007) 282:4102–12. doi: 10.1074/jbc.M609503200

36. Jiang Z, Ninomiya-Tsuji J, Qian Y, Matsumoto K, Li X. Interleukin-1 (IL-1) receptor-associated kinase-dependent IL-1-induced signaling complexes phosphorylate TAK1 and TAB2 at the plasma membrane and activate TAK1 in the cytosol. *Mol Cell Biol.* (2002) 22:7158–67. doi: 10.1128/mcb.22.20.7158-7167.2002

37. Sun SC, Ganchi PA, Ballard DW, Greene WC. NF-kappa B controls expression of inhibitor I kappa B alpha: evidence for an inducible autoregulatory pathway. *Science.* (1993) 259:1912–5. doi: 10.1126/science.8096091

38. Li Q, Lu Q, Bottero V, Estepa G, Morrison L, Mercurio F, et al. Enhanced NF-kappaB activation and cellular function in macrophages lacking IkappaB kinase 1 (IKK1). *Proc Natl Acad Sci U S A.* (2005) 102:12425–30. doi: 10.1073/pnas.0505997102

39. Tanaka T, Grusby MJ, Kaisho T. PDLIM2-mediated termination of transcription factor NF-kappaB activation by intranuclear sequestration and degradation of the p65 subunit. *Nat Immunol.* (2007) 8:584–91. doi: 10.1038/ni1464

40. Boone DL, Turer EE, Lee EG, Ahmad RC, Wheeler MT, Tsui C, et al. The ubiquitin-modifying enzyme A20 is required for termination of Toll-like receptor responses. *Nat Immunol.* (2004) 5:1052–60. doi: 10.1038/ni1110

41. Brummelkamp TR, Nijman SM, Dirac AM, Bernards R. Loss of the cylindromatosis tumour suppressor inhibits apoptosis by activating NF-kappaB. *Nature.* (2003) 424:797–801. doi: 10.1038/nature01811

42. Karim ZA, Zhang J, Banerjee M, Chicka MC, Al Hawas R, Hamilton TR, et al. IκB kinase phosphorylation of SNAP-23 controls platelet secretion. *Blood.* (2013) 121:4567–74. doi: 10.1182/blood-2012-11-470468

43. Chen ZJ. Ubiquitination in signaling to and activation of IKK. *Immunol Rev.* (2012) 246:95–106. doi: 10.1111/j.1600-065X.2012.01108.x

44. Zarnegar BJ, Wang Y, Mahoney DJ, Dempsey PW, Cheung HH, He J, et al. Noncanonical NF-kappaB activation requires coordinated assembly of a regulatory complex of the adaptors cIAP1, cIAP2, TRAF2 and TRAF3 and the kinase NIK. *Nat Immunol.* (2008) 9:1371–8. doi: 10.1038/ni.1676

45. Dixit V, Mak TW. NF-kappaB signaling. Many roads lead to madrid. *Cell.* (2002) 111:615–9. doi: 10.1016/s0092-8674(02)01166-2

46. Huxford T, Ghosh G. A structural guide to proteins of the NF-kappaB signaling module. *Cold Spring Harb Perspect Biol.* (2009) 1:a000075. doi: 10.1101/cshperspect.a000075

47. Xiao G, Harhaj EW, Sun SC. NF-kappaB-inducing kinase regulates the processing of NF-kappaB2 p100. *Mol Cell.* (2001) 7:401–9. doi: 10.1016/s1097-2765(01)00187-3

48. Fong A, Sun SC. Genetic evidence for the essential role of beta-transducin repeat-containing protein in the inducible processing of NF-kappa B2/p100. *J Biol Chem.* (2002) 277:22111–4. doi: 10.1074/jbc.C200151200

49. Liang C, Zhang M, Sun SC. Beta-TrCP binding and processing of NF-kappaB2/p100 involve its phosphorylation at serines 866 and 870. *Cell Signal.* (2006) 18:1309–17. doi: 10.1016/j.cellsig.2005.10.011

50. Sun M, Li S, Yu K, Xiang J, Li F. An E3 ubiquitin ligase TRIM9 is involved in WSSV infection via interaction with β-TrCP. *Dev Comp Immunol.* (2019) 97:57–63. doi: 10.1016/j.dci.2019.03.014

51. Arabi A, Ullah K, Branca RM, Johansson J, Bandarra D, Haneklaus M, et al. Proteomic screen reveals Fbw7 as a modulator of the NF-κB pathway. *Nat Commun.* (2012) 3:976. doi: 10.1038/ncomms1975

52. Hu H, Brittain GC, Chang JH, Puebla-Osorio N, Jin J, Zal A, et al. OTUD7B controls non-canonical NF-κB activation through deubiquitination of TRAF3. *Nature.* (2013) 494:371–4. doi: 10.1038/nature11831

53. Hansson GK, Hermansson A. The immune system in atherosclerosis. *Nat Immunol.* (2011) 12:204–12. doi: 10.1038/ni.2001

54. Libby P. The changing landscape of atherosclerosis. *Nature.* (2021) 592:524–33. doi: 10.1038/s41586-021-03392-8

55. Frostegård J. Immunity, atherosclerosis and cardiovascular disease. *BMC Med.* (2013) 11:117. doi: 10.1186/1741-7015-11-117

56. Shah PK. Mechanisms of plaque vulnerability and rupture. *J Am Coll Cardiol.* (2003) 41:15s–22s. doi: 10.1016/s0735-1097(02)02834-6

57. Pateras I, Giaginis C, Tsigris C, Patsouris E, Theocharis S. NF-κB signaling at the crossroads of inflammation and atherogenesis: searching for new therapeutic links. *Expert Opin Ther Targets.* (2014) 18:1089–101. doi: 10.1517/14728222.2014.938051

58. Bornfeldt KE, Tabas I. Insulin resistance, hyperglycemia, and atherosclerosis. *Cell Metab.* (2011) 14:575–85. doi: 10.1016/j.cmet.2011.07.015

59. Schrijvers DM, De Meyer GR, Kockx MM, Herman AG, Martinet W. Phagocytosis of apoptotic cells by macrophages is impaired in atherosclerosis. *Arterioscler Thromb Vasc Biol.* (2005) 25:1256–61. doi: 10.1161/01.ATV.0000166517.18801.a7

60. Thorp E, Tabas I. Mechanisms and consequences of efferocytosis in advanced atherosclerosis. *J Leukoc Biol.* (2009) 86:1089–95. doi: 10.1189/jlb.0209115

61. Tabas I, García-Cardeña G, Owens GK. Recent insights into the cellular biology of atherosclerosis. *J Cell Biol.* (2015) 209:13–22. doi: 10.1083/jcb.201412052

62. Jeziorska M, Woolley DE. Local neovascularization and cellular composition within vulnerable regions of atherosclerotic plaques of human carotid arteries. *J Pathol.* (1999) 188:189–96. doi: 10.1002/(sici)1096-9896(199906)188:23.0.Co;2-n

63. Brogi E, Winkles JA, Underwood R, Clinton SK, Alberts GF, Libby P. Distinct patterns of expression of fibroblast growth factors and their receptors in human atheroma and nonatherosclerotic arteries. Association of acidic FGF with plaque microvessels and macrophages. *J Clin Invest.* (1993) 92:2408–18. doi: 10.1172/jci116847

64. Collins T, Cybulsky MI. NF-kappaB: pivotal mediator or innocent bystander in atherogenesis? *J Clin Invest.* (2001) 107:255–64. doi: 10.1172/jci10373

65. Monaco C, Andreakos E, Kiriakidis S, Mauri C, Bicknell C, Foxwell B, et al. Canonical pathway of nuclear factor kappa B activation selectively regulates proinflammatory and prothrombotic responses in human atherosclerosis. *Proc Natl Acad Sci U S A.* (2004) 101:5634–9. doi: 10.1073/pnas.0401060101

66. de Winther MP, Kanters E, Kraal G, Hofker MH. Nuclear factor kappaB signaling in atherogenesis. *Arterioscler Thromb Vasc Biol.* (2005) 25:904–14. doi: 10.1161/01.Atv.0000160340.72641.87

67. Wolfrum S, Teupser D, Tan M, Chen KY, Breslow JL. The protective effect of A20 on atherosclerosis in apolipoprotein E-deficient mice is associated with reduced expression of NF-kappaB target genes. *Proc Natl Acad Sci U S A.* (2007) 104:18601–6. doi: 10.1073/pnas.0709011104

68. Kanters E, Pasparakis M, Gijbels MJ, Vergouwe MN, Partouns-Hendriks I, Fijneman RJ, et al. Inhibition of NF-kappaB activation in macrophages increases atherosclerosis in LDL receptor-deficient mice. *J Clin Invest.* (2003) 112:1176–85. doi: 10.1172/jci18580

69. Yang S, Wu M, Li X, Zhao R, Zhao Y, Liu L, et al. Role of endoplasmic reticulum stress in atherosclerosis and its potential as a therapeutic target. *Oxid Med Cell Longev.* (2020) 2020:9270107. doi: 10.1155/2020/9270107

70. Battson ML, Lee DM, Gentile CL. Endoplasmic reticulum stress and the development of endothelial dysfunction. *Am J Physiol Heart Circ Physiol.* (2017) 312:H355–67. doi: 10.1152/ajpheart.00437.2016

71. Vanhoutte PM, Shimokawa H, Feletou M, Tang EH. Endothelial dysfunction and vascular disease - a 30th anniversary update. *Acta Physiol (Oxf).* (2017) 219:22–96. doi: 10.1111/apha.12646

72. Burleigh ME, Babaev VR, Yancey PG, Major AS, McCaleb JL, Oates JA, et al. Cyclooxygenase-2 promotes early atherosclerotic lesion formation in ApoE-deficient and C57BL/6 mice. *J Mol Cell Cardiol.* (2005) 39:443–52. doi: 10.1016/j.yjmcc.2005.06.011

73. Elnabawi YA, Garshick MS, Tawil M, Barrett TJ, Fisher EA, Lo Sicco K, et al. CCL20 in psoriasis: a potential biomarker of disease severity, inflammation, and impaired vascular health. *J Am Acad Dermatol.* (2021) 84:913–20. doi: 10.1016/j.jaad.2020.10.094

74. Calvayrac O, Rodríguez-Calvo R, Alonso J, Orbe J, Martín-Ventura JL, Guadall A, et al. CCL20 is increased in hypercholesterolemic subjects and is upregulated by LDL in vascular smooth muscle cells: role of NF-κB. *Arterioscler Thromb Vasc Biol.* (2011) 31:2733–41. doi: 10.1161/atvbaha.111.235721

75. Montanari E, Stojkovic S, Kaun C, Lemberger CE, de Martin R, Rauscher S, et al. Interleukin-33 stimulates GM-CSF and M-CSF production by human endothelial cells. *Thromb Haemost.* (2016) 116:317–27. doi: 10.1160/th15-12-0917

76. Civelek M, Manduchi E, Riley RJ, Stoeckert CJ Jr., Davies PF. Coronary artery endothelial transcriptome in vivo: identification of endoplasmic reticulum stress and enhanced reactive oxygen species by gene connectivity network analysis. *Circ Cardiovasc Genet.* (2011) 4:243–52. doi: 10.1161/circgenetics.110.958926

77. Ye J, Rawson RB, Komuro R, Chen X, Davé UP, Prywes R, et al. ER stress induces cleavage of membrane-bound ATF6 by the same proteases that process SREBPs. *Mol Cell.* (2000) 6:1355–64. doi: 10.1016/s1097-2765(00)00133-7

78. Bobrovnikova-Marjon E, Hatzivassiliou G, Grigoriadou C, Romero M, Cavener DR, Thompson CB, et al. PERK-dependent regulation of lipogenesis during mouse mammary gland development and adipocyte differentiation. *Proc Natl Acad Sci U S A.* (2008) 105:16314–9. doi: 10.1073/pnas.0808517105

79. Ning J, Hong T, Ward A, Pi J, Liu Z, Liu HY, et al. Constitutive role for IRE1α-XBP1 signaling pathway in the insulin-mediated hepatic lipogenic program. *Endocrinology.* (2011) 152:2247–55. doi: 10.1210/en.2010-1036

80. Gordon JW, Shaw JA, Kirshenbaum LA. Multiple facets of NF-κB in the heart: to be or not to NF-κB. *Circ Res.* (2011) 108:1122–32. doi: 10.1161/circresaha.110.226928

81. Mehrhof FB, Schmidt-Ullrich R, Dietz R, Scheidereit C. Regulation of vascular smooth muscle cell proliferation: role of NF-kappaB revisited. *Circ Res.* (2005) 96:958–64. doi: 10.1161/01.Res.0000166924.31219.49

82. Yang D, Sun C, Zhang J, Lin S, Zhao L, Wang L, et al. Proliferation of vascular smooth muscle cells under inflammation is regulated by NF-κB p65/microRNA-17/RB pathway activation. *Int J Mol Med.* (2018) 41:43–50. doi: 10.3892/ijmm.2017.3212

83. Lu QB, Wan MY, Wang PY, Zhang CX, Xu DY, Liao X, et al. Chicoric acid prevents PDGF-BB-induced VSMC dedifferentiation, proliferation and migration by suppressing ROS/NFκB/mTOR/P70S6K signaling cascade. *Redox Biol.* (2018) 14:656–68. doi: 10.1016/j.redox.2017.11.012

84. Monaco C, Paleolog E. Nuclear factor kappaB: a potential therapeutic target in atherosclerosis and thrombosis. *Cardiovasc Res.* (2004) 61:671–82. doi: 10.1016/j.cardiores.2003.11.038

85. Kong P, Yu Y, Wang L, Dou YQ, Zhang XH, Cui Y, et al. circ-Sirt1 controls NF-κB activation via sequence-specific interaction and enhancement of SIRT1 expression by binding to miR-132/212 in vascular smooth muscle cells. *Nucleic Acids Res.* (2019) 47:3580–93. doi: 10.1093/nar/gkz141

86. Shi C, Deng J, Chiu M, Chen YX, O'Brien ER. Heat shock protein 27 immune complex altered signaling and transport (ICAST): novel mechanisms of attenuating inflammation. *Faseb J.* (2020) 34:14287–301. doi: 10.1096/fj.202001389RR

87. Crane ED, Al-Hashimi AA, Chen J, Lynn EG, Won KD, Lhoták S, et al. Anti-GRP78 autoantibodies induce endothelial cell activation and accelerate the development of atherosclerotic lesions. *JCI Insight.* (2018) 3:e99363. doi: 10.1172/jci.insight.99363

88. Xie Z, Wang X, Liu X, Du H, Sun C, Shao X, et al. Adipose-derived exosomes exert proatherogenic effects by regulating macrophage foam cell formation and polarization. *J Am Heart Assoc.* (2018) 7:e007442. doi: 10.1161/jaha.117.007442

89. Isa SA, Ruffino JS, Ahluwalia M, Thomas AW, Morris K, Webb R. M2 macrophages exhibit higher sensitivity to oxLDL-induced lipotoxicity than other

monocyte/macrophage subtypes. *Lipids Health Dis.* (2011) 10:229. doi: 10.1186/1476-511x-10-229

90. Yamada Y, Doi T, Hamakubo T, Kodama T. Scavenger receptor family proteins: roles for atherosclerosis, host defence and disorders of the central nervous system. *Cell Mol Life Sci.* (1998) 54:628–40. doi: 10.1007/s000180050191

91. Stewart CR, Stuart LM, Wilkinson K, van Gils JM, Deng J, Halle A, et al. CD36 ligands promote sterile inflammation through assembly of a Toll-like receptor 4 and 6 heterodimer. *Nat Immunol.* (2010) 11:155–61. doi: 10.1038/ni.1836

92. Yang S, Li J, Chen Y, Zhang S, Feng C, Hou Z, et al. MicroRNA-216a promotes M1 macrophages polarization and atherosclerosis progression by activating telomerase via the Smad3/NF-κB pathway. *Biochim Biophys Acta Mol Basis Dis.* (2019) 1865:1772–81. doi: 10.1016/j.bbadis.2018.06.016

93. Plotkin JD, Elias MG, Dellinger AL, Kepley CL. NF-κB inhibitors that prevent foam cell formation and atherosclerotic plaque accumulation. *Nanomedicine.* (2017) 13:2037–48. doi: 10.1016/j.nano.2017.04.013

94. Sage AP, Nus M, Bagchi Chakraborty J, Tsiantoulas D, Newland SA, Finigan AJ, et al. X-Box binding protein-1 dependent plasma cell responses limit the development of atherosclerosis. *Circ Res.* (2017) 121:270–81. doi: 10.1161/circresaha.117.310884

95. Zeng L, Zampetaki A, Margariti A, Pepe AE, Alam S, Martin D, et al. Sustained activation of XBP1 splicing leads to endothelial apoptosis and atherosclerosis development in response to disturbed flow. *Proc Natl Acad Sci U S A.* (2009) 106:8326–31. doi: 10.1073/pnas.0903197106

96. Oh J, Riek AE, Weng S, Petty M, Kim D, Colonna M, et al. Endoplasmic reticulum stress controls M2 macrophage differentiation and foam cell formation. *J Biol Chem.* (2012) 287:11629–41. doi: 10.1074/jbc.M111.338673

97. Gough PJ, Gomez IG, Wille PT, Raines EW. Macrophage expression of active MMP-9 induces acute plaque disruption in apoE-deficient mice. *J Clin Invest.* (2006) 116:59–69. doi: 10.1172/jci25074

98. Wang N, Zhang X, Ma Z, Niu J, Ma S, Wenjie W, et al. Combination of tanshinone IIA and astragaloside IV attenuate atherosclerotic plaque vulnerability in ApoE(−/−) mice by activating PI3K/AKT signaling and suppressing TRL4/NF-κB signaling. *Biomed Pharmacother.* (2020) 123:109729. doi: 10.1016/j.biopha.2019.109729

99. Zhang M, Xue Y, Chen H, Meng L, Chen B, Gong H, et al. Resveratrol inhibits MMP3 and MMP9 expression and secretion by suppressing TLR4/NF-κB/STAT3 activation in Ox-LDL-Treated HUVECs. *Oxid Med Cell Longev.* (2019) 2019:9013169. doi: 10.1155/2019/9013169

100. Park L, Raman KG, Lee KJ, Lu Y, Ferran LJ Jr., Chow WS, et al. Suppression of accelerated diabetic atherosclerosis by the soluble receptor for advanced glycation endproducts. *Nat Med.* (1998) 4:1025–31. doi: 10.1038/2012

101. Cuccurullo C, Iezzi A, Fazia ML, De Cesare D, Di Francesco A, Muraro R, et al. Suppression of RAGE as a basis of simvastatin-dependent plaque stabilization in type 2 diabetes. *Arterioscler Thromb Vasc Biol.* (2006) 26:2716–23. doi: 10.1161/01.Atv.0000249630.02085.12

102. Martín-Ventura JL, Blanco-Colio LM, Muñoz-García B, Gómez-Hernández A, Arribas A, Ortega L, et al. NF-kappaB activation and Fas ligand overexpression in blood and plaques of patients with carotid atherosclerosis: potential implication in plaque instability. *Stroke.* (2004) 35:458–63. doi: 10.1161/01.Str.0000114876.51656.7a

103. Zhou J, Werstuck GH, Lhoták S, de Koning AB, Sood SK, Hossain GS, et al. Association of multiple cellular stress pathways with accelerated atherosclerosis in hyperhomocysteinemic apolipoprotein E-deficient mice. *Circulation.* (2004) 110:207–13. doi: 10.1161/01.Cir.0000134487.51510.97

104. Wu R, Zhang QH, Lu YJ, Ren K, Yi GH. Involvement of the IRE1α-XBP1 pathway and XBP1s-dependent transcriptional reprogramming in metabolic diseases. *DNA Cell Biol.* (2015) 34:6–18. doi: 10.1089/dna.2014.2552

105. Scull CM, Tabas I. Mechanisms of ER stress-induced apoptosis in atherosclerosis. *Arterioscler Thromb Vasc Biol.* (2011) 31:2792–7. doi: 10.1161/atvbaha.111.224881

106. Myoishi M, Hao H, Minamino T, Watanabe K, Nishihira K, Hatakeyama K, et al. Increased endoplasmic reticulum stress in atherosclerotic plaques associated with acute coronary syndrome. *Circulation.* (2007) 116:1226–33. doi: 10.1161/circulationaha.106.682054

107. Thorp E, Li G, Seimon TA, Kuriakose G, Ron D, Tabas I. Reduced apoptosis and plaque necrosis in advanced atherosclerotic lesions of Apoe-/- and Ldlr-/- mice lacking CHOP. *Cell Metab.* (2009) 9:474–81. doi: 10.1016/j.cmet.2009.03.003

108. Gao J, Ishigaki Y, Yamada T, Kondo K, Yamaguchi S, Imai J, et al. Involvement of endoplasmic stress protein C/EBP homologous protein in arteriosclerosis acceleration with augmented biological stress responses. *Circulation.* (2011) 124:830–9. doi: 10.1161/circulationaha.110.014050

109. Dong Y, Zhang M, Liang B, Xie Z, Zhao Z, Asfa S, et al. Reduction of AMP-activated protein kinase alpha2 increases endoplasmic reticulum stress and atherosclerosis in vivo. *Circulation.* (2010) 121:792–803. doi: 10.1161/circulationaha.109.900928

110. Erbay E, Babaev VR, Mayers JR, Makowski L, Charles KN, Snitow ME, et al. Reducing endoplasmic reticulum stress through a macrophage lipid chaperone alleviates atherosclerosis. *Nat Med.* (2009) 15:1383–91. doi: 10.1038/nm.2067

111. Mogilenko DA, Haas JT, L'Homme L, Fleury S, Quemener S, Levavasseur M, et al. Metabolic and innate immune cues merge into a specific inflammatory response via the UPR. *Cell.* (2019) 177:1201–16.e19. doi: 10.1016/j.cell.2019.03.018

112. Burgos-Morón E, Abad-Jiménez Z, Marañón AM, Iannantuoni F, Escribano-López I, López-Domènech S, et al. Relationship between oxidative stress, ER stress, and inflammation in Type 2 diabetes: the battle continues. *J Clin Med.* (2019) 8:1385. doi: 10.3390/jcm8091385

113. Cubillos-Ruiz JR, Bettigole SE, Glimcher LH. Tumorigenic and immunosuppressive effects of endoplasmic reticulum stress in cancer. *Cell.* (2017) 168:692–706. doi: 10.1016/j.cell.2016.12.004

114. Inagi R. Glycative stress and glyoxalase in kidney disease and aging. *Biochem Soc Trans.* (2014) 42:457–60. doi: 10.1042/bst20140007

115. Zhou AX, Tabas I. The UPR in atherosclerosis. *Semin Immunopathol.* (2013) 35:321–32. doi: 10.1007/s00281-013-0372-x

116. Rosenzweig R, Nillegoda NB, Mayer MP, Bukau B. The Hsp70 chaperone network. *Nat Rev Mol Cell Biol.* (2019) 20:665–80. doi: 10.1038/s41580-019-0133-3

117. Chen HW, Kuo HT, Wang SJ, Lu TS, Yang RC. In vivo heat shock protein assembles with septic liver NF-kappaB/I-kappaB complex regulating NF-kappaB activity. *Shock.* (2005) 24:232–8. doi: 10.1097/01.shk.0000174020.87439.f2

118. Kim I, Shin HM, Baek W. Heat-shock response is associated with decreased production of interleukin-6 in murine aortic vascular smooth muscle cells. *Naunyn Schmiedebergs Arch Pharmacol.* (2005) 371:27–33. doi: 10.1007/s00210-004-1007-5

119. Stöhr D, Jeltsch A, Rehm M. TRAIL receptor signaling: from the basics of canonical signal transduction toward its entanglement with ER stress and the unfolded protein response. *Int Rev Cell Mol Biol.* (2020) 351:57–99. doi: 10.1016/bs.ircmb.2020.02.002

120. Bodmer JL, Holler N, Reynard S, Vinciguerra P, Schneider P, Juo P, et al. TRAIL receptor-2 signals apoptosis through FADD and caspase-8. *Nat Cell Biol.* (2000) 2:241–3. doi: 10.1038/35008667

121. Sullivan GP, O'Connor H, Henry CM, Davidovich P, Clancy DM, Albert ML, et al. TRAIL receptors serve as stress-associated molecular patterns to promote ER-Stress-Induced inflammation. *Dev Cell.* (2020) 52:714–30.e5. doi: 10.1016/j.devcel.2020.01.031

122. Ren J, Bi Y, Sowers JR, Hetz C, Zhang Y. Endoplasmic reticulum stress and unfolded protein response in cardiovascular diseases. *Nat Rev Cardiol.* (2021) 18:499–521. doi: 10.1038/s41569-021-00511-w

123. Shen CH, Tung SY, Huang WS, Lu CC, Lee KC, Hsieh YY, et al. Exploring the effects of tert-butylhydroperoxide induced liver injury using proteomic approach. *Toxicology.* (2014) 316:61–70. doi: 10.1016/j.tox.2013.12.007

124. Chen J, Zhang M, Zhu M, Gu J, Song J, Cui L, et al. Paeoniflorin prevents endoplasmic reticulum stress-associated inflammation in lipopolysaccharide-stimulated human umbilical vein endothelial cells via the IRE1α/NF-κB signaling pathway. *Food Funct.* (2018) 9:2386–97. doi: 10.1039/c7fo01406f

125. Keestra-Gounder AM, Byndloss MX, Seyffert N, Young BM, Chávez-Arroyo A, Tsai AY, et al. NOD1 and NOD2 signalling links ER stress with inflammation. *Nature.* (2016) 532:394–7. doi: 10.1038/nature17631

126. Lencer WI, DeLuca H, Grey MJ, Cho JA. Innate immunity at mucosal surfaces: the IRE1-RIDD-RIG-I pathway. *Trends Immunol.* (2015) 36:401–9. doi: 10.1016/j.it.2015.05.006

127. Tam AB, Koong AC, Niwa M. Ire1 has distinct catalytic mechanisms for XBP1/HAC1 splicing and RIDD. *Cell Rep.* (2014) 9:850–8. doi: 10.1016/j.celrep.2014.09.016

128. Zhang H, Song G, Zhang Z, Song H, Tang X, Deng A, et al. Colitis is effectively ameliorated by (±)-8-Acetonyl-dihydrocoptisine via the XBP1-NF-κB pathway. *Front Pharmacol.* (2017) 8:619. doi: 10.3389/fphar.2017.00619

129. Kim S, Joe Y, Kim HJ, Kim YS, Jeong SO, Pae HO, et al. Endoplasmic reticulum stress-induced IRE1α activation mediates cross-talk of GSK-3β and XBP-1 to regulate inflammatory cytokine production. *J Immunol.* (2015) 194:4498–506. doi: 10.4049/jimmunol.1401399

130. Sun H, Wei G, Liu H, Xiao D, Huang J, Lu J, et al. Inhibition of XBP1s ubiquitination enhances its protein stability and improves glucose

homeostasis. *Metabolism.* (2020) 105:154046. doi: 10.1016/j.metabol.2019.154046

131. Schwabe RF, Brenner DA. Role of glycogen synthase kinase-3 in TNF-alpha-induced NF-kappaB activation and apoptosis in hepatocytes. *Am J Physiol Gastrointest Liver Physiol.* (2002) 283:G204–11. doi: 10.1152/ajpgi.00016.2002

132. Demarchi F, Bertoli C, Sandy P, Schneider C. Glycogen synthase kinase-3 beta regulates NF-kappa B1/p105 stability. *J Biol Chem.* (2003) 278:39583–90. doi: 10.1074/jbc.M305676200

133. Zhang H, Zhao C, Wang S, Huang Y, Wang H, Zhao J, et al. Anti-dsDNA antibodies induce inflammation via endoplasmic reticulum stress in human mesangial cells. *J Transl Med.* (2015) 13:178. doi: 10.1186/s12967-015-0536-7

134. Mendez JM, Kolora LD, Lemon JS, Dupree SL, Keestra-Gounder AM. Activation of the endoplasmic reticulum stress response impacts the NOD1 signaling pathway. *Infect Immun.* (2019) 87:e826–818. doi: 10.1128/iai.00826-18

135. Stępkowski TM, Kruszewski MK. Molecular cross-talk between the NRF2/KEAP1 signaling pathway, autophagy, and apoptosis. *Free Radic Biol Med.* (2011) 50:1186–95. doi: 10.1016/j.freeradbiomed.2011.01.033

136. Jain A, Lamark T, Sjøttem E, Larsen KB, Awuh JA, Øvervatn A, et al. p62/SQSTM1 is a target gene for transcription factor NRF2 and creates a positive feedback loop by inducing antioxidant response element-driven gene transcription. *J Biol Chem.* (2010) 285:22576–91. doi: 10.1074/jbc.M110.118976

137. Duran A, Linares JF, Galvez AS, Wikenheiser K, Flores JM, Diaz-Meco MT, et al. The signaling adaptor p62 is an important NF-kappaB mediator in tumorigenesis. *Cancer Cell.* (2008) 13:343–54. doi: 10.1016/j.ccr.2008.02.001

138. Thimmulappa RK, Lee H, Rangasamy T, Reddy SP, Yamamoto M, Kensler TW, et al. Nrf2 is a critical regulator of the innate immune response and survival during experimental sepsis. *J Clin Invest.* (2006) 116:984–95. doi: 10.1172/jci25790

139. Soares MP, Seldon MP, Gregoire IP, Vassilevskaia T, Berberat PO, Yu J, et al. Heme oxygenase-1 modulates the expression of adhesion molecules associated with endothelial cell activation. *J Immunol.* (2004) 172:3553–63. doi: 10.4049/jimmunol.172.6.3553

140. Li J, Holbrook NJ. Elevated gadd153/chop expression and enhanced c-Jun N-terminal protein kinase activation sensitizes aged cells to ER stress. *Exp Gerontol.* (2004) 39:735–44. doi: 10.1016/j.exger.2004.02.008

141. Alonso-Piñeiro JA, Gonzalez-Rovira A, Sánchez-Gomar I, Moreno JA, Durán-Ruiz MC. Nrf2 and heme oxygenase-1 involvement in atherosclerosis related oxidative stress. *Antioxidants (Basel).* (2021) 10:1463. doi: 10.3390/antiox10091463

142. Hosoya T, Maruyama A, Kang MI, Kawatani Y, Shibata T, Uchida K, et al. Differential responses of the Nrf2-Keap1 system to laminar and oscillatory shear stresses in endothelial cells. *J Biol Chem.* (2005) 280:27244–50. doi: 10.1074/jbc.M502551200

143. Harada N, Ito K, Hosoya T, Mimura J, Maruyama A, Noguchi N, et al. Nrf2 in bone marrow-derived cells positively contributes to the advanced stage of atherosclerotic plaque formation. *Free Radic Biol Med.* (2012) 53:2256–62. doi: 10.1016/j.freeradbiomed.2012.10.001

144. Ruotsalainen AK, Inkala M, Partanen ME, Lappalainen JP, Kansanen E, Mäkinen PI, et al. The absence of macrophage Nrf2 promotes early atherogenesis. *Cardiovasc Res.* (2013) 98:107–15. doi: 10.1093/cvr/cvt008

145. Freigang S, Ampenberger F, Spohn G, Heer S, Shamshiev AT, Kisielow J, et al. Nrf2 is essential for cholesterol crystal-induced inflammasome activation and exacerbation of atherosclerosis. *Eur J Immunol.* (2011) 41:2040–51. doi: 10.1002/eji.201041316

146. Ishii T, Itoh K, Ruiz E, Leake DS, Unoki H, Yamamoto M, et al. Role of Nrf2 in the regulation of CD36 and stress protein expression in murine macrophages: activation by oxidatively modified LDL and 4-hydroxynonenal. *Circ Res.* (2004) 94:609–16. doi: 10.1161/01.Res.0000119171.44657.45

147. Yamazaki H, Hiramatsu N, Hayakawa K, Tagawa Y, Okamura M, Ogata R, et al. Activation of the Akt-NF-kappaB pathway by subtilase cytotoxin through the ATF6 branch of the unfolded protein response. *J Immunol.* (2009) 183:1480–7. doi: 10.4049/jimmunol.0900017

148. Chen Z, Liu Y, Yang L, Liu P, Zhang Y, Wang X. MiR-149 attenuates endoplasmic reticulum stress-induced inflammation and apoptosis in nonalcoholic fatty liver disease by negatively targeting ATF6 pathway. *Immunol Lett.* (2020) 222:40–8. doi: 10.1016/j.imlet.2020.03.003

149. Rao J, Yue S, Fu Y, Zhu J, Wang X, Busuttil RW, et al. ATF6 mediates a pro-inflammatory synergy between ER stress and TLR activation in the pathogenesis of liver ischemia-reperfusion injury. *Am J Transplant.* (2014) 14:1552–61. doi: 10.1111/ajt.12711

150. Schmitz ML, Shaban MS, Albert BV, Gökçen A, Kracht M. The crosstalk of endoplasmic reticulum (ER) stress pathways with NF-κB: complex mechanisms relevant for cancer, inflammation and infection. *Biomedicines.* (2018) 6:58. doi: 10.3390/biomedicines6020058

151. Kim YG, Kim SM, Kim KP, Lee SH, Moon JY. The role of inflammasome-dependent and inflammasome-independent NLRP3 in the kidney. *Cells.* (2019) 8:1389. doi: 10.3390/cells8111389

152. Lamkanfi M, Dixit VM. Mechanisms and functions of inflammasomes. *Cell.* (2014) 157:1013–22. doi: 10.1016/j.cell.2014.04.007

153. Awad F, Assrawi E, Louvrier C, Jumeau C, Georgin-Lavialle S, Grateau G, et al. Inflammasome biology, molecular pathology and therapeutic implications. *Pharmacol Ther.* (2018) 187:133–49. doi: 10.1016/j.pharmthera.2018.02.011

154. Tang D, Kang R, Berghe TV, Vandenabeele P, Kroemer G. The molecular machinery of regulated cell death. *Cell Res.* (2019) 29:347–64. doi: 10.1038/s41422-019-0164-5

155. Hoseini Z, Sepahvand F, Rashidi B, Sahebkar A, Masoudifar A, Mirzaei H. NLRP3 inflammasome: its regulation and involvement in atherosclerosis. *J Cell Physiol.* (2018) 233:2116–32. doi: 10.1002/jcp.25930

156. Paik S, Kim JK, Silwal P, Sasakawa C, Jo EK. An update on the regulatory mechanisms of NLRP3 inflammasome activation. *Cell Mol Immunol.* (2021) 18:1141–60. doi: 10.1038/s41423-021-00670-3

157. Hu X, Li D, Wang J, Guo J, Li Y, Cao Y, et al. Melatonin inhibits endoplasmic reticulum stress-associated TXNIP/NLRP3 inflammasome activation in lipopolysaccharide-induced endometritis in mice. *Int Immunopharmacol.* (2018) 64:101–9. doi: 10.1016/j.intimp.2018.08.028

158. Du RH, Tan J, Yan N, Wang L, Qiao C, Ding JH, et al. Kir6.2 knockout aggravates lipopolysaccharide-induced mouse liver injury via enhancing NLRP3 inflammasome activation. *J Gastroenterol.* (2014) 49:727–36. doi: 10.1007/s00535-013-0823-0

159. Yarmohammadi F, Hayes AW, Karimi G. Possible protective effect of resolvin D1 on inflammation in atrial fibrillation: involvement of ER stress mediated the NLRP3 inflammasome pathway. *Naunyn Schmiedebergs Arch Pharmacol.* (2021) 394:1613–9. doi: 10.1007/s00210-021-02115-0

160. Menu P, Mayor A, Zhou R, Tardivel A, Ichijo H, Mori K, et al. ER stress activates the NLRP3 inflammasome via an UPR-independent pathway. *Cell Death Dis.* (2012) 3:e261. doi: 10.1038/cddis.2011.132

161. Zeng W, Wu D, Sun Y, Suo Y, Yu Q, Zeng M, et al. The selective NLRP3 inhibitor MCC950 hinders atherosclerosis development by attenuating inflammation and pyroptosis in macrophages. *Sci Rep.* (2021) 11:19305. doi: 10.1038/s41598-021-98437-3

162. Sharma BR, Kanneganti TD. NLRP3 inflammasome in cancer and metabolic diseases. *Nat Immunol.* (2021) 22:550–9. doi: 10.1038/s41590-021-00886-5

163. Van Hauwermeiren F, Van Opdenbosch N, Van Gorp H, de Vasconcelos N, van Loo G, Vandenabeele P, et al. Bacillus anthracis induces NLRP3 inflammasome activation and caspase-8-mediated apoptosis of macrophages to promote lethal anthrax. *Proc Natl Acad Sci U S A.* (2022) 119:e2116415119. doi: 10.1073/pnas.2116415119

164. Wan Z, Fan Y, Liu X, Xue J, Han Z, Zhu C, et al. NLRP3 inflammasome promotes diabetes-induced endothelial inflammation and atherosclerosis. *Diabetes Metab Syndr Obes.* (2019) 12:1931–42. doi: 10.2147/dmso.S222053

165. Burger F, Baptista D, Roth A, da Silva RF, Montecucco F, Mach F, et al. NLRP3 inflammasome activation controls vascular smooth muscle cells phenotypic switch in atherosclerosis. *Int J Mol Sci.* (2021) 23:340. doi: 10.3390/ijms23010340

166. Zheng F, Xing S, Gong Z, Mu W, Xing Q. Silence of NLRP3 suppresses atherosclerosis and stabilizes plaques in apolipoprotein E-deficient mice. *Mediators Inflamm.* (2014) 2014:507208. doi: 10.1155/2014/507208

167. Menu P, Pellegrin M, Aubert JF, Bouzourene K, Tardivel A, Mazzolai L, et al. Atherosclerosis in ApoE-deficient mice progresses independently of the NLRP3 inflammasome. *Cell Death Dis.* (2011) 2:e137. doi: 10.1038/cddis.2011.18

168. Bleda S, de Haro J, Varela C, Esparza L, Ferruelo A, Acin F. NLRP1 inflammasome, and not NLRP3, is the key in the shift to proinflammatory state on endothelial cells in peripheral arterial disease. *Int J Cardiol.* (2014) 172:e282–4. doi: 10.1016/j.ijcard.2013.12.201

169. Takada Y, Mukhopadhyay A, Kundu GC, Mahabeleshwar GH, Singh S, Aggarwal BB. Hydrogen peroxide activates NF-kappa B through tyrosine phosphorylation of I kappa B alpha and serine phosphorylation of p65: evidence for the involvement of I kappa B alpha kinase and Syk protein-tyrosine kinase. *J Biol Chem.* (2003) 278:24233–41. doi: 10.1074/jbc.M212389200

170. Schoonbroodt S, Ferreira V, Best-Belpomme M, Boelaert JR, Legrand-Poels S, Korner M, et al. Crucial role of the amino-terminal tyrosine residue 42 and the carboxyl-terminal PEST domain of I kappa B alpha in NF-kappa B activation by an oxidative stress. *J Immunol.* (2000) 164:4292–300. doi: 10.4049/jimmunol.164.8.4292

171. Toledano MB, Leonard WJ. Modulation of transcription factor NF-kappa B binding activity by oxidation-reduction in vitro. *Proc Natl Acad Sci U S A.* (1991) 88:4328–32. doi: 10.1073/pnas.88.10.4328

172. Liu J, Yoshida Y, Yamashita U. DNA-binding activity of NF-kappaB and phosphorylation of p65 are induced by N-acetylcysteine through phosphatidylinositol (PI) 3-kinase. *Mol Immunol.* (2008) 45:3984–9. doi: 10.1016/j.molimm.2008.06.012

173. Morgan MJ, Kim YS, Liu ZG. TNFalpha and reactive oxygen species in necrotic cell death. *Cell Res.* (2008) 18:343–9. doi: 10.1038/cr.2008.31

174. Ochoa CD, Wu RF, Terada LS. ROS signaling and ER stress in cardiovascular disease. *Mol Aspects Med.* (2018) 63:18–29. doi: 10.1016/j.mam.2018.03.002

175. Li W, Zhou X, Cai J, Zhao F, Cao T, Ning L, et al. Recombinant Treponema pallidum protein Tp0768 promotes proinflammatory cytokine secretion of macrophages through ER stress and ROS/NF-κB pathway. *Appl Microbiol Biotechnol.* (2021) 105:353–66. doi: 10.1007/s00253-020-11018-8

176. Kim HK, Lee GH, Bhattarai KR, Junjappa RP, Lee HY, Handigund M, et al. PI3Kδ contributes to ER stress-associated asthma through ER-redox disturbances: the involvement of the RIDD-RIG-I-NF-κB axis. *Exp Mol Med.* (2018) 50:e444. doi: 10.1038/emm.2017.270

177. Ma YM, Peng YM, Zhu QH, Gao AH, Chao B, He QJ, et al. Novel CHOP activator LGH00168 induces necroptosis in A549 human lung cancer cells via ROS-mediated ER stress and NF-κB inhibition. *Acta Pharmacol Sin.* (2016) 37:1381–90. doi: 10.1038/aps.2016.61

178. Incalza MA, D'Oria R, Natalicchio A, Perrini S, Laviola L, Giorgino F. Oxidative stress and reactive oxygen species in endothelial dysfunction associated with cardiovascular and metabolic diseases. *Vascul Pharmacol.* (2018) 100:1–19. doi: 10.1016/j.vph.2017.05.005

179. Ungvari Z, Tarantini S, Kiss T, Wren JD, Giles CB, Griffin CT, et al. Endothelial dysfunction and angiogenesis impairment in the ageing vasculature. *Nature Reviews Cardiology.* (2018) 15:555–65. doi: 10.1038/s41569-018-0030-z

180. Lara-Guzmán OJ, Gil-Izquierdo A, Medina S, Osorio E, Alvarez-Quintero R, Zuluaga N, et al. Oxidized LDL triggers changes in oxidative stress and inflammatory biomarkers in human macrophages. *Redox Biol.* (2018) 15:1–11. doi: 10.1016/j.redox.2017.11.017

181. Forrester SJ, Kikuchi DS, Hernandes MS, Xu Q, Griendling KK. Reactive oxygen species in metabolic and inflammatory signaling. *Circ Res.* (2018) 122:877–902. doi: 10.1161/circresaha.117.311401

182. Gutierrez J, Ballinger SW, Darley-Usmar VM, Landar A. Free radicals, mitochondria, and oxidized lipids: the emerging role in signal transduction in vascular cells. *Circ Res.* (2006) 99:924–32. doi: 10.1161/01.RES.0000248212.86638.e9

183. Niki E. Do free radicals play causal role in atherosclerosis? Low density lipoprotein oxidation and vitamin E revisited. *J Clin Biochem Nutr.* (2011) 48:3–7. doi: 10.3164/jcbn.11-007FR

184. Wang Z, Liu B, Zhu J, Wang D, Wang Y. Nicotine-mediated autophagy of vascular smooth muscle cell accelerates atherosclerosis via nAChRs/ROS/NF-κB signaling pathway. *Atherosclerosis.* (2019) 284:1–10. doi: 10.1016/j.atherosclerosis.2019.02.008

185. Lozhkin A, Vendrov AE, Pan H, Wickline SA, Madamanchi NR, Runge MS. NADPH oxidase 4 regulates vascular inflammation in aging and atherosclerosis. *J Mol Cell Cardiol.* (2017) 102:10–21. doi: 10.1016/j.yjmcc.2016.12.004

186. Hu P, Wu X, Khandelwal AR, Yu W, Xu Z, Chen L, et al. Endothelial Nox4-based NADPH oxidase regulates atherosclerosis via soluble epoxide hydrolase. *Biochim Biophys Acta Mol Basis Dis.* (2017) 1863:1382–91. doi: 10.1016/j.bbadis.2017.02.004

187. Craige SM, Kant S, Reif M, Chen K, Pei Y, Angoff R, et al. Endothelial NADPH oxidase 4 protects ApoE-/- mice from atherosclerotic lesions. *Free Radic Biol Med.* (2015) 89:1–7. doi: 10.1016/j.freeradbiomed.2015.07.004

188. Gray SP, Di Marco E, Kennedy K, Chew P, Okabe J, El-Osta A, et al. Reactive oxygen species can provide atheroprotection via NOX4-dependent inhibition of inflammation and vascular remodeling. *Arterioscler Thromb Vasc Biol.* (2016) 36:295–307. doi: 10.1161/atvbaha.115.307012

189. Li G, Scull C, Ozcan L, Tabas I. NADPH oxidase links endoplasmic reticulum stress, oxidative stress, and PKR activation to induce apoptosis. *J Cell Biol.* (2010) 191:1113–25. doi: 10.1083/jcb.201006121

190. Ewald CY, Hourihan JM, Bland MS, Obieglo C, Katic I, Moronetti Mazzeo LE, et al. NADPH oxidase-mediated redox signaling promotes oxidative stress resistance and longevity through memo-1 in C. elegans. *Elife.* (2017) 6:e19493. doi: 10.7554/eLife.19493

191. Wu RF, Liao C, Hatoum H, Fu G, Ochoa CD, Terada LS. RasGRF couples Nox4-dependent endoplasmic reticulum signaling to Ras. *Arteriosclerosis Thrombosis Vasc Biol.* (2017) 37:98–107. doi: 10.1161/ATVBAHA.116.307922

192. Lee J, Rhee MH, Kim E, Cho JY. BAY 11-7082 is a broad-spectrum inhibitor with anti-inflammatory activity against multiple targets. *Mediators Inflamm.* (2012) 2012:416036. doi: 10.1155/2012/416036

193. Irrera N, Vaccaro M, Bitto A, Pallio G, Pizzino G, Lentini M, et al. BAY 11-7082 inhibits the NF-κB and NLRP3 inflammasome pathways and protects against IMQ-induced psoriasis. *Clin Sci (Lond).* (2017) 131:487–98. doi: 10.1042/cs20160645

194. Scuderi SA, Casili G, Basilotta R, Lanza M, Filippone A, Raciti G, et al. NLRP3 inflammasome inhibitor BAY-117082 reduces oral squamous cell carcinoma progression. *Int J Mol Sci.* (2021) 22:11108. doi: 10.3390/ijms222011108

195. Moon SK, Jung SY, Choi YH, Lee YC, Patterson C, Kim CH. PDTC, metal chelating compound, induces G1 phase cell cycle arrest in vascular smooth muscle cells through inducing p21Cip1 expression: involvement of p38 mitogen activated protein kinase. *J Cell Physiol.* (2004) 198:310–23. doi: 10.1002/jcp.10728

196. Bhat OM, Kumar PU, Giridharan NV, Kaul D, Kumar MJ, Dhawan V. Interleukin-18-induced atherosclerosis involves CD36 and NF-κB crosstalk in Apo E-/- mice. *J Cardiol.* (2015) 66:28–35. doi: 10.1016/j.jjcc.2014.10.012

197. Zhang W, Li XJ, Zeng X, Shen DY, Liu CQ, Zhang HJ, et al. Activation of nuclear factor-κB pathway is responsible for tumor necrosis factor-α-induced up-regulation of endothelin B2 receptor expression in vascular smooth muscle cells in vitro. *Toxicol Lett.* (2012) 209:107–12. doi: 10.1016/j.toxlet.2011.12.005

198. Feng Y, Pathria G, Heynen-Genel S, Jackson M, James B, Yin J, et al. Identification and characterization of IMD-0354 as a glutamine carrier protein inhibitor in melanoma. *Mol Cancer Ther.* (2021) 20:816–32. doi: 10.1158/1535-7163.Mct-20-0354

199. Prola A, Pires Da Silva J, Guilbert A, Lecru L, Piquereau J, Ribeiro M, et al. SIRT1 protects the heart from ER stress-induced cell death through eIF2α deacetylation. *Cell Death Differ.* (2017) 24:343–56. doi: 10.1038/cdd.2016.138

200. Zheng G, Li H, Zhang T, Yang L, Yao S, Chen S, et al. Irisin protects macrophages from oxidized low density lipoprotein-induced apoptosis by inhibiting the endoplasmic reticulum stress pathway. *Saudi J Biol Sci.* (2018) 25:849–57. doi: 10.1016/j.sjbs.2017.08.018

201. Zhang Y, Song H, Zhang Y, Wu F, Mu Q, Jiang M, et al. Irisin inhibits atherosclerosis by promoting endothelial proliferation through microRNA126-5p. *J Am Heart Assoc.* (2016) 5:e004031. doi: 10.1161/jaha.116.004031

202. Remuzgo-Martínez S, Rueda-Gotor J, Pulito-Cueto V, López-Mejías R, Corrales A, Lera-Gómez L, et al. Irisin as a novel biomarker of subclinical atherosclerosis, cardiovascular risk and severe disease in axial spondyloarthritis. *Front Immunol.* (2022) 13:894171. doi: 10.3389/fimmu.2022.894171

203. Gouni-Berthold I, Berthold HK, Huh JY, Berman R, Spenrath N, Krone W, et al. Effects of lipid-lowering drugs on irisin in human subjects in vivo and in human skeletal muscle cells ex vivo. *PLoS One.* (2013) 8:e72858. doi: 10.1371/journal.pone.0072858

204. Agh F, Mohammadzadeh Honarvar N, Djalali M, Nematipour E, Gholamhoseini S, Zarei M, et al. Omega-3 fatty acid could increase one of myokines in male patients with coronary artery disease: a randomized, double-blind, placebo-controlled trial. *Arch Iran Med.* (2017) 20:28–33.

205. Lebeaupin C, Vallée D, Rousseau D, Patouraux S, Bonnafous S, Adam G, et al. Bax inhibitor-1 protects from nonalcoholic steatohepatitis by limiting inositol-requiring enzyme 1 alpha signaling in mice. *Hepatology.* (2018) 68:515–32. doi: 10.1002/hep.29847

206. Zhang F, Tang B, Zhang Z, Xu D, Ma G. DUSP6 Inhibitor (E/Z)-BCI hydrochloride attenuates lipopolysaccharide-induced inflammatory responses in murine macrophage cells via activating the Nrf2 signaling axis and inhibiting the NF-κB pathway. *Inflammation.* (2019) 42:672–81. doi: 10.1007/s10753-018-0924-2

207. Bian H, Wang G, Huang J, Liang L, Zheng Y, Wei Y, et al. Dihydrolipoic acid protects against lipopolysaccharide-induced behavioral deficits and neuroinflammation via regulation of Nrf2/HO-1/NLRP3 signaling in rat. *J Neuroinflamm.* (2020) 17:166. doi: 10.1186/s12974-020-01836-y

208. Wu NN, Tian H, Chen P, Wang D, Ren J, Zhang Y. Physical exercise and selective autophagy: benefit and risk on cardiovascular health. *Cells.* (2019) 8:1436. doi: 10.3390/cells8111436

209. Chang P, Zhang X, Zhang M, Li G, Hu L, Zhao H, et al. Swimming exercise inhibits myocardial ER stress in the hearts of aged mice by enhancing cGMP-PKG signaling. *Mol Med Rep.* (2020) 21:549–56. doi: 10.3892/mmr.2019.10864

210. Shen M, Wang L, Yang G, Gao L, Wang B, Guo X, et al. Baicalin protects the cardiomyocytes from ER stress-induced apoptosis: inhibition of CHOP through induction of endothelial nitric oxide synthase. *PLoS One.* (2014) 9:e88389. doi: 10.1371/journal.pone.0088389

211. Cai X, Bao L, Dai X, Ding Y, Zhang Z, Li Y. Quercetin protects RAW264.7 macrophages from glucosamine-induced apoptosis and lipid accumulation via the endoplasmic reticulum stress pathway. *Mol Med Rep.* (2015) 12:7545–53. doi: 10.3892/mmr.2015.4340

212. Zwicker JI, Schlechter BL, Stopa JD, Liebman HA, Aggarwal A, Puligandla M, et al. Targeting protein disulfide isomerase with the flavonoid isoquercetin to improve hypercoagulability in advanced cancer. *JCI Insight.* (2019) 4:e125851. doi: 10.1172/jci.insight.125851

213. Dagher O, Mury P, Noly PE, Fortier A, Lettre G, Thorin E, et al. Design of a randomized placebo-controlled trial to evaluate the anti-inflammatory and senolytic effects of quercetin in patients undergoing coronary artery bypass graft surgery. *Front Cardiovasc Med.* (2021) 8:741542. doi: 10.3389/fcvm.2021.741542

214. Kar P, Laight D, Rooprai HK, Shaw KM, Cummings M. Effects of grape seed extract in Type 2 diabetic subjects at high cardiovascular risk: a double blind randomized placebo controlled trial examining metabolic markers, vascular tone, inflammation, oxidative stress and insulin sensitivity. *Diabet Med.* (2009) 26:526–31. doi: 10.1111/j.1464-5491.2009.02727.x

215. Lin Y, Zhu J, Zhang X, Wang J, Xiao W, Li B, et al. Inhibition of cardiomyocytes hypertrophy by resveratrol is associated with amelioration of endoplasmic reticulum stress. *Cell Physiol Biochem.* (2016) 39:780–9. doi: 10.1159/000447788

216. Lou Y, Wang Z, Xu Y, Zhou P, Cao J, Li Y, et al. Resveratrol prevents doxorubicin-induced cardiotoxicity in H9c2 cells through the inhibition of endoplasmic reticulum stress and the activation of the Sirt1 pathway. *Int J Mol Med.* (2015) 36:873–80. doi: 10.3892/ijmm.2015.2291

217. van der Made SM, Plat J, Mensink RP. Trans-resveratrol supplementation and endothelial function during the fasting and postprandial phase: a randomized placebo-controlled trial in overweight and slightly obese participants. *Nutrients.* (2017) 9:596. doi: 10.3390/nu9060596

218. Marques B, Trindade M, Aquino JCF, Cunha AR, Gismondi RO, Neves MF, et al. Beneficial effects of acute trans-resveratrol supplementation in treated hypertensive patients with endothelial dysfunction. *Clin Exp Hypertens.* (2018) 40:218–23. doi: 10.1080/10641963.2017.1288741

219. Pecoraro L, Zoller T, Atkinson RL, Nisi F, Antoniazzi F, Cavarzere P, et al. Supportive treatment of vascular dysfunction in pediatric subjects with obesity: the OBELIX study. *Nutr Diabetes.* (2022) 12:2. doi: 10.1038/s41387-021-00180-1

220. Dong L, Qiao H, Zhang X, Zhang X, Wang C, Wang L, et al. Parthenolide is neuroprotective in rat experimental stroke model: downregulating NF-κB, phospho-p38MAPK, and caspase-1 and ameliorating BBB permeability. *Mediators Inflamm.* (2013) 2013:370804. doi: 10.1155/2013/370804

221. Yang X, Gao X, Cao Y, Guo Q, Li S, Zhu Z, et al. Anti-inflammatory effects of boldine and reticuline isolated from litsea cubeba through JAK2/STAT3 and NF-κB signaling pathways. *Planta Med.* (2018) 84:20–5. doi: 10.1055/s-0043-113447

222. Lee S, Choi SY, Choo YY, Kim O, Tran PT, Dao CT, et al. Sappanone A exhibits anti-inflammatory effects via modulation of Nrf2 and NF-κB. *Int Immunopharmacol.* (2015) 28:328–36. doi: 10.1016/j.intimp.2015.06.015

223. Zeng J, Chen Y, Ding R, Feng L, Fu Z, Yang S, et al. Isoliquiritigenin alleviates early brain injury after experimental intracerebral hemorrhage via suppressing ROS- and/or NF-κB-mediated NLRP3 inflammasome activation by promoting Nrf2 antioxidant pathway. *J Neuroinflamm.* (2017) 14:119. doi: 10.1186/s12974-017-0895-5

224. Su Y, Yuan J, Zhang F, Lei Q, Zhang T, Li K, et al. MicroRNA-181a-5p and microRNA-181a-3p cooperatively restrict vascular inflammation and atherosclerosis. *Cell Death Dis.* (2019) 10:365. doi: 10.1038/s41419-019-1599-9

225. Simion V, Zhou H, Pierce JB, Yang D, Haemmig S, Tesmenitsky Y, et al. LncRNA VINAS regulates atherosclerosis by modulating NF-κB and MAPK signaling. *JCI Insight.* (2020) 5:e140627. doi: 10.1172/jci.insight.140627

226. Bian W, Jing X, Yang Z, Shi Z, Chen R, Xu A, et al. Downregulation of LncRNA NORAD promotes Ox-LDL-induced vascular endothelial cell injury and atherosclerosis. *Aging (Albany NY).* (2020) 12:6385–400. doi: 10.18632/aging.103034

frontiers | Frontiers in Cardiovascular Medicine

TYPE Original Research
PUBLISHED 07 June 2023
DOI 10.3389/fcvm.2023.1149113

OPEN ACCESS

EDITED BY
Wen-Jun Tu,
Chinese Academy of Medical Sciences and Peking Union Medical College, China

REVIEWED BY
Ning Hou,
Guangzhou Medical University, China
Ding-Sheng Jiang,
Huazhong University of Science and Technology, China

*CORRESPONDENCE
Yiming Leng
lyming2010@csu.edu.cn

RECEIVED 21 January 2023
ACCEPTED 23 May 2023
PUBLISHED 07 June 2023

CITATION
Zhao Q, Liu R, Chen H, Yang X, Dong J, Bai M, Lu Y and Leng Y (2023) Transcriptome-wide association study reveals novel susceptibility genes for coronary atherosclerosis.
Front. Cardiovasc. Med. 10:1149113.
doi: 10.3389/fcvm.2023.1149113

Transcriptome-wide association study reveals novel susceptibility genes for coronary atherosclerosis

Qiuping Zhao[1], Rongmei Liu[1], Hui Chen[1], Xiaomo Yang[1], Jiajia Dong[1], Minfu Bai[1], Yao Lu[2] and Yiming Leng[3,4]*

[1]Heart Center of Henan Provincial People's Hospital, Fuwai Central China Cardiovascular Hospital, Zhengzhou, China, [2]School of Life Course Sciences, King's College London, London, United Kingdom, [3]Clinical Research Center, The Third Xiangya Hospital, Central South University, Changsha, China, [4]Department of Cardiology, The Third Xiangya Hospital, Central South University, Changsha, China

Background: Genetic risk factors substantially contributed to the development of coronary atherosclerosis. Genome-wide association study (GWAS) has identified many risk loci for coronary atherosclerosis, but the translation of these loci into therapeutic targets is limited for their location in non-coding regions. Here, we aimed to screen the potential coronary atherosclerosis pathogenic genes expressed though TWAS (transcriptome wide association study) and explore the underlying mechanism association.

Methods: Four TWAS approaches (PrediXcan, JTI, UTMOST, and FUSION) were used to screen genes associated with coronary atherosclerosis. Enrichment analysis of TWAS-identified genes was applied through the Metascape website. The summary-data-based Mendelian randomization (SMR) analysis was conducted to provide the evidence of causal relationship between the candidate genes and coronary atherosclerosis. At last, the cell type-specific expression of the intersection genes was examined by using human coronary artery single-cell RNA-seq, interrogating the immune microenvironment of human coronary atherosclerotic plaque at different stages of maturity.

Results: We identified 19 genes by at least three approaches and 1 gene (*NBEAL1*) by four approaches. Enrichment analysis enriching the genes identified at least by two TWAS approaches, suggesting that these genes were markedly enriched in asthma and leukocyte mediated immunity reaction. Further, the summary-data-based Mendelian randomization (SMR) analysis provided the evidence of causal relationship between *NBEAL1* gene and coronary atherosclerosis, confirming the protecting effects of *NBEAL1* gene and coronary atherosclerosis. At last, the single cell cluster analysis demonstrated that *NBEAL1* gene has differential expressions in macrophages, plasma cells and endothelial cells.

Conclusion: Our study identified the novel genes associated with coronary atherosclerosis and suggested the potential biological function for these genes, providing insightful guidance for further biological investigation and therapeutic approaches development in atherosclerosis-related diseases.

KEYWORDS

GWAS, coronary atherosclerosis, TWAS, genetic risk factors, genetic mechanisms

Introduction

Coronary artery disease (CAD), a leading global cause of death, is influenced by lifestyle, interactions of environmental, genetic risk factors and so on (1). Environmental and lifestyle factors were well-established coronary atherosclerosis risk factors, including physical activity, body mass index (BMI), smoking, healthy diet score and blood pressure (BP), total

cholesterol (TC) and fasting plasma glucose (FPG), as defined by American Heart Association (2, 3).

Meanwhile, genetic risk factors substantially contributed to the development of coronary atherosclerosis (4, 5). A study of more than 20,000 Swedish twins confirmed a heritability of ~50% for fatal coronary atherosclerosis among close relatives. Another analysis study using updated genome-wide approaches similarly quantified the heritability of coronary atherosclerosis at 40%–50% (6, 7). Recently, the genome-wide approaches have laid the foundation to understand the underlying genetic architecture of coronary atherosclerosis, to uncover novel biology and to apply these findings to clinical practice. More than 250 risk loci for coronary atherosclerosis have been identified though genome-wide association study (GWAS), helping to inform experimental interrogation of putative causal mechanisms for coronary atherosclerosis (8).

However, the translation of these loci into therapeutic targets is limited. One of the possible reasons is that most of these risk loci are located in the non-coding region of the human genome. The biological explanations are thus not straightforward. In order to solve this problem, TWAS (transcriptome wide association study) has been developed to identify and prioritize disease genes. TWAS may point to causal genes at risk sites identified by GWAS, thereby providing further insight into biological mechanisms (9, 10). In addition, TWAS can provide higher sensitivity to identify susceptibility genes missed by traditional GWAS analyses.

In this study, four different TWAS methods were used to systematically prioritize the potential coronary atherosclerosis pathogenic genes expressed in coronary arteries tissues, and to further reveal the underlying mechanism association through pathway enrichment analysis, providing novel evidence for the genetic mechanisms of coronary atherosclerosis.

Methods

Study design

First, we extracted the complete summary data from the GWASs for coronary atherosclerosis. Then we performed a TWAS analysis using four different methods with pre-trained gene expression models. Third, the summary-data-based Mendelian randomization (SMR) was used to assess the causal relationship between the intersection of genes and coronary atherosclerosis risk. Finally, we utilized public single-cell transcriptome data to explore the cell type-specific expression of the intersection genes in the coronary artery.

The data source for gene-expression models and coronary atherosclerosis

We used the recently released data of the Genotype-Tissue Expression (GTEx, https://gtexportal.org/home/) project (V8), which includes RNA sequencing data and whole-genome sequencing (WGS) data of coronary artery ($N = 213$). The training methods of gene-expression models can be found in previous studies (11–13). We utilized the pre-trained prediction models from Zenodo (https://doi.org/10.5281/zenodo.3842289) and TWAS/FUSION website (https://s3.us-west-1.amazonaws.com/gtex.v8.fusion/EUR/GTExv8.EUR.Artery_Coronary.tar.gz) for further transcriptome-wide association analyses. We collected the GWAS summary data of coronary atherosclerosis from FinnGen, a significant public-private partnership that aims to gather and analyze genetic and health data from more than 500,000 people. The latest release is from December 2022, including 342,499 participants (190,879 females and 151,620 males) and 20,175,454 variants. The diagnosis of coronary atherosclerosis from the hospital discharge registry and cause of death registry was based on the International Classification of Disease. In total, 42,421 cases and 285,621 controls were identified (https://www.finngen.fi/en/access_results).

Transcriptome-wide association study

We performed a summary-based TWAS using four different approaches, including the joint-tissue imputation (JTI) method (11), the PrediXcan (12), the modified unified test for molecular signatures (UTMOST) (11, 13), and the FUSION (14). Overall, the JTI borrows information on each tissue-tissue pair (or cell type) to improve the prediction quality. The PrediXcan uses the elastic net to determine the optimal hyperparameter. UTMOST borrows information across tissues using a sparse group-LASSO method. Similarly, FUSION is a suite of tools for performing TWAS. A combination of complementary methods may improve the reliability of results. We also applied Bonferroni corrections for multiple comparisons, considering the total number of tested genes across different methods.

Summary-data-based Mendelian randomization

We further validated the TWAS results using the SMR analysis followed by the heterogeneity in dependent instrument (HEIDI) test (15). The SMR was used to test for the potential causal effect of the expression level of a gene on coronary atherosclerosis using summary GWAS data and expression quantitative trait loci (eQTLs) studies. Genes were considered plausible causal gene only if they passed both SMR and HEIDI tests ($P_{SMR} < 0.05$ and HEIDI $P > 0.05$).

Enrichment analysis and cell-type specificity analysis

We performed the enrichment analysis of TWAS-identified genes using the Metascape website (16). We examined the cell type-specific expression of the intersection genes by using human coronary artery single-cell RNA-seq, interrogating the immune microenvironment of human coronary atherosclerotic plaque at different stages of maturity. Clusters were annotated by taking default parameters with an online tool to visualize single-cell

data (17). Finally, we performed differential expression analysis to determine whether these candidate genes were differentially expressed in some specific cell types.

Results

Transcriptome-wide significant genes for coronary atherosclerosis

Four TWAS approaches (PrediXcan, JTI, UTMOST, and FUSION) were used to screen genes associated with coronary atherosclerosis (**Supplementary Tables S1–S4**). Finally, we identified 19 genes with TWAS *P*-value passing multiple testing, such as *NBEAL1*, *CEACAM19*, *AC243964.3*, *INO80E*, et al. Among these candidate genes, only one gene (*NBEAL1*) was identified by all TWAS approaches. **Figure 1** shows the Venn diagram of the TWAS-identified genes. **Table 1** summarizes the 19 associated genes identified by at least three TWAS approaches.

Enrichment analysis of the TWAS-identified genes

Enrichment analysis of the genes identified at least by two TWAS approaches results were shown in **Figure 2**. Several significant biological process terms and pathways were detected, such as asthma (hsa05310), positive regulation of telomere maintenance (GO:0032206), positive regulation of biological process (GO:0048518), negative regulation of neuron projection development (GO:0010977), immune system process (GO:0002376) and so on. We found that among all the significant biological process terms and pathways, the genes identified at least by two TWAS approaches were markedly enriched in asthma and leukocyte mediated immunity reaction (**Figure 2**).

Causal relationships between *NBEAL1* and coronary atherosclerosis

The NBEAL1 gene was identified by all the four TWAS approaches, suggesting that this gene might be the most reliable associated gene. We therefore explored the causal relationship between *NBEAL1* expression in the coronary artery and coronary atherosclerosis using SMR. Our results showed *NBEAL1* was a plausible causal gene in the coronary artery and coronary atherosclerosis. And it provided a protective role in coronary atherosclerosis incidence (odds ratio (OR) = 0.84, 95% confidence interval (CI) = 0.79–0.90, *P*-value = 5.84^{-8}) (**Supplementary Table S5**), showing the same direction as that in TWAS analysis.

Single-cell cluster analysis

To analyze the expression of *NBEAL1* gene in immune cells during the immune response process, we also performed single cell cluster analysis. Our results showed the human coronary atherosclerotic plaque tissue were annotated into seven clusters, including endothelial cells, plasma cells, erythrocyte, T cells, mast cells, macrophages, and Natural killer (NK) cells. The single cell cluster analysis demonstrated that *NBEAL1* gene has differential expressions in macrophages, plasma cells and endothelial cells (**Figure 3**).

Discussion

In this study, we identified 19 genes by at least three TWAS approaches and one gene (*NBEAL1*) by four TWAS approaches. Next, we found that these genes were markedly enriched in asthma and leukocyte mediated immunity reaction though gene enrichment analysis approaches. Further, the SMR analysis provide the evidence of causal relationship between *NBEAL1* gene and coronary atherosclerosis, confirming the protective effects of *NBEAL1* gene and coronary atherosclerosis. Finally, the single cell cluster analysis demonstrated that *NBEAL1* gene has differential expressions in macrophages, plasma cells and endothelial cells.

CAD is one kind of cardiovascular diseases with a high prevalence rate, and its etiology is complex, among which genetic factors play the primary role. Although GWAS has identified many risk loci for CAD, only a minority of candidate genes could be experimentally demonstrated for their potential causal role in atherosclerosis. TWAS, a bioinformatics method based on expression levels of specific genes in defined tissues, could shed further insights into biological mechanisms in the pathophysiological process of diseases. There has been TWAS analysis identifying 18 novel genes in association with CAD based on two genetics-of-gene-expression panels (STARNET and GTEx) (18). More TWAS analyses are needed to explore genes associated with coronary atherosclerosis diseases.

Atherosclerosis is a chronic, complex inflammatory disease that is mediated by adaptive and innate immunity (19, 20). However, the specific molecular mechanisms and gene associated causal effects on coronary atherosclerosis are still unclear. Our study identified 19 novel genes by three TWAS approaches and one novel gene (*NBEAL1*) by four TWAS approaches associated with coronary atherosclerosis, and all these genes could be enriched in leukocyte mediated immunity reaction pathway. Abnormal immune response could interact with inflammation, metabolic risk factors, and other effector molecules to initiate and activate lesions in the arterial tree, inducing and accelerating the progression of coronary atherosclerosis (21, 22). Leukocytes, as the body's predominant immune cells, have traditionally been recognized as markers of acute or chronic inflammation. Previous studies have reported leukocytes and their subpopulations (lymphocytes, neutrophils, monocytes, eosinophils, and basophils) are associated with CAD (23, 24). Our recent research has also confirmed the causal relationship between leukocytes and CAD though Mendelian randomization (MR) approach. This study reconfirmed the relationship between leukocyte-mediated immune response and coronary atherosclerosis at the level of gene and gene function.

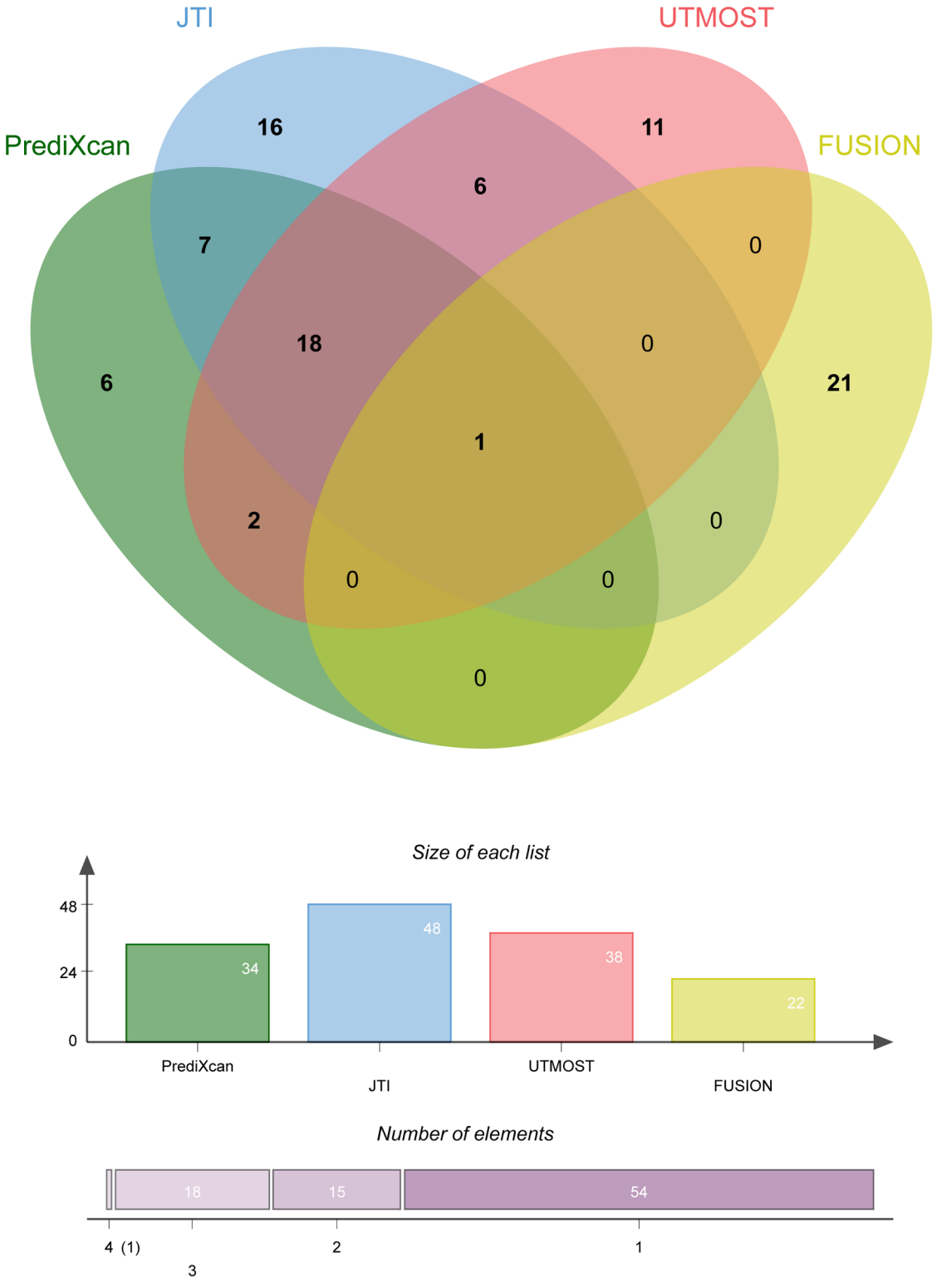

FIGURE 1
Overlap analysis of the coronary atherosclerosis associated genes by different TWAS approaches.

In addition, the study found the genes identified by TWAS could also be enriched in asthma pathway. There have been many researches focusing on the relationship between asthma and CAD. Some studies demonstrated that adult-onset asthma was associated with CAD, especially in females (25, 26), and the potential mechanism may involve systemic inflammation and cellular immunity. However, some bioinformatics analyses (such as MR) found that asthma was a causal factor for atrial

TABLE 1 TWAS-identified genes associated with coronary atherosclerosis.

	PrediXcan		JTI		UTMOST		FUSION	
	Z score	*P* value	*Z* score	*P* value	*Z* score	*P* value	*Z* score	*P* value
NBEAL1	−5.16	2.47×10^{-7}	−5.26	1.43×10^{-7}	−5.02	5.12×10^{-7}	−7.62	2.43×10^{-14}
CEACAM19	11.85	2.13×10^{-32}	9.12	6.90×10^{-20}	9.43	3.88×10^{-21}	–	–
AC243964.3	9.37	6.98×10^{-21}	7.82	4.93×10^{-15}	7.35	1.95×10^{-13}	–	–
INO80E	6.50	8.30×10^{-11}	6.26	3.74×10^{-10}	6.59	4.33×10^{-11}	–	–
WNT3	−6.09	1.10×10^{-9}	−5.86	4.51×10^{-9}	−6.13	8.52×10^{-10}	–	–
C17orf107	6.09	1.15×10^{-9}	5.01	5.28×10^{-7}	5.18	2.13×10^{-7}	–	–
SCIMP	6.06	1.34×10^{-9}	6.04	1.48×10^{-9}	4.84	1.25×10^{-6}	–	–
HLA-DQA2	−5.81	6.09×10^{-9}	−5.87	4.29×10^{-9}	−5.47	4.36×10^{-8}	–	–
YPEL3	−5.81	6.25×10^{-9}	−4.92	8.58×10^{-7}	−6.05	1.40×10^{-9}	–	–
KANSL1-AS1	−5.71	1.08×10^{-8}	−5.61	1.99×10^{-8}	−5.36	7.98×10^{-8}	–	–
LACTB	5.48	4.05×10^{-8}	5.65	1.55×10^{-8}	5.34	9.07×10^{-8}	–	–
SLC26A1	−5.45	4.89×10^{-8}	−5.10	3.31×10^{-7}	−5.00	5.65×10^{-7}	–	–
KAT8	−5.39	6.95×10^{-8}	−6.27	3.50×10^{-10}	−6.08	1.18×10^{-9}	–	–
EPHX2	5.38	7.27×10^{-8}	5.10	3.28×10^{-7}	4.86	1.16×10^{-6}	–	–
CHRNE	5.26	1.41×10^{-7}	5.30	1.11×10^{-7}	5.33	9.68×10^{-8}	–	–
LRRC37A2	−5.25	1.51×10^{-7}	−5.51	3.44×10^{-8}	−5.19	2.10×10^{-7}	–	–
NDUFAF6	4.78	1.68×10^{-6}	5.00	5.73×10^{-7}	5.43	5.61×10^{-8}	–	–
AC135050.3	−4.65	3.29×10^{-6}	−4.71	2.38×10^{-6}	−4.50	6.55×10^{-6}	–	–
EARS2	4.46	7.97×10^{-6}	4.72	2.34×10^{-6}	4.68	2.83×10^{-6}	–	–

fibrillation and heart failure, but not for CAD (27, 28). Therefore, more research is needed to explore the relationship between asthma and coronary atherosclerosis.

The *NBEAL1* is a new coronary atherosclerosis associated maker gene screened by four TWAS approaches in our study. The *NBEAL1* gene, located on human chromosome 2q33–2q34 was consisted of 25 exons spanning about 73 kb of the human genome. *NBEAL1* gene transcripts showed high expression in the human brain, kidney, prostate, and testis while low expression in the ovary, small intestine, colon and peripheral blood leukocyte. *NBEAL1* was first found higher expression in glioma tissues compared to the normal brain tissue, suggesting its correlation with the glioma (29). Besides, some research also revealed its association with stroke, cerebral small vessel disease and hereditary breast cancer (30–32).

Recently, a gene-based analyses from the NIH Exome Sequencing Project has identified the association between *NBEAL1* gene and early onset myocardial infarction, emphasizing the potential contributions of genetic variation in *NBEAL1* to the pathogenesis of premature atherosclerosis (33). However, there is few reports on the causal relationship between *NBEAL1* gene and coronary atherosclerosis. In this research, we further identified

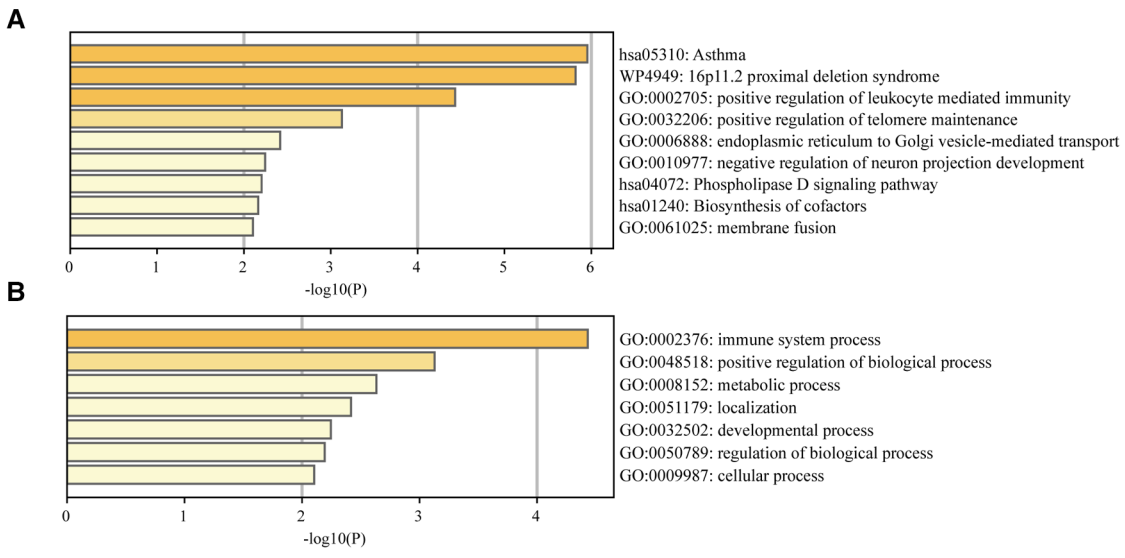

FIGURE 2
(A) Enrichment analysis of the TWAS-identified genes. (B) Enrichment analysis of the immune system process.

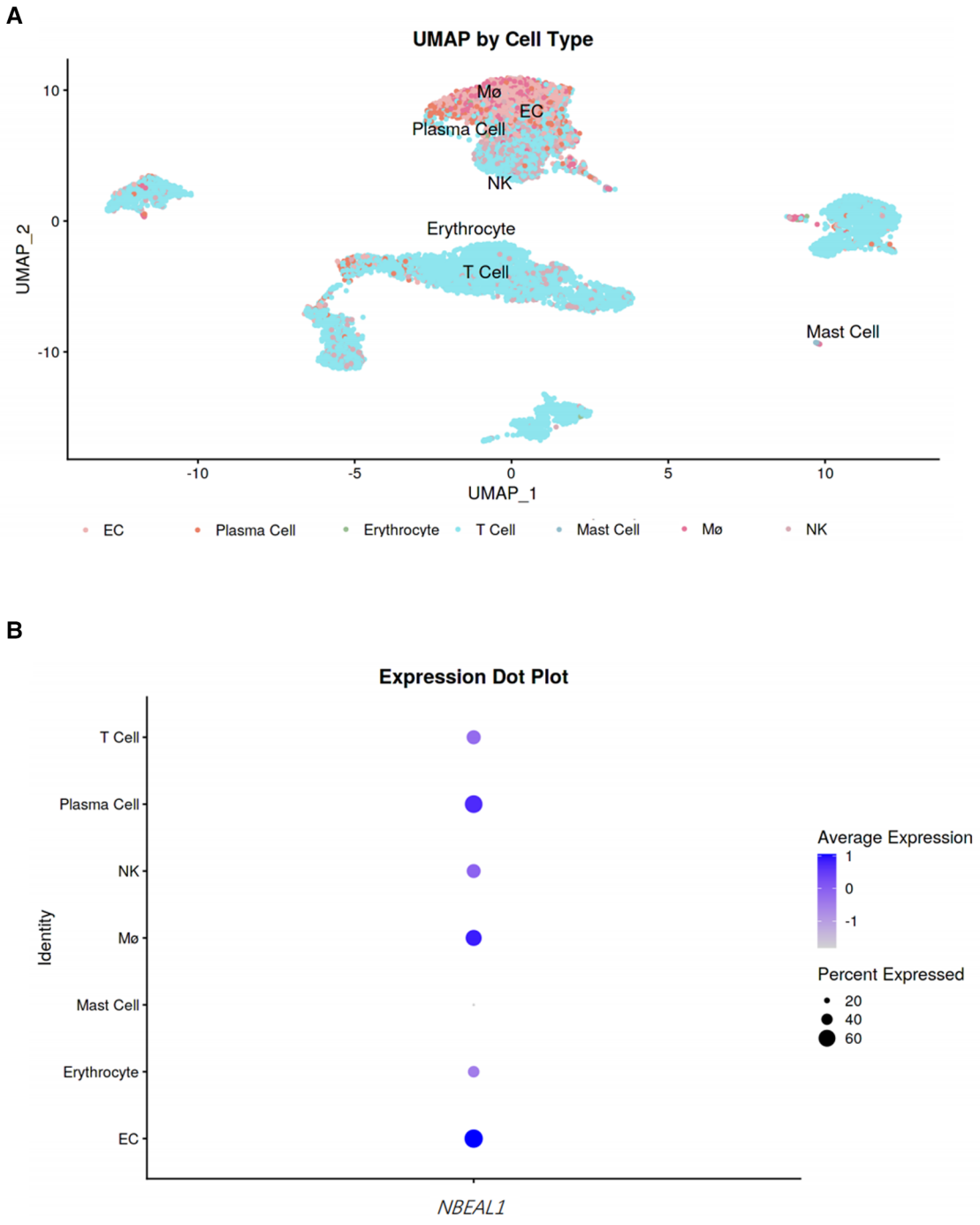

FIGURE 3
Single cell cluster analysis. (A) UMAP by cell type. To observe the expression of *NBEAL1* gene in cells, the darker the color, the higher the expression. (B) Expression dot plot. The size of the dot represents the proportion of the *NBEAL1* gene in the immune cells and the shade of the dot represents the degree of expression, the darker the color, the higher the expression.

the causal relationship between *NBEAL1* gene and coronary atherosclerosis though SMR analysis, and we found *NBEAL1* gene was a protective causal gene maker for CAD. Combined with our previous enrichment analysis results, we speculate that *NBEAL1* gene might mediate the development of coronary atherosclerosis through the immune inflammatory pathway. Christian et al. found that *NBEAL1* is shown to be expressed most abundantly in arteries and could regulate cholesterol metabolism through modulation of LDLR expression in a mechanism which involves interaction with SCAP and PAQR3

and subsequent SREBP2-processing (34). Low expression of *NBEAL1* may lead to increased risk of CAD by downregulation of LDLR levels. In depth, it is still unclear whether *NBEAL1* gene associated immune inflammatory reaction could lead to the occurrence and development of coronary atherosclerosis though cholesterol metabolism pathway, and more research are needed to identify this.

Further, single cell cluster analysis found that *NBEAL1* gene has differential expressions in macrophages, plasma cells and endothelial cells. All these cells are the key cells involved in the occurrence and development of coronary atherosclerosis. Macrophages contribute to the maintenance of the local inflammatory response by producing reactive oxygen and nitrogen species and secreting chemokines, proinflammatory cytokines (including IL-6, TNF-α and IL-1β) (35–37). In pathological condition, the inflammatory cycle can be amplified with increased retention of lipoproteins (38, 39), finally promoting the formation of complicated atherosclerotic plaques. Endothelial cells are important barrier covering the wall of the arteries, regulating vascular tone, preventing platelet aggregation, and maintaining fluid homeostasis (40–42). Endothelial dysfunction plays a central role in all phases of the atherosclerotic process. Once more, the single cell cluster analysis results illustrate that the *NBEAL1* gene enriched in these key cells may be an important intervention target for prevention and treatment of coronary atherosclerosis.

However, there are still some limitations in our study. We did not exhibit molecular biology experiment to further explore the specific mechanism association between the maker genes and coronary atherosclerosis, and we will perform this part of research in future. Besides, our research results are obtained through bioinformatics methods, and we did not revalidate our findings in the coronary atherosclerosis population. This is also an important part of our future research directions.

Conclusion

In conclusion, we identified the novel genes associated with coronary atherosclerosis and suggested the potential biological function (inflammatory immune pathway) for these genes, providing insightful guidance for further research and therapeutic approaches development in atherosclerosis-related diseases.

Data availability statement

The original contributions presented in the study are included in the article/**Supplementary Material**, further inquiries can be directed to the corresponding author.

Ethics statement

This study is a secondary analysis conducted through existing GWAS data. The specific ethics and consent statements reviewed in this study can be accessed in the original publication.

Author contributions

All authors participated in the field survey and data collection. QZ and YML contributed to the study conception. QZ, RL, MB and XY drafted the manuscript. YML, HC, YL and JD analyzed the data. QZ obtained the funding. All authors contributed to the article and approved the submitted version.

Funding

Henan Provincial Medical Science and Education Research Program project jointly built by the Ministry (SB201903022), Henan Province Key and Joint Construction Project of Medical Science and Technology (LHGJ20210102), Henan Province Key and Joint Construction Project of Medical Science and Technology (LHGJ20220103).

Conflict of interest

The authors declare that the research was conducted in the absence of any commercial or financial relationships that could be construed as a potential conflict of interest.

Publisher's note

Supplementary material

The Supplementary Material for this article can be found online at: https://www.frontiersin.org/articles/10.3389/fcvm.2023.1149113/full#supplementary-material

SUPPLEMENTARY FIGURE S1
Transcriptome comparison of NBEAL1 gene in publicly available data (GSE43292). G1 is for control group, G2 is for experimental group.

References

1. Malakar AK, Choudhury D, Halder B, Paul P, Uddin A, Chakraborty S. A review on coronary artery disease, its risk factors, and therapeutics. *J Cell Physiol*. (2019) 234:16812–23. doi: 10.1002/jcp.28350

2. Lloyd-Jones DM, Hong Y, Labarthe D, Mozaffarian D, Appel LJ, Van Horn L, et al. Defining and setting national goals for cardiovascular health promotion and disease reduction: the American Heart Association's strategic impact goal through 2020 and beyond. *Circulation*. (2010) 121:586–613. doi: 10.1161/CIRCULATIONAHA.109.192703

3. Arnett DK, Blumenthal RS, Albert MA, Buroker AB, Goldberger ZD, Hahn EJ, et al. 2019 ACC/AHA guideline on the primary prevention of cardiovascular disease: executive summary: a report of the American College of Cardiology/American Heart Association task force on clinical practice guidelines. *J Am Coll Cardiol*. (2019) 74:1376–414. doi: 10.1016/j.jacc.2019.03.009

4. Kathiresan S, Srivastava D. Genetics of human cardiovascular disease. *Cell*. (2012) 148:1242–57. doi: 10.1016/j.cell.2012.03.001

5. Khera AV, Kathiresan S. Genetics of coronary artery disease: discovery, biology and clinical translation. *Nat Rev Genet*. (2017) 18:331–44. doi: 10.1038/nrg.2016.160

6. Marenberg ME, Risch N, Berkman LF, Floderus B, de Faire U. Genetic susceptibility to death from coronary heart disease in a study of twins. *N Engl J Med*. (1994) 330:1041–6. doi: 10.1056/NEJM199404143301503

7. Zdravkovic S, Wienke A, Pedersen NL, Marenberg ME, Yashin AI, De Faire U. Heritability of death from coronary heart disease: a 36-year follow-up of 20 966 Swedish twins. *J Intern Med*. (2002) 252:247–54. doi: 10.1046/j.1365-2796.2002.01029.x

8. Aragam KG, Jiang T, Goel A, Kanoni S, Wolford BN, Atri DS, et al. Discovery and systematic characterization of risk variants and genes for coronary artery disease in over a million participants. *Nat Genet*. (2022) 54:1803–15. doi: 10.1038/s41588-022-01233-6

9. Wainberg M, Sinnott-Armstrong N, Mancuso N, Barbeira AN, Knowles DA, Golan D, et al. Opportunities and challenges for transcriptome-wide association studies. *Nat Genet*. (2019) 51:592–9. doi: 10.1038/s41588-019-0385-z

10. Zhang W, Voloudakis G, Rajagopal VM, Readhead B, Dudley JT, Schadt EE, et al. Integrative transcriptome imputation reveals tissue-specific and shared biological mechanisms mediating susceptibility to complex traits. *Nat Commun*. (2019) 10:3834. doi: 10.1038/s41467-019-11874-7

11. Zhou D, Jiang Y, Zhong X, Cox NJ, Liu C, Gamazon ER. A unified framework for joint-tissue transcriptome-wide association and Mendelian randomization analysis. *Nat Genet*. (2020) 52:1239–46. doi: 10.1038/s41588-020-0706-2

12. Gamazon ER, Wheeler HE, Shah KP, Mozaffari SV, Aquino-Michaels K, Carroll RJ, et al. A gene-based association method for mapping traits using reference transcriptome data. *Nat Genet*. (2015) 47:1091–8. doi: 10.1038/ng.3367

13. Hu Y, Li M, Lu Q, Weng H, Wang J, Zekavat SM, et al. A statistical framework for cross-tissue transcriptome-wide association analysis. *Nat Genet*. (2019) 51:568–76. doi: 10.1038/s41588-019-0345-7

14. Gusev A, Ko A, Shi H, Bhatia G, Chung W, Penninx BW, et al. Integrative approaches for large-scale transcriptome-wide association studies. *Nat Genet*. (2016) 48:245–52. doi: 10.1038/ng.3506

15. Zhu Z, Zhang F, Hu H, Bakshi A, Robinson MR, Powell JE, et al. Integration of summary data from GWAS and eQTL studies predicts complex trait gene targets. *Nat Genet*. (2016) 48:481–7. doi: 10.1038/ng.3538

16. Zhou Y, Zhou B, Pache L, Chang M, Khodabakhshi AH, Tanaseichuk O, et al. Metascape provides a biologist-oriented resource for the analysis of systems-level datasets. *Nat Commun*. (2019) 10:1523. doi: 10.1038/s41467-019-09234-6

17. Ma WF, Hodonsky CJ, Turner AW, Wong D, Song Y, Mosquera JV, et al. Enhanced single-cell RNA-seq workflow reveals coronary artery disease cellular cross-talk and candidate drug targets. *Atherosclerosis*. (2022) 340:12–22. doi: 10.1016/j.atherosclerosis.2021.11.025

18. Li L, Chen Z, von Scheidt M, Li S, Steiner A, Güldener U, et al. Transcriptome-wide association study of coronary artery disease identifies novel susceptibility genes. *Basic Res Cardiol*. (2022) 117:6. doi: 10.1007/s00395-022-00917-8

19. Wolf D, Ley K. Immunity and inflammation in atherosclerosis. *Circ Res*. (2019) 124:315–27. doi: 10.1161/CIRCRESAHA.118.313591

20. Ruparelia N, Choudhury R. Inflammation and atherosclerosis: what is on the horizon? *Heart*. (2020) 106:80–5. doi: 10.1136/heartjnl-2018-314230

21. Hansson GK. Inflammation, atherosclerosis, and coronary artery disease. *N Engl J Med*. (2005) 352:1685–95. doi: 10.1056/NEJMra043430

22. Gerling IC, Ahokas RA, Kamalov G, Zhao W, Bhattacharya SK, Sun Y, et al. Gene expression profiles of peripheral blood mononuclear cells reveal transcriptional signatures as novel biomarkers of cardiac remodeling in rats with aldosteronism and hypertensive heart disease. *JACC Heart Fail*. (2013) 1:469–76. doi: 10.1016/j.jchf.2013.09.003

23. Wheeler JG, Mussolino ME, Gillum RF, Danesh J. Associations between differential leucocyte count and incident coronary heart disease: 1764 incident cases from seven prospective studies of 30,374 individuals. *Eur Heart J*. (2004) 25:1287–92. doi: 10.1016/j.ehj.2004.05.002

24. Madjid M, Fatemi O. Components of the complete blood count as risk predictors for coronary heart disease: in-depth review and update. *Tex Heart Inst J*. (2013) 40:17–29.

25. Lee HM, Truong ST, Wong ND. Association of adult-onset asthma with specific cardiovascular conditions. *Respir Med*. (2012) 106:948–53. doi: 10.1016/j.rmed.2012.02.017

26. Liu H, Fu Y, Wang K. Asthma and risk of coronary heart disease: a meta-analysis of cohort studies. *Ann Allergy Asthma Immunol*. (2017) 118:689–95. doi: 10.1016/j.anai.2017.03.012

27. Chen H, Chen W, Zheng L. Genetic liability to asthma and risk of cardiovascular diseases: a Mendelian randomization study. *Front Genet*. (2022) 13:879468. doi: 10.3389/fgene.2022.879468

28. Zhou Y, Liang ZS, Jin Y, Ding J, Huang T, Moore JH, et al. Shared genetic architecture and causal relationship between asthma and cardiovascular diseases: a large-scale cross-trait analysis. *Front Genet*. (2021) 12:775591. doi: 10.3389/fgene.2021.775591

29. Chen J, Lu Y, Xu J, Huang Y, Cheng H, Hu G, et al. Identification and characterization of NBEAL1, a novel human neurobeachin-like 1 protein gene from fetal brain, which is up regulated in glioma. *Brain Res Mol Brain Res*. (2004) 125:147–55. doi: 10.1016/j.molbrainres.2004.02.022

30. Wu BS, Chen SF, Huang SY, Ou YN, Deng YT, Chen SD, et al. Identifying causal genes for stroke via integrating the proteome and transcriptome from brain and blood. *J Transl Med*. (2022) 20:181. doi: 10.1186/s12967-022-03377-9

31. Traylor M, Zhang CR, Adib-Samii P, Devan WJ, Parsons OE, Lanfranconi S, et al. Genome-wide meta-analysis of cerebral white matter hyperintensities in patients with stroke. *Neurology*. (2016) 86:146–53. doi: 10.1212/WNL.0000000000002263

32. Glentis S, Dimopoulos AC, Rouskas K, Ntritsos G, Evangelou E, Narod SA, et al. Exome sequencing in BRCA1- and BRCA2-negative Greek families identifies MDM1 and NBEAL1 as candidate risk genes for hereditary breast cancer. *Front Genet*. (2019) 10:1005. doi: 10.3389/fgene.2019.01005

33. Hixson JE, Jun G, Shimmin LC, Wang Y, Yu G, Mao C, et al. Whole exome sequencing to identify genetic variants associated with raised atherosclerotic lesions in young persons. *Sci Rep*. (2017) 7:4091. doi: 10.1038/s41598-017-04433-x

34. Bindesbøll C, Aas A, Ogmundsdottir MH, Pankiv S, Reine T, Zoncu R, et al. NBEAL1 controls SREBP2 processing and cholesterol metabolism and is a susceptibility locus for coronary artery disease. *Sci Rep*. (2020) 10:4528. doi: 10.1038/s41598-020-61352-0

35. Xue J, Schmidt SV, Sander J, Draffehn A, Krebs W, Quester I, et al. Transcriptome-based network analysis reveals a spectrum model of human macrophage activation. *Immunity*. (2014) 40:274–88. doi: 10.1016/j.immuni.2014.01.006

36. Martinez FO, Gordon S, Locati M, Mantovani A. Transcriptional profiling of the human monocyte-to-macrophage differentiation and polarization: new molecules and patterns of gene expression. *J Immunol*. (2006) 177:7303–11. doi: 10.4049/jimmunol.177.10.7303

37. Mosser DM, Edwards JP. Exploring the full spectrum of macrophage activation. *Nat Rev Immunol*. (2008) 8:958–69. doi: 10.1038/nri2448

38. Moore KJ, Sheedy FJ, Fisher EA. Macrophages in atherosclerosis: a dynamic balance. *Nat Rev Immunol*. (2013) 13:709–21. doi: 10.1038/nri3520

39. Williams KJ, Tabas I. The response-to-retention hypothesis of early atherogenesis. *Arterioscler Thromb Vasc Biol*. (1995) 15:551–61. doi: 10.1161/01.ATV.15.5.551

40. Herrero-Fernandez B, Gomez-Bris R, Somovilla-Crespo B, Gonzalez-Granado JM. Immunobiology of atherosclerosis: a complex net of interactions. *Int J Mol Sci*. (2019) 20. doi: 10.3390/ijms20215293

41. Marchio P, Guerra-Ojeda S, Vila JM, Aldasoro M, Victor VM, Mauricio MD. Targeting early atherosclerosis: a focus on oxidative stress and inflammation. *Oxid Med Cell Longev*. (2019) 2019:8563845. doi: 10.1155/2019/8563845

42. Lee DY, Chiu JJ. Atherosclerosis and flow: roles of epigenetic modulation in vascular endothelium. *J Biomed Sci*. (2019) 26:56. doi: 10.1186/s12929-019-0551-8

frontiers | Frontiers in Cardiovascular Medicine

TYPE Original Research
PUBLISHED 27 June 2023
DOI 10.3389/fcvm.2023.1167132

OPEN ACCESS

EDITED BY
Mark Slevin,
Manchester Metropolitan University,
United Kingdom

REVIEWED BY
Mirjana Macvanin,
University of Belgrade, Serbia
Mustafa Yalcinkaya,
Columbia University Irving Medical Center,
United States

*CORRESPONDENCE
Gang Li
ligang20210203@163.com

†These authors have contributed equally to this work

RECEIVED 16 February 2023
ACCEPTED 14 June 2023
PUBLISHED 27 June 2023

CITATION
Guo F, He M, Hu B and Li G (2023) Levels and clinical significance of the m6A methyltransferase METTL14 in patients with coronary heart disease.
Front. Cardiovasc. Med. 10:1167132.
doi: 10.3389/fcvm.2023.1167132

Levels and clinical significance of the m6A methyltransferase METTL14 in patients with coronary heart disease

Fengxia Guo[1†], Mei He[2†], Bing Hu[3] and Gang Li[1*]

[1]Department of Clinical Laboratory, Henan Provincial People's Hospital; People's Hospital of Zhengzhou University, Zhengzhou, China, [2]Zhengzhou Key Laboratory, Zhengzhou No. 7 People's Hospital, Zhengzhou, China, [3]Department of Clinical Laboratory, Affiliated Cancer Hospital of Zhengzhou University, Zhengzhou, China

Objective: To investigate the association of methyltransferase-like protein 14 (METTL14) expression with coronary heart disease (CHD).
Methods: Three hundred and sixteen patients who attended Henan Provincial People's Hospital between June 2019 and February 2021 with principal symptoms of pain or tightness in the chest and who underwent coronary angiography for definitive diagnosis were enrolled. The uric acid, TG, TC, LDL-C, HDL-C, apolipoprotein A1, free fatty acid, lipoprotein a, homocysteine, CRP, and SAA levels were examined. The levels of METTL14, TNF-α, MCP-1, VCAM-1, ICAM-1, and IL-6 were evaluated by ELISA.
Results: Patients with CHD had significantly higher m6A methyltransferase activity. In addition, the incidence of diabetes and hypertension, as well as the concentrations of TC, CRP, and SAA were higher in CHD patients. Patients with coronary lesion branches also had significantly increased TG, LDL-C, CRP, and SAA levels. TNF-α, MCP-1, VCAM-1, ICAM-1, and IL-6 expression was also markedly increased in the CHD group ($P < 0.001$) as was the expression of METTL14 ($P < 0.001$). The METTL14 expression levels also differed significantly in relation to the number of branches with lesions ($P < 0.01$) and were correlated with SAA, VCAM-1, ICAM-1, IL-6, and the Gensini score. ROC curve analyses of METTL14 in CHD indicated an AUC of 0.881 (0.679, 0.894) with a cut-off value of 342.37, a sensitivity of 77%, and a specificity of 84%. MCP-1, VCAM-1, IL-6, SAA, and METTL14 were found to independently predict CHD risk.
Conclusions: METTL14 levels were found to be positively associated with inflammatory markers and to be an independent predictor of CHD risk.

KEYWORDS
coronary heart disease, m6A methylation, METTL14, inflammatory markers, atherosclerosis

1. Introduction

Coronary heart disease (CHD) is increasing in incidence. The current tests used to assist in the diagnosis of CHD have limited specificity and sensitivity and are invasive; thus, the identification of specific biomarkers is important for the early detection of CHD. CHD is both chronic and progressive and evidence suggests a close association between CHD and inflammation, which can be assessed by a variety of inflammatory indicators, suggesting that the levels of these indicators may be useful for preventing, diagnosing, and treating CHD (1–4). Thus, a comprehensive analysis of potential indicators and biomarkers for CHD development and progression would be highly useful for the assessment of CHD risk.

The importance of epigenetic modification is increasingly recognized. Nucleic acid methylation is a major form of epigenetic modification, with N6-methyladenosine (m6A) methylation representing approximately 80% of RNA modifications in eukaryotes (5). m6A methylation is controlled by a series of enzymes, specifically, the "writers" or m6A methyltransferases, such as METTL3/14, VIRMA, RBM15/15B, WTAP, and ZC3H13, responsible for the methylation, the "erasers" or demethylases, such as ALKBH5, FTO, and ALKBH3, that remove the modification, and "readers", such as hnRNP, YTHDF1/2/3, eIF3, and IGF2BP1/2/3 (6, 7). Evidence suggests the close involvement of m6A methylation in regulating RNA function and these modifications have been associated with pathological processes in in physiological and pathological processes of cardiovascular diseases (8). Methyltransferase-like 14 (METTL14), a well-known m6A writer protein, widely participated in the progression of major diseases, such as cardiovascular pathogenesis (9). In addition, METTL14 plays an important role in maintaining cardiac homeostasis (10). Knocking down METTL14 could inhibit the development of atherosclerosis in high-fat diet-treated APOE-/- mice (11). Here, the clinical significance of alterations in the METTL14 levels of CHD patients was investigated to clarify the association between METTL14 and the severity of CHD. It is hoped that these findings will suggest new directions for CHD prevention and treatment.

2. Study participants and methods

2.1. Patients

A total of 316 patients who attended Henan Provincial People's Hospital between June 2019 and February 2021 with principal symptoms of pain or tightness in the chest and who received coronary angiography for definitive diagnosis were recruited. The patients were allocated to a CHD group and a control group based on the angiographic findings. Patients in the control group had no stenosis of the coronary arteries or only myocardial bridge alterations (i.e., congenital abnormal coronary artery development where a part of the coronary artery crosses the myocardium). The inclusion criterion for the CHD group was the presence of a >50% stenosis in at least one coronary artery (left main, left circumflex, left anterior descending, or right coronary artery). Patients who had undergone earlier coronary angiography and coronary artery bypass grafting were excluded, as were those with hematological disorders, tumors, severe liver and renal insufficiencies, acute or chronic infectious diseases, active bleeding from all causes, peripheral vascular disease, diabetes mellitus, cardiac arrhythmia, or chronic obstructive pulmonary disease. The study was approved by the Ethics Committee of the hospital, and all participants provided written informed consent.

2.2. Collection and analysis of blood samples

Five-milliliter venous blood samples were collected after an overnight fast. After centrifugation (3,000 rpm, 15 min), the uric acid, TG, TC, LDL-C, free fatty acid, lipoprotein a, homocysteine, HDL-C, Apolipoprotein A1 (ApoA1), CRP, and plasma amyloid A (SAA) levels were determined.

2.3. Methods

2.3.1 ELISA

ELISA kits (Abcam, Cambridge, UK) were used to measure the plasma levels of METTL14, TNF-α, MCP-1, VCAM-, ICAM-1, and IL-6.

2.3.2. Methylase activity assay

The m6A methylase activity was determined using an Epigenase m6A Methylase Activity Assay kit (Epigentek, NY, USA).

2.3.3. qRT-PCT

Total RNA was isolated from plasma using a TRIzol kit (Invitrogen, Carlsbad, CA, USA). The RNA concentration was measured with a spectrophotometer (NanoDrop® 2000; Thermo Fisher Scientific, Waltham, MA, USA). All experimental procedures were performed according to the manufacturer's instructions. Ploidy differences in expression levels were determined using the 2-ΔΔCt method.

METTL14 Forward: 5′-GTT GGA ACA TGG ATA GCC GC-3′; Reverse: 5′-CAA TGC TGT CGG CAC TTT CA-3′.

GAPDH Forward:5′-GGTGGTCTCCTCTGACTTCAA-3′; Reverse: 5′-GTTGCTGTAGCCAAATTCGTTGT-3′.

FTO forward: 5′-CTTCACCAAGGAGACTGCTATTTC; Reverse: 5′-CAAGGTTCCTGTTGAGCACTCTG-3′.

2.3.4. Gensini score

The Gensini score equals the sum of all segment scores (each segment score equals a segment weighting factor multiplied by a severity score). The segment weighting factors range from 0.5 to 5.0. The severity scores reflecting the specific percentage of luminal diameter reduction in the coronary artery segment are 32 for 100%, 16 for 99%, 8 for 90%, 4 for 75%, 2 for 50%, and 1 for 25% reduction. Thus, segments supplying a larger area of the myocardium are more heavily weighted and the highest scores are associated with multiple severe proximal lesions. Scoring was performed according to internationally recognized methods and the score of the individual patients represented the summed scores for each branch (12).

Narrowness	Score	Lesion	Score
1%–25%	1	Left main stem	5
26%–50%	2	Left anterior descending branch or left gyral branch	2.5
51%–75%	4	Middle left anterior descending branch	1.5
76%–90%	8	Distal segment of the left anterior descending branch	1.0
91%–99%	16	Middle and distal left gyral branch	1.0
Fully closed	32	Right coronary artery	1
		Small branch	0.5

2.4. Statistical analysis

Data were analyzed using SPSS 23.0. Data distributions were assessed by Kolmogorov–Smirnov tests and normally distributed data were expressed as means ± standard deviations and compared using independent-sample *t*-tests for two groups and one-way ANOVAs for multiple groups. Data that did not conform to a normal distribution were expressed as medians (interquartile spacing) and compared with the Mann–Whitney *U* rank-sum test for two groups and the Kruskal–Wallis rank-sum test for multiple groups. Associations between variables were assessed by Pearson or Spearman correlation analysis, and the sensitivity and specificity of METTL14 were evaluated by ROC curves and logistic regression analysis of risk factors for CHD. The discrimination ability of the logistic regression model was assessed by estimating the area under the receiver operating characteristic (ROC) curve. Model calibration was assessed using the Hosmer–Lemeshow test for good-ness of fit. Differences were statistically significant at $P < 0.05$.

3. Results

3.1. Activity of the methyltransferase are significantly raised in CHD

Firstly, we used ELISA to determine the activity of methyltransferase in the plasma of patients with CHD, finding the activity of the methyltransferase significantly raised in CHD patients relative to the controls (**Figure 1**). In addition, the mRNA levels of METTL14 were markedly increased while the FTO levels were significantly reduced in the CHD group (**Figure 2**).

3.2. Comparison of patient characteristics between the groups

No significant differences were observed between the groups in relation to age, sex, smoking, drinking, UA, TC, TG, LDL-C, FFA, LPa, HCY, HDL-C, or ApoA1 ($P > 0.05$). However, as shown in **Table 1**, the incidence of diabetes and hypertension, as well as the concentrations of TC, CRP, and SAA were higher in CHD patients.

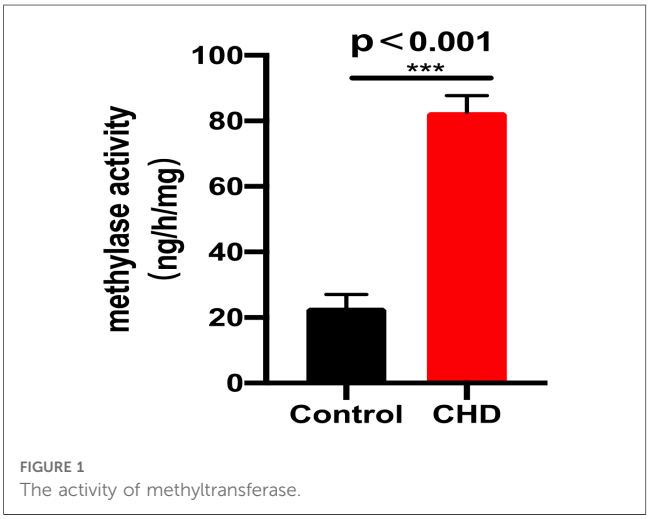

FIGURE 1
The activity of methyltransferase.

3.3. Numbers of coronary branches with lesions

Patients with CHD were then classified by the number of coronary branches containing lesions. Seventy-two patients had a single lesion in one branch, 80 had lesions in two branches, and 64 had lesions in three branches. Analysis of the clinical parameters of the patients in these different subgroups showed no inter-group differences in terms of age, sex, hypertension, diabetes, smoking, alcohol consumption, LDL-C, FFA, LPa, HCY, HDL-C, and ApoA1 while significant differences were observed for TG, LDL-C, CRP, and SAA (**Table 2**).

3.4. Levels of inflammatory factors in patients with CHD

It was observed that the contents of TNF-α, VCAM-1, ICAM-1, MCP-1, and IL-6, measured by ELISA, were significantly raised in the CHD group in comparison with the controls ($P < 0.001$) (**Table 3**).

3.5. METTL14 levels in the CHD group

METTL14 levels were observed to be markedly increased in the CHD group relative to the controls ($P < 0.001$) (**Table 4**).

3.6. METTL14 levels in relation to lesioned branches

Patients with CHD were grouped as described above based on the number of branches containing coronary lesions. The groups were defined as the 1-branch lesion ($n = 72$), 2-branch lesion ($n = 80$), and 3-branch lesion ($n = 64$) groups. The control was the 0-branch lesion group. The results are shown in **Table 5**.

3.7. Associations between METTL14 levels and clinical characteristics of CHD patients

There was no correlation between METTL14 and age, sex, diabetes, hypertension, alcohol consumption, smoking, TG, TC, LDL-C, FFAs, LPa, HCY, HDL-C, or ApoA1 ($P > 0.05$). A significant association, however, was observed with SAA ($P < 0.01$) (**Table 6**).

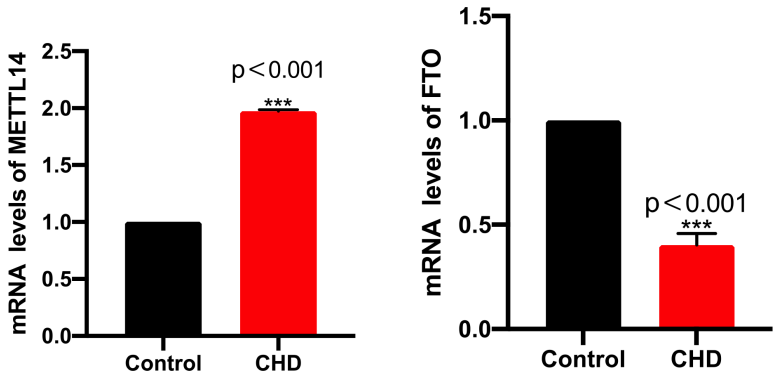

FIGURE 2
The mRNA levels of METTL14 and FTO.

TABLE 1 Characteristics of patients in the two groups.

	Control ($n = 100$)	CHD ($n = 216$)	*P*
Age (year)	55.38 ± 10.02	56.03 ± 5.19	0.359
Sex (Male/Female)	48/52	97/119	0.054
Hypertension [case (%)]	37 (37%)	138 (63.8%)	0.001
Diabetes [case (%)]	42 (42%)	103 (47.6)	0.034
Smoking [case (%)]	37 (37%)	78 (36.1%)	0.421
Drinking [case (%)]	34 (34%)	69 (31.9%)	0.390
UA (umol/L)	302.48 ± 79.55	322 ± 67.5	0.311
TG (mmol/L)	1.34 (0.88,2.14)	1.39 (1.21,1.95)	0.688
TC (mmol/L)	1.03 ± 0.79	4.1 ± 0.83	0.001
LDL-C (mmol/L)	2.88 ± 0.78	2.96 ± 0.84	0.603
FFA (mmol/L)	0.51 ± 0.34	0.68 ± 0.49	0.062
Lpa (mg/dl)	129.4 (72,321.3)	141.9 (69.46,423.4)	0.087
HCY (umol/L)	10.3 (9.3,13)	10.7 (9.6,15.9)	0.059
HDL-C (mmol/L)	1.13 ± 0.47	1.05 ± 0.22	0.074
ApoA1 (g/L)	1.43 ± 0.38	1.45 ± 0.30	0.183
CRP (mg/dl)	5.90 ± 3.18	30.28 ± 6.7	<0.001
SAA	4.35 ± 0.25	23 ± 2.21	<0.001

TABLE 2 Association between the number of coronary branches with lesions and clinical parameters in CHD patients.

	1 sticks ($n = 72$)	2 sticks ($n = 80$)	3 sticks ($n = 64$)	*P*
Age (year)	55.48 ± 5.93	55.8 ± 6.29	56.01 ± 4.38	0.403
Sex (Male/Female)	37/35	38/42	34/30	0.078
Hypertension [case (%)]	25 (34.7%)	30 (37.5%)	21 (32.8%)	0.055
Diabetes [case (%)]	21 (29.1%)	25 (31.2%)	22 (34.3%)	0.451
Smoking [case (%)]	24 (33.3%)	30 (37.5%)	24 (37.5%)	0.053
Drinking [case (%)]	20 (27.7%)	27 (33.7%)	21 (32.8%)	0.064
TG (mmol/L)	1.17 (1.12,1.5)	1.19 (0.89,1.6)	2.57 (1.32,2.99)	0.028
TC (mmol/L)	4.34 ± 0.58	4.46 ± 0.04	4.82 ± 0.75	0.348
LDL-C (mmol/L)	2.17 ± 0.71	3.02 ± 1.19	3.35 ± 0.23	0.017
FFA (mmol/L)	0.65 ± 0.31	0.69 ± 0.28	0.62 ± 0.34	0.178
LPa (mg/dl)	109.4 (73,205.4)	120.5 (84.3,450.9)	113.9 (69.6,423.4)	0.058
HCY (umol/L)	11.2 (8.7,18.4)	11.9 (9,21)	10 (8.7,17.6)	0.231
HDL-C (mmol/L)	1.01 ± 0.28	1.04 ± 0.39	1.12 ± 0.46	0.129
ApoA1 (g/L)	1.39 ± 0.42	1.45 ± 0.64	1.43 ± 0.29	0.274
CRP (mg/dl)	13.3 ± 4.39	29.5 ± 3.43	36.5 ± 5.4	0.001
SAA	19.3 ± 2.12	45.2 ± 1.38	88.7 ± 0.12	0.001

TABLE 3 Levels of inflammatory factors.

	Control ($n = 100$) P50 (P25, P75)	CHD ($n = 216$) P50 (P25, P75)	*P*
TNF-α (pg/ml)	197 (95.23, 294.39)	403.5 (209.2, 488.90)	<0.001
MCP-1 (pg/ml)	302 (139.20, 388.47)	537 (219.3, 573.9)	<0.001
VCAM-1 (pg/ml)	153.6 (142.29, 232.3)	340.8 (267.4, 473.98)	<0.001
ICAM-1 (pg/ml)	109 (78.38, 236.4)	302.3 (148.3, 335.39)	<0.001
IL-6 (pg/ml)	174.3 (133.2, 289.3)	392.4 (212.3, 478.2)	<0.001

TABLE 4 METTL14 in the two groups.

	Control	CHD	*P*
METTL14 (pg/ml)	123.39 (112.67, 298.45)	438.17 (239.04, 468.23)	<0.001

3.8. Associations between METTL14 and inflammatory factor levels and Gensini scores in CHD patients

METTL14 levels were significantly linked to those of VCAM-1, ICAM-1, SAA, and IL-6, as well as the Gensini scores in the CHD group (Table 7).

3.9. ROC curve analysis of METTL14 sensitivity and specificity

The cut-off values and sensitivity and specificity according to the maximum Jorden index were determined from the ROC curves. The results showed that METTL14 had a cut-off value of 342.37, a sensitivity of 77%, a specificity of 84%, and an AUC of 0.881 (0.679, 0.894).

3.10. Binary logistic regression

In the regression analysis, CHD was set as the dependent variable with inflammatory factor and METTL14 levels as independent variables. The analysis showed that MCP-1, VCAM-

TABLE 5 Levels of METTL14 in relation to the number of branches containing lesions.

Number of sticks	METTL14
0	123.4 (98.3,147.9)[a,b,c]
1	281 (234.5, 318.2)[a,b,d]
2	367.4 (325.8, 390.2)[a,c,d]
3	490.2 (436.18, 576.32)[b,c,d]

[a]Compared with the 0-branch lesion group, $P < 0.01$ was statistically significant.
[b]Compared with the 1-branch lesion group, $P < 0.01$ was statistically significant.
[c]Compared with the 2-branch lesion group, $P < 0.01$ was statistically significant.
[d]Compared with the 3-branch lesion group, $P < 0.01$ was statistically significant.

TABLE 6 Relationships between METTL14 and clinical characteristics.

	METTL14	*P*
	R	
Age	0.045	0.509
Sex	−0.74	0.083
Hypertension	0.015	0.783
Diabetes	0.098	0.054
Smoking	−0.018	0.801
Drinking	0.023	0.612
TG	0.271	0.064
TC	0.382	0.078
LDL-C	0.641	0.392
FFA	−0.029	0.075
LPa	0.218	0.175
HCY	0.193	0.204
HDL-C	0.143	0.169
ApoA1	−0.292	0.403
SAA	0.012	0.03

R denotes correlation coefficient.

TABLE 7 Correlations of METTL14 with TNF-α, MCP-1, VCAM-1, ICAM-1, IL-6 and gensini scores.

	METTL14	*P*
	R	
TNF-α	0.372	0.062
MCP-1	0.4830	0.0594
VCAM-1	0.075	0.013
ICAM-1	0.05	0.029
IL-6	0.39	0.003
SAA	0.013	0.011
Gensini	0.493	0.027

1, IL-6, SAA, and METTL14 were independent risk factors for CHD ($P < 0.05$) (**Table 8**).

TABLE 8 Logistic regression analysis of METTL14 in CHD.

	β	Sx	Wald	RR (95% CI)	*P*
TNF-α	0.07	0.01	10.738	1.0007 (1.004,1.015)	0.312
MCP-1	0.05	0.03	10.487	1.005 (1.003,1.040)	<0.001
VCAM-1	0.09	0.04	11.783	1.013 (1.005,1.025)	<0.001
ICAM-1	0.05	0.02	1.291	1.003 (0.999,1.015)	0.382
IL-6	0.08	0.02	10.649	1.008 (1.005,1.023)	<0.001
SAA	0.04	0.04	3.204	1.019 (1.004,1.027)	<0.001
METTL14	0.05	0.03	13.08	1.002 (1.001,1.029)	<0.001

4. Discussion

Although the specific risk factors for CHD have not been fully elucidated, it is known that factors such as hypertension, hyperlipidemia, diabetes, and inflammation are associated with its development (13–15). A characteristic feature of CHD is the presence of atherosclerotic plaques, formed by a combination of lipid, calcium, and inflammation-associated cells (16, 17). The presence of plaque narrows the lumen of the artery, and, in the case of coronary arteries, can lead to the development of angina, either persistent or episodic. Plaque rupture can lead to the development of blood clots which can cause myocardial infarction through blockage of the vessels. Atherosclerosis is also linked with inflammation. It is thus possible to assess the severity and progression of CHD by measuring the levels of specific inflammatory indicators (18). Here, it was found that the presence of hypertension and diabetes, as well as the levels of TC, CRP, and SAA, were significantly associated with CHD. This suggests that both hyperlipidemia and the inflammatory response are closely associated with CHD pathogenesis, as has been found in earlier studies (17, 18).

Recent evidence has indicated that epigenetic modifications are associated with both the initiation and subsequent promotion of atherosclerosis, playing important parts in the development of atherosclerotic plaque. This suggests the potential significance of using markers of epigenetic modifications as indicators or biomarkers for CHD risk and progression (19). This appears to be the first investigation of the role of the methyltransferase METTL14 in CHD, and demonstrated that METTL14 levels were markedly raised in the sera of patients with CHD. However, the METTL14 levels were not found to be linked to either the TC or TG levels, which were used in the inclusion criteria.

Studies have shown that the m6A methylation process affects various types of cells, including those associated with blood vessels, such as vascular endothelial and smooth muscle cells, as well as macrophages, and that changes in methylation levels contribute to the pathogenesis of atherosclerosis. METTL14 is documented to methylate pri-miR-19a and promote the processing of the mature miR-19a, stimulating the proliferation and invasion of atherosclerotic vascular endothelial cells, indicating that the METTL14/m6A/miR-19a axis may represent a novel target for anti-atherosclerosis treatment (20). In addition, METTL14 reduction inhibits the endothelial cell inflammatory response, thereby preventing atherosclerotic plaque formation (21). A study using mass spectrometry to analyze m6A levels in non-atherosclerotic arterial and carotid atherosclerotic tissues found that m6A methylesterase and demethylase levels were altered in atherosclerotic tissues (22). More importantly, knockdown of METTL14 inhibited the m6A modification of FOXO1 and decreased FOXO1 expression to suppress the endothelial inflammatory response and atherosclerotic plaque formation (21). It has also been shown that METTL14 promotes inflammatory responses in atherosclerosis-associated macrophages via NF-κB/IL-6 signaling (23). WTAP promotes myocardial I/R

injury through promoting ER stress and cell apoptosis by regulating m6A modification of ATF4 mRNA (24). NCBP3, a novel hypoxia-specific response protein, functions as a scaffold for the coordination of METTL3 and eIF4A2 for enhancing gene translation by m6A RNA methylation in cardiomyocytes subjected to hypoxic stress (25). Moreover, METTL14 promotes the renal ischemia-reperfusion injury (IRI) via suppressing YAP1 pathway (26). UCHL5 modified by METTL14/YTHDF1 axis could facilitate the inflammation and vascular remodeling in atherosclerosis by activating the NLRP3 inflammasome (27).

Here, plasma concentrations of inflammatory factors were analyzed by ELISA, showing that CHD patients had significantly elevated concentrations of TNF-α, MCP-1, ICAM-1, VCAM-1, and IL-6, which is consistent with previous findings (28–31). Notably, METTL14 levels were found to be significantly associated with those of VCAM-1, IL-6, ICAM-1, and SAA, suggesting a close relationship between METTL14 and the inflammatory response. The relationship between SAA and METTL14 has not yet been reported and the precise mechanisms underlying this association require further elucidation in future work. METTL14 was also observed to correlate with the Gensini score and higher numbers of coronary artery branches containing lesions, suggesting a relationship between METTL14 and CHD stenosis and severity. The above studies provide a stronger theoretical basis for the relationship between METTL14 and inflammation. Although studies have identified the role of METTL14 in CHD and its relationship with inflammatory markers, the biological effects of METTL14 on the initiation and progression of CHD have not been investigated. Combined with previous and our results, it is speculated that it is possible to delay the progression of CHD by intervening or inhibiting potential molecular targets. Nevertheless, there are still several shortcomings in this study. First, it was a single-center study with a small sample size, with some variation in the clinical baseline data of the study population, so a subsequent large-sample study is needed to further confirm these results. In addition, there are many risk factors for CHD and only a single inclusion criterion was used. Thus, although we observed a significant link between METTL14 levels and CHD risk, the use of METTL14 as a CHD biomarker requires further verification with large-sample and multi-center studies. Specific targeting is challenging in disease treatment and it is possible that the combination of transcription factors with targets may be useful, providing a stronger theoretical basis for the prevention of CHD.

Data availability statement

The raw data supporting the conclusions of this article will be made available by the authors, without undue reservation.

Author contributions

FG and GL: conceived and supervised the study. FG: designed experiments. FG and MH: performed experiments. FG and BH: analyzed the data. FG: wrote the manuscript; and FG and GL: revised the manuscript. All authors contributed to the article and approved the submitted version.

Funding

This study was funded by the National Natural Sciences Foundation of China (grant no 82002199).

Conflict of interest

The authors declare that the research was conducted in the absence of any commercial or financial relationships that could be construed as a potential conflict of interest.

Publisher's note

All claims expressed in this article are solely those of the authors and do not necessarily represent those of their affiliated organizations, or those of the publisher, the editors and the reviewers. Any product that may be evaluated in this article, or claim that may be made by its manufacturer, is not guaranteed or endorsed by the publisher.

References

1. Tian Y, Deng P, Li B, Wang J, Li J, Huang Y, et al. Treatment models of cardiac rehabilitation in patients with coronary heart disease and related factors affecting patient compliance. *Rev Cardiovasc Med*. (2019) 20:27–33. doi: 10.31083/j.rcm.2019.01.53

2. Chen D, Liang M, Jin C, Sun Y, Xu D, Lin Y. Expression of inflammatory factors and oxidative stress markers in serum of patients with coronary heart disease and correlation with coronary artery calcium score. *Exp Ther Med*. (2020) 20 (3):2127–33. doi: 10.3892/etm.2020.8958

3. Ndrepepa G, Holdenrieder S, Cassese S, Fusaro M, Xhepa E, Laugwitz KL, et al. A comparison of gamma-glutamyl transferase and alkaline phosphatase as prognostic markers in patients with coronary heart disease. *Nutr Metab Cardiovasc Dis*. (2018) 28(1):64–70. doi: 10.1016/j.numecd.2017.09.005

4. Hou P, Xue HP, Mao XE, Li YN, Wu LF, Liu YB. Inflammation markers are associated with frailty in elderly patients with coronary heart disease. *Aging (Albany NY)*. (2018) 10(10):2636–45. doi: 10.18632/aging.101575

5. Qin Y, Li L, Luo E, Hou J, Yan G, Wang D, et al. Role of m6A RNA methylation in cardiovascular disease (review). *Int J Mol Med*. (2020) 46:1958–72. doi: 10.3892/ijmm.2020.4746

6. Zhang B, Jiang H, Dong Z, Sun A, Ge J. The critical roles of m6A modification in metabolic abnormality and cardiovascular diseases. *Genes Dis*. (2021) 8:746–58. doi: 10.1016/j.gendis.2020.07.011

7. Kumari R, Ranjan P, Suleiman ZG, Goswami SK, Li J, Prasad R, et al. mRNA modifications in cardiovascular biology and disease: with a focus on m6A modification. *Cardiovasc Res*. (2022) 118:1680–92. doi: 10.1093/cvr/cvab160

8. Zhao K, Yang CX, Li P, Sun W, Kong XQ. Epigenetic role of N6-methyladenosine (m6A) RNA methylation in the cardiovascular system. *J Zhejiang Univ Sci B*. (2020) 21:509–23. doi: 10.1631/jzus.B1900680

9. Meng L, Lin H, Huang X, Weng J, Peng F, Wu S. METTL14 suppresses pyroptosis and diabetic cardiomyopathy by downregulating TINCR lncRNA. *Cell Death Dis*. (2022) 13:38. doi: 10.1038/s41419-021-04484-z

10. Wang L, Wang J, Yu P, Feng J, Xu GE, Zhao X, et al. METTL14 is required for exercise-induced cardiac hypertrophy and protects against myocardial ischemia-reperfusion injury. *Nat Commun*. (2022) 13:6762. doi: 10.1038/s41467-022-34434-y

11. Liu Y, Luo G, Tang Q, Song Y, Liu D, Wang H, et al. Methyltransferase-like 14 silencing relieves the development of atherosclerosis via m(6)A modification of p65 mRNA. *Bioengineered*. (2022) 13:11832–43. doi: 10.1080/21655979.2022.2031409

12. Zencirci AE, Zencirci E, Degirmencioglu A, Karakus G, Ugurlucan M, Gunduz S, et al. The relationship between gensini score and ST-segment resolution in patients with acute ST-segment elevation myocardial infarction undergoing primary percutaneous coronary intervention. *Kardiol Pol*. (2014) 72(6):494–503. doi: 10.5603/KP.a2013.0355

13. Luscher TF, von Eckardstein A, Simic B. Therapeutic targets to raise HDL in patients at risk or with coronary artery disease. *Curr Vasc Pharmacol*. (2012) 10 (6):720–4. doi: 10.2174/157016112803520972

14. de Araújo Gonçalves P, Garcia-Garcia HM, Carvalho MS, Dores H, Sousa PJ, Marques H, et al. Diabetes as an independent predictor of high atherosclerotic burden assessed by coronary computed tomography angiography: the coronary artery disease equivalent revisited. *Int J Cardiovasc Imaging*. (2013) 29(5):1105–14. doi: 10.1007/s10554-012-0168-4

15. Mahalle N, Kulkarni MV, Naik SS. Is hypomagnesaemia a coronary risk factor among Indians with coronary artery disease? *J Cardiovasc Dis Res*. (2012) 3(4):280–6. doi: 10.4103/0975-3583.102698

16. Li H, Sun K, Zhao R, Hu J, Hao Z, Wang F, et al. Inflammatory biomarkers of coronary heart disease. *Front Biosci (Schol Ed)*. (2018) 10(1):185–96. doi: 10.2741/s508

17. Qian H, Luo Z, Xiao C, Chen J, Li D, Xu H, et al. Red cell distribution width in coronary heart disease: prediction of restenosis and its relationship with inflammatory markers and lipids. *Postgrad Med J*. (2018) 94(1115):489–94. doi: 10.1136/postgradmedj-2018-135806

18. Asztalos BF, Horvath KV, Schaefer EJ. High-density lipoprotein particles, cell-cholesterol efflux, and coronary heart disease risk. *Arterioscler Thromb Vasc Biol*. (2018) 38(9):2007–15. doi: 10.1161/ATVBAHA.118.311117

19. Wu S, Zhang S, Wu X, Zhou X. M(6)A RNA methylation in cardiovascular diseases. *Mol Ther*. (2020) 28(10):2111–9. doi: 10.1016/j.ymthe.2020.08.010

20. Jian D, Wang Y, Jian L, Tang H, Rao L, Chen K, et al. METTL14 aggravates endothelial inflammation and atherosclerosis by increasing FOXO1 N6-methyladeosine modifications. *Theranostics*. (2020) 10(20):8939–56. doi: 10.7150/thno.45178

21. Quiles-Jimenez A, Gregersen I, Mittelstedt Leal de Sousa M, Abbas A, Kong XY, Alseth I, et al. N6-methyladenosine in RNA of atherosclerotic plaques: an epitranscriptomic signature of human carotid atherosclerosis. *Biochem Biophys Res Commun*. (2020) 533(4):631–7. doi: 10.1016/j.bbrc.2020.09.057

22. Aslibekyan S, Agha G, Colicino E, Do AN, Lahti J, Ligthart S, et al. Association of methylation signals with incident coronary heart disease in an epigenome-wide assessment of circulating tumor necrosis factor alpha. *JAMA Cardiol*. (2018) 3 (6):463–72. doi: 10.1001/jamacardio.2018.0510

23. Zheng Y, Li Y, Ran X, Wang D, Zheng X, Zhang M, et al. METTL14 mediates the inflammatory response of macrophages in atherosclerosis through the NF-κB/IL-6 signaling pathway. *Cell Mol Life Sci*. (2022) 79(6):311. doi: 10.1007/s00018-022-04331-0

24. Wang J, Zhang J, Ma Y, Zeng Y, Lu C, Yang F, et al. WTAP promotes myocardial ischemia/reperfusion injury by increasing endoplasmic reticulum stress via regulating m(6)A modification of ATF4 mRNA. *Aging (Albany NY)*. (2021) 13:11135–49. doi: 10.18632/aging.202770

25. Ye F, Wang X, Tu S, Zeng L, Deng X, Luo W, et al. The effects of NCBP3 on METTL3-mediated m6A RNA methylation to enhance translation process in hypoxic cardiomyocytes. *J Cell Mol Med*. (2021) 25:8920–8. doi: 10.1111/jcmm.16852

26. Xu Y, Yuan XD, Wu JJ, Chen RY, Xia L, Zhang M, et al. The N6-methyladenosine mRNA methylase METTL14 promotes renal ischemic reperfusion injury via suppressing YAP1. *J Cell Biochem*. (2020) 121:524–33. doi: 10.1002/jcb.29258

27. Yang X, Wang C, Zhu G, Guo Z, Fan L. METTL14/YTHDF1 axis-modified UCHL5 aggravates atherosclerosis by activating the NLRP3 inflammasome. *Exp Cell Res*. (2023) 427:113587. doi: 10.1016/j.yexcr.2023.113587

28. Leocadio PCL, Menta P, Dias MTS, Fraga JR, Goulart AC, Santos IS, et al. Low serum levels of CCL2 are associated with worse prognosis in patients with acute coronary syndrome: 2-year survival analysis. *Biomed Pharmacother*. (2019) 109:1411–6. doi: 10.1016/j.biopha.2018.10.087

29. Santos JCD, Cruz MS, Bortolin RH, Oliveira KM, Araujo JNG, Duarte VHR, et al. Relationship between circulating VCAM-1, ICAM-1, E-selectin and MMP9 and the extent of coronary lesions. *Clinics*. (2018) 73:e203. doi: 10.6061/clinics/2018/e203

30. Wang Y, Sun X, Xia B, Le C, Li Z, Wang J, et al. The role of OX40l and ICAM-1 in the stability of coronary atherosclerotic plaques and their relationship with sudden coronary death. *BMC Cardiovasc Disord*. (2019) 19(1):272. doi: 10.1186/s12872-019-1251-8

31. Held C, White HD, Stewart RAH, Budaj A, Cannon CP, Hochman JS, et al. Inflammatory biomarkers interleukin-6 and C-reactive protein and outcomes in stable coronary heart disease: experiences from the STABILITY (stabilization of atherosclerotic plaque by initiation of darapladib therapy) trial. *J Am Heart Assoc*. (2017) 6(10):e005077. doi: 10.1161/JAHA.116.005077

Frontiers in
Cardiovascular Medicine

Innovations and improvements in cardiovascular treatment and practice

Focuses on research that challenges the status quo of cardiovascular care, or facilitates the translation of advances into new therapies and diagnostic tools.

Discover the latest Research Topics

See more →

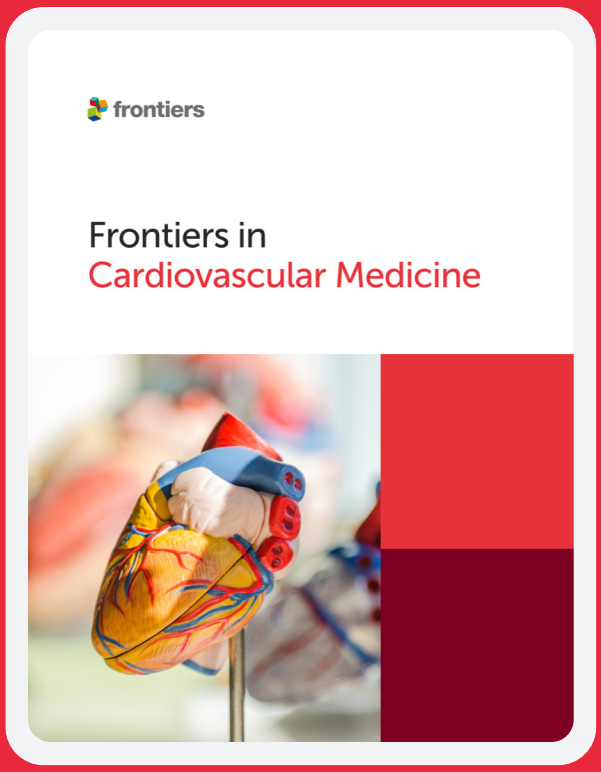

Frontiers

Avenue du Tribunal-Fédéral 34
1005 Lausanne, Switzerland
frontiersin.org

Contact us

+41 (0)21 510 17 00
frontiersin.org/about/contact